

# The Origin of Granites and Related Rocks



III  
HUTTON  
SYMPOSIUM

ABSTRACTS



U.S. GEOLOGICAL SURVEY CIRCULAR 1129

**Cover.** Boudins on several scales within layered amphibolite, Tolstik Peninsula, Karelia, Russia. Anatectic melt represented by leucosome has migrated preferentially parallel to the tectonic foliation to the boudin necks, at each of the scales, in response to applied differential stress. Width of field of view about 1 m. Photograph taken by Michael Brown. Cover design by Jane B. Russell.

**T H E O R Y**  
**O F T H E**  
**E A R T H,**  
**W I T H**  
**P R O O F S A N D I L L U S T R A T I O N S.**

---

**I N F O U R P A R T S.**

---

**By JAMES HUTTON, M. D. & F. R. S. E.**

---

**V O L. I.**

---

**E D I N B U R G H :**  
**P R I N T E D F O R M E S S R S C A D E L L , J U N I O R , A N D D A V I E S ,**  
**L O N D O N ; A N D W I L L I A M C R E E C H , E D I N B U R G H .**

---

**1795.**

**Frontispiece.** Facsimile of the title page of James Hutton's seminal work, *Theory of the Earth*, two volumes, Edinburgh, 1795. The geological writings of James Hutton (1726–1797) provide the foundation of modern geology. Hutton recognized the length of geological time, the uniformity of geological processes through time, and the role of igneous activity, sedimentation, and erosion in forming the Earth as we know it. It is fitting that this Third Hutton Symposium on the Origin of Granites and Related Rocks should occur during the bicentenary of the publication of this great work, which records among its content an important stage in the development of ideas about igneous rocks.

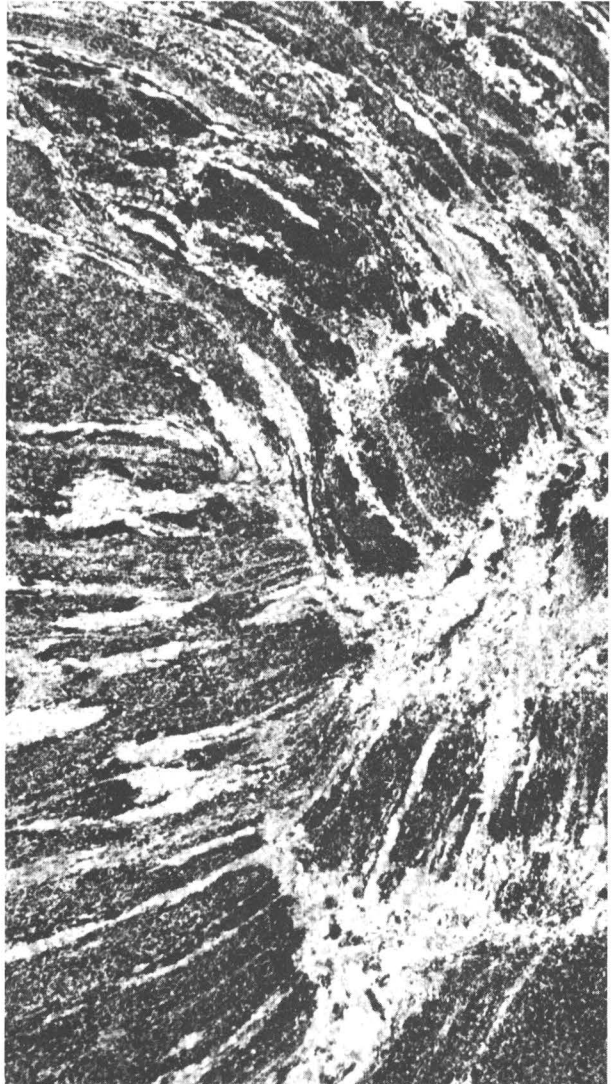
**THE ORIGIN OF GRANITES  
AND RELATED ROCKS**

# The Origin of Granites and Related Rocks

THIRD HUTTON SYMPOSIUM  
A B S T R A C T S

College Park, Maryland  
August 26–September 2, 1995

*Edited by* Michael Brown and  
Philip M. Piccoli



U.S. GEOLOGICAL SURVEY CIRCULAR 1129

---

**U.S. DEPARTMENT OF THE INTERIOR  
BRUCE BABBITT, Secretary**

**U.S. GEOLOGICAL SURVEY  
GORDON P. EATON, Director**

For sale by U.S. Geological Survey, Information Services  
Box 25286, Federal Center, Denver, CO 80225

This report has been prepared by the University of Maryland in cooperation with the U.S. Geological Survey; the report has not been reviewed for conformity with U.S. Geological Survey editorial standards or with the North American Stratigraphic Code. Any use of trade, product, or firm names in this publication is for descriptive purposes only and does not imply endorsement by the U.S. Government.

Published in the Eastern Region, Reston, Va.  
Manuscript approved for publication May 25, 1995.

# CONTENTS

Introduction .....	1
Program of Oral Presentations .....	4
Abstracts .....	7
Author Index .....	169



# THE ORIGIN OF GRANITES AND RELATED ROCKS

Michael Brown and Philip M. Piccoli, *Editors*

## INTRODUCTION

Towards the end of his life, James Hutton (1726-1797) set forth his "Theory of the Earth" in which he recognized the length of geological time, the uniformity of geological processes through time, and the role of igneous activity, sedimentation, and erosion in forming the Earth as we know it. These ideas had been formulated as a result of much thought and discussion, and were based on a long and critical study of rocks in the field. Hutton's four part two-volume book was preceded by a public presentation of these ideas in 1785, in a paper on "Examination of the System of the Habitable Earth with Regard to its Duration and Stability" read to members of the Royal Society of Edinburgh on March 7 and April 4. Subsequently, the paper was published in Volume I of the *Transactions of the Royal Society of Edinburgh* in 1788. In the ten years between presentation of the paper to the Royal Society of Edinburgh and publication of his book, Hutton occupied himself in accumulating the "proofs and illustrations" of his *Theory of the Earth* which enhance the fuller exposition of the *Theory* as presented in the book. Indeed, for the three summers that followed his 1785 presentations to the Royal Society of Edinburgh, Hutton examined key field relationships along Glentilt in the Grampians (1785), around Loch Ken in Galloway (1786) and on Goatfell in the north of Arran (1787), because he concluded, that if his account in 1785 was correct, some confirmation of it must appear at those places where granite and stratified rock are in contact. The development of Hutton's views on the origin of igneous rocks was presented to members of the Royal Society of Edinburgh on January 4, 1790, and subsequently published in Volume III of the *Transactions* in 1794. The questions in Hutton's mind in 1785 concerned whether granites represented material "transfused from the subterraneous regions, and made to break and invade the strata". During his field work, Hutton was able to find unequivocal evidence to show that molten granite had invaded the surrounding stratified rock, that is to say it was an intrusive igneous rock of younger age than the

country rocks. This represents the first demonstration of the class of rocks that we now refer to as *intrusive igneous rocks*. The conclusions of his short paper "Observations on Granite" are important to all of us, and were:

*"We are now fully assured that granite has been made to break, displace and invade the Alpine schistus or primary strata having been previously forced to flow in the bowels of the earth, and reduced into a state of fusion. From this too we are to draw the following conclusion: Granite, which has been hitherto considered by naturalists as being the original or primitive part of the earth, is now found to be posterior to the Alpine schistus; which schistus, being stratified, is not itself original; though it may be considered, perhaps, as primary, in relation to other strata, which are evidently of a later date."*

The subject of the origin of granite and related rocks has remained of intense topical interest since the time of Hutton, and the Hutton Symposium Series began as a result of the success of a symposium on "The Origin of Granites" organized jointly by the Royal Society of Edinburgh and the Royal Society of London in 1987 to celebrate the bicentenary of the work of James Hutton. Implicit in Hutton's conclusions concerning granite are the ideas of crustal anatexis, melt segregation, magma transfer and granite emplacement into lower-grade upper-crustal rocks. How far have we progressed in our understanding of these processes during the following 200 years?

Detailed field studies, such as those completed by Hutton 200 years ago, remain the foundation of our understanding of granites and related rocks. Since Hutton's time, field work has provided a necessary framework for the interpretation of studies of, for example: granite crystallization; coeval and cogenetic felsic volcanic systems; pegmatite genesis; and granite-related hydrothermal systems (which may represent the culmination of the granite crystallization process). After several decades of experimental investigation, we have a firm understanding of the melt production of common crustal protoliths as a function of pressure, temperature and activity of water.

The thermal budget of continental collision belts that involve thickening, thermal relaxation and exhumation has been modeled, and in many cases extension and/or delamination of part of the lithosphere to increase the heat flux across the Moho is necessary to explain observed features of granite magmatism in orogenic belts. Nonetheless, it remains unclear exactly how the thermal requirements for melting crustal protoliths are met in individual cases. Additionally, the role of mantle-derived magma in crustal anatexis remains a matter of debate, although hybridization and assimilation-fractional crystallization are well-established processes and in many cases the isotopic evidence seems unambiguous. Our understanding of controls on the geochemistry of crustal melts has improved significantly with increases in experimental data and better understanding of rates of, for example, diffusion and mineral dissolution. In contrast, our knowledge of pressure, temperature, fugacity of oxygen and fugacity of water in magmas during ascent and emplacement remains sketchy at best. Since 1980 our understanding of and our ability to model the processes that cause change in magma composition during ascent, emplacement and final solidification has advanced considerably, but the relative importance of these processes, such as fractional crystallization, assimilation-fractional crystallization, restite entrainment and unmixing, and hybridization remains uncertain. The past decade has seen a return to experimental work which is producing data to advance our understanding of the physics of magma, a renewed interest in textural interpretation and a quantitative approach to rates of, for example, melt segregation, ascent and emplacement; there is much progress still to be made in these areas of research.

The whole concept of melt segregation is changing. The current view is that melt segregation is governed by the type of melting reaction, the rate of melting, the depth of melting, and the rate of deformation. In most circumstances, there will be no specific rheological critical melt percentage at which melt automatically will begin to segregate, although before any melt will segregate from the crustal protolith, connectivity of the melt-filled porosity must be achieved. Models for melt segregation include compaction, convection, filter-pressing, dilatancy-pumping and magma fracture, each of which may operate cyclically and at different strain rates in active tectonic environments undergoing syn-anatectic deformation. In some circumstances melt may be generated and accumulate until bulk magma mobility facilitates transfer of the whole system (*i.e.* melt plus residual material) but in other circumstances melt at fractions clearly below the rheological critical melt percentage has transferred from the melting environment to the upper crust. Thus, segregation of low melt fractions from residual solid can be an efficient process. Studies in migmatite complexes, in which at least part of the product

of the melting reaction remains *in situ*, provide information about plumbing in the crust and melt transfer pathways. The relationship between lower crust that exhibits depleted geochemistry and fragments of apparently undepleted lower crustal material entrained as xenoliths in basalts, remains unresolved.

There has been considerable debate concerning the mechanisms of ascent of granitic magma through the continental crust. During the past decade support for the traditionally assumed mechanism of diapirism has been waning as emphasis has been increasingly placed on the relationship between plutons and shear zones. More recently, magma transfer through the crust in dikes has become popular. Rates of melt segregation in response to applied differential stress and melt ascent in dikes or major shear zones have been modeled, and in some circumstances are thought to be fast. Both the processes themselves and the rates at which they proceed have important implications for the geochemistry of granites and for the potential to advect heat into higher levels of the crust. Additionally, the rheological consequences of partially molten crust are significant. For example, if major crustal shear zones initiate in partially molten regions subjected to applied differential stress, then melt will migrate to the lower-pressure shear zone. In this way the shear zone may localize the ascent path and emplacement site, but the driving forces both for ascent and emplacement will be some combination of the regional applied differential stress and buoyancy forces of gravity. At the emplacement site, the amount of strain may relate to the interaction between the rate of space creation by regional deformation and the rate at which magma arrives if the ascent mechanism is fast. During magma emplacement crust must be displaced at a rate equal to the growth of the pluton. Further, the evidence cited by Hutton and many others subsequently demonstrates a variety of small-scale mechanisms that may act in combination to enhance the space available for magma accumulation at the emplacement site. Multiple horizontal and vertical material transfer processes acting in different proportions from pluton to pluton may well be more realistic than the extremes implied by a single model either of ascent or of emplacement.

The importance of mass transfer in dikes was recognized by Hutton during field work at Water of Leith, Scotland, where he examined many whinstone (diabase) dikes. Since that time, several questions have been answered concerning the origin, evolution and structure of simple and rare-metal granitic dikes (pegmatites and aplites), particularly concerning the role of volatiles in the generation of these highly evolved liquids, and yet many questions still remain unanswered. Detailed experimental studies provide an understanding of the phase equilibria, the role of trace metals (fluxes) on those equilibria (*e.g.*,

B, Li, F, and Cl), textures (including nucleation and crystal growth rates, and grain size), and the diverse mineralogies and structural complexities (*e.g.*, zoning) of these systems. Our knowledge of the internal structure of granite-related pegmatites and controls on processes such as fractional crystallization, including the pressure-temperature-time conditions under which such structures form, is good in some systems. However, our knowledge of various pegmatite groups, and the ultimate origin of these granite-related pegmatite melts, is less clear.

The role of volatiles (*e.g.*, H<sub>2</sub>O and CO<sub>2</sub>), both as structural constituents of granite melts and as a discrete volatile phase or phases, has been realized for some time. Evidence from rhyolites, the erupted counterpart of granites, with dissolved water of between 3 and 7 wt % (upon eruption), suggests magma degassing during ascent and decompression of H<sub>2</sub>O-rich phases may be prevalent at depths less than *c.* 10 km. The magmatic volatile phase may be responsible for: modification of geochemical characteristics of source regions, in addition to modifying granite phase equilibria; alteration and mineralization of granite and country rock upon cooling; and, controlling fugacity of oxygen in some systems. Detailed, combined chemical-physical modeling still needs to be done to obtain a better understanding of these degassing processes. Degassing leads to hydrofracturing, which is an important control on the formation of well developed hydrothermal and ore systems. Granite-related hydrothermal systems and mineral deposits (*e.g.* porphyry-type deposits and granite skarns), develop from the synergistic effects of a multitude of processes and conditions. All mineral deposits have a common requirement - a process whereby an element is brought from a dispersed state to a state of higher concentration. There has been considerable debate over the ultimate origin of metals in granite related ore-systems, but several conditions including emplacement level within the crust, initial water concentration in the melt, fugacity of oxygen, and halide concentration in the melt play a role in both the final chemistry of granite bodies and the ore deposits they sometimes form. The close spatial and temporal relationships of some ore-deposits with granitic systems suggest a genetic affinity; observed ore element ratios in some systems (*e.g.* eastern Australia) exhibit correlation with composition of the related granites at the present level of erosion. Granite porphyry systems (*e.g.* Cu, Mo, Pb, and Zn, with minor Au and Ag) often consist of several distinct periods of mineralization within a system, in which magmatic volatile phases associated with granites (*sensu lato*) appear to play a significant role in scavenging ore-metals from granite melts. Granite skarns form when volatile phases (vapor and vapor-brine mixtures) are exsolved and interact with country rocks. Understanding these processes which

produce economically important mineral deposits is fundamental if geology is to continue to support the economic development of humankind.

The Third Hutton Symposium has been structured to promote discussion. A number of oral presentations (abstracts of these are identified as such) will provide an overview of recent developments in our understanding of one of several themes identified as foci for this symposium (crustal anatexis and pressure-temperature-composition relations in granites; physics and chemistry of melts; segregation, ascent and emplacement of granite magmas; volcano-plutonic systems; granite-related hydrothermal systems, mineralization and pegmatites; and, the contribution from isotope geochemistry). However, the majority of papers will be presented as posters during more informal afternoon and evening sessions to facilitate discussion with the evidence on hand. Furthermore, two evening discussions will be organized on "Current Debates and Future Research Directions", which will provide both a stimulus to research in areas where we need a better understanding as well as setting up some topics for possible elaboration at the Fourth Hutton Symposium in 1999.

This Symposium has been organized by a committee that comprised Prof. Michael Brown (University of Maryland at College Park, General Chair of the Third Hutton Symposium), Prof. Philip Candela (University of Maryland at College Park, Technical Program Chair), Dr. Judy Ehlen (U.S. Army Topographic Engineering Center, Registration), Jane Hammarstrom (U.S. Geological Survey, Poster Session Chair), Prof. E-an Zen (University of Maryland at College Park, Field Excursions Chair), Prof. Eirik Krogstad (University of Maryland at College Park), Prof. Eileen McLellan (University of Maryland at College Park), Dr. Dallas Peck (U.S. Geological Survey), Dr. Philip Piccoli (University of Maryland at College Park), Mr. Kent Ratajeski (University of Maryland at College Park), Dr. Steven Shirey (Department of Terrestrial Magnetism, Carnegie Institution of Washington), Mr. Paul Tomascak (University of Maryland at College Park), and Prof. Richard Walker (University of Maryland at College Park). The Symposium is co-sponsored by the Department of Geology, University of Maryland at College Park, the U.S. Geological Survey, Reston, Virginia, and the Department of Terrestrial Magnetism & Geophysical Laboratory, Carnegie Institution of Washington. The Organizing Committee acknowledges a grant from the National Science Foundation to subsidize the cost of travel to the meeting by U.S.-based graduate students, and the assistance of staff in the Department of Geology at UMCP. The editors thank the BETR for support in producing this Abstracts Volume as a U.S. Geological Survey Circular, and acknowledge the professional help of Dona Brizzi, Jane Russell, and Connie Schafer.

## PROGRAM OF ORAL PRESENTATIONS

(Speaker identified in bold)

### MONDAY, AUGUST 28, 1995

**Alan Bruce Thompson**

Fertility of Crustal Rocks During Anatexis

**Alberto E. Patiño Douce** and James S. Beard,

Effects of Pressure, H<sub>2</sub>O Activity, and Fe/Mg Ratio on the Compositions of Anatectic Melts

**Fernando Bea**

Controls on the Trace Element Chemistry of Crustal Melts

**Francois Holtz** and Bruno Scaillet

Effects of Dissolved C-O-H Species on Chemical and Physical Properties of Ascending Granitic Magmas

**D.B. Dingwell**, K. Hess, R. Knoche and S.L. Webb

New Experimental Constraints on the Physical Properties of Granitic Melts

**J. Lawford Anderson**

Status of Thermobarometry in Granitic Batholiths

**Hanna Nekvasil**, Charles Jensen and William Carroll

Experimental and Theoretical Constraints on the Differentiation of High Temperature Crustal Magmas

Malcolm P. Roberts and **John D. Clemens**

The Perils of AFC Modelling

### TUESDAY, AUGUST 29, 1995

**E.B. Watson** and J.M. Hanchar

Zircon Dissolution and Overgrowth in Granitic Melts: Effects of Thermal History and Local Melt Volume, with Implications for Chemical Zoning and Relative Core Size in Natural Zircons Showing an Inherited Isotopic Component

**J.P. Hogan**

Insights From Igneous Reaction Space: A Holistic Approach to Granite Crystallization

**Tracy Rushmer**

Application of Rock Deformation Experiments to Melt Segregation in the Lower Crust

**E.W. Sawyer**

Melt Segregation or Magma Mobility - The Difference Between Migmatites and Granites

**G.W. Bergantz**

Linking Phase Relations, Thermal Budgets and Deformation During Partial Melting: Two Contrasting Styles of Basalt-Crust Interaction

**Jean Louis Vigneresse**

Granites From Source to Emplacement: The View from Geophysics

**Roberto F. Weinberg**

Diapirism of Crustal Magmas

**Nick Petford**

Granite Ascent: Dykes or Diapirs?

**Scott R. Paterson, T. Kenneth Fowler, Jr. and Robert B. Miller**

Pluton Emplacement in Arcs: A Crustal-Scale Recycling Process

**WEDNESDAY, AUGUST 30, 1995**

**Mid-Conference Excursions**

**THURSDAY, AUGUST 31, 1995**

**Takashi Nakajima**

Cretaceous Granitoids in Southwest Japan and Their Bearing on Crust-Forming Processes in the Eastern Eurasian Margin

**Bruce W. Chappell**

Causes of Compositional Variation Within Granite Suites

**W.J. Collins**

S- and I-Type Granitoids of the Eastern Lachlan Fold Belt: Three-Component Mixing, Not Restite Unmixing

**C.W. Rapela and R.J. Pankhurst**

Monzonite Suites: The Innermost Cordilleran Plutonism of Patagonia

**Mark S. Drummond**, Marc J. Defant and Pavel K. Kepezhinskas  
The Petrogenesis of Slab-Derived Trondhjemite-Tonalite-Dacite/Adakite Magmas

**G. Poli**, G.R. Davies and S. Tommasini  
Trace Element and Isotopic Exchange During Acid-Basic Magma Interaction

**R.A. Wiebe**  
Mafic-Silicic Layered Intrusions

**Leslie Baker** and Malcolm J. Rutherford  
Crystallization of Pinatubo Magma

**R. Brooks Hanson**  
Hydrodynamics of Magmatic and Meteoric Fluids in the Vicinity of Granite Plutons

## **FRIDAY, SEPTEMBER 1, 1995**

**Mark D. Barton**  
Phanerozoic Granitoids and Associated Mineral Deposits in Southwestern North America

**Phillip L. Blevin**, Charlotte M. Allen, Colleen J. Bryant and Bruce W. Chappell  
A Metallogenic Template for Eastern Australia Based on Granite Source and Evolution

**Jacob B. Lowenstern**  
Intrusive Degassing at the Magma/Wallrock Interface

**David London**  
Pegmatites

**Robert A. Creaser**  
Radiogenic Isotopes in Granitic Systems: Studies of Melting and Mixing at the Source

**M. Pichavant** and T. Hammouda  
Control of Redox State and Sr Isotopic Composition of Magmas: Source or Processes?

**Richard J. Walker** and Eirik J. Krogstad  
Heterogeneous Sources for Granitic Rocks, Black Hills, South Dakota: Do Granites Really Serve as Interpretable Crustal Probes?

**Clark Johnson**, Katlin M. Barovich and Steven B. Shirey  
New Approaches to Crustal Evolution Studies Through the Lu-Hf and Re-Os Isotope Systems

## ABSTRACTS

### **Petrology and Geochemistry of the Polly Wright Cove Pluton, Blue Ridge Province, Virginia: Perspectives on Late Neoproterozoic Anorogenic Magmatism, Central Laurentian Appalachians**

<sup>1</sup>Abbey, W.J., <sup>1</sup>Tollo, R.P.  
and <sup>2</sup>Aleinikoff, J.N.

<sup>1</sup>*Department of Geology, George Washington University,  
Washington, DC 20052, USA*

<sup>2</sup>*U.S. Geological Survey, Denver, CO 80225, USA*

The Late Neoproterozoic Polly Wright Cove Pluton (PWCP) intruded Grenville-age (1.1-1.0 Ga) basement rocks of the Blue Ridge anticlinorium in central Virginia. The PWCP is part of a regional Late Neoproterozoic (760-700 Ma) anorogenic supersuite comprised of more than twenty granite plutons exposed throughout the Laurentian terrains of Virginia and North Carolina. These plutons were emplaced during an early period of crustal extension that preceded a younger period (at about 600 Ma) during which rifting of Laurentia (ancestral North America) produced the Iapetus ocean basin. The PWCP includes four major lithologic phases (from oldest to youngest): 1) fine-grained biotite granite (present only as xenoliths); 2) medium-grained biotite granite (the most areally extensive lithologic unit); 3) medium-grained biotite leucogranite; and, 4) fine- to medium-grained biotite granite (occurs only as dikes). The PWCP granites are metaluminous in composition and have geochemical signatures characteristic of A-type affinity, including: 1) high Ga/Al and Fe/Mg; 2) marked enrichment (relative to other granite types) of Y, Nb, Zr, Ce, and Ga; and, 3) low Ba and Sr. These geochemical characteristics are shared by other members of the anorogenic supersuite, as well as by anorogenic granites worldwide. The broad range in SiO<sub>2</sub> values (67.1 - 76.5 wt %), FeO/MgO (12.6 - 41.6), and Ba/Rb (0.34 - 3.50) indicates that fractionation of major minerals was responsible for developing significant compositional variation within the PWCP. The late-stage granites (leucogranites and dikes) of the pluton show marked depletion in Ba and Sr, as well as an increase in Ga/Al, relative to the older units suggesting that fractionation of alkali feldspar and plagioclase was a major factor controlling differentiation of the PWCP magmatic system.

Removal of ferromagnesian silicate minerals is suggested by the range in FeO/MgO and by development of late-stage leucogranite. Additionally, a marked decrease in Ce/Nb relative to Y/Nb in the late stage granites suggest fractionation of allanite. U-Pb isotopic data for zircons from the medium-grained biotite granite yield an upper intercept age of  $706 \pm 4$  Ma, indicating that most of the PWCP was emplaced near the end of the first period of regional anorogenic magmatism. A <sup>207</sup>Pb/<sup>206</sup>Pb age of 972 Ma from a single xenocrystic zircon preserves isotopic evidence of an inherited component of possible Middle Proterozoic, post-Grenville age. Emplacement of anorogenic plutons in this region has been linked only indirectly to rift-related faulting. However, detailed structural studies by other workers have demonstrated that the PWCP was intruded syn-tectonically as a series of sheeted dikes into actively extending country rock. For this reason, the age of the PWCP has important implications for the timing of extensional tectonics in the region. The PWCP was one of the last plutons to be emplaced during the earlier period of Laurentian crustal extension and overlaps in age with an interval of peralkaline plutonism in the nearby anorogenic Robertson River batholith. Marked differences in related trace element ratios suggest that the metaluminous PWCP and coeval peralkaline magmas of the Robertson River may have been derived from different sources.

### **Melting and Generation of Leucogranites Associated with the Emplacement of Ronda Peridotites**

Acosta, Antonio and Menéndez, Luis G.

*Department of Mineralogy and Petrology,  
Campus Fuentenueva, University of Granada,  
18002 Granada, Spain*

The Ronda peridotite is a tectonic slab emplaced during the Alpine orogeny within high-grade crustal metamorphic rocks. The peridotite body has sheet-like geometry with a maximum thickness of about 4.5 km. It overlies a tectonically inverted metasedimentary sequence, composed from top to bottom of a low-*P* peraluminous migmatites of probable Hercynian age and Permo-Triassic sequences (marble and micaschist) that include meta-evaporites. The peridotite is crowded with subvertical leucogranite dikes

(thickness ~10 cm - 10 m) with predominant NW-SE direction. In the lower zone of the peridotite body, dikes consist of an agmatitic breccia formed by metapelitic enclaves of uniform size (c. 2-3 cm) within a leucogranitic groundmass. Within the same dike, the relative proportions of enclaves and groundmass are highly variable. In the uppermost zone of the peridotite body the dikes have no metapelitic enclaves, have complex geometrical relations between medium-grained granites, fine-grained granites, aplites, and pegmatites, and some of them are internally differentiated. Mirolitic cavities are abundant. Luxillianitic textures sometimes occur. In some cases, the material of border zones and apophyses of dikes is a leucodiorite with a color index lower than 1. Available Rb/Sr data gave an age of  $22 \pm 4$  Ma with  $(^{87}\text{Sr}/^{86}\text{Sr})_i = 0.7219$ . The Ronda leucogranites are formed of quartz, microcline, and albitic plagioclase as essential minerals, with tourmaline, minor cordierite, muscovite and rare biotite as varietal minerals. The accessory mineral assemblage is composed of apatite, zircon, monazite, xenotime, ilmenite, titanite, uraninite, brannerite, uranospherite, Th-orthosilicate (huttonite?), columbotantalite, rutile, pyrite, arsenopyrite, galena, barite, and occasional native gold. The chemical composition of the Ronda leucogranites is very unusual. Boron contents are in the range 500 - 1250 ppm. The aluminium saturation index,  $\text{ASI} = \text{mol Al}_2\text{O}_3/(\text{CaO} + \text{Na}_2\text{O} + \text{K}_2\text{O})$ , ranges from 1.40 to 0.92, with an average of 1.06. ASI values show an excellent negative correlation with  $\text{SiO}_2$ ,  $\text{TiO}_2$ , and  $\text{FeO}^T$ , such that most leucocratic dikes are metaluminous.  $\text{Fe}/(\text{Fe}+\text{Mg})$  ratios are uncommonly low for granites, ranging from 0.75 to 0.22, with an average of 0.48.  $\text{Na}_2\text{O}$  and  $\text{K}_2\text{O}$  show a clear antipathetic relation. K-rich facies are less silicic, more aluminous, richer in Th, with higher  $\text{Fe}/(\text{Fe}+\text{Mg})$ , lower K/Rb ratios and negative Eu anomalies, and may contain native gold. In contrast, Na-rich facies are more silicic, less aluminous, richer in U, with positive Eu anomalies, "gabbroic"  $\text{Fe}/(\text{Fe}+\text{Mg})$  ratios, and abnormally high K/Rb values (~500 - 1300). Remarkably,  $\text{Na}_2\text{O}$  and K/Rb have an excellent positive correlation ( $R \sim 0.85$ ). Leucodiorites share many features of Na-rich facies with  $\text{Fe}/(\text{Fe}+\text{Mg}) < 0.1$ ,  $\text{K}/\text{Rb} > 800$  and high Ni, and occasionally, high Cr contents. The Ronda leucogranites were generated by partial melting of underlying migmatites due to the emplacement of the peridotite. Heat for melting was mostly provided by frictional heating along the thrust plane. This plane also acted as a trap for a B-rich volatile phase released from Permo-Triassic sequences, so easing the partial melting of the tectonic melange and producing

a low-viscosity melt. Pods of this partially molten material were emplaced as dikes along fractures in the peridotite body and formed agmatitic dikes. The low viscosity of B-rich leucogranite melt as well as sustained high temperature (the temperature of peridotite was higher than 600°C during dike emplacement) favored restite unmixing, differentiation, and some contamination of leucogranitic melt with material from peridotite. Restite-rich high melt-fraction leucogranites are K-rich, whereas restite-poor, low melt-fraction leucogranites are Na-rich, formed by melting of quartz plus feldspars in a volatile-rich environment, with no participation of biotite or other Fe-Mg minerals. This explains why they have such high K/Rb ratios and positive Eu anomalies. Due to the very low Fe and Mg contents of these melts, just a little contamination from peridotitic material produced their abnormally low  $\text{Fe}/(\text{Fe}+\text{Mg})$  ratios. Geological position of leucodiorites and the fact that they have simultaneous leucogranitic and peridotitic geochemical features support the idea that the leucodiorites are the result of an interaction between leucogranitic magma and ultramafic wall rock.

**Migmatite Sheaths as Indicators  
of the Emplacement Mechanisms  
of Granitic Plutons:  
A Case Study from the Al-Amar Suture,  
Eastern Arabian Shield,  
Kingdom of Saudi Arabia**

Al-Saleh, Ahmad

*Geology Department, King Saud University,  
Riyadh, Saudi Arabia*

The Al-Amar Suture is made up essentially of a thick and monotonous sequence of sericite-chlorite schists known as the Abt schist. This unit was derived from graywackes that were deposited in a short-lived (15 Ma) back-arc basin which separated the Afif microcontinent in the west from the Ar Rayn island arc in the east, and was closed at around 680 Ma. The Abt Schist is intruded by granitic bodies of various sizes, the majority of which are thought to have been produced by the partial melting of the Abt graywackes during a period of crustal thickening that followed basin closure. Radiometric dating of these granites, however, has revealed that most of them post-

date basin inversion by 60-80 Ma. The thermal anomaly that existed beneath the back-arc basin largely would have decayed during that time, and it is, therefore, obvious that a later phase of tectonic rejuvenation was responsible for the widespread granitic magmatism within the Al-Amar Suture.

Using the  $^{40}\text{Ar}/^{39}\text{Ar}$  step-heating technique it was possible to recognize the effects of two episodes of tectonism. A first period coincided with the juxtaposition of the Ar Rayn island arc against the Afif block (c. 680 Ma). A second phase took place in the period 610-600 Ma, and is thought to be the outcome of the collision between the eastern part of the Arabian Shield and a large continental mass now concealed beneath the sedimentary cover of the Arabian Platform. This final collisional orogeny was contemporaneous with the development of the strike-slip Najd Fault System and its associated syntectonic plutonism. It is widely believed that this zone of transcurrent displacement was induced by oblique collision with a large continental mass near the end of the cratonization process of the Arabian Shield.

Many of the Al-Amar Suture granites, especially near its southern end, are surrounded by sheaths of high-grade migmatites, and lie mainly near or within large-scale transpressive shear zones belonging to the Najd system. It is believed that these metamorphites represent thermal envelopes that have risen with the granites as ductile sheaths from lower crustal levels to their present positions. Evidence for the rapid (diapiric) emplacement of the granites come from the coincidence of biotite and hornblende  $^{40}\text{Ar}/^{39}\text{Ar}$  ages obtained from their associated migmatites. P-T estimates from the same rocks (using the GRIPS, biotite - garnet, amphibole - plagioclase and THERMOCALC techniques) indicate near isothermal decompression, a feature that is also consistent with the rapid ascent of a hot ballooning granite. The compressive stresses that accompanied transcurrent displacement along the Najd Fault System have produced similar and well-documented granitic diapirs in other parts of the shield that are coeval with those of the Al-Amar Suture.

## ORAL PRESENTATION

### Status of Thermobarometry in Granitic Batholiths

Anderson, J. Lawford

*Department of Earth Sciences,  
University of Southern California,  
Los Angeles, CA 90089-0740, USA*

Knowledge of the intensive parameters that characterize formation and emplacement of granitic rocks lags behind that of metamorphic systems. In many cases this is due to the presence of high-variance phase assemblages, resetting during slow cooling, or the lack of well characterized, experimentally calibrated reactions. Yet portions of most granitic batholiths contain low-variance plutons that are amenable to detailed quantification of  $P - T - f_{\text{O}_2} - f_{\text{H}_2\text{O}}$  conditions acquired during ascent and emplacement. Several igneous mineral phases resist subsolidus exchange and critical magmatic compositions can be retrieved through careful analysis. Detailed quantification of intensive parameters, however, is often not rigorously attempted and/or it is assumed that granitic magmas crystallize on or near a wet solidus.

*Thermometry.* Based either on cation exchange or solvus relations, there are several thermometers applicable to granitic rocks. Many granites contain two ternary feldspars and/or two Fe-Ti oxides, but both systems are known to undergo subsolidus re-equilibration. Other more robust thermometers, such as hornblende - plagioclase, hornblende - clinopyroxene, pyroxene - ilmenite, pyroxene - biotite, garnet - hornblende, garnet - clinopyroxene, and garnet - biotite, are applicable. Some are well calibrated, others less so. A major challenge resides in the large range of liquidus to solidus crystallization temperature incompletely preserved in mineral profiles coupled with the significant addition of components that affect  $K_D$  relations between non-ideal solutions. Liquidus temperatures, based on the solubility of early crystallizing apatite or zircon, are often in excess of 900°C, whereas estimation of solidus and near solidus conditions often yield results  $> 740^\circ\text{C}$ , far above that expected on experimental grounds for crystallization in the presence of a  $\text{H}_2\text{O}$ -saturated fluid.

*Fugacity of Volatile Components.* Volatile composition and the degree of fluid saturation dramatically affect solidus temperature and the stability of solid phases that incorporate volatile components. The observation from thermometry that many granitic plutons crystallize at

temperatures in excess of a water-saturated solidus argues for fluid undersaturation and/or dilution of H<sub>2</sub>O with CO<sub>2</sub> or other volatiles. In contrast, fluid-saturated granitic melts containing substantial F or B can be expected to have solidus temperatures < 600°C. Hence, well grounded knowledge of crystallization temperature occupies a fundamental role in estimation of volatile contents of magmas. Equilibria including sillimanite (or andalusite) - biotite - garnet - alkali feldspar, hypersthene - biotite - alkali feldspar - quartz and biotite - alkali feldspar - magnetite allow estimation of  $f_{H_2O}$ . Estimates by the latter assemblage, however, are highly dependent on  $f_{O_2}$ .

Oxygen fugacity varies widely and can have a great affect on mafic phase composition. Granitic magmas are known to have  $f_{O_2}$  ranging from two or more log units below the QFM buffer to a few log units below the HM buffer, a range that spans more than five orders of magnitude. Ilmenite - magnetite, quartz - ulvöspinel - ilmenite - fayalite (QUILF), biotite - alkali feldspar - magnetite, biotite - almandine - muscovite - magnetite (BAMM), and titanite - magnetite - quartz (TMQ) are well characterized equilibria that provide a basis for calculation of  $f_{O_2}$ .

**Pressure.** Granite barometry plays a critical role in constraining tectonic history. Barometric estimates for multiply intruded crustal sections has allowed successful tracking of the tectonic ascent of metamorphic core complexes and the deep residence periods of several allochthonous terranes. Thus, plutons can serve as "tectonic nails" in constraining *P-T-t* paths.

Peraluminous granites often contain mineral assemblages that enable pressure determinations, including garnet - aluminosilicate - silica - plagioclase (GASP), garnet - biotite - muscovite - plagioclase (GBMP), and muscovite - biotite - alkali feldspar - quartz (MBAQ). Metaluminous granites likewise offer a range of barometers. Most well calibrated are barometers based on the assemblages garnet - hornblende - plagioclase - quartz (GHBQ) and garnet - ferrosilite - plagioclase - quartz (GFPQ). The Al-in-hornblende (AH) barometer remains at a developmental stage but potentially could serve as the basis for the most widely applied barometer for granitic batholiths. Recent work has incorporated the effects of temperature, but the complete reaction remains uncalibrated. Limiting pressures can be obtained from the presence of magmatic epidote and for low-Ca pegmatites or aplites, the presence of subsolvus versus hypersolvus alkali feldspars.

As with all barometers, the influence of temperature,  $f_{O_2}$ , and choice of activity model are critical factors. Moreover, the nature and quality of calibration is variable.

Foremost is the fact that batholiths are not static features. Mineral compositions imperfectly record conditions acquired during ascent and over a range of temperature and great care must be taken in properly quantifying intensive parameters.

### **An Experimental Method for Determining Compositions of Aqueous Fluids Coexisting with Silicate Melts**

Anovitz, Lawrence M., Blencoe, James G.,  
Horita, Juske and Cole, David R.  
*Chemical and Analytical Sciences Division,  
Oak Ridge National Laboratory, P.O. Box 2008,  
Building 4500-S, Oak Ridge, TN 37831-6110, USA*

There have been numerous field, experimental and theoretical studies of the genesis and evolution of granitic systems. However, the chemistry of aqueous fluids in equilibrium with granitic melts is poorly known. Such data would be of extreme utility, as an understanding of the solubility of components of both molten and subsolidus igneous rocks in aqueous fluids is critical to understanding and modeling the chemistry of geothermal and other magma-hydrothermal systems.

A number of factors have limited the ability of previous researchers to determine the composition of aqueous fluids coexisting with haplogranitic melts. The most important is that the high *P-T* composition of a silica-saturated aqueous fluid is not retained on quenching. Silicate materials precipitate out of the fluid as films and "quench roe" (amorphous silica-rich spheres). This prevents direct analysis of the fluid extant at high *P-T*. The tendency of the silicate to precipitate on the glass further complicates the analysis.

We have developed a method that overcomes many of these difficulties, and we are currently investigating the compositions of aqueous fluids in the haplogranite system. These experiments will determine the Na, K, Si, and Al composition, as well as  $\delta D$  and  $\delta^{18}O$ , of a vapor coexisting with haplogranitic melt. Hydrous haplogranitic glasses of known chemical and isotopic composition are synthesized to serve as starting materials for the experiments. Nine such compositions have been prepared, five in the haplogranite system, three on the bounding binaries (2.5 kbar minimum melt compositions), and albite. In each

case, water-oversaturated and undersaturated glasses are prepared to allow reversal of the equilibrium water content of the melt.

Several experimental capsule configurations have been evaluated. The successful design satisfied three criteria. The melt had to be confined within a section of the capsule to permit its separation from the precipitate after the run. It was also necessary, however, that it remain in contact with the aqueous fluid during the experiment. In addition, the volume of fluid in contact with the melt at any time had to be minimized to limit the amount of precipitate on the glass after the quench. Such precipitate is inseparable from the melt and would therefore reduce the calculated solubility. This had to be done, however, without reducing the area of fluid/melt contact to the extent that the time to equilibrium would extend inordinately. Finally, both the composition and amount of precipitate had to be analyzable.

Our approach is to load two inner 3 mm x 1 cm capsules into a 5 mm x 3.75 cm outer capsule. The lower end of each inner capsule is welded shut. The capsule is then partially filled with glass and its top plugged with a ball of Pt mesh. Both inner capsules and a water of known  $\delta D$  and  $\delta^{18}O$  different from the glass are then sealed in the outer capsule, and the capsule is run vertically to prevent the melt from flowing out of the inner capsules. Two capsule assemblies with different waters are run to reverse the isotopic fractionation. The Pt mesh permits contact between the melt and fluid while minimizing the amount of fluid actually present at the interface during the quench.

The first step in analyzing the run products is to remove the water, leaving the precipitate and any remaining solute behind. The capsule is frozen in liquid nitrogen, punctured under vacuum and then allowed to warm slowly, which prevents escape of precipitate from the capsule. The water is vacuum distilled into a break-seal tube for isotopic analysis. Next, the capsule is opened and the inner capsules removed for analysis of water content, chemical, and isotopic composition. The precipitate-encrusted outer capsule is then placed in a Pt crucible, to which a known amount of Mg and Ca are added. This is then fused in a Li-borate flux, which is re-dissolved in nitric acid for ICPS analysis. This procedure yields the composition of the precipitate. The original amount of precipitate is then determined by ratioing the analyses to the original weight of Mg and/or Ca.

Experiments have been performed at 2.5 kbar and 950°C, for periods of time ranging from 1 to 11 days, to

constrain the reaction kinetics and determine the time required to achieve equilibrium. Additional experiments will reverse the equilibrium water contents of the melts. These results will constrain the equilibrium and kinetics of major element and isotopic exchange between melts and aqueous fluids.

Research sponsored by the Geothermal Technology Program of the Office of Energy Efficiency and Renewable Energy, U.S. Department of Energy, under contract number DE-AC05-84OR21400 with Martin Marietta Energy Systems, Inc.

### Compositional Variations in Granitic Rocks of the Northern Appalachians, USA

<sup>1</sup>Ayuso, R. A. and <sup>2</sup>Arth, J. G.

<sup>1</sup>U.S. Geological Survey, MS 954,  
Reston, VA 22092, USA

<sup>2</sup>U.S. Geological Survey, MS 937,  
Menlo Park, CA 94025, USA

Silurian and Devonian granitic plutons of the Northern Appalachians in the U.S.A. were used to assess the contributions of juvenile magmas and the extent of crustal recycling during terrane accretion. Petrologic, chemical, and isotopic-tracer studies were done on a total of 32 plutons from the Brompton-Cameron and Central Maine terranes in western New England (WNE), and from the Peri-Gondwanan Merrimack-Harpswell, and St. Croix terranes in eastern New England (ENE). Remarkable heterogeneity exists in field (*e.g.*, range of rock types, mode of emplacement, and types of enclaves) and petrographic features (*e.g.*, hornblende/biotite ratios, presence of aluminous minerals, fabrics, accessory minerals, and magnetite/ilmenite ratios) even in temporally and geographically related groups of granitic rocks within single terranes. No consistent trends in most petrographic features have been identified, although in ENE, composite igneous intrusions commonly contain significant volumes of quartz gabbro and diorite associated with leucogranite. Intrusive rocks in WNE, in contrast, consist predominantly of granodiorite and granite, although gabbro may be present.

Notable chemical differences exist between WNE (*e.g.*, Northeast Kingdom batholith, Vermont) and ENE (*e.g.*, Spruce Head pluton and the South Penobscot Intrusive Series in coastal Maine). For example, in WNE the

granitic rocks are largely calc-alkaline and at a given SiO<sub>2</sub> content have lower A/CNK and K<sub>2</sub>O/Na<sub>2</sub>O values, as well as lower contents of alkalis, Rb, and HFS elements than granitic rocks in ENE (see Table for ranges of selected trace element contents). Higher Sr and Ba contents are also found in granitic rocks of WNE. Granitic rocks of the St. Croix terrane (coastal Maine) in ENE, are more alkaline in character. An additional distinction is that plutons from WNE have associated porphyry Cu-Mo deposits whereas in ENE the plutons contain occurrences of Sn and W skarns.

The table shows the range of selected trace elements and calculated isotopic values at 400 Ma for granitic rocks from ENE and WNE. The granitic rocks show the same range of initial Nd isotopic ratios regardless of their position relative to the North American craton or within the accreted terranes. Thus, underlying basement to the terranes cannot be differentiated on the basis of the initial Nd isotopic values of the plutons. This is in contrast to Pb isotopic values which distinguish between the relatively unradiogenic granites from WNE (Brompton-Cameron terrane) and the generally more radiogenic granites from ENE (St. Croix terrane).

Table

(trace elements in ppm; initial isotopic ratios at 400 Ma)

	WNE	ENE
Rb	70-300	50-400
Sr	200-800	50-350
Ta	0.4-1.1	0.2-2.1
<sup>143</sup> Nd/ <sup>144</sup> Nd	0.51177-0.51215	0.51181-0.51221
<sup>207</sup> Pb/ <sup>204</sup> Pb	15.53-15.61	15.59-15.75
( <sup>87</sup> Sr/ <sup>86</sup> Sr) <sub>i</sub>	0.7041-0.7125	0.7045-0.7150
δ <sup>18</sup> O	+6 to +12‰	+9 to +11‰

Isotopic and chemical variations in the granitic rocks indicate significant diversity in the contribution of crustal and mantle rocks in all the terranes. Nd and Sr initial ratios of Grenville basement rocks during the Paleozoic overlap the range in isotopic values in granitic rocks from both WNE and ENE. More importantly, source regions of the mafic plutons have chemical features that resemble those of magmatic compositions in island arcs. The largest volume of granitic magma in the terranes is represented by quartz monzodiorite, granodiorite, and granite; the smallest volume of magma is represented by two-mica granites, and they indicate a source region

dominated by metasediments (upper crustal) as suggested by the high initial Sr and δ<sup>18</sup>O values.

Terrane amalgamation during the Paleozoic was associated with granitic magma generation which involved a substantial amount of recycling of older crust. The most inboard terranes (Brompton-Cameron) contain granitic rocks that were generated from remobilization of Grenville-like basement; those from the most outboard terranes (St. Croix) were produced from non-Grenvillian (Avalon-like) basement. Source region characteristics in intermediate terranes (Central Maine, Merrimack-Harpswell) are non-unique and cannot be distinguished from the other basement types - the granitic rocks may reflect mixtures of Grenville- and Avalon-like sources.

## ORAL PRESENTATION

### Crystallization of Pinatubo Magma

Baker, Leslie and Rutherford, Malcolm J.

*Department of Geological Sciences,  
Brown University, Providence, RI 02912, USA*

The dacite magma erupted by Mount Pinatubo in June of 1991 was unusual for several reasons. At a temperature of 780°C, it was sulfur-rich enough to contain almost 1 vol % phenocrystic anhydrite, and it had a very high oxidation state (3 log units above NNO). It was extremely water-rich (6.4 wt %) and probably volatile-saturated, but almost too crystalline (up to 50 vol %) to erupt. The conditions in the pre-eruptive magma as deduced from existing phase equilibria have been corroborated by experiments which show these exact conditions are required to crystallize cummingtonite, a prominent overgrowth on hornblende in the Pinatubo magma. Unanswered questions still remain regarding the origin of the sulfur-rich and highly oxidized character of the magma and the amount of excess volatiles present prior to eruption. Experiments in the H-O-S system to determine the composition of the pre-eruptive volatile phase have shown that it contains approximately 1 mol % SO<sub>2</sub> at 800°C and 2 kbar.

The highly crystalline Pinatubo dacite was essentially forced to erupt by the intrusion of basalt into its magma chamber. Had this not taken place, the dacite would presumably have continued to cool and solidify into a pluton. An interesting set of unanswered questions concerns the solid-liquid-vapor reactions that would take

place as the magma crystallized. In fact, the dacite may at one time have been more crystalline, as suggested by partially resorbed quartz and biotite phenocrysts, and by plagioclase phenocrysts whose cores are more albitic than their rims. Probable reactions in the cooling magma include production of orthoclase and the regrowth of biotite and quartz.

A question of particular interest concerns the fate of the anhydrite phenocrysts. While anhydrite was a stable phase in the pre-eruptive magma, it has not to our knowledge been reported in plutonic equivalents of this dacite. While it is possible that anhydrite is dissolved into the H<sub>2</sub>O-rich vapor exsolved from the magma during crystallization, limited data on the temperature dependence of the vapor composition coexisting with anhydrite suggest that the efficiency of this process will drop as the magma cools. It may be that a minor and unexpected anhydrite component has been overlooked in some arc plutons.

We are conducting experiments to determine the crystallization path of the Pinatubo dacite. The experiments place particular emphasis on the fate of anhydrite phenocrysts, in order to determine whether they might be preserved to some extent in plutonic rocks. If ancient anhydrite-bearing magmatic systems can be identified in the rock record, then this will yield more insight into the frequency and evolution of sulfur-rich eruptions than can be obtained from studying only modern, active volcanoes.

### **The Enclave Swarms in Some Granitoids of the Sierra Nevada Batholith, California: Indicators of Magma Interactions and Evolution**

Barbarin, Bernard

*Université de Paris-Sud et URA 1369 CNRS,  
Laboratoire de Pétrographie-Volcanologie,  
Bâtiment 504, F-91405 Orsay Cedex, France*

Enclave swarms are abundant in the granitoids of the Sierra Nevada batholith. In these swarms are associated enclaves of various natures, shapes and sizes. Three groups of swarms can be distinguished.

Enclave swarms of the first group consist of many different types of mafic microgranular enclaves (MME) and of granitoid or hornfels xenoliths, generally enclosed in a coarse-grained and mafic-mineral-rich matrix. Lo-

cally, two MME can touch without any deformation of their globular shapes. Contacts between the matrix of these "polygenic" swarms and the host granitoids are either sharp or progressive. These swarms are generally located in the margins of the normally-zoned plutons where they are frequently associated with magmatic layering.

Enclaves swarms of the second group consist of a single type of fine-grained, isogranular MME, enclosed in a fine-grained relatively felsic matrix. The MME are also globular but they can deform each other when they are touching. Contacts between these "monogenic" swarms and the host granitoids are invariably sharp. These swarms occur locally in the areas where plutons are crosscut by swarms of mafic or composite dikes.

Enclaves swarms of the third group also consist of a single type of fine-grained, isogranular MME, enclosed in a granitic matrix. The MME generally present lobate contacts, frequently underlined by extremely fine-grained margins. Their shape can pass in a very narrow distance from globular to angular. In these swarms, MME frequently display planar contacts on one side and lobate contacts on the other. These swarms, roughly described as "magmatic breccias", surround the large (hectometric to kilometric) dioritic or gabbroic bodies isolated in the granitoid plutons.

The two last groups of enclave swarms differ from the first one because they result from *in situ* mingling and hybridization between mafic magma and felsic magma at the emplacement level. The MME are of a single type because they are all formed at the same time and in a relatively defined mixing system. In the largely crystallized granitic plutons, lately injected mafic magmas can only mix with the residual granitic magmas channelled in the early fractures to form composite dikes. The "monogenic" enclave swarms are obtained after disruption of the earliest composite dikes in granitic magmas which could be affected by some late magmatic displacements. "Magmatic breccias" result from disruption at emplacement level of the margins of large mafic bodies. Depending on the importance of the rheology contrasts between the mafic and felsic magmas, the mafic blobs can either occur as globular enclaves, frequently with lobated limits, or be broken into angular fragments.

Genesis of the "polygenic" enclave swarms is more complex. They represent aggregations and accumulation, on the rheologic interface between the magma and the relatively viscous margins of the plutons, of the many relatively solid elements present in the magma (*i.e.* phenocrysts of mafic and accessory minerals, K-feldspar

phenocrysts where present, xenoliths, and MME). The various types of MME result from mingling and hybridization between contrasted mafic and felsic magmas, in many small and limited mixing systems, at depth in the magma chamber or in the feeding conduits during ascent.

Pipe-, funnel- or vortex-shapes displayed by the "polygenic" enclave swarms and some associated magmatic layerings also indicate that close to the contacts with the metamorphic screens, the margins of the magmatic body can be affected by magmatic movements that witness displacements of volatiles obtained through dehydration of the close metamorphic host rocks.

### **The Dynamics of Dehydration Melting and Implications for Melt Extraction in the Lower Crust Following Underplating: An Example from the Ivrea-Verbanò Zone, Northern Italy**

Barboza, Scott A.  
and Bergantz, George W.

*Department of Geological Sciences, AJ-20,  
University of Washington, Seattle, WA 98195, USA*

We have developed a thermo-mechanical model for the generation and flow of melts during the dehydration melting of pelitic rocks. Melt movement is modeled as a fully coupled two regime system of percolative flow through a variable permeability mush and convective flow in regions where the volume melt fraction (MF) exceeds some critical melt fraction (CMF) for viscous flow. The model also includes latent heat effects, temperature-composition-MF dependent viscosity, and both thermal and compositional buoyancy. The effects of compaction are not considered. The model phase relations include two solid solution loops and two invariant points. As our model composition, we chose the pelite of Vielzeuf and Holloway (1988) which, during melting, exhibits large jumps in MF at the reaction temperatures of the hydrous phases (muscovite, biotite). The major element composition of this pelite closely corresponds to the average composition of the roof rocks in the Ivrea-Verbanò Zone (IVZ).

For a constant temperature boundary condition, the amount of melt generated was found to be a maximum when the contact between the country rock and the intru-

sion was horizontal. Increasing contact dip angles decreased the total amount of melt that was generated, particularly shortly after emplacement. The total amount of melt generated by different contact angles tended to converge after more time had passed. For calculations in which convection initiated, convective velocities in the region of viscous flow were found to be small ( $1 \times 10^{-3}$  m  $\text{yr}^{-1}$ ), but high enough to exceed a Peclet number of one. Convection strongly affected the position of the biotite isograd relative to that predicted by conduction (500 m versus 250 m after 12,700 years), but the position of the muscovite isograd remained relatively unaffected. With a constant temperature boundary condition, the model over predicts the location of the muscovite-out isograd at the IVZ. This indicates that there was probably not a continuous supply of magma to the Mafic Complex but rather a periodic supply punctuated by long intervals of stagnation.

In the region of porous flow, the relative potential for a melt to be extracted under a given pressure field can be estimated by the permeability of the porous medium divided by the viscosity of the melt ( $K/\mu$ ). A region of higher  $K/\mu$  is found to occur at low melt fractions (between 5 and 15%) due to the high water content (near 10 wt %) of these liquids. With respect to the extractability of these melts, the drop in viscosity far outweighs the effect of the low permeability. A peak in the magnitude of the velocities was observed to correspond with the region of high  $K/\mu$ . The compositions of the melts in this region were that of a high silica (74-77%), peraluminous rhyolitic liquid. Interestingly, with few exceptions, the predicted major element composition of the liquids in the high  $K/\mu$  region corresponds reasonably well to average compositions of some of the late-Hercynian granites in regions near the IVZ.

Bulk convection of the molten country rock did not occur until well above the CMF. Peclet numbers near one exist only when the MF in the pelite exceeds 0.6 for models in which the CMF was 0.5. This required a floor temperature of over 1000°C. Convection is suppressed until higher MF because the large amount of solids in the melt increases the effective viscosity enough to inhibit convection. Bulk convection of melt in the country rock therefore does not occur unless the initial temperature of the country rock is high or the intruding magma is unusually hot. Thermobarometry in the IVZ has shown that peak contact temperatures were never sufficient to create the high MF required for viscous flow.

We found that buoyancy forces alone were not sufficient to drive crystal liquid segregation within the chosen model

parameters. The pressure field generated by buoyant convection was not sufficient to drive enough melt by porous flow to effect the bulk composition over geologically reasonable times. Maximum melt velocities observed in the region of porous flow were found to be on the order of  $1 \times 10^{-10} \text{ m yr}^{-1}$ . We submit that some other mechanism such as hydrofracturing, shear, or diking must occur to achieve significant crystal-liquid segregation. We also suggest that the melts most likely to be extracted from the source region are the high water content melts that exist at low melt fractions.

Vielzeuf, D. and Holloway, J.R., 1988. Experimental determination of the fluid-absent melting relations in the pelitic system. *Contrib. Mineral. Petrol.*, **98**, 257-276.

## Grenville-Age A-Type Granitic Rocks in Texas

<sup>1</sup>Barnes, C.G., <sup>1</sup>Shannon, W.M.,

<sup>2</sup>Smith, D.R. and <sup>3</sup>James, E.

<sup>1</sup>Department of Geosciences, Texas Tech University,  
Lubbock, TX 79409, USA

<sup>2</sup>Department of Geosciences, Trinity University,  
San Antonio, TX 78212, USA

<sup>3</sup>Department of Geological Sciences,  
University of Texas, Austin, TX 78712, USA

The Red Bluff granitic suite (RBGS) in the Franklin Mountains of west Texas was emplaced inboard of the Grenville suture into a Middle Proterozoic shelf sequence at  $\sim 1.135$  Ga. It lies  $\sim 290$  km west of a subsurface occurrence of a 1.15 Ga layered intrusion interpreted as an extension of the Mid-Continent Rift (Adams and Keller, 1994). Early workers proposed a subduction-related origin for the RBGS. However, recognition of widespread and coeval extension in the region provides an incentive to reevaluate the origin of the RBGS.

The order of intrusion of the RBGS was: granitic to quartz syenitic sills, alkali feldspar granite, alkali feldspar syenite, leucogranitic dikes, and pegmatitic peralkaline arfvedsonite granite. Late-stage, transitional ferrobasaltic dikes are also present. Compositional variation is continuous from quartz syenite to leucogranite. Ferromagnesian silicates are ferrohedenbergite, ferroedenite, annite and relict fayalite, with accessory ilmenite and magnetite. Estimated  $f_{\text{O}_2}$  was near FMQ for the entire suite. Initial

emplacement temperature was near  $1050^\circ\text{C}$  for the syenites;  $T$  decreased to  $\sim 725^\circ\text{C}$  among late-stage leucogranites. Initial  $\text{H}_2\text{O}$  content was  $\sim 0.3$  wt % and  $f_{\text{HF}}/f_{\text{H}_2\text{O}}$  was  $\sim 10^{-2.5}$ , consistent with the presence of magmatic fluorite. The suite is predominantly meta-luminous and is characterized by high concentrations of HFSE and REE typical of A-type, "within-plate" granites.

$\epsilon_{\text{Nd}}(1.13 \text{ Ga})$  values average  $\sim +3.0$ ; measured Pb isotope ratios show the following ranges:  $^{206}\text{Pb}/^{204}\text{Pb}$  from 16.76 to 17.43,  $^{207}\text{Pb}/^{204}\text{Pb}$  from 15.36 to 15.44, and  $^{208}\text{Pb}/^{204}\text{Pb}$  from 36.40 to 37.11. Although hydrothermally "disturbed",  $(^{87}\text{Sr}/^{86}\text{Sr})_i$  can be shown to be low ( $\sim 0.7034$ ).  $\delta^{18}\text{O}$  of quartz separates ranges from  $+7.7$  to  $+8.9\text{‰}$ .

The isotope values are consistent with an origin either by fractional crystallization of a mantle-derived OIB-like basaltic parent or by partial melting of young lower crustal rocks. However, partial melting models that use basement rocks as parental compositions fail to reproduce the observed trace element patterns. Models that assume other crustal compositions can produce good fits to the trace element patterns, but fail to explain the continuous compositional variation of the suite. In contrast, trace element data are consistent with mass balance fractionation models if the assumption is made that crystal separation was inefficient (*i.e.*, *in situ* crystallization). Assimilation of  $< 10\%$  crustal material can account for the slightly elevated  $\delta^{18}\text{O}$  values.

Petrologic and geochemical characteristics of the RBGS are virtually identical to those of the  $\sim 1.08$  Ga Pikes Peak batholith (PPB) of central Colorado. Late stage, alkaline intrusions emplaced within the PPB include a sodic and a potassic series. The PPB sodic series and the RBGS share characteristics typical of A-type, "within-plate" granites. They are suites of cogenetic syenites, quartz syenites, and granites with iron- and alkali-rich silicates, mineral assemblages consistent with water-poor magmas, high  $\text{FeO}^T/\text{MgO}$ , and high abundances of  $\text{Na}_2\text{O} + \text{K}_2\text{O}$ , HFSE and REE. Both suites are associated with coeval mafic rocks and are interpreted to arise by fractional crystallization ( $\pm$  crustal assimilation) of basaltic magmas derived from OIB-like mantle sources.

Earlier workers correlated the RBGS with 1.07-1.13 Ga high-K granites in the Llano uplift to the east, but recent work has shown the Llano granites to be geochemically distinct with generally higher  $\text{P}_2\text{O}_5$  and Sr, lower  $\text{Na}_2\text{O}$ ,  $\text{FeO}^T/\text{MgO}$ , Zr, Y, and REE, and much lower Ta and Nb compared to the RBGS and PPB sodic suites. Geochemical characteristics of Llano granites are consistent with an

origin involving partial melting of slightly older subduction-related tonalitic crust, but a mantle component cannot be ruled out, as suggested by Nd data (Patchett and Ruiz, 1989) and the presence of microgranular magmatic enclaves.

Derivation of the RBGS and PPB sodic series from basaltic parental magmas indicates that they represent additions of juvenile material to continental crust during Grenville time. The RBGS and PPB apparently developed in a broad regional zone of mild extension; both lay to the west (modern coordinates) of continental rift zones. In contrast, the Llano granites were late-stage intrusions associated with the Grenville orogenic belt.

Adams, D.C. and Keller, G.R., 1994. Possible extension of the Midcontinent Rift in west Texas and eastern New Mexico. *Can. J. Earth Sci.*, **31**, 709-720.

Patchett, P.J. and Ruiz, J., 1989. Nd isotopes and the origin of Grenville-age rocks in Texas: Implications for Proterozoic evolution of the United States, Mid-continental region. *J. Geol.*, **97**, 685-695.

**Petrochemistry and Origin of  
Silurian - Devonian Plutons in  
the "Central Mobile Belt" of  
Cape Breton Island, Nova Scotia, Canada,  
in Comparison with  
Newfoundland and New Brunswick**

Barr, Sandra M. and O'Neill, Michael

*Department of Geology,  
Acadia University, Wolfville,  
Nova Scotia, BOP 1X0, Canada*

Cape Breton Island is interpreted to preserve a condensed cross-section of the northern Appalachian orogen, analogous to the Humber - Avalon section preserved in Newfoundland. The Aspy terrane in central Cape Breton Island occurs between Laurentian Grenvillian basement (Humber Zone) to the north and Late Proterozoic former peri-Gondwanan terranes (Bras d'Or and Mira) to the south. It consists of Ordovician to Devonian rocks comparable to those in the eastern and southern parts of the Central Mobile Belt of Newfoundland and New Brunswick. As in those other parts of the Central Mobile Belt, one of the unresolved questions about the Aspy terrane is the nature of the underlying crust. This question is closely related to the nature of the "Central Crustal

Block" identified on seismic reflection profiles - is it really a separate crustal entity or is it a variety of either Grenvillian or Avalonian crust, or a mixture of both?

Evidence about the nature of the crust underlying central Cape Breton Island is provided by granitoid plutons which form more than half of the present level of exposure of the Aspy terrane. They are mainly of granodioritic and granitic compositions and Silurian through Devonian ages, but vary widely in depth of emplacement and petrochemical character. Based on standard parameters, their tectonic settings ranged from subduction through collision to extension, but overall, their petrochemical characteristics and Pb, Nd, and O isotopic signatures are consistent with derivation from mid-Proterozoic and older continental crust. Comparison with plutons in the Humber Zone and Avalon terrane indicates that the Aspy terrane plutons were not derived from either a Grenvillian or Avalonian basement. Their source may have been a complex crustal package similar to that underlying the now-adjacent Bras d'Or terrane, a peri-Gondwanan terrane isotopically and tectonically distinct from Avalon terrane *sensu stricto*.

Recently published petrochemical and isotopic data from Silurian and Devonian plutons in the Central Mobile Belt of both Newfoundland and New Brunswick confirm earlier preliminary interpretations of the postulated similarity in pluton type and magmatic evolution between these areas and the Aspy terrane. However, early Silurian plutons in the Aspy terrane are mainly gneissic, and both Silurian and Devonian plutons are more deformed than their counterparts in Newfoundland and New Brunswick - this is attributed to the location of the area on a Laurentian promontory during terrane assembly. The Aspy terrane plutons are also petrochemically distinct from plutons in the Meguma terrane in southern Nova Scotia, although they overlap in age.

## ORAL PRESENTATION

## Phanerozoic Granitoids and Associated Mineral Deposits in Southwestern North America

Barton, Mark D.

*Department of Geosciences, University of Arizona,  
Tucson, AZ 85721, USA*

Southwestern North America (California - Colorado through Mexico) has a complex history of granitic magmatism from the early Proterozoic through the Cenozoic. A broad mix of hydrothermal systems and contact metamorphism formed with these granitoids during the late Phanerozoic (Mesozoic-Cenozoic convergent margin) portion of this record. Interpretation of these granitoids and their related rocks must be made through the tripartite filter of provincial, exposure level, and process controls.

Voluminous Cordilleran magmatism began with development of one or more Permo-Triassic arcs along the western margin of Pangaea, spanning both Laurentian and Gondwanan basement and their marginal sequences. Plutonism continued with few major interruptions through the Mesozoic and Tertiary, reaching maximum fluxes in the Middle Jurassic, Late Cretaceous, and Oligocene. Two types of suites are present: the first type is associated with relatively stable convergence in the late Mesozoic and early-middle Cenozoic, and the second type is associated with variably extensional tectonics in the middle-Mesozoic and middle-late Cenozoic. Diachronous plutonic suites, 20-50 Ma in duration, vary systematically from older mafic-intermediate to younger felsic compositional ranges along major portions of the late Mesozoic and early Tertiary Andean margin (California-NW Mexico Cretaceous, Great Basin Cretaceous, Arizona-New Mexico Laramide, Colorado-north-central Mexico Tertiary). Compositional suites vary from calc-alkaline in the western regions (dioritic to granodioritic, commonly strongly peraluminous) to moderately alkalic (monzonitic to alkali granitic) in eastern areas. In contrast, coeval multi-modal magmatism characterizes middle-Tertiary and portions of the middle-Mesozoic events, particularly in the Basin and Range province of the US through northern Mexico. Higher crustal levels are typically preserved with these multi-modal events, consistent with the extensional interpretation. Some of the overall variability is interpretable in

terms of contrasting lithosphere; for example, basement signatures are clearly transmitted in isotopic systematics. Nevertheless, many of the suites of intrusive centers are built upon common lithospheric columns indicating that variability reflects process control (thermal structure, mantle flux, stress regime) linked to tectonic drives. Simple thermal and mechanical models of limits on assimilation and magma uprise, when constrained by regional tectonics, are broadly consistent with the general petrogenetic patterns, predicting the observed time variations in composition. In turn, these compositional variations help govern the characteristics of igneous-related mineralization and metamorphism.

Igneous-driven processes including hydrothermal activity and contact metamorphism vary through time, reflecting exposure and province, as well as process controls. Major types of mineralization associated with upper crustal plutonic and hypabyssal suites of Phanerozoic granitoids include hydrothermal porphyry, skarn, epithermal, replacement, and syngenetic deposits of widely varying styles and metal contents. Orthomagmatic deposits are apparently absent. Late Mesozoic and early to middle-Cenozoic magmatic series show metallogenic progressions from oldest Cu (-Au-Fe) mineralization associated with intermediate composition intrusive centers through polymetallic suites (Zn-Pb-Ag-W-Cu-Au) associated with broadly granodioritic centers, and finally to lithophile-element-dominated suites (F-Mo-Be-W-Zn) associated with young granitic centers (alkalic to strongly peraluminous). Extensional magmatic series (Jurassic, middle-late Cenozoic) are metallogenically varied, with a predominant Cu-Fe-Au metal suite, but with common coeval base-metal (Pb-Zn-Ag) and lithophile-element (Mo-F-Be) suites in more felsic centers. The first-order filter on the modern distribution of mineralization and other features is level of exposure, a consequence of burial/erosional history. Simple isostatic-diffusional erosional models, again constrained by tectonic and geochemical evidence, help rationalize the temporal and spatial distributions of hydrothermal, metamorphic, and igneous features: at shallow levels (< 3 km, epithermal, syngenetic deposits; hydrothermal metamorphism, volcanic-dominated suites), at intermediate levels (2-8 km, porphyry, skarn; defined thermal aureoles; variably porphyritic intrusions), and at deeper levels (> 8-10 km; unmineralized; regionally extensive metamorphism; equigranular intrusions). Time-space distributions are consistent with erosional half-lives on the order of a few 10s of millions of years. Systematic regional variations in metal ratios suggest a basement

control in some regions (*e.g.* Arizona), but the overall variability within single provinces points to the importance of magmatic controls. The strong correlations between lithology and associated alteration and metal suites indicate that magmatic compositions provide the fundamental control on type of mineralization. Compositional patterns are broadly interpretable in terms of metal inventories, redox controls, and major element variations. Aluminosity (activity of alumina) and alkalinity (activity ratio of soda to lime) help quantitatively rationalize the variations in hydrothermal alteration with composition. Open questions include sources and controls on sulfur, redox, and halogens.

**Time-Space Evolution of a  
Two-Mica Granite:  
The Birch Creek Pluton,  
California, USA**

<sup>1</sup>Barton, Mark, <sup>1</sup>Ghidotti, Gregory,  
<sup>2</sup>Holden, Peter, <sup>3</sup>Goodwin, Laurel  
and <sup>3</sup>Heizler, Matt

<sup>1</sup>*Department of Geosciences, University of Arizona,  
Tucson, AZ 85721, USA*

<sup>2</sup>*Department of Earth and Space Sciences, UCLA,  
Los Angeles, CA 90024, USA*

<sup>3</sup>*Department of Geoscience, New Mexico Tech,  
Socorro, NM 87801, USA*

Detailed field, petrographic, and geochemical studies of the composite Birch Creek pluton and its aureole reveal complex concurrent development of the magma chamber, deformation, contact metamorphism, and hydrothermal activity. The strongly peraluminous Birch Creek granite intruded and deformed Late Proterozoic and Early Cambrian sedimentary rocks in the White Mountains of east-central California at ~82 Ma (Rb-Sr, Ar-Ar, K-Ar). It belongs to a large suite of Late Cretaceous strongly peraluminous granitoids in the hinterland of the Cordilleran batholithic belt which commonly have lithophile-element mineralization and strongly deformed margins.

The intrusion consists of equigranular to porphyritic biotite-muscovite granodiorite to monzogranite formed from two isotopically distinct but coeval felsic magmas and accompanied by minor (<1 ppm by volume) mafic magma. All three magmas were emplaced broadly

synchronously over at least three pulses. Episodic formation of aplite dike swarms and associated metasomatism provides time lines that allow evolution of the magma chamber to be tied to deformation and metasomatism in the periphery. Large subsolidus strains (>100%, mainly flattening?) accumulated during emplacement by high- and moderate-temperature ductile mechanisms in both the outer portions of the pluton and the inner portions of the contact aureole. These fabrics are crosscut by slightly younger undeformed phases of the intrusion, confirming early interpretations of dominantly synintrusive deformation (Nelson and Sylvester, 1971). Overall, intrusive mechanisms evolved from early diking with orientations controlled by regional stresses, through an intrusion-centered stress regime (radial dikes, concentric foliation), to a late set of regionally consistent dikes and brittle veins. Thermal constraints and Ar-Ar dates on igneous and metamorphic muscovites indicate that emplacement took <1 Ma, probably <100 ka.

Isotopic (Nd, Pb, Sr, O), whole rock (XRFS, INAA), and electron microprobe analyses combined with the field relationships indicate that crystal fractionation dominated chemical evolution on small scales (20-200 m, by sidewall crystallization and filter pressing), but that the intrusion underwent at most minor overall fractionation. Fluid evolution was nearly continuous as evidenced by the distribution of aplitic, pegmatitic and quartz-bearing dikes and veins, but it reached distinct maxima during major diking episodes. An antithetic spatial distribution of K-feldspar megacrysts and immediately surrounding dike/vein events suggests that fluid evolution operated on scales of 2-5 times that of major and trace element fractionation. Thermal metamorphism, deformation, and metasomatism in the metasedimentary rocks relate directly to particular emplacement and fluid release episodes. Ductile fabrics in the host carbonate and clastic rocks of the inner aureole (hornblende hornfels) occur as much as 1 km from the intrusion on its western side. These fabrics both overprint and are cut by fluorine-rich metasomatic features that formed from infiltration of magmatic fluids. Brittle deformation in the distal (lower greenschist) portions of the aureole may accommodate some of the space for the intrusion, and it hosts intrusion-related hydrothermal veins. The lack of economically significant mineralization in this system probably reflects a combination of the dilution effect of high water contents, the lack of effective internal fractionation, and the relatively deep level of exposure.

Overall, the Birch Creek system had a complex physical evolution and a modest chemical evolution that are best interpretable in terms of the progressive (though geologically rapid) emplacement of a viscous, water-rich magma. Recognition of internal structures allows documentation of the interplay between magmatic, deformational, and metasomatic processes. This pluton-wall rock system is representative of peraluminous granitoids in the Great Basin, and has many common features with other such systems worldwide.

Nelson, C.A. and Sylvester, A.G., 1971. Wall rock decarbonation and forcible emplacement of the Birch Creek pluton, southern White Mountains, California. *Geol. Soc. Am. Bull.*, **82**, 2891-2904.

## ORAL PRESENTATION

### Controls on the Trace Element Chemistry of Crustal Melts

Bea, Fernando

*Department of Mineralogy and Petrology,  
Campus Fuentenueva, University of Granada,  
18002 Granada, Spain*

The behavior of trace elements during crustal anatexis depends primarily on whether they reside 1) as trace elements in major phases (*e.g.* Li, Rb, Cs, Sr, Ba, Eu, Ga, and Ge), 2) as essential structural components in accessory phases (*e.g.* Zr, Y, Th, U, and REE other than Eu), or 3) as trace elements in accessories (*e.g.* Nb, Ta, V, Cr, Cu, Zn, Ni, and Co).

Melt/solid partitioning of elements residing as traces in major phases is, in principle, controlled by crystal/melt partition coefficients ( $K$ ), the extent of melting, modal mineralogy of source rock, and the proportions of minerals that melt. However, at  $P$ - $T$  conditions of crustal anatexis, kinetic effects related to the balance between melting rate and rate of intracrystalline diffusion within restitic phases strongly affect trace-element partitioning. If melting is faster than diffusion, all  $K_{effective}$  tend to be equal to 1, regardless of their  $K_{equilibrium}$  values. Some experimentally determined Arrhenius relations consistently indicate that diffusion coefficients at  $P$ - $T$  conditions of crustal anatexis are  $D \leq 10^{-16} \text{ cm}^2 \text{ s}^{-1}$ . With this value, all  $K_{effective}$  for trace elements residing for example within 2 mm-sized crystals that melt faster than  $10^{-13} - 10^{-14} \text{ cm}^2 \text{ s}^{-1}$  are equal to 1, and

$K_{effective}$  become equal to  $K_{equilibrium}$  only when the melting rate is lower than  $10^{-17} - 10^{-18} \text{ cm}^2 \text{ s}^{-1}$ . When  $K_{effective}$  and  $K_{equilibrium}$  are equal, the rate of melt segregation determines whether partial melting is equilibrium or Rayleigh type. For  $D = 10^{-16} \text{ cm}^2 \text{ s}^{-1}$ , 2 mm-sized restitic crystals need about  $1.6 \times 10^6$  years to equilibrate with the melt. When  $K_{effective}$  and  $K_{equilibrium}$  are different, disequilibrium melting occurs. If  $K_{effective} = 1$ , the concentration of a given trace element in melt is simply given by:

$$C_{melt} = \Sigma (C_m \cdot Z_m) - \Sigma (C_n \cdot P_n),$$

where  $C_m$  is the concentration of trace elements in source minerals,  $C_n$  is the concentration of elements in newly formed phases,  $Z_m$  is the weight fraction of source minerals that melt, and  $P_n$  is the melt fraction of each new phase. Melts produced in these conditions tend to inherit the patterns of those trace elements which reside essentially within major minerals of the source rock.

Trace elements which are essential structural components in accessory phases do not obey Henry's law and their concentrations in melt are ruled by accessories solubility and solution kinetics instead of partition coefficients. For a given temperature, the solubility of accessories depends on the melt bulk chemistry and volatile contents. The textural position of accessories controls whether they are available to the melt. Included accessories may be physically isolated from the melt and retained in restites together with their host. Biotite is especially prone to this effect because it usually includes about 85% mass fraction of monazite, xenotime, zircon, Th-orthosilicates, *etc.*, present in common crustal protoliths. Isolation of accessories produces leucosomes with low contents of Zr, Y, Th, U, LREE, HREE, *etc.* and positive Eu anomalies, simply due to the fact that feldspars are the only REE-bearing minerals that melt. Since dissolution rates of accessories are slow, fast segregation of melt could eventually produce the same effect. Sometimes, this process is also referred to as disequilibrium melting (but with a different sense than above) and leucosomes with the above composition are interpreted as proof of fast melt extraction. However, since the segregation of tiny crystals ( $\phi_{max} \approx 50$ -1 microns) from a highly viscous melt is a very inefficient process, one would expect that accessories, once available for the melt at any time during anatexis, cannot be removed and will therefore dissolve either completely or, if they were in excess, until they saturate the melt, regardless of how fast melt is extracted from bulk restites. Accessories may also be entrained in the melt

as inclusions within restitic crystals, especially in biotite. This effect produces leucosomes with spurious positive correlations between such elements as Ti, Li, and Rb (characteristic of the host) with LREE, HREE, Y, and Th (characteristic of inclusions).

Lastly, elements which occur as abundant traces within accessories are affected by both the kinetics of intracrystalline diffusion and the effects of accessories.

### **The Residence of REE, Y, Th, and U in Granites and Crustal Protoliths. Implications for the Chemistry of Crustal Melts**

Bea, Fernando

*Department of Mineralogy and Petrology,  
Campus Fuentenueva, University of Granada,  
18002 Granada, Spain*

A systematic study (SEM, LA-ICP-MS, electron microprobe analyses) on unmineralized granites, migmatites, and granulites from Iberia, the Urals, Kola and Transbaikalia revealed 25 (REE, Y, Th, U)-rich mineral species. Nineteen species - monazite, cheralite, xenotime, huttonite, thorite, allanite, cerianite, uraninite, betafite, pyrochlore, brannerite, uranosferite, bastnaesite, parisite, samarskite, aeschinite, fergusonite, zirkelite, and fluocerite - have at least one REE, Y, Th, or U as an essential structural component. Another six species - zircon, baddeleyite, epidote, apatite, titanite, and fluorite - occasionally contain these elements as abundant impurities. The diameter of all primary (REE, Y, Th, U)-rich minerals (except fluorite, epidote, titanite, apatite, and occasionally allanite), usually is smaller than a few tens of microns, and they tend to occur included within other major or accessory phases, showing a definite preference for biotite, garnet, zircon, and apatite. The accessory assemblage changes with the rock bulk-chemistry and always accounts for an elevated fraction of REE, Y, Th, and U. Eu, however, resides almost completely within plagioclase, K-feldspar, and (in subaluminous granites) amphibole. Low-Ca peraluminous leucogranites have monazite + xenotime + apatite + Th-orthosilicate + zircon ± uraninite ± betafite ± uranosferite ± brannerite, which account for more than 90% of LREE, HREE, Th, and U. Peraluminous granites and

granodiorites have monazite + apatite + zircon + Th-orthosilicate (huttonite?) ± allanite, also accounting for more than 90% of total LREE, HREE, Y, Th, and U. Metaluminous granites have allanite + apatite + zircon ± Th-orthosilicate (thorite?) ± titanite ± monazite ± epidote ± REE-carbonates, which account for 70% LREE, 70-60% HREE and Y, 80-85% Th, and 95% U, although amphibole contains about 30% LREE, 40% HREE, and 15% Th. Peralkaline granites have complex associations of niobotantalates, allanite, monazite, xenotime, bastnaesite, thorite, fluocerite, zircon, apatite, titanite, fluorite, zirkelite and baddeleyite, accounting for c. 90% of total LREE, HREE, Y, Th, and U. Migmatites and high-grade metamorphic rocks have practically the same accessory assemblage as granites with similar bulk composition. In garnet-bearing rocks, garnet rarely accounts for more than 15% HREE and Y, whereas xenotime + zircon + Th-orthosilicate usually account for more than 80%.

The fact that REE, Y, Th, and U are essential structural components in at least one accessory of every crystallizing granite and melting protolith implies that these elements will not obey Henry's law, and that their concentration in partial melts is ruled by accessory solubility and dissolution kinetics. During anatexis, the mass fraction of accessories located at major-phase grain boundaries (and therefore available to the melt) depends on the nature of the mineral and decreases with grain size. In common crustal protoliths from Iberia, for example, about 90% of the mass of monazite and xenotime, and 65% of the mass of zircon are included within biotite, which thus indirectly controls the behavior of REE, Y, Th, and U during melt segregation.

Crystal settling of (REE, Y, Th, U)-rich accessories in granite melts is physically impossible, due to their small grain size. Crystallized accessories must remain in suspension until a growing major mineral includes them. Selective inclusion is caused by heterogeneous nucleation coupled to local saturation adjacent to a growing crystal. High surface/volume ratios and almost zero contents of REE, Y, Th, and U make biotite an ideal host for (REE, Y, Th, U)-rich accessories. Due to selective inclusion, host minerals may exert an indirect yet significant control on the geochemistry of REE, Y, Th, and U. The melt bulk-chemistry determines the nature of crystallized accessories, their appearance within the paragenetic sequence, and, hence, the partitioning of REE, Y, Th, and U between melt and crystals. During magmatic differentiation, the contrasting behavior of REE, Y, Th, and U in

peraluminous granites (extreme depletion) as opposed to subaluminous granites (moderate enrichment) is caused by the low solubility of monazite and xenotime in peraluminous melts. The low-Ca activity related to high aluminosity inhibits apatite precipitation, thus increasing phosphorus activity and easing the precipitation of (REE, Y) phosphates. The elevated REE fraction contained in accessory minerals, non-Henry's law behavior, indirect control by major minerals, the effects of textural position of accessories during anatexis, and the controls of melt bulk-chemistry on the stability of accessories, mean that REE-based modeling for deciphering the behavior of major minerals during melting and crystallization is of little, if any, use in granite rocks.

**Tonalites as Barometers  
and Hygrometers:  
An Example from the  
Southern Virginia Appalachians**

Beard, James S.

*Virginia Museum of Natural History,  
Martinsville, VA 24112, USA*

Both total pressure and water pressure have profound effects on the phase equilibria of amphibolite melting and on the compositions of the tonalitic liquids so derived. High total pressure favors the formation of garnet and dissolution of plagioclase. Little is known about the effect of  $P_{H_2O}$  on garnet stability *per se*, but, by analogy with other non-tectosilicate phases, it is likely to be less strongly affected than plagioclase. Even at  $P_{H_2O}$  as low as 2-3 kbar, the stability limits of plagioclase are greatly reduced. Thus, amphibolite melting at high  $P_{H_2O}$  in the middle crust may yield a garnet-rich, plagioclase-absent residual assemblage similar to that produced by dehydration-melting at significantly higher pressure. Under these circumstances, the concentrations of major elements in the derivative melts may be useful in determining whether melting occurred in a system with or without excess water. Alumina content should be particularly useful in that high  $P_{H_2O}$  melting at moderate total pressures simultaneously promotes the dissolution of plagioclase and the formation of metaluminous, Ca-bearing minerals such as amphibole and clinopyroxene.

Tonalite dikes within the Smith River Allochthon (SRA) in south-central Virginia have high Sr (average 710 ppm), positive Eu anomalies, and are depleted in HREE and Y ( $La_N/Yb_N$  average 25, Y average 7.4 ppm). These characteristics are the signature of tonalite melts generated by partial melting of amphibolite under conditions where garnet is stable and plagioclase is not. Tonalites having these characteristics are generally interpreted as having formed either below the crust or at or near its base. The SRA tonalites, however, are, in addition, aluminous ( $Al_2O_3 = 17\%$  at 70%  $SiO_2$ ), peraluminous, and Fe-poor (most  $< 2\%$   $FeO^T$  at 70%  $SiO_2$ ). The tonalites appear to be too aluminous and Fe-poor to have formed by dehydration melting, even at pressures  $> 30$  kbar. The chemistry of the tonalites is consistent with their formation by water-excess melting of basalt or amphibolite in the garnet stability field and above plagioclase stability at  $P_{total} > 8-10$  kbar and  $P_{H_2O}$  between 1 and 3 kbar. Trace element modeling suggests that the tonalites can be generated by partial melting of a local crustal source (Basset Amphibolite). The models require a high proportion of residual amphibole (40-85% of the residuum mode) and large (25-40%) melt fractions, consistent with melting under relatively wet conditions. Melting may have been induced by influx of water from the cool, upper portion of the lower plate into the hot, lower portion of the SRA during or after emplacement of the thrust sheet.

ORAL PRESENTATION

**Linking Phase Relations,  
Thermal Budgets and Deformation  
During Partial Melting:  
Two Contrasting Styles of  
Basalt-Crust Interaction**

Bergantz, G.W.

*Department of Geological Sciences, AJ-20,  
University of Washington, Seattle, WA 98195, USA*

The importance of basaltic input in granite generation has been well established and the evidence is discussed extensively elsewhere (Bergantz and Dawes, 1994; Kay *et al.*, 1992). What isn't well understood are the physical processes and the attendant time and length scales of basalt-crust interaction. In this presentation, we will focus

only on the partial melting regime, we do not consider magma mixing in high level chambers.

Two geologically motivated endmembers for basalt-crust interaction are presented. The first is the "Ivrea" type, the second, the "Chelan" type; these are named for their type locations in northern Italy and Washington State, respectively. The Ivrea type is the more commonly cartooned endmember. It is characterized by a mafic system with dimensions on the order of kilometers, discrete (or regionally mappable) contacts with broadly horizontal upper boundaries, and a compositional variation largely consistent with fractionation with contamination by crustal material. These systems typically originate by incremental assembly into chambers which may be largely crystal liquid mush, like mid-ocean ridge chambers, as suggested by Quick *et al.* (1994). Heat and mass transfer between the country rock and the mafic magma takes place across a conjugate interface, and geologic evidence indicates that the enthalpy exchange is largely conductive. The dominant means of mass transfer is the wholesale incorporation of roof blocks or septa into the largely mushy, mafic magma (Sinigoi *et al.*, 1994). Extensional deformation plays a key role in crystal-liquid organization and movement, both in the mafic complex and near the contact.

The Chelan type endmember has been documented and discussed by Hopson and Mattinson (1994). The distinctive feature of this endmember is that the basalt intrudes regionally as sequences of dikes. This yields a temporal and spatial sequence of partial melting with an intimate association between basalt and partial melt. It produces an efficient means for basalt-melt interaction and a variety of mingling and mixing features have been documented. The type region as a whole has undergone incipient diapiric upwelling. Petrologic diversity in the Chelan type is readily generated at all scales.

Thermo-mechanical models for partial melting and melt migration have been developed for both endmembers. The Ivrea type model is discussed by Barboza and Bergantz (this volume). One key point is that buoyancy alone, whether driven by thermal or compositional density contrasts, does not lead to appreciable amounts of melt segregation. This is in contrast to some laboratory models that suggest large amounts of melting (above the contiguity limit) will occur at the contact driven only by density differences. Our model predictions agree remarkably well with geological observations, and suggest a key role for shearing or diking in melt migration.

Models for the Chelan type are more difficult to constrain as the volume-time interval-dike spacing relation-

ships for the intrusion of the basalt have yet to be determined from the field area. In addition, our model protolith is different than that at the Chelan (we are currently working up the appropriate protolith composition). Nonetheless, the essential dynamic features of the Chelan type have been obtained: melting at many scales, and a regional change in bulk rheology that would initiate a "proto-diapir" type of structure (after Hopson and Mattinson, 1994). Note however, that this is not a simple diapir of material heated from below. The buoyancy originates from a region that is effectively heated internally, and thus the usual types of time dependent behavior and kinematic indicators associated with a classic Rayleigh-Taylor instability, or "hot Stokes" diapir, do not obtain. The geometry and rise time of the proto-diapir depends on the basalt intrusion rate, distribution, and the rheological model chosen for the unheated crust.

Despite the conceptual popularity of the Ivrea type, we propose (following Hopson) that the Chelan type may be more important in the development of granitoids which have a substantial mantle signature and metaluminous composition. The Chelan type may be difficult to recognize, or may be commonly misinterpreted in regional geological mapping. Shearing of some type is a fundamental feature for substantial melt migration in both types. In the Ivrea type, such shearing may originate from far field stresses combined with intrusion. In the Chelan type, it is a natural consequence of the thermal maturing and bulk buoyancy, following the basalt intrusion episode.

Bergantz, G.W. and Dawes, R., 1994. Aspects of magma generation and ascent in continental lithosphere. In Ryan, M.P. (ed), *Magmatic Systems*, Academic Press, 291-317.

Hopson, C.A. and Mattinson, J., 1994. Chelan migmatite complex, Washington: Field evidence for mafic magmatism, crustal anatexis, mixing and protodiapiric emplacement. In Swanson, D.A. and Haugerud, R.A. (eds), *Geological Field Trips in the Pacific Northwest*. Department of Geological Sciences, University of Washington, 2K, 1-21.

Kay, R.W., Mahlburg Kay, S. and Arculus, R.J., 1992. Magma genesis and crustal processing. In Fountain, D.M., Arculus, R.J. and Kay, R.W. (eds), *Continental Lower Crust*, Elsevier, 423-441.

Quick, J.E., Sinigoi, S. and Mayer, A., 1994. Emplacement dynamics of a large mafic intrusion in the lower crust, Ivrea-Verbanese Zone, northern Italy. *J. Geophys. Res.*, **99**, 21,559-21,573.

Sinigoi, S., Quick, J.E., Clemens-Knot, D., Mayer, A., Demarchi, G., Mazzuchelli, M., Negrini, L. and Rivalenti, G., 1994. Chemical evolution of a large mafic intrusion in the lower crust, Ivrea-Verbanese Zone, northern Italy. *J. Geophys. Res.*, **99**, 21,575-21,590.

## Mineralogy and Geochemistry of Tertiary A-Type Granitoids at a Continental Rift Margin, Southern Red Sea.

Blakey, Suzanne, Thirlwall, M.F.  
and Menzies, M.A.

*Geology Department, Royal Holloway College,  
University of London, Egham, Surrey,  
TW20 0EX, UK*

Oligo-Miocene continental rifting of the Red Sea was associated with intense magmatic activity in Yemen, expressed as a thick sequence (> 3500 m) of basalt-rhyolite flows. Associated granitoids are up to 25 km across, located along a linear trend parallel to the Red Sea. The granitoids are smaller in the south and further inland than along the coastal escarpment and to the north. This could be a function of uplift and erosion, with the southern granitoids being unroofed to a lesser extent than those in the north.

The granitoids are intruded late in the history of the volcanic margin, they intrude the Precambrian basement, the Mesozoic sedimentary cover and the Tertiary lavas. An Rb-Sr whole rock isochron for a southern granitoid gave  $24.5 \pm 1.4$  Ma. Despite the altered nature of whole rock samples, fresh amphibole and biotite separates yield an identical age of  $23.1 \pm 0.6$  Ma.

The mineralogy and texture of the granitoids offer insight into magmatic processes. Quartz displays undulose extinction resulting from transformation of  $\beta$ -quartz to  $\alpha$ -quartz, and may exhibit granophyric intergrowths with orthoclase as a result of eutectic crystallization. Feldspars occur as orthoclase, plagioclase and perthite. Perthite is the most common texture, suggesting sub-solidus cooling. Both hypersolvus and subsolvus granitoids are present, reflecting different pressures and temperatures of emplacement. Amphibole occurs as clusters of arfvedsonite, with minor riebeckite, these alkali amphiboles are typical of A-type granites. Minor amounts of eckermannite and katophorite occur in more mafic samples. Pyroxene is rare, occurring as optically continuous interstitial aegirine-augite, representing orthocumulate textures forming between the liquidus and solidus temperatures. Biotite is annite-rich, and often results from alteration. There are many accessory minerals, *e.g.* fluorapatite, titanite, magnetite, ilmenite, rutile, monazite, fluorite, uraninite and epidote. Apart from apatite and Ti-magnetite, these do not

appear to affect the chemistry of the rocks and may be the result of subsolidus/*in situ* crystallization.

The granitoids of Yemen have an unusual alkaline chemistry which led them to be classified as A-type granitoids, they are characterised by high SiO<sub>2</sub>, Na<sub>2</sub>O, K<sub>2</sub>O, Zr (> 1000 ppm), Nb, Ga, Y, F, Sn, REE (except Eu), low Al, Mg, Ca, Ba, V and Sr. Typical spiderdiagrams display strong negative anomalies in K<sub>2</sub>O, Ba, Sr, Eu, P and Ti. The Sr anomalies are caused by either plagioclase fractionation, or a crustal source for the granitoids. High <sup>143</sup>Nd/<sup>144</sup>Nd ratios (*c.* 0.512887) and Ce/Pb ratios close to mantle values (~25 - 30) suggest the granitoids are not crustal melts and that plagioclase fractionation causes the Sr anomalies. P and Ti anomalies are due to the fractionation of apatite and Ti-magnetite respectively.

The granitoids plot in the "within plate granite" field of Pearce *et al.* (1984), with the exception of a few samples which plot in the field of volcanic arc granites (VAG), possibly due to plagioclase accumulation. The granitoids contain very little ammonium, 1-4 ppm, contrasting with high ammonium contents of VAG granites.

Evolution of the textures observed in the granites is largely a result of subsolidus reactions. A-type magmas have high halogen contents and movement of the halogens through the magma depresses the melt viscosity and also overprints the original texture of the granites, *e.g.* in the Yemen granitoids a large proportion of the original mineralogy has been pseudomorphed by quartz, with only ghost structures of minerals remaining.

Initial isotope data display a range of compositions from  $(^{87}\text{Sr}/^{86}\text{Sr})_i = 0.7039 - 0.7083$ ,  $^{206}\text{Pb}/^{204}\text{Pb} = 18.15 - 19.17$ ,  $^{207}\text{Pb}/^{204}\text{Pb} = 15.59 - 15.67$ ,  $^{208}\text{Pb}/^{204}\text{Pb} = 38.53 - 39.03$ ,  $^{143}\text{Nd}/^{144}\text{Nd} = 0.512591 - 0.512887$ . There is a great variation in Sr, Nd and Pb isotopes between individual granitoids. For instance the Jabal Sabir granitoid displays no isotopic variation,  $(^{87}\text{Sr}/^{86}\text{Sr})_i$  is high, 0.705,  $^{143}\text{Nd}/^{144}\text{Nd}$  is low, 0.512596, therefore there must have been crustal involvement and homogenisation of the isotopic composition before emplacement. In Jabal Dubas,  $^{143}\text{Nd}/^{144}\text{Nd}$  is identical to the Yemen basalts, therefore little bulk crust can have been assimilated, but  $(^{87}\text{Sr}/^{86}\text{Sr})_i$  is high, 0.7068. The high  $(^{87}\text{Sr}/^{86}\text{Sr})_i$  occurs because Sr has been removed by feldspar fractionation at high SiO<sub>2</sub>, this is therefore very sensitive to a small crustal input. A good relationship between Sr isotopic compositions and Sr content indicates AFC-type processes.

Pb isotopic data vary markedly between each granitoid and to a lesser extent within individual intrusions. Provin-

ciality in Pb isotopic data reflect the Pb isotopic heterogeneity of the Pan-African lithosphere. Pb isotopic data for granitoids in central Yemen overlap those of coeval and spatially related silicic pyroclastic units. The A-type granitoids may be the exposed roots of a chain of caldera centers that fed the ignimbrites.

Pearce J.A., Harris, N.B.W. and Tindle, A.G., 1984. Trace element discrimination diagrams for the tectonic interpretation of granitic rocks. *J. Petrol.*, **25**, 956-983.

### Methods for Determining the Thermodynamic Mixing Properties of Hydrous Haplogranitic Melts: Progress, Problems and Prospects

Blencoe, James G. and  
Anovitz, Lawrence M.

*Chemical and Analytical Sciences Division,  
Oak Ridge National Laboratory, P.O. Box 2008,  
Building 4500S, Oak Ridge, TN 37831, USA*

Quantitative modeling of phase equilibria in granitic systems would be greatly facilitated if the thermodynamic mixing properties of  $\text{NaAlSi}_3\text{O}_8$  -  $\text{KAlSi}_3\text{O}_8$  -  $\text{Si}_4\text{O}_8$  -  $\text{H}_2\text{O}$  melts were known accurately. Recognizing this, numerous investigators have attempted to measure these properties experimentally. However, these efforts have been hindered by difficulties encountered in performing experiments on *hydrous* haplogranitic melts. High pressures and temperatures are required to stabilize melt compositions that correspond to natural granitic magmas, and it can be difficult to achieve complete equilibrium during experimentation. Moreover,  $\text{H}_2\text{O}$ -rich haplogranitic melts tend to exsolve water during quenching, and hydrous haplogranitic glasses lose dissolved water readily when heated at one atmosphere. Owing to these and other difficulties, very few calorimetric and volumetric data have been obtained for hydrous haplogranitic melts and glasses.

On the other hand, some very useful phase-equilibrium and spectroscopic data have been obtained for hydrous haplogranitic melts and glasses. These data have been used to elucidate melt - crystal - fluid reactions, water solubility, and water speciation, and to constrain thermodynamic models. However, almost all of the phase-equilibrium data for haplogranitic melts are unreversed, and spectroscopic data on water speciation in haplogranitic

glasses must be interpreted with caution because the relative proportions of the two principal types of water species (OH groups and molecular water) change when a haplogranitic melt is quenched. Furthermore, because data on melt - crystal - fluid phase relations and water speciation do not provide direct information on the *activities* of the components and species in haplogranitic melts, supplementary thermochemical data are required for accurate thermodynamic modeling.

Another difficulty is that the standard-state free energies of fusion of high albite, sanidine and quartz are poorly known. This is so not only because relevant 1-atm thermochemical data are either absent or of low accuracy, but also because fusion temperatures are not well known at high pressures. If the standard-state free energies of fusion of high albite, sanidine and quartz were known accurately in *P-T* regions where haplogranitic melts are stable, accurate activities for these components could be calculated from tightly reversed melt-crystal-fluid phase-equilibrium data.

Because conventional experimental and thermodynamic approaches have failed to yield reliable equations for the thermodynamic mixing properties of hydrous haplogranitic melts, researchers have developed ad hoc thermodynamic models based on one or more key assumptions. For example, in speciation models for hydrous haplogranitic melts it is commonly assumed that the species either mix ideally, or obey Henry's law. However, all speciation models for hydrous haplogranitic melts are inconsistent with one or more sets of high-quality phase-equilibrium, calorimetric or spectroscopic data. We suggest that these inconsistencies arise partly because both fictive and real melt species do not interact thermodynamically in accordance with any simple mixing law.

An alternative method for determining the thermodynamic mixing properties of hydrous haplogranitic melts is to measure the chemical potential of  $\text{H}_2\text{O}$  ( $\mu_{\text{H}_2\text{O}}$ ) in these melts. With these data, activities for the stoichiometric silicate components ( $\text{NaAlSi}_3\text{O}_8$ ,  $\text{KAlSi}_3\text{O}_8$  and  $\text{Si}_4\text{O}_8$ ) can be quantified by fitting calculated chemical potentials for  $\text{H}_2\text{O}$  to a formulation which is consistent with the Gibbs-Duhem relation. Currently, we are exploring the possibility that reliable  $\mu_{\text{H}_2\text{O}}-X_{\text{H}_2\text{O}}$  data for haplogranitic melts can be obtained from: 1) fluid-saturated, mixed-volatile experiments with  $\text{CO}_2$ ,  $\text{N}_2$  or Xe; and, 2) fluid-undersaturated experiments at fixed hydrogen and oxygen fugacity (controlled- $f_{\text{H}_2\text{O}}$  experiments). Also, we are collecting reversed experimental data on the boundaries of hypersolidus phase fields in hydrous haplogranitic

systems. These data will constrain melt-crystal-fluid phase relations in these systems, and permit evaluations of the standard-state free energies of fusion of high albite, sanidine and quartz.

Finally, binary and ternary haplogranitic systems should be investigated thoroughly before collecting large quantities of  $\mu_{H_2O}$ - $X_{H_2O}$  and other phase equilibrium data for quaternary haplogranitic melts. This is advisable because it is possible that no quaternary mixing parameters will be required to develop an accurate excess free energy equation for  $NaAlSi_3O_8$  -  $KAlSi_3O_8$  -  $Si_4O_8$  -  $H_2O$  melts.

Research sponsored by the Geothermal Technology Program of the Office of Energy Efficiency and Renewable Energy, U.S. Department of Energy, under contract number DE-AC05-84OR21400 with Martin Marietta Energy Systems, Inc.

## ORAL PRESENTATION

### **A Metallogenic Template for Eastern Australia Based on Granite Source and Evolution**

Blevin, Phillip L., Allen, Charlotte M.,  
Bryant, Colleen J. and Chappell, Bruce W.

*Department of Geology,  
Australian National University,  
Canberra, 0200, ACT, Australia*

Phanerozoic granite-related mineralization in eastern Australia is heterogeneously distributed both temporally and spatially. Three broad mineralization categories have been recognized: porphyry Cu-Mo-Au deposits associated with continental margin type, dominantly low- to medium-K granites in the northern New England Orogen (NEO); Cu-Au associated with isotopically primitive, medium- to high-K and shoshonitic Ordovician magmatism in the central Lachlan Fold Belt (LFB); and W, W-Sn, and Mo-W mineralization associated with high-K, felsic, I- and S-type Siluro-Devonian, and Carboniferous to Triassic magmatism in Tasmania, the southern NEO, LFB, and northern Queensland. A-type granites are not associated with significant mineralization. The ore element associations found in granite-related mineralization; Cu-Au, W, Mo-W, Sn-W, and complex polymetallic (Pb-Zn-Ag-Sn-As, etc.), are typical of intermediate to felsic granite magmatism worldwide. A widespread, though often

genetically tenuous, relationship between granite magmatism and Au mineralization is also present in eastern Australia.

The ore element associations, in combination with age, compositional and source features for the associated granites allow recognition of several distinct granite-metallogenic provinces in eastern Australia. Granite-metallogenic provinces defined by S-type granites are wholly restricted within individual terranes and fold belts. In contrast, some granite-metallogenic provinces defined by I-type granites cross the boundaries between terranes and fold belts. These contrasting distributions probably reflect that S-type magma sources were located within the mid crust, whereas I-types were derived from lower crustal sources whose compositions and origins are not reflected in the exposed geology.

Copper mineralizing systems are associated with granites that are chemically and isotopically primitive; these granites were derived through the rapid igneous reworking of juvenile igneous crust. Relatively isotopically primitive ( $(^{87}Sr/^{86}Sr)_i \sim 0.705$ ), but highly fractionated high-K granites, such as those in the southern NEO, are associated with substantial Sn mineralization. Elsewhere in eastern Australia Sn mineralization is genetically related to S- and I-type granites that are both isotopically ( $(^{87}Sr/^{86}Sr)_i > 0.710$ ) and chemically evolved. Tungsten mineralization occurs in scheelite skarns associated with moderately chemically evolved I-type granites, or as wolframite with Mo or Sn in highly fractionated granites that are oxidized and reduced, respectively. Molybdenum mineralization is widespread through eastern Australia and is associated with porphyry Cu systems, but also occurs as Mo-rich greisen and pipe hosted deposits in highly fractionated K-rich granites. Climax-type porphyry Mo systems are rare and small in eastern Australia despite the presence of large volumes of compositionally similar granites in the southern NEO and north Queensland.

The observed granite-metallogenic relationships in eastern Australia display a strong correlation between the ore element ratios in mineral deposits and the composition of the related granites. This is mirrored in the evolutionary trend from Cu dominant deposits associated with less evolved granite suites through W, to Mo- and Sn-dominant deposits associated with highly fractionated K-rich granite suites. Elsewhere, these relationships may be affected by the action of granite composition modifying processes such as assimilation. While thousands of small deposits and showings are associated with the granites of eastern Australia, the number of world class deposits is remark-

ably restricted given the volume of granite. In some cases this may reflect the relative degree of erosion and subsequent removal of epizonal ore deposits. However, most of these unmineralized granites, as typified by the LFB I- and S-type granites, define a compositional field based on fractionation and oxidation state parameters that is distinct from granites associated elsewhere with significant mineralization. Granites formed by the remagmatization of evolved, older continental crust appear to be capable of generating Mo and Sn mineralization only if they have an appropriate oxidation state and have undergone substantial crystal fractionation to even more evolved compositions. The association of certain metal commodities with certain tectonic settings is in part a function of these relationships, as tectonic processes affects the range of protolith materials, and heat and volatile fluxes available for magma generation.

### **Intraplate A-Type Bimodal Magmatism: Why and How?**

Bonin, Bernard

*CNRS-URA 1369, Département des Sciences de la Terre,  
Bâtiment 504 Université de Paris-Sud,  
F-91405 Orsay Cedex, France*

Intraplate post-orogenic to anorogenic igneous suites are markedly bimodal and made up of large but varying amounts of basic and felsic rocks with scarce intermediate rocks. The volcanic (plutonic) series display liquid lines of descent contrasting from Ne-normative basalt (gabbro) to: 1) Q-normative rhyolite (granite); 2) saturated trachyte (syenite); and, 3) Ne-normative phonolite (nepheline syenite). Differentiation paths from the metaluminous basic end-member to the three possible A-type (per)alkaline felsic end-members are chiefly controlled by fractionation of anhydrous (olivine, pyroxene, plagioclase) and hydrous (amphibole, more rarely mica) silicate minerals in mantle and crustal magma chambers.

The silica oversaturated igneous complexes are commonly characterized by huge volumes of rhyolite (granite) and comparatively minor volumes of basalt (gabbro). On the contrary, in the mixed and silica undersaturated igneous complexes, basalt (gabbro) compositions predominate largely over trachyte (syenite) and phonolite (nepheline syenite) intrusions.

In continental areas, the distribution of rock types changes as a function of time elapsed since the end of the last orogenic event. Beginning at the very end of the late-orogenic episode and lasting less than 25 Ma, the onset of the post-orogenic episode is marked by rhyolite (granite) complexes predominating over scarce basic formations, and evidence exists for availability of large amounts of water (subsolvus granites). Then, during the 500 Ma-long post-orogenic to anorogenic episode, subsolvus granites are progressively replaced by hypersolvus granites, occasionally altered by aqueous fluids. After this long period, mixed and silica undersaturated complexes are emplaced, where low-silica basic rocks predominate over rare nepheline syenitic differentiates, frequently altered by mixed (H<sub>2</sub>O + CO<sub>2</sub>) fluids.

In oceanic islands, a systematic evolution in time from tholeiitic, largely submarine, to transitional to alkaline, mainly aerial, magmatism has been documented and interpreted in terms of either decreasing partial melting of the same mantle source, or of mantle sources varying from depleted MORB types to variously enriched OIB (plume-like) types. The younger alkaline volcanic (plutonic) complexes display the typical twofold evolution toward silica oversaturated trachyte ± rhyolite (syenite ± granite) and undersaturated phonolite (nepheline syenite) differentiates.

Whether the liquid line of descent yields ultimate silica oversaturation or undersaturation, calcic amphibole, a silica-deficient hydrous mineral, plays a critical role. If the amount of water dissolved into the melt exceeds approximately 2 wt %, which corresponds to a vapour pressure of at least 50 MPa, magmatic amphibole can crystallize near the liquidus. As melt viscosities and solidus temperatures are significantly lowered, diffusion processes are enhanced and promote efficient liquid-mineral separation. Massive and fast precipitation of early calcic amphibole favours nearly complete consumption of basalt (gabbro) melts and generation of large volumes of highly silicic rhyolite (granite) residual liquids.

In water-deficient and/or very shallow environments, amphibole can no longer crystallize and early crystals dissolve ultimately into the melt. Melt viscosities and solidus temperatures increase, so that liquid-mineral separation becomes sluggish. Late *in situ* resorption of early calcic amphibole can generate strongly silica undersaturated phonolite (nepheline syenite) residual liquids but in small volumes only, due to inefficient liquid-mineral separation within basalt (gabbro) melts.

Thus, magma differentiation is chiefly governed by the water molecule which combines two separate chemical effects: 1) calcic amphibole upper stability limit by filling its hydroxyl site; and, 2) catalysis of liquid-mineral reactions by lowering melt viscosities and solidus temperatures. Water dissolved into the melts at depths may come from at least two distinct reservoirs: 1) rock-forming hydrous minerals, which can release water by dehydration melting reactions; and, 2) aqueous fluids, which can percolate through permeable host rocks at the magma chamber level.

### Rapid Ascent Rates of Granitoid Magmas Determined from Epidote Dissolution Kinetics

<sup>1</sup>Brandon, Alan D., <sup>2</sup>Creaser, Robert A. and <sup>2</sup>Chacko, T.

<sup>1</sup>*Department of Terrestrial Magnetism, Carnegie Institution of Washington, 5241 Broad Branch Road, N.W., Washington, DC 20015, USA*

<sup>2</sup>*Department of Geology, University of Alberta, Edmonton, Alberta, T6G 2E3 Canada*

Time scales for ascent of silicic magmas from the lower to upper crust are important in controlling their compositions. During rapid ascent, little modification occurs and magma compositions likely are controlled by source characteristics, extent of melting, and separation processes. During slow ascent, more modification can occur, and resultant magma compositions may not accurately reflect the nature of the source rock. In addition, magma ascent times are a function of the method of migration, either diapirism ( $\sim 1 \text{ m yr}^{-1}$ ), or dike transport ( $> > 1 \text{ m yr}^{-1}$ ). Numerical models suggest that dike transport of granitoid magma is viable, and such dikes can fill large silicic plutons in  $< 1000$  years (Clemens and Mawer, 1992). Here, we use direct petrologic constraints to evaluate the transport rates and mechanisms of some granitoid magmas.

Epidote is stable at  $> 6$  kbar in granitoid magmas. Magmatic epidote formed at  $\sim 8$  kbar is known from dacite dikes in the Colorado Front Range emplaced at 2 - 4 kbar, and is present because of the rapid ascent rate (Dawes and Evans, 1991). Magmatic epidote is present in the mid-Cretaceous White Creek batholith in SE British

Columbia (Brandon and Lambert, 1994), and has compositional characteristics typical for magmatic epidote reported elsewhere. Very low  $\text{TiO}_2$  ( $< 0.1 \text{ wt } \%$ ) and pistacite contents ( $\text{Ps} = [\text{Fe}^{3+}/(\text{Fe}^{3+} + \text{Al})]$ ) of  $\text{Ps}_{27}$  to  $\text{Ps}_{29}$  are diagnostic of magmatic epidote. The White Creek batholith was emplaced into metapelites and the mineral assemblage of its contact aureole consists of quartz, muscovite, sillimanite, and staurolite, with an emplacement level of 2.3 to 3.8 kbar (7 to 11 km depth). Emplacement pressures determined using two calibrations of the Al-in-hornblende geobarometer for White Creek hornblende rims range from 2.2 to 4.0 kbar, overlapping with the range of pressures indicated by the contact aureole assemblage. Occurrence of epidote in this shallow-level pluton suggests epidote was preserved by rapid magma transport from the source region.

We have quantitatively constrained magma transport rates from the deep crust by calibrating the low-pressure dissolution of epidote in granitoid magmas experimentally. The experiments show that epidote in the White Creek granodiorites are stable at pressures greater than 8 kbar, but breaks down at less than 6 kbar (temperatures of 750 to 780°C). Reaction rims in the low pressure experiments consist of quenched melt, plagioclase and magnetite. Reaction rim growth is modeled by a parabolic rate law, and is controlled by diffusivity of major elements across the reaction rim. Measured reaction rim widths in the experiments produce effective diffusion coefficients from  $2.3 \times 10^{-15}$  to  $6.1 \times 10^{-15} \text{ m}^2 \text{ s}^{-1}$  at 750 to 780°C. Using these coefficients, at 780°C a 2 mm diameter epidote crystal will dissolve in  $< 100$  years with reaction rim melt fractions of  $> 10\%$ . At 700°C, just above the 3 kbar water-saturated granite solidus, a 2 mm diameter epidote will dissolve in  $< 1200$  years.

Epidote phenocrysts within the dacite dikes have highly corroded rims indicative of reaction and dissolution. Epidote resorption begins at 6 kbar during ascent and continues until final solidification at 2 kbar, equating to at least 14 km of epidote-reactive transport. The phenocryst assemblage in the dikes equilibrated at 800-880°C at 7 to 12 kbar (Dawes and Evans, 1991). If the dikes were at 800°C upon emplacement at 2 kbar, a minimum rate of  $350 \text{ m yr}^{-1}$  is calculated using the reaction rim growth data. For epidote within the White Creek batholith, a minimum ascent rate of  $1750 \text{ m yr}^{-1}$  is obtained at 780°C. These rates suggest that rapid magma ascent is required for epidote preservation in low pressure granitoid rocks consistent with models for dike transport, but not diapirism. In conclusion, the petrological and experimen-

tal evidence presented here support a model where magmatic epidote in shallow-level granitoid plutons results from rapid magma transport from the deep crust, likely via dikes, precluding large amounts of interaction with the surrounding country rocks.

- Brandon, A.D. and Lambert, R.St.J., 1994. Crustal melting in the Cordilleran interior: the Mid-Cretaceous White Creek batholith in the southern Canadian Cordillera. *J. Petrol.*, **35**, 239-269.
- Clemens, J.D. and Mawer, C.K., 1992. Granitic magma transport by fracture propagation. *Tectonophysics*, **204**, 339-360.
- Dawes, R.L. and Evans, B.W., 1991. Mineralogy and geothermobarometry of magmatic epidote-bearing dikes, Front Range, Colorado. *Geol. Soc. Am. Bull.*, **103**, 1017-1031.

## Generation of Leucogranites at Granulite Facies Conditions: A Case Study from the Kerala Khondalite Belt in Southern India

Braun, I.

*Mineralogisch-Petrologisches Institut, Universität Bonn,  
Poppelsdorfer Schloss, 53115 Bonn, Germany*

Leptynitic garnet-biotite gneisses in the central and northern part of the Neoproterozoic Kerala Khondalite Belt (KKB) in southern India were regarded as the main source rocks for garnet-bearing leucogranites (Braun and Raith, 1994). From geochemical and petrological work it was suggested that granulite facies metamorphism ( $P = 5.5 - 6$  kbar,  $T = 800 - 850^\circ\text{C}$ ,  $a_{H_2O} \sim 0.3$ ) during the Pan-African orogeny  $\sim 550$  Ma ago led to fluid-absent dehydration-melting of biotite-bearing gneisses according to the reaction biotite + plagioclase + quartz = garnet (+ potassic feldspar) + granitic melt. This which gave rise to the development of garnet-bearing in-situ leucosomes in the leptynitic gneisses and the generation of leucogranitic melts. Although this model may explain the relationship between partial anatexis of the leptynitic gneisses and the generation of the leucogranites in general, some details of this process are still poorly known. Principally, a more precise knowledge of the source rock composition is required, the mechanisms of melt segregation at the assumed low melting degree ( $< 10\%$ ) are not known, and the question of participation of melt intrusions from greater distances and short-range melt segregation from the adjacent gneisses in the formation of leucogranite dykes, needs to be addressed.

This study presents Rb and Sr isotope and REE data of selected leucogranite and leptynitic gneiss samples and first results of major and trace element modeling, which were carried out to achieve a more detailed understanding of the process that led to the generation of the leucogranites.

In feldspar mineralogy and CaO and K<sub>2</sub>O abundances the leptynitic gneisses are highly variable. Gneisses which exclusively contain plagioclase ( $\sim \text{An}_{25}$ ) are rich in CaO ( $\sim 3$  wt %) and poor in K<sub>2</sub>O ( $\sim 1$  wt %). They contrast with mesoperthite-bearing gneisses with CaO and K<sub>2</sub>O abundances of 2 and 3 wt %, respectively. Rocks that contain both plagioclase and mesoperthite are less abundant and yield intermediate CaO and K<sub>2</sub>O values.

Leucogranites form small dykes and veins in mesoperthite-bearing leptynitic gneisses and occur subparallel or discordant to the foliation. The granuloblastic texture consists of euhedral garnet ( $\text{Alm}_{64}\text{Pyr}_{30}\dots$ ), quartz and mesoperthite ( $\text{Ab}_{38}\text{Or}_{57}\text{An}_{05}$ ), plagioclase is rare or absent. Accessory phases and opaque minerals are almost absent and only in very few cases gradations into fluorapatite-rich rocks are recognized. The chemical composition is characterized by high K<sub>2</sub>O and low FeO, MgO and Zr contents. REE abundances are low and yield flat chondrite-normalized patterns, which hardly show any Eu-anomaly. Compared to the leptynitic gneisses they are enriched in K<sub>2</sub>O, Rb and Ba, while Na<sub>2</sub>O, CaO, FeO, Sr, Zr and LREE are strongly depleted.

REE and Rb-Sr isotope investigations were carried out on whole-rock samples of leptynitic gneisses, their in-situ leucosomes and gneiss domains and of leucogranites. Rb-Sr isotope ratios of mesoperthite-bearing gneisses and their leucosome and gneiss domains plot in the same range and are weakly fractionated. REE patterns of these samples show a strong enrichment of HREE in the leucosomes, while LREE remain unfractionated. This suggests that dehydration-melting of the gneisses principally resulted in the formation of garnet which controlled the REE distribution between leucosome and gneiss domain. Furthermore these Rb-Sr and REE systematics preclude a high melting degree and significant melt extraction from the leucosomes. Leucogranites display HREE patterns similar to those of the leptynitic gneisses, while LREE are significantly depleted. Rb-Sr ratios of a leucogranite vein in a mesoperthite-bearing leptynitic gneiss are significantly higher than those obtained for the gneiss and do not plot on an isochron calculated for the gneiss and its both domains. This supports the idea that leucogranites intruded the gneisses from greater distances and that short-range

melt segregation from the adjacent gneisses largely did not contribute to their generation.

The source rock composition of the leucogranites was estimated from major and trace element mass balance calculations. It became obvious, that if equilibrium melting and low melting degrees are required, mesoperthite-bearing leptynitic gneisses may not serve as source rocks. Instead, such rocks should be more sodic and less potassic and silicic in composition and also should have higher REE abundances. At the present stage plagioclase-bearing leptynitic gneisses provide the best results and thus are considered to approximate the source rock composition of the leucogranites.

Braun, I. and Raith, M., 1994. The leptynitic gneisses of the Kerala Khondalite Belt, southern India: phenomena and mechanism of dehydration/melting at granulite facies conditions. *Mineral. Mag.*, 58A, 119-120.

### **The Taku Transect and its Granitic Rocks, Coast Mountains Complex, Southeastern Alaska**

Brew, David A., Drinkwater, James L.,  
Ford, Arthur B. and Himmelberg, Glen R.  
*U.S. Geological Survey, Branch of Alaskan Geology,  
MS 904, 345 Middlefield Road,  
Menlo Park, CA 94025, USA*

The Taku transect near Juneau, Alaska, is one of four transects that are currently used, together with reconnaissance field mapping, to define the Coast Mountains Complex. This complex has previously been informally called the Coast Mountains plutonic-metamorphic complex and by other names. The other transects are the Ketchikan and Skagway transects studied by Barker and Arth (1990) and the Stikine River transect studied in part by the present authors. The Taku transect is the only one that contains all of the magmatic, lithostratigraphic-terrane, metamorphic, and structural features that make up the Coast Mountains Complex.

The Taku transect is about 40 km wide and 80 km long, and extends in a NE direction from Douglas and Admiralty Islands on the west to the Alaska-British Columbia boundary on the east. It is made up of these major units and structural features, with their lithotectonic terrane assignments: 1) low-pressure, low-temperature, mafic-composi-

tion metavolcanic and lesser amounts of metapelitic sedimentary rocks assigned to the Douglas Island Volcanics of the Stephens Passage Group of the Gravina overlap assemblage; they are intruded by the 95 Ma granodiorite, tonalite, and quartz diorite plutons of the Admiralty-Revillagigedo belt; 2) the Coast Range megalineament, which is here the high-angle Gastineau Channel fault; 3) low- to medium-pressure, low- to medium-temperature, mafic-composition metavolcanic and some metapelitic and metacarbonate sedimentary rocks belonging to the Wrangellia terrane; 4) medium- to high-pressure, medium- to high-temperature, Barrovian series pelitic schists together with minor amphibolitic schist and marble that are presently assigned to the Behm Canal structural zone; they are intruded by Late Cretaceous tonalite and granodiorite sills of the Mount Juneau pluton; 5) well-foliated and locally lineated and mylonitized intermediate-composition granitic rocks of the 69 - 56 Ma Great tonalite sill composite batholith, which was emplaced at or close to the contact between the Behm Canal structural zone to the west and the metamorphic rocks of the Nisling terrane to the east; 6) layered biotite-hornblende gneiss, amphibole gneiss, quartz- and feldspar-rich schist, and multicomponent migmatite intruded by a series of 60 - 55 Ma hornblende-biotite granodiorite sills related to the Great tonalite sill; 7) generally unfoliated and homogeneous 50 Ma sphene-biotite-hornblende granodiorite and granite of the Turner Lake batholith, which contains sporadic screens of metamorphic rocks and local migmatite zones; and, 8) locally hornfelsed intermediate-composition metavolcanic rocks of the Stikine terrane and pelitic and semipelitic schists of the Nisling terrane at and near the international boundary.

The 95 Ma Admiralty-Revillagigedo belt plutons are discrete and discordant, locally well foliated, medium-grained, magnetite-free porphyritic biotite and hornblende quartz diorite and tonalite that contain primary epidote and garnet. The Mount Juneau pluton and the Great tonalite sill both are thick composite sill- or sheet-like bodies of foliated and locally well lineated medium- to coarse-grained tonalite. The Late Cretaceous Mount Juneau pluton is magnetite-free epidote-bearing biotite-hornblende tonalite and the 69 - 56 Ma Great tonalite sill is magnetite-bearing biotite-hornblende tonalite. The 60 - 55 Ma sills to the east of and related to the Great tonalite sill are heterogeneous hornblende-biotite leucotonalite and granodiorite. The 50 Ma Turner Lake batholith consists of homogeneous, massive, porphyritic to equigranular magnetite-bearing sphene-hornblende - biotite granodiorite to the west and

homogeneous, massive, porphyritic, coarse-grained allanite-bearing hornblende -biotite granite to the east.

The metamorphic rocks that occur between these belts are assigned to several lithotectonic terranes and resulted from multiple metamorphic episodes both older than and about the same age as the plutonic events. Taken all together, the rocks of the Coast Mountains Complex record a long history of magmatism and metamorphism first near the converging plate margin between the Insular and Intermontane superterranes and then in a subsequent transtensional to extensional regime.

Barker, F. and Arth, J.G., 1990. Two traverses across the Coast batholith, southeastern Alaska. In Anderson, J.L. (ed), *The Nature and Origin of Cordilleran Magmatism*, Geological Society of America Memoir 174, 395-405.

## Prosecuting the Connection Between Migmatites and Granites

Brown, Michael

*Department of Geology, University of Maryland at  
College Park, MD 20742, USA*

".....the intensity of the conviction that a hypothesis is true has no bearing on whether it is true or not".

P.B. Medawar  
Advice to a Young Scientist

Migmatites are mixed rocks comprising granite in a metamorphic host. Regional migmatites typically occur in the higher-grade parts of orogenic belts, belts that exhibit polyphase and heterogeneous deformation at all scales (Brown, 1994). Many granites are located in orogenic belts: associated with high-grade metamorphic rocks; emplaced along shear zones associated with uplift and exhumation; and, emplaced in lower-grade metamorphic rocks at higher structural levels. *Q.E.D.* the crust is migmatitic at all scales! The plumbing by which melt segregates and magma transfers through the crust is marked by former melt (or its cumulate product) and magma that became stuck in the system. Outcrop-scale information in migmatite terranes indicates the importance of deformation during anatexis, both to drive melt segregation and to provide sites for accumulation. The same features occur at map-scale in orogenic belts, where

regional tectonic features may control location of granite plutons.

Static models of melt segregation by gravity-driven porous medium flow based on the dihedral angle model are unlikely to apply during most natural crustal melting. The application of differential stress to an anisotropic body such as the crust, in particular when it contains some volume of melt, leads to heterogeneous deformation and the development of sites for melt accumulation, as well as a driving force for melt movement. Melt may migrate through structurally-created pathways, such as fractures and shear zones, accumulate in a variety of dilatant sites, such as boudin necks, or immigrate as discordant bodies of leucosome. Melting at high  $a_{H_2O}$  involves a volume reduction, segregation may be by convection and filter pressing, and melt retention is expected, since the system tends to "suck in" the melt (Brown *et al.*, 1995a,b). Melt fraction may increase until the contiguity of the solid framework breaks down and bulk magma mobility with restite entrainment may occur; unless deformation drives out the melt at lower melt fractions. Major crustal melting involves hydrate breakdown at low  $a_{H_2O}$  under volatile phase-absent conditions, which leads to an increase in volume, and will promote segregation by convection and filter pressing. Increasing volume may lead to pore fluid pressures high enough to facilitate melt-enhanced embrittlement, cataclastic flow and fracture to allow melt escape; effectively the system "blows out" the melt (Brown *et al.*, 1995a,b). Field evidence is consistent with this - excess melt in leucosomes commonly has been frozen while draining through an interconnected network of structurally-created pathways and dilatant sites to a higher structural level. Anatexis has a significant implication for crustal rheology. It is clear from studies of orogenic belts that there are feedback mechanisms between deformation and melting. Melting can lead to a concentration of deformation which not only facilitates melt segregation and ascent but partitions deformation preferentially back into the zones in which partial melting has occurred.

Generally there are considered to be three end-member models by which melt might ascend through the crust to its level of emplacement, *viz.* as a diapir, in a fracture as a dike or along a shear zone (Brown, 1994; Brown *et al.*, 1995a,b). Magma will flow to low-pressure regions and migration of melt along major crustal shear zones appears fundamental in some orogenic settings, particularly transcurrent shear zones. The buoyancy force of the magma then will interact with regional stresses in the most convenient way to facilitate ascent. Zones dominated by

buoyant magma flow may be characterized by a steep magmatic lineation, whereas zones characterized by strike-slip shearing may record sub-horizontal magmatic lineations. One consequence of an anisotropically layered lower crust is that melting in one zone may be capped by an unmolten layer above. If the partially molten zone within the crust did develop instabilities due to gravity, then melt might be expected to migrate parallel to the foliation and accumulate at dome culminations produced by the instability. If shear zones preferentially nucleate at these sites, then collection of melt followed by ascent within a shear zone would occur.

An example of a middle crustal zone that preserves evidence for ductile transpression synchronous with melting is the St. Malo migmatite belt (Brown, 1995). Here melt has frozen during transfer along an interconnected system of shallow-oriented shear zones within the migmatite belt, and marginal to the migmatite belt larger volumes of magma have been frozen during transfer upward within major strike-slip shear zones. In this case, magma ascent through the crust from the zone of generation to the level of emplacement is inferred to have been channelized, having occurred through the strike-slip shear zones. Adjacent to the migmatite belt at a higher structural level the Mancellian granites are interpreted to represent emplacement into the upper crust of fugitive magma from migmatitic rocks analogous to the St. Malo migmatite belt at deeper structural levels (D'Lemos *et al.*, 1992; Brown, 1994, 1995). Ascent is inferred to have been channelized along steeply-oriented strike-slip shear zones with emplacement into tensile bridges developed between left-stepping segments of a major transcurrent fault zone. Along individual granite pluton/country rock contacts, however, local space creation by stoping clearly was the method by which emplacement was completed.

Brown, M., 1994. The generation, segregation, ascent and emplacement of granite magma: The migmatite-to-crustally-derived granite connection in thickened orogens. *Earth-Sci. Rev.*, **36**, 83-130.

Brown, M., 1995. The late-Precambrian geodynamic evolution of the American segment of the Cadomian belt (France): Distortion of an active continental margin during south-west directed convergence and subduction of a bathymetric high. *Géologie de la France*, in press.

Brown, M., Averkin, Y.A., McLellan, E.M. and Sawyer, E.W., 1995a. Melt segregation in migmatites. *J. Geophys. Res.*, **100**, in press.

Brown, M., Rushmer, T. and Sawyer, E.W., 1995b. Mechanisms and consequences of melt segregation from crustal protoliths. *J. Geophys. Res.*, **100**, in press.

D'Lemos, R.S., Brown, M. and Strachan, R.A., 1992. Granite magma generation, ascent and emplacement within a transpressional orogen. *J. Geol. Soc. London*, **149**, 487-490.

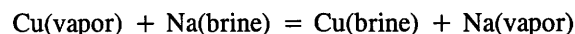
## Optimal Conditions for Porphyry Copper Ore Genesis Based on Experimental, Theoretical and Field Observations: An Overview

Candela, P.A.

*Laboratory for Mineral Deposits Research,  
Department of Geology, University of Maryland at  
College Park, MD 20742, USA*

Extensive experimental, theoretical and field investigations by the Laboratory for Mineral Deposits Research, have shed light on the optimal conditions for the generation of Porphyry Copper Deposits, and other granite-related mineral deposits.

Candela and Holland (1984) demonstrated that copper partitions strongly into a chloride-bearing supercritical gas phase from a rhyolitic melt at 1.4 kbar and 750°C. Williams *et al.* (1995) confirmed those results and showed, further, that 1) copper partitioning is enhanced at 1 kbar and 800°C relative to 1.4 kbar and 750°C; and, 2) copper partitioning is *not* further enhanced by changing the *P* and *T* to 0.5 kbar and 850°C. Further, whereas copper partitions strongly into a brine, as expected, the inferred exchange constant for the equilibrium:



was found to be on the order of unity.

Regarding the partitioning of copper into crystalline phases, the univalent copper that prevails during magmatic processes does not have an affinity for ferromagnesian minerals. The uptake of copper by magnetite, biotite and amphibole can be related to subsolidus alteration (Simon, 1995). Lynton *et al.* (1993) demonstrated experimentally that copper partitions strongly into pyrrhotite from a rhyolitic melt at 1 kbar and 800°C with  $D^{(p/m)}=775$  (averaged over oxygen fugacities of graphite - methane - (water) and nickel-nickel oxide). These results indicate that magmatic sulfides are important, potentially, in sequestering copper at the magmatic stage. Whereas these data are necessary to demonstrate that sulfides are important hosts for copper in intermediate to felsic magmas, they are not sufficient. In a discussion of the conditions for the generation of giant ore systems, Candela and Blevin (1995) have shown that the variation in the copper concentration in the units of the Boggy Plain Suite of the Lachlan Fold Belt is consistent with the removal of copper

by pyrrhotite crystallization. Given the pyrrhotite/melt partition coefficient of Lynton *et al.* (1993) and the data on pyrrhotite solubility in high K melts from Luhr (1990) a bulk partition coefficient for copper on the order of 1.5-2 is predicted. Further, given the Rayleigh fractionation formalism, treating the units of the Boggy Plain Suite as aliquots of melt, and assuming that Th is a perfectly incompatible element, yields a bulk partition coefficient for copper equal to  $1.83 \pm 0.17$  ( $1\sigma$ ). These results do not falsify the hypothesis that copper sequestration in intermediate to felsic systems is controlled by the crystallization of pyrrhotite.

The models of Candela and Holland (1986) and Candela (1989) showed that the critical variable for controlling the relative partitioning of a crystal-compatible element between crystalline phases and the magmatic volatile phase (MVP) is  $C_w^{l,o}/C_w^{l,s}$ , the ratio of the initial water concentration in the melt to the solubility of water in the melt. High values of  $C_w^{l,o}/C_w^{l,s}$  induce water saturation early, providing the MVP early access to copper dissolved in the melt.  $C_w^{l,o}/C_w^{l,s}$  is maximized when hot, wet magma is emplaced at high levels in crust. Further, the physical model of Candela (1991) suggests that interconnected volumes of the MVP are favored at upper crustal ( $P < 2$  kbar) conditions, facilitating the efficient removal of the MVP through spanning clusters of volumes of the MVP.

Piccoli and Candela (1994) showed, from an analysis of apatite, that the Cl/H<sub>2</sub>O in the Tuolumne Intrusive Suite of the Sierra Nevada Batholith, USA, decreases with increasing (<sup>87</sup>Sr/<sup>86</sup>Sr)<sub>i</sub>, suggesting that Cl/H<sub>2</sub>O is higher in more primitive melts in arc environments. Further, high oxygen fugacities (>QFM) promote sulfide destruction after volatile saturation, and oxygen fugacities higher than NNO + 3 log units may destabilize sulfides altogether.

In summary, we can now understand, in a preliminary manner, the conditions that *affect the probability of Porphyry Copper ore formation*. According to the theoretical hypothesis outlined herein, emplacement of primitive, oxidized, hot, and wet melts at shallow levels of Earth's crust with devolatilization at approximately 1 kbar (with ore deposition at shallower levels) is optimal, in accord with observations.

Candela, P.A., 1989. Magmatic ore-forming fluids: thermodynamic and mass transfer calculations of metal concentrations. In Whitney, J.A. and Naldrett, A.J. (eds), *Reviews in Economic Geology*, v. 4; *Ore Deposition Associated with Magmas*, Society of Economic Geologists Publishing Company, 203-221.

Candela, P.A., 1991. Physics of aqueous phase exsolution in plutonic environments. *Am. Mineral.*, **76**, 1081-1091.

Candela, P.A. and Holland, H.D., 1984. The partitioning of copper and molybdenum between silicate melts and aqueous fluids. *Geochim. Cosmochim. Acta*, **48**, 373-388.

Candela, P.A. and Holland, H.D., 1986. A mass transfer model for copper and molybdenum in magmatic hydrothermal systems: the origin of porphyry-type ore deposits. *Econ. Geol.*, **81**, 1-19.

Candela, P.A. and Blevin, P.L., 1995. Physical and chemical magmatic controls on the size of magmatic-hydrothermal ore deposits. In Clark, A.H. (ed), *Giant Ore Deposits-II*, QminEx Associates and Queen's University, 2-37.

Luhr, J.F., 1990. Experimental phase relations of water and sulfur saturated arc magmas and the 1982 eruptions of El Chichon volcano. *J. Petrol.*, **31**, 1071-1114.

Lynton, S.J., Candela, P.A. and Piccoli, P.M., 1993. Experimental study of the partitioning of copper between pyrrhotite and a high-silica rhyolitic melt. *Econ. Geol.*, **88**, 901-915.

Piccoli, P.M. and Candela, P.A., 1994. Apatite in felsic rocks: a model for the estimation of initial halogen concentrations in the Bishop Tuff (Long Valley) and Tuolumne Intrusive Suite (Sierra Nevada Batholith) magmas. *Am. J. Sci.*, **294**, 92-135.

Simon, A., 1995. *Copper in the Tuolumne Intrusive Suite: Is its behavior controlled by ferromagnesian phases*. Unpublished B.S. thesis, University of Maryland at College Park.

Williams, T.J., Candela, P.A. and Piccoli, P.M., 1995. The partitioning of copper between silicate melts and two-phase aqueous fluids: an experimental investigation at 1 kilobar, 800°C and 0.5 kilobar, 850°C. *Contrib. Mineral. Petrol.*, in press.

## **Hercynite-Bearing Granites and Associated Metasedimentary Enclaves from the Taltson Magmatic Zone, Alberta, Canada: A Natural Example of High-Temperature Pelite Melting.**

Chacko, Thomas and Creaser, Robert A.  
*Department of Geology, University of Alberta,  
Edmonton, Alberta, T6G 2E3, Canada*

The Taltson Magmatic Zone (TMZ) is the product of the 1.9-2.0 Ga collision between the Buffalo Head Terrane and the Churchill Craton (Ross *et al.*, 1991). This collision produced a large amount of strongly peraluminous granitoid (Goff *et al.*, 1986; Theriault, 1992). The present study focuses on a spectacular outcrop of one such granitoid and its associated metasedimentary enclaves. The rocks found at this outcrop (and in other parts of the TMZ) are remarkable in that the enclaves and some of the granites contain the high temperature mineral assemblage hercynitic spinel - quartz - garnet - cordierite ± sillimanite. Below, we argue that these enclaves are refractory vestiges

of the pelitic composition protolith that gave rise to the granitoids. Furthermore, we suggest that the granites have not travelled very far from their source region. As such, this locality is an excellent natural laboratory for studying high-temperature, peraluminous magmas at their point of origin.

The rocks in question are from Pelican Rapids (PR), a locality in northeast Alberta that is part of the regionally extensive Slave Batholith. The outcrop comprises two phases (I and II) of medium-grained, leucocratic, alkali feldspar granite. The sharp but sinuous contact between the two granite phases suggests that Phase I granite was still at high temperature and behaving plastically when intruded by Phase II. The two granites are very similar in field appearance and are distinguished from each other by relatively subtle mineralogical and textural differences. Phase I contains garnet, sparse biotite and mesoperthite as the only feldspar. Phase II granite lacks a primary mica but contains a small amount of plagioclase, hercynitic spinel, garnet and cordierite. Both phases of granite contain large (up to 60 meters across), lozenge-shaped enclaves of pelitic to psammitic composition paragneiss. The pelitic enclaves have migmatitic textures with variable amounts of quartz-alkali feldspar or quartz-rich leucosome. Interestingly, the accessory mineralogy of Phase II granite is identical to the mineral assemblage present in the enclaves. Thus, the enclaves and Phase II granite, although radically different in appearance, differ primarily in their modal proportions of minerals and their mineral textures.

Both granite phases are characterized by high  $\text{SiO}_2$  (>73 wt %) and low  $\text{FeO}+\text{MgO}$  (<2 wt %) but can be distinguished from each other on the basis of the higher  $\text{K}_2\text{O}/\text{Na}_2\text{O}$ ,  $\text{A}/\text{CNK}$ , REE and Th of Phase II. The pelitic enclaves show a large range in chemical compositions depending on the amount of migmatitic leucosome remaining in the enclave; however, enclaves with little leucosome are characterized by a very refractory composition (49%  $\text{SiO}_2$ , 29%  $\text{Al}_2\text{O}_3$ ). This suggests that the enclaves have been extensively melted and that some have experienced a large degree of melt extraction. This observation is consistent with the extreme temperatures (900-1000°C) derived for these samples using TWEEQU thermobarometry and quartz-garnet oxygen isotope thermometry (Farquhar *et al.*, 1994).

The high temperatures, the mineralogical similarities, the peraluminous composition of the granites and the refractory nature of the enclaves all point to a melt-restite relationship between the granites and pelitic enclaves. If

this is correct then first order Stokes law calculations indicate that enclaves as large as those at PR could not have been transported a great distance from their point of origin by the granite magma. Therefore, the PR outcrop represents the root zone of a regionally extensive, S-type granite batholith.

We suggest the protolith for the granites at PR was a high-Al pelite with a relatively low plagioclase content. The early-formed melts derived from this protolith (*i.e.*, Phase I) incorporated the plagioclase component leaving behind a residue rich in quartz, K-feldspar, sillimanite, and ferromagnesian minerals. Continued, higher temperature melting produced more potassic melts that were also richer in REE and Th (Phase II). These higher temperature melts, however, remained very leucocratic. This somewhat surprising result is consistent with recent experimental melting studies of true pelite bulk compositions (Patiño Douce and Johnston, 1991) which indicate that melts produced from such protoliths remain leucocratic to  $T > 1000^\circ\text{C}$ . Therefore, the term leucogranite should not necessarily be taken as synonymous with "low-temperature" granite.

Many questions remain regarding the PR outcrop. In particular, how were the high temperature conditions recorded at the outcrop generated during a collisional orogen? This question is especially enigmatic because field and geophysical data do not indicate the presence of any contemporaneous basaltic magmatism or underplating.

- Farquhar, J., Chacko, T. and Ellis, D.J., 1994. High-temperature oxygen isotope thermometry in two contrasting terranes, the Taltson Magmatic Zone, Canada and the Napier Complex, Antarctica. *Mineral. Mag.*, **58A**, 265-266.
- Goff, S.P., Godfry, J.D. and Holland, J.D., 1986. Petrology and geochemistry of the Canadian Shield of northeastern Alberta. *Alberta Res. Council Bull.*, **51**, 1-60.
- Patiño Douce, A.E. and Johnson, A.D., 1991. Phase equilibria and melt productivity in the pelitic system: Implications for the origin of peraluminous granitoids and aluminous granulites. *Contrib. Mineral. Petrol.*, **107**, 202-218.
- Ross, G.M., Parrish, R.R., Villeneuve, M.E. and Bowring, S.A., 1991. Geophysics and geochronology of the crystalline basement of the Alberta Basin, western Canada. *Can. J. Earth Sci.*, **28**, 512-522.
- Theriault, R.J., 1992. Nd isotopic evolution of the Taltson Magmatic Zone, Northwest Territories, Canada: insights into early Proterozoic accretion along the western margin of the Churchill Province. *J. Geol.*, **100**, 465-475.

## ORAL PRESENTATION

## Causes of Compositional Variation Within Granite Suites

Chappell, Bruce W.

*Department of Geology,  
Australian National University,  
Canberra, 0200, ACT, Australia*

Variation within granite suites potentially can be produced in several ways, which will be discussed with particular reference to the granites of the Lachlan Fold Belt (LFB).

*Magma mixing and/or mingling* is generally proposed in terms of blending a crustal melt and the mafic material from the mantle which caused that melting. The Bega Batholith is the largest I-type granite complex in the LFB and shows many features that have elsewhere been interpreted as supporting magma mixing, such as the development of local hybrids, common mafic enclaves in the more mafic granites, linear patterns on variation diagrams, and systematic changes in isotopic composition across the batholith. However, when suites from the batholith are examined in detail, there are features of the chemical variation that are not compatible with mixing on a scale that would have produced the major variations in those suites. Any difference in compositions at either end of the range in composition of a suite is also seen at the other end, so that both the most mafic and felsic rocks show similar relative abundances of particular elements. Since such observations are not consistent with magma mixing or mingling, it cannot have produced the major compositional variations. This observation is more widely applicable to the granites of the LFB, both I- and S-type.

*Assimilation of country rock* had no detectable role in producing variations within granite suites of the LFB. While such processes would be accompanied by fractional crystallization and therefore be more complex than the variations expected with magma mixing or mingling, the within-suite correlations between isotopic and chemical compositions that would be expected are not seen. For the Bega Batholith, the variations in isotopic compositions correlate with differences in chemical composition between suites, but not within suites, so that the incorporation of sedimentary material occurred before the partial melting of the source rock. It has been argued that the variations in isotopic compositions of the LFB granites resulted from mixing of basaltic material and granitic melt derived from

the melting of the Ordovician sedimentary rocks. However, the chemical compositions of many isotopically evolved I-type granites are not consistent with the addition of the amounts of sedimentary material that would have been required. Likewise, the chemical compositions of the S-type granites are not consistent with derivation from a mixture of basalt and the exposed sedimentary rocks.

*Fractional crystallization* played a dominant role in producing the variation in the Boggy Plain Supersuite, which shows textural and compositional features which clearly indicate that the rocks, which range from 50% to 75% SiO<sub>2</sub>, formed progressively as cumulates from a liquid or largely liquid magma. Most of the granites of the LFB area are so distinct from the Boggy Plain rocks that an origin by fractional crystallization is certainly not self evident. Moreover, there are specific patterns of chemical variation that either make an origin by fractional crystallization unlikely, or in some cases preclude it, except at the most felsic compositions. Many of the most felsic granites of the LFB, particularly the S-types, have trace element abundances that resulted from extended fractional crystallization of a magma that had approached or reached minimum temperature compositions through the loss of restite (below), although not all such granites evolved further in that way.

The *restite model* proposes that many granite suites contain crystals residual from melting, or restite, and that it is differences in the proportion of this restite that accounts for variation in composition. Melting within the crust will produce a magma comprising granitic melt in equilibrium with restite. The composition of a granite that results will be a function of the degree of separation between those two components. The difficulties of generating most of the granite suites of the LFB by the three processes discussed above are generally resolved with this model.

*Hydrothermal alteration* has the potential to greatly alter the composition of a granite. Destruction of feldspar has chemical effects analogous to those of feldspar fractionation at higher temperatures. The primary evidence for alteration is generally petrographic; however chemical data show that its effects are overrated. Many rocks in which there are petrographic signs of alteration plot in a very tight field or array on chemical diagrams, and for felsic granites the compositions are very close to minimum-temperature compositions, so that alteration occurred over a scale much smaller than that at which the rocks are sampled for chemical analysis.

## Plutons Emplaced in Dextral Strike-Slip Deformation Zones in the Abitibi Subprovince, Canada

Chown, E.H.

*Sciences de la terre, Université du Québec à Chicoutimi, Chicoutimi, Québec, G7H 2B1, Canada*

Numerous plutons in the Archean Abitibi Subprovince fall in the 2696 - 2692 Ma age bracket. The Colombourg (2696 Ma) and Franquet (2692 Ma) intrusions are representative of the two principal petrologic suites (monzodiorite and tonalite-granodiorite), and both occur adjacent to major southeast-trending dextral strike-slip faults. The strike-slip faulting is the final episode of regional deformation in the area.

The Colombourg pluton is an elongate southeast-trending mass bounded on the north and south by dextral strike-slip faults. The southern fault dies out near where it encounters the buttress of a large pre-existing tonalite-diorite complex just south of the intrusion site. The pluton is composed of quartz monzodiorite and granodiorite which grade almost imperceptibly into one another. The rocks are calc-alkaline, with LREE enrichment patterns similar to other intrusions of the monzodiorite suite. Magmatic foliation within the pluton defines a shallow northwest plunging trough, with steep sides and a prominent NW plunging lineation. Magmatic foliation is defined by alignment of xenoliths and hornblende and plagioclase grains. A later submagmatic foliation is subvertical and parallel to the foliation in the bounding faults. This foliation is defined by polygonized quartz, bent and broken biotite and plagioclase. Pressure estimates using the Al-in-hornblende barometer give two signatures at 2.2 kbar and 3.2 kbar suggesting that the lower value indicates the emplacement and the higher denotes earlier crystallization in a subjacent magma chamber. The unique shape and position of the intrusion suggest that it was emplaced where the principal displacement on the strike-slip faults shifted from south to north forming a left-stepping dextral pull-apart.

The Franquet stock, although outwardly appearing to be a standard subcircular pipe, is a composite stock formed of an inner L-shaped dyke of granodiorite enclosed in a later fine-grained leucogranodiorite phase, occurring between two branches of dextral strike-slip fault which splits around the resistant mass of an earlier tonalite batholith. The central dyke is north-south parallel to the local tensional

direction, with the L-extension along the north-bounding fault. The outer partial rim of leucogranodiorite fills the angle of the L. This calc-alkaline series evolves from metaluminous to peraluminous. Pressure estimates using the Al-in-hornblende barometer indicate an emplacement pressure of 1.75 kbar with an early-crystallization signature of 2.3 kbar. The reverse-zoned stock formed in a right-stepping dextral pull-apart structure, and is possibly a pipe feeding a higher level intrusion, but more likely a cupola rising from a differentiating body at depth.

The study shows that deformation-related plutons may take on a variety of forms in response to local conditions, and that the late strike-slip faulting episode of regional deformation exercised considerable control on pluton emplacement.

## Granites, Subduction, and Extension in the Basin and Range Province, Western USA

Christiansen, Eric H.

*Department of Geology, Brigham Young University, Provo, Utah 84602, USA*

Two plutons emplaced only 15 km apart and separated in time by about 13 Ma illustrate the contrasting compositional effects of subduction and extension on granite geochemistry. The Desert Mountain granite (34.8 Ma) and the Sheeprock granite (21.4 Ma) are both small, shallowly emplaced plutons. The older Desert Mountain pluton formed above a gently dipping slab of subducting oceanic lithosphere; it was emplaced in a southward migrating zone of magmatism that transected the Great Basin during the middle Tertiary. Late Tertiary normal faults cut the pluton and may have tilted it. The pluton is slightly peraluminous and comprised mostly of biotite monzogranite with titanite, magnetite, ilmenite, zircon, and apatite. Magnetic susceptibilities of the pluton average 0.015 SI units - typical of magnetite-series granites. The Desert Mountain granite appears to have crystallized at a relatively high oxygen fugacity - based on its mineral assemblage and low Fe/Mg ratios in the mafic silicates. It has trace element concentrations and patterns typical of subduction-related granites on continents, including deep Nb and Ti anomalies. Mineralization related to the granite consists of partially oxidized Cu deposits and F- and metal-poor greisen. Isotopic ratios are typical of middle Tertiary granites from this region ( $(^{87}\text{Sr}/^{86}\text{Sr})_i = 0.709$  and

$\epsilon_{Nd} = -18$ ) and consistent with a major contribution from felsic crust of Proterozoic age known to underlie the eastern Great Basin. Heat for crustal melting was apparently derived from mafic magmas generated in the subduction zone. Contemporaneous andesites are apparently mixtures of crust and mantle components.

The younger Sheeprock granite was emplaced after the subducting slab had slipped away to be replaced by warm asthenosphere. This is also near the beginning of the episode of late Tertiary extension that formed the Basin and Range province. The pluton consists of monzogranite with zircon, fluorite, monazite, thorite, uraninite, complex Ta-Nb-Sn-W-Fe-Ti oxides and local topaz, beryl, zinnwaldite, and muscovite. It is also slightly peraluminous, but appears to have crystallized at a low oxygen fugacity based on the Fe-rich character of the biotites and low magnetic susceptibilities (0.001 SI units - typical of ilmenite-series granites). The Sheeprock granite has high concentrations of incompatible trace elements and fluorine and is similar in composition and mineralogy to topaz-bearing rhyolites erupted contemporaneously in the region. Mineralization consists of scattered clots of beryl - albite - zinnwaldite - muscovite and thin veins of W- and Sn-rich greisen with F-rich muscovite. The trace element pattern of the Sheeprock granite is typical of other highly evolved granites and, in many respects, to those of anorogenic granites. Nb concentrations approach 100 ppm and Rb concentrations 1000 ppm. However, contributions from old felsic continental crust are limited by the isotopic composition of the pluton ( $(^{87}\text{Sr}/^{86}\text{Sr})_i = 0.706$  and  $\epsilon_{Nd} = -6$ ). Perhaps, the magma was derived by partial melting of young mafic crust underplated during the middle Tertiary, but it is difficult to obtain fluorine-rich magmas with low oxygen fugacities by this process. Alternatively, the source may be granulite-facies Proterozoic rocks in the lower crust. The elevated concentrations of fluorine and low oxygen fugacity are more easily explained by the latter hypothesis. In either case, lithospheric extension appears to have been important because it allowed very small melt fractions (less than 10%) to accumulate and migrate upwards without mixing with contemporaneous mafic magmas. Heat for partial melting was probably provided by: 1) replacement of the cold lithospheric slab by hot asthenosphere when subduction ceased; 2) consequent extension, uplift, and crustal thinning; and, 3) emplacement of hot but dense mafic magma at the base of the crust.

## Respective Roles of Source Composition and Melting Conditions in the High-K Content of Some Magmas: Geochemical Constraints

Cocherie, Alain and Rossi, Philippe  
BRGM, B.P. 6009,  
F-45060 Orléans Cedex 2, France

The origin of potassic to ultrapotassic rocks, which are also Mg-enriched, is still not clear. Such rocks occur in the Variscan batholiths of Europe (Bohemia, Vosges, Alps, Corsica), and we have studied the respective roles of source composition and melting conditions in the formation of acid and intermediate components emplaced contemporaneously with mafic components.

Special attention was paid to occurrences in Corsica and Bohemia. Major- and trace-element data indicate similar geochemical characteristics for all rocks of the Mg-K associations, *i.e.* high Mg, Co, Cr and Ni concentrations, high contents of incompatible elements ( $\text{K}_2\text{O}$ , Rb, Cs, LREE, Th, U, Zr, Hf, *etc.*), and strong REE fractionation without large Eu anomalies. Mineral composition varies only slightly from mafic to felsic rock-types. These points indicate a genetic link between rocks found in the same area, but isotope data rule out such a link. A common origin for granites ranging from monzodiorite to leucosyenogranite is possible, as indicated by trace-element isotope data, but mafic rocks show a wide range of variation for Sr and Nd initial ratios, suggesting a mixing process between two end-members consisting of mantle-derived material and a crustal component. According to the isotope data, the crustal component appears to be  $^{87}\text{Sr}$ -enriched and  $^{143}\text{Nd}$ -depleted, compared to the associated granite source. The most contaminated mafic rocks show REE, Sr and Nd evidence of a crustal end-member resembling that of normal detrital sedimentary rock, with a flatter HREE pattern, and higher  $^{87}\text{Sr}/^{86}\text{Sr}$  and lower  $^{143}\text{Nd}/^{144}\text{Nd}$  ratios than Mg-K granite. The  $\text{K}_2\text{O}/\text{Na}_2\text{O}$  ratio also decreases as a function of the importance of the crustal component. In other words, the high  $\text{K}_2\text{O}$  and LREE contents seem characteristic of a mantle-derived magma, but not of the associated Mg-K granites, nor of any other crustal component.

Thus, based on the geochemical data of mafic Mg-K and associated acid rocks of Corsica, at least three end-members are involved.

A mantle end-member shows isotope compositions of syenomonzonite:  $(^{87}\text{Sr}/^{86}\text{Sr})_i = 0.7046$ ;  $\epsilon_{\text{Nd}}(t) = +0.7$  and  $\delta^{18}\text{O} = +6$  ‰. Several models have been proposed for the origin of a highly potassic mantle-derived magma: 1) an extremely small degree of partial melting of garnet-peridotite mantle material; 2) fusion of a metasomatized mantle source; 3) zone refining; 4) leaching of wall rock leading to an enrichment of incompatible elements during ascent of the melt; and, 5) separation of very small melt fractions from a thick mantle layer and accumulation in a metasomatized layer, which, upon remelting, would yield a strongly potassic magma. In our opinion, if metasomatic fluids are involved, their main role would be to favour the melting process, which could take place as a two-stage-model: a phlogopite- ( $\pm$ garnet) bearing source melts at  $\sim 200$  km depth; and the rising magma induces a zone-refining process in the traversed mantle, leading to a significant increase of incompatible elements and LREE, whereas the isotope characteristics of the melt retain their mantle affinity, despite the increase in Sr and Nd concentrations.

A second end-member is typical detrital material. Its interaction with the  $\text{H}_2\text{O}$ -enriched mafic mantle-derived magma will lead to flatter LREE patterns of the most contaminated syenomonzonites.

A third source has the isotope composition of granitic rocks:  $(^{87}\text{Sr}/^{86}\text{Sr})_i = 0.706$ ;  $\epsilon_{\text{Nd}}(t) = -3$  and  $\delta^{18}\text{O} = +8$  ‰. Using trace elements and especially REE, we found that partial-melting of a non-modal batch ( $F = 0.3$ ) of dry granulite with a graywacke composition fits monzodiorite data. Under wet melting conditions, this protolith could yield a calc-alkaline monzogranitic magma, characterized by the same isotopic feature and a distinct chemical composition compared to high-Mg-K granites. High Mg-K granites from Bohemia and the Vosges show similar chemical compositions as the same rock types from Corsica, but with another isotopic signature (*i.e.* Pb).

## ORAL PRESENTATION

### **S- and I-Type Granitoids of the Eastern Lachlan Fold Belt: Three-Component Mixing, Not Restite Unmixing**

Collins, W.J.

*Department of Geology, University of Newcastle, Newcastle, NSW 2308, Australia*

425-400 Ma old I-type granite suites of the eastern Lachlan Fold Belt (LFB) show strong linear chemical variation, which is considered to reflect crystal fractionation from parent magmas with  $\sim 60\%$   $\text{SiO}_2$ , rather than restite unmixing from intermediate-composition source rocks. The characteristic chemistry of I-type suites is evident in coeval gabbroic complexes, indicating an intrinsic link. The I-types are a mix of subordinate gabbroid, representing mantle-derived melts, and a dominant metaigneous, 500 - 600 Ma old lower crustal component, identified from Nd isotopic data and the ages of inherited zircons in granites and mafic enclaves. Mafic microgranular enclaves are considered to be the final vestiges of the mixing process, reflecting mingling of contaminated, mantle-derived melts with granite magma in high-level, almost-solidified plutons.

S-type granite suites of the eastern LFB are not chemically imaged by any metasediment of Early Palaeozoic or Proterozoic age in eastern or central Australia, but the zircon populations from S-types and Ordovician LFB sediments fall into similar patterns of age groups. Furthermore, gneissic metasedimentary inclusions in S-type granites closely approximate the Ordovician sediments, implying a genetic link. The Cooma granite is "remobilized" Ordovician sediment and represents one of the few restite-controlled granites in the LFB. It formed at 3.5 - 4 kbar, whereas most S-types were generated at 4 - 5 kbar. Chemical tie-lines between Cooma granite and mafic I-type Jindabyne tonalite encompass almost all mafic S-type granites of the vast Bullenbalong suite, for all elements, consistently in the proportion Jindabyne:Cooma, 30:70. This 30:70 mix corresponds to the Bullenbalong parent magma, and chemical variation in the suite is a response to crystal fractionation.

A three-component mixing model is presented, whereby mantle-derived basaltic magmas intruded, melted, and mixed with metaigneous lower-crust to produce I-type

granites in the LFB. Continued underplating and intra-plating of mantle material expanded the elevated geotherms into the mid-crust (~15 km depth), where locally underthrust Ordovician metasediment was remobilized and mixed with the hybrid I-type magmas to produce S-type granites. Therefore, S-type granites of the LFB are heavily contaminated I-types. The model is consistent with the simple Nd-Sr-O-Pb isotope mixing arrays defined for LFB S- and I-type granites. The remarkable east-west, chemical and isotopic asymmetry across the Bega Batholith demonstrates a progressive westward increase of Ordovician metasediment that mixed with the I-type granitoid magmas, as the thickened crustal welt generated by the ~430 Ma old "Benambran Orogeny" is approached. The model explains the paucity of I-types in areas dominated by S-types, and their later emplacement. Finally, the mixing model implies that Proterozoic continental basement does not exist, which is consistent with the known tectono-stratigraphy of the LFB.

### **Pervasive Magma Transfer Through the Lower Middle Crust During Non-Coaxial Compressional Deformation: an Alternative to Diking**

<sup>1</sup>Collins W.J. and <sup>2</sup>Sawyer, E.W.

<sup>1</sup>*Department of Geology, University of Newcastle, Newcastle, NSW 2308, Australia*

<sup>2</sup>*Sciences de la Terre, Université du Québec à Chicoutimi, Chicoutimi, Québec, G7H 2B1, Canada*

Theoretical studies of diapirism and diking suggest that these are efficient mechanisms of magma transfer through the crust. We examine the structural location of leucosomes and granitoids in the deep crust of the Arunta Inlier in central Australia to test whether these were the actual mechanisms of magma transfer.

At Mt. Hay, granitoid magmas migrated through the middle-lower crust during a period (D1 - D4) of WSW-directed thrusting. The magmas utilized whatever channels were locally available, *i.e.* opportunistic use of existing folds, boudins and shear zones, or created new channels by magmatic fracture either parallel to layering or, much less commonly, in irregular arrays. Because the channelways were principally fold hinges, or controlled by the orientation of layering anisotropy (S0 or S1), the melt

could not migrate vertically, but rose buoyantly parallel to the regional elongation direction, which is defined by coaxial folds and a strong elongation lineation. As a result of these factors, melt transfer in the Mt. Hay area was not focussed along a few conduits (*i.e.* dikes), but was distributed over a wide area and occurred through a diverse network of various structurally-linked channelways.

The upper middle crust of the Anmatjira - Reynolds Range area contains abundant granitoid sheets that are of similar age, geochemistry and structure to granite leucosomes in the deeper Mt. Hay region. Thus, granitic melts formed at the base of the continental crust are believed to have passed through the middle-lower crustal level (25-30 km) exposed at Mt. Hay and accumulated, in batholithic proportions, at shallower crustal levels (12-20 km) represented by the Anmatjira - Reynolds Range area.

The observations demonstrate that magmas are capable of pervasive migration through, and accumulation in, the crust during a major compressive, non-coaxial shear deformation because the crust is anisotropic and, therefore, deforms heterogeneously to create innumerable interconnected dilatant sites. Diking is expected to be the principal magma transfer mechanism in comparatively isotropic crust.

### ORAL PRESENTATION

### **Radiogenic Isotopes in Granitic Systems: Studies of Melting and Mixing at the Source**

Creaser, Robert A.

*Department of Geology, University of Alberta, Edmonton, Alberta, T6G 2E3, Canada*

Radiogenic isotope systems (Sr, Nd, Pb) play a critical role in many aspects of granite petrology, such as evaluating petrogenetic models, interpreting deep crustal characteristics and tectonic studies. Isotopic studies of granites are, by nature, removed from the mechanisms by which magmas are produced; we typically only see (and analyze) the products of larger-scale tectonothermal processes once granitic magmas move from their formation region. Intuitively, this does not present any limitations, as radiogenic isotopic systems should directly record the characteristics of source region(s) or component(s) of

formation; granites, after all, are "images of their sources". However, model studies of Pb isotopes in granites have advocated large Pb isotopic shifts between melt and source as a result of differential mineral solubility. Models of crustal heating by basalt intrusion suggest melting on very short timescales ( $< 0.01$  Ma); far less than timescales required for (diffusional) isotopic equilibration of a protolith. To better constrain the meaning of isotopic signatures carried by granites, studies of granites at their source have been undertaken. The localities reported on here cover two popular models for granite origins, namely partial melting of crustal rocks and magma mixing in a mafic-felsic magma system.

Granite and associated high-grade metasedimentary enclaves from Pelican Rapids (PR) in NE Alberta are part of the 1.93 Ga Slave Batholith from the Taltson Magmatic Zone. The outcrop at PR comprises three phases of leucocratic granite (migmatitic leucosome, Phase I, Phase II) containing large (up to 60 m), refractory enclaves of pelitic to psammitic paragneiss showing evidence of extensive partial melting and granite production. *P-T* estimates are 6-8 kbar, 900-1000°C for granites and enclaves. When compared with experimental melt compositions, granites from leucosome to Phase I to Phase II appear to represent sequentially higher degrees of partial melting from a pelite source. Geochemical data support this hypothesis, particularly REE and Th contents which systematically increase with degree of melting reflecting increasing monazite solubility. Refractory pelitic xenoliths yield  $\epsilon_{Nd}$  values of -4 to -7. Leucosome and Phase I granites yield  $\epsilon_{Nd}$  values of -10 to -11, and Phase II granite -5 to -6.  $t_{DM}$  values for these granites differ by  $>1$  Ga. At face value, these data indicate that the leucosome and Phase I granites are unrelated to the refractory enclaves, despite intimate field and geochemical relationships. Alternatively, these systematics can be explained by partial melting of a pelite where Nd isotopic budget of a melt is controlled by the melting behavior (solubility) of two mineral phases (garnet and monazite) with vastly different Sm/Nd and Nd isotopic compositions at the time of melting. Significant isotopic contrasts can be produced between a (total-rock) protolith and the initial partial melts. Later, higher-temperature, melts approach the source (total-rock) isotopic composition as diffusion- and recrystallization-driven isotopic equilibration occurs.

Field evidence of mafic-felsic magma interaction occurs in the Campanas Igneous Complex (CIC), Argentina. The CIC comprises the Campanas Granite (CG) which is intruded by mafic dikes and zoned mafic intrusions (ZMI).

The ZMI, which consist of gabbroic cores surrounded by concentric rings of diorite, tonalite and granodiorite, extend in an approximately 6 km long N-S band along the central axis of the CIC. Major and trace element abundances vary systematically from the core of each ZMI to the surrounding CG. Samples of CG close to the ZMI have lower abundances of  $SiO_2$  and incompatible elements than samples far from the ZMI, reflecting chemical interaction with the ZMI. The ZMI are heterogeneous in composition and contain mineral disequilibrium features such as reverse zoned plagioclase and quartz ocelli. Sr and Nd isotope analyses along a profile from the gabbro to the granite define a mixing curve in Nd-Sr isotopic space with  $\epsilon_{Nd}$  variations from +4 to -3 and  $\epsilon_{Sr}$  variations from -60 to +60; the Sr data likely reflect, in part, secondary processes after crystallization of the  $468 \pm 3$  Ma CIC. This wide isotopic variation occurs in samples separated from each other by only a few meters, highlighting the absence of diffusion-controlled isotopic equilibration in this mixing system. Petrographic, geochemical and isotopic data suggest that the evolution of the complex was controlled by fractional crystallization and replenishment of mafic magma inside a granite magma chamber, followed by extensive magma mixing between the CG and the fractionated end-members of the ZMI to produce intermediate calc-alkaline rocks.

### Granitoid Magmatism and Crustal Evolution in the Southwest Baltic Shield.

<sup>1</sup>Darbyshire, D.P.F., <sup>2</sup>Brewer, T.S.,

<sup>3</sup>Larson, S.-Å. and <sup>3</sup>Åhäll, K.-I.

<sup>1</sup>NERC Isotope Geosciences Laboratory, Kingsley Dunham Centre, Nottingham NG12 5GG, UK

<sup>2</sup>Borehole Research Group, Department of Geology, Leicester University, Leicester LE1 7RH, UK

<sup>3</sup>Institute of Geology, University of Göteborg, S-412 96 Göteborg, Sweden

The Baltic Shield forms the major exposure of Precambrian crust in northern Europe and is the principal component of Fennoscandia, one of the crustal segments of the East European Craton. Crust in the Baltic Shield defines a simple age pattern, with the Archaean in the north east and progressively younger Proterozoic terranes to the south and west. The northern Archaean nuclei provided a

cratonic region onto which the Palaeoproterozoic Svecofennian juvenile arc terranes were accreted between 1.9 - 1.8 Ga. This accretionary event represents a major episode of juvenile crustal growth, which was followed by the intrusion of granitoids in the Transscandinavian Igneous Belt (TIB) and by rapakivi magmatism in Finland, Estonia, Russia and Sweden, between 1.8 and 1.65 Ga. The final stages of Proterozoic crustal growth in the Baltic Shield are recorded in the southwest Scandinavian Domain. Here Palaeoproterozoic juvenile arc accretion and crustal growth occurred between 1.76 - 1.61 Ga and is post dated by granitoid intrusions of the Göteborg Batholith. Subsequent crustal development in the southwest Scandinavian Domain involved extensive reworking during the Meso- and Neoproterozoic. The last event prior to cratonisation of the crust in this domain was the intrusion of mafic and felsic plutons at 1.56 Ga.

The Transscandinavian Igneous Belt (TIB) is a c.1600 km long by 20-150 km wide belt composed predominantly of granitoid intrusions emplaced on the western margin of the Svecofennian Province. Published U-Pb zircon geochronology indicates magmatism in the interval 1.81-1.65 Ga, although within the belt there appear to be three discrete magmatic episodes termed TIB 1 (1.81 - 1.77 Ga), TIB 2 (1.7 Ga) and TIB 3 (1.68 - 1.65 Ga). In SW Sweden TIB 1 magmatism appears to predominate on the eastern side of the belt, whereas TIB 2 and 3 plutons outcrop on the western side. The granitoids range in composition from quartz monzonites to granites, having I- or transitional A-type geochemical affinities. TIB 3 plutonism is synchronous with the earliest rapakivi magmatism in Finland.

The Göteborg Batholith (GB) comprises c. 1.59 Ga granitoids which outcrop in the western part of SW Sweden and in the Western Gneiss Region of Norway. The granitoids range from tonalites to granites, although granodiorites are the most abundant, and all have I-type affinities. Both the TIB and GB granitoids formed after a hiatus of juvenile Proterozoic crustal accretion, but they display contrasting geochemical signatures.

This study seeks to provide a better understanding of the origin of the magmatism and its relationship to crustal evolution in the southwest Baltic Shield. Any genetic model for this region must accommodate the differing styles of plutonism and in particular, the rapakivi magmatism.

The TIB is characterised by  $\epsilon_{\text{Nd}}$  values of 0.7 to 2.8 and depleted mantle model ages ( $t_{\text{DM}}$ ) of 1.94 - 2.11 Ga. There appears to be a trend towards more depleted

signatures with time which is consistent with the whole rock geochemistry. The Nd-isotope systematics suggest derivation from a juvenile source, such as the Svecofennian crust, with the addition of a mantle component. In SW Sweden there is no evidence for a significant Archaean contribution to the TIB. The 1.59 Ga GB plutons yield more depleted  $\epsilon$  values of 1.6 to 4.2 and  $t_{\text{DM}}$  of 1.71 - 1.89 Ga, indicating a larger mantle component than is seen in the TIB granitoids.

The final episode at 1.56 Ga produced granites with  $\epsilon_{\text{Nd}}$  of 2.4 to 3.6 and  $t_{\text{DM}}$  1.74 - 1.82 Ga. These Nd isotope signatures are more depleted than those displayed by the synchronous rapakivi plutons in Finland which would suggest either derivation from a different source or melting at different crustal levels.

Arc accretion processes have significantly influenced the whole rock and isotope geochemistry of Proterozoic granitoids in the southwest Baltic Shield. The Svecofennian terrane, formed by the amalgamation and accretion of 2.1 - 1.9 Ga juvenile arcs, was the major source component for the TIB plutons. In the southwest Scandinavian Domain, a later episode of arc accretion 1.76 - 1.61 Ga provided a more juvenile source for the Göteborg Batholith.

### S-type Granites in the Northern Slave Province, Northwest Territories, Canada?

Davis, A.M. and Krogstad, E.J.

*Isotope Geochemistry Laboratory,  
Department of Geology, University of Maryland  
at College Park, MD 20742, USA*

The Archean Slave Province, located in the Northwest Territories, Canada, comprises c. 2700 Ma supracrustal belts, which include gneiss fragments older than 2900 Ma in the western Slave, separated and intruded by c. 2600 Ma granitoid rocks (Isachsen and Bowring, 1994). Davis and Hegner (1992) found  $\epsilon_{\text{Nd}}(2600 \text{ Ma}) = -6$  to 0 for late granites in the western central Slave Province and +1 to +4 for late granites in the east, indicating that long term LREE enriched basement is present in the western Slave Province and not in the east. In the northern Slave Province, late Archean (c. 2600 Ma) granites of the Kangguyak gneiss, Anialik River, High Lake, Torp Lake, and Hood River supracrustal belts, have  $\epsilon_{\text{Nd}}(2600 \text{ Ma}) = -2$  to +1.

These data can be interpreted to mean that the granites had isotopically homogeneous source materials that were somewhat evolved compared to "depleted mantle". A petrogenetic model for the granites involves mixing of magmas from long term LREE depleted (mantle) and long term LREE enriched (continental crust) sources. Alternatively, the late Archean granite magmas may have been derived exclusively from supracrustal sources. Two groups of granite REE patterns can be explained by a model that involves melting of materials chemically similar to supracrustal rocks exposed in the Slave Province. Country rocks include metavolcanic units with  $\epsilon_{Nd}(2600 \text{ Ma}) = -1$  to  $+2$ , and heterogeneous gneisses with  $\epsilon_{Nd}(2600 \text{ Ma}) = -8$  to  $-7$  and  $t_{DM} = 3200 \text{ Ma}$ . Some granites with  $Ce_N/Yb_N = 4$  to  $8$  (e.g., Chin Lake Stock of the Anialik River Belt) may have been derived by 10-20% partial melting of metavolcanic rocks, whereas other granites (e.g., Tough Run and Torp Lake granites) with steeper patterns ( $Ce_N/Yb_N > 11$ ) may have been derived by melting of metasedimentary rocks. Long term LREE enriched continental crust was not necessarily a component of the sources of c. 2600 Ma granite.

Davis, W.J. and Hegner, E., 1992. Neodymium isotopic evidence for the tectonic assembly of Late Archean crust in the Slave Province, northwest Canada. *Contrib. Mineral. Petrol.*, **111**, 493-504.

Isachsen, C.E. and Bowring, S.A., 1994. Evolution of the Slave craton. *Geology*, **22**, 917-920.

## Microgranitoid Enclaves and Associated Intrusives: A Comparative Petrographic and Geochemical Study

Dean, A.A.

*Department of Earth Sciences, Monash University,  
Clayton 3168, Australia*

Rame Head and Petrel Point are prominent rocky headlands, within Croajingolong National Park, 25 km southwest of Mallacoota, East Gippsland, Victoria, Australia. The headlands comprise granitic outcrop that contains abundant microgranitoid enclaves and closely related dyke-like minor intrusive bodies. This plutonic complex intrudes folded Late Ordovician age metasediments of the Bega basement terrane, and is considered a component of the eastern arm of the composite "I-type" Bega batholith (390-400 Ma), within the

Palaeozoic Lachlan Fold Belt of southeastern Australia.

Sr-Nd-Pb isotopic systematics indicate a more primitive character for some intrusives of the Bega batholith than those elsewhere in the Lachlan Fold Belt (e.g.  $(^{87}\text{Sr}/^{86}\text{Sr})_i \sim 0.7041$ ,  $\epsilon_{Nd} \sim +3.0$ ; McCulloch and Chappell, 1982). It has been suggested that the eastern arm intrusives, close to the supposed margin of the Australian continental plate, exhibit isotopic evidence for limited mixing associated with underplating and late stage intrusion into the crust of mantle-derived magmas. (McCulloch and Woodhead, 1993).

Investigations of field and microstructural relationships have given insights into physical and chemical evolution within the Croajingolong plutonic complex. Four granitoid phases that exhibit distinct lithological features were determined in the field. Petrographic and geochemical evidence confirms these initial distinctions. The lack of chilled margins and sharp contact relationships indicate simultaneous intrusion of several fluid magmas that may have interacted.

The predominant granitic phase is a weakly foliated coarse grained biotite granodiorite. The generally fine grained ovoid enclaves (usually between 10 mm - 1 m in diameter) are of biotite microgranodiorite to microdiorite composition and have a lower quartz and higher mafic content ( $\pm$ hornblende) relative to the host granodiorite. There is considerable variation in enclave abundance. Where densely packed swarms occur enclaves exceed 70% of the total rock volume. In other areas they comprise < 20%. The enclaves are typically ellipsoidal and preferential alignment of some minerals defines an incipient magmatic foliation. Within the microgranitoid enclaves there is a gradation from homogeneous fine grained to coarser grained with megacrysts of zoned plagioclase. Feldspar megacrysts also accumulate around enclaves within swarms. Schlieren swirls are common.

Enclave/host granodiorite contacts are generally sharp and featureless, marked by a change in crystal size and corresponding increase in mafic content which in some enclaves forms a concentrated rim. Textural analysis shows primary igneous quench textures. Acicular apatite is abundant throughout enclaves. Megacrysts within enclaves show clear evidence of textural and chemical disequilibrium with their surroundings. Electron microprobe analyses distinguish complex compositional zoning. Plagioclase megacrysts have overgrowth rims more calcic than most core regions.

Microgranitoid enclaves and the mafic dike-like intrusives have similar petrographic and geochemical

characteristics. However, the hornblende present within the dyke-like bodies is usually prismatic and megacrysts are rare. Dyke-like bodies have convoluted margins and disaggregate into pillow-like enclaves indicating a genetic, spatial and temporal relationship between the two.

This study represents the initial stages of a research program that will incorporate data from several areas within the Lachlan Fold Belt that also contain spatially and temporally related mafic and felsic intrusives. Trace element abundances and isotope systematics will be used to support observations and to indicate likely cogenetic relationships.

McCulloch, M.T. and Chappell, B.W., 1982. Nd isotopic characteristics of S- and I-type granites. *Earth Planet. Sci. Let.*, **58**, 51-64.

McCulloch, M.T. and Woodhead, J.D., 1993. Lead isotopic evidence for deep crustal-scale fluid transport during granite petrogenesis. *Geochim. Cosmochim. Acta*, **57**, 659-674.

## ORAL PRESENTATION

### **New Experimental Constraints on the Physical Properties of Granitic Melts**

Dingwell, D.B., Hess, K.,  
Knoche, R. and Webb, S.L.

*Bayerisches Geoinstitut, Universität Bayreuth,  
95440 Bayreuth, Germany*

The determination of physical properties of granitic and pegmatitic melts under the conditions of pressure and temperature relative to their emplacement in the Earth's crust provide valuable physical constraints on the behavior of such magmatic systems during igneous petrogenesis. The superliquidus properties of melts of relatively low viscosity are reasonably well-constrained by experimental geochemical investigations where methods borrowed from the metallurgical and glass sciences have been applied to geologically relevant compositions. The low viscosities that are a prerequisite for most of these conventional methods preclude the direct determination of the physical properties of relatively viscous granitic and pegmatitic melts using such conventional means.

Recently, we have begun to employ methods more commonly used for glass-ceramics and extremely viscous glassmelts in order to obtain much new data for the properties of granitic and pegmatitic melt compositions at

the low temperatures relevant to their intrusion and crystallization. We are in the process of applying these methods to hydrothermal pressures.

The data for the supercooled liquids, at temperatures just above the glass transition, are complementary to those obtained at superliquidus temperatures on the same compositions. Such metastable liquids generate, in general, values of expansivity and activation energy of viscosity that are considerably higher than the values obtained from the superliquidus determinations. Nevertheless, both data sets (supercooled and superliquidus) are completely reconcilable with each other through a temperature-dependence of the expansivity and of the activation energy of viscosity. These complementary data sets provide strong constraints on the interpolation of temperature-dependence property data to the intermediate temperature range relevant to crystallization of granitic and pegmatitic melts. With the examples of viscosity and density we illustrate the development of multicomponent studies of the temperature-dependence of the viscosity of melts and the temperature-dependent density of melts in the multicomponent system  $\text{SiO}_2$  -  $\text{Al}_2\text{O}_3$  -  $\text{Na}_2\text{O}$  -  $\text{K}_2\text{O}$  -  $\text{Rb}_2\text{O}$  -  $\text{Cs}_2\text{O}$  -  $\text{Li}_2\text{O}$  -  $\text{BaO}$  -  $\text{SrO}$  -  $\text{CaO}$  -  $\text{MgO}$  -  $\text{TiO}_2$  -  $\text{B}_2\text{O}_3$  -  $\text{P}_2\text{O}_5$  -  $\text{F}_2\text{O}_{.1}$  -  $\text{Ta}_2\text{O}_5$  -  $\text{Nb}_2\text{O}_5$  -  $\text{WO}_3$ .

The systematics of the viscosity-temperature relationships are discussed in terms of the structural contribution of each added oxide to the granitic melt base. The density data are inverted to partial molar volumes for each component. The development of a database including the effects of water on these properties using the methods outlined above is in progress.

### **Generation, Ascent and Emplacement of Granitic Magma in the Northeastern Gander Zone, Newfoundland Appalachians**

D'Lemos, R.S., King, T.R.,  
Pembroke, J.W. and Tribe, I.R.

*Geology and Cartography Division,  
Oxford Brookes University, Oxford, OX3 0BP, UK*

Ordovician to Devonian deformation, migmatization, and granite emplacement within the Gander Zone of northeastern Newfoundland resulted from the closure of Iapetus and transcurrent docking of Avalon (Gondwana)

with North America. From west to east, Gander Zone rocks pass transitionally from low greenschist facies Gander Group metasediment to upper amphibolite facies migmatite, coincident with an increase in structural complexity and intensity of deformation and volume of granite intruded. The migmatitic region is characterized by the *c.* 425 Ma Hare Bay Gneiss and occupies a *c.* 20 km wide zone of syn-migmatization sinistral shear adjacent to the Avalon - Gander boundary. Sillimanite is the dominant aluminosilicate within the migmatites, although andalusite rimmed by muscovite and sillimanite occurs rarely. Mineral reactions, amphibole - plagioclase geothermometry and  $X_{Mg}$  cordierite, indicate high-temperature and low-pressure anatexis (*c.* 640-740°C, 4-5 kbar) requiring high geothermal gradients.

Sm-Nd isotopic characteristics of metasedimentary rocks, gneisses and intrusive granitoids place some constraints upon their origins. A marked similarity in  $\epsilon_{Nd}$  (-8 - -6) for low grade Gander Group metasediments and sillimanite paragneisses of the Hare Bay Gneiss are most consistent with derivation from the same protolith. Despite some open system behavior these isotopic signatures can be traced into zones of local (contact) and regional migmatization and partial melting fingerprinting the possible contribution to granite magmatism. Voluminous Silurian and Devonian granites ( $\epsilon_{Nd} = -5 - 0$ ) were not derived from such a source, nor were they derived exclusively from the mantle. The most likely source was lower crust and mantle, variably contaminated by mid- to upper crust, the range of  $\epsilon_{Nd}$  resulting from systematic changes in relative contributions through time.

Silurian (*c.* 425-415 Ma) plutons are characterized by foliated K-feldspar megacrystic granite. Fabric elements within plutons parallel those developed in country rocks and show a broad continuum of down-temperature magmatic through solid-state microstructures resulting from emplacement synchronous with sinistral transpression. The plutons from elongate sheets often several km in width which parallel the regional structural grain. Contact-generated migmatites are common along margins demonstrating considerable convective heat. Ambient regional metamorphic conditions and pluton microstructures indicate emplacement at mid-crustal levels. These plutons record the ascent routes for large volumes of granitic magma transported through the crust during the Silurian.

Devonian (*c.* 385 Ma) plutons are characterized by extensive bodies of K-feldspar megacrystic granite markedly discordant to the regional tectonic grain and metamorphic isograds. Contacts are typically sharp and stoped

blocks of country rock occur near margins. These features demonstrate emplacement at upper crustal levels and after the main ductile (Silurian) deformation consistent with rapid regional exhumation. The plutons exhibit internal, often cryptic, contacts and heterogeneities indicative of assembly by batch filling, although differences between magma batches were small. Evidence for mixing between batches includes numerous grain-scale disequilibrium textures, outcrop heterogeneity and subtle pluton-wide lithological variation. Weak to moderate fabrics formed prior to extensive crystallization, and record flow during emplacement of magma batches. Pre-existing country rock fabrics on the northern side of the N-S trending Newport Granite are rotated anti-clockwise of the regional trend indicating emplacement into a tear structure initiated by dextral movements along a major, NE-SW trending crustal-deep transcurrent structure, the Dover Fault, located at the Avalon - Gander boundary. Passive emplacement during regionally important brittle dextral movements is further supported by local vein arrays at pluton contacts and by the orientation of internal contacts. The Newport Granite is itself displaced by, and cataclased within the Dover Fault system indicating that fault movements continued after emplacement.

Our ongoing studies in the Gander Zone indicate that voluminous Silurian to Devonian megacrystic granites were generated during transpressional thickening followed by rapid exhumation of the region, possibly in response to delamination, leading to adiabatic decompressive melting of unexposed (amphibolitic?) lower crust. High temperature - low pressure migmatization recorded in the region resulted from a combination of ambient regional metamorphic conditions due to initial crustal thickening, coupled with advected heat from voluminous, syntectonic granites generated at deeper levels. The granites ascended through the mid-crust with relatively narrow zones (kms) of transcurrent shear to be emplaced passively as broadened, fault controlled bodies in the upper crust. Throughout the region there is clear evidence for a tectonic control on the location of granite plutonism. In turn, magmas may have controlled the local focusing of strain, thus creating a positive feedback loop.

## ORAL PRESENTATION

## The Petrogenesis of Slab-Derived Trondhjemite-Tonalite-Dacite/Adakite Magmas

<sup>1</sup>Drummond, Mark S., <sup>2</sup>Defant, Marc J.  
and <sup>2</sup>Kepezhinskas, Pavel K.

<sup>1</sup>Geology Department, University of Alabama  
at Birmingham, Birmingham, AL 35294, USA

<sup>2</sup>Geology Department, University of South Florida,  
Tampa, FL 33620, USA

The focus of "granite" petrology has leaned towards the study of granite and rhyolites and their relevance to the generation and growth of continental crust through time. This pursuit has allowed us to find that a significant proportion of granites (*sensu stricto*) represent recycling of continental crustal components and contribute sparingly to new net addition for continental crustal growth. In order to understand the birth of continental crust and its subsequent growth we should refocus our studies towards the sodic end of the "granite" spectrum, the trondhjemite-tonalite-dacite suite (TTD). Most continental growth models indicate that over three quarters of the present-day continental crust was produced in the Archean with the majority of this Archean crust represented by TTD.

	Adakite	high-Al TTD	CARC	IARC	low-Al TTD	Plagiogranite
(#)	(131)	(386)	(825)	(476)	(124)	(53)
Y	10	9	27	28	45	83
Yb	0.93	0.64	2.42	4.26	4.03	7.19
Sr	858	659	428	229	133	150
Cs	1.2	2.0	9.2	0.8	0.8	0.1
U	0.9	0.9	3.6	0.7	0.9	1.4
Ni	41	26	19	9	18	6
Mg#	48	43	41	34	33	31
La/Yb	18	35	12	8	3	2
Sr/Y	107	103	19	9	5	2
Zr/Y	14	24	7	5	4	5

TTD may be subdivided into high-Al TTD and low-Al TTD (> 15% and < 15% Al<sub>2</sub>O<sub>3</sub> at 70% SiO<sub>2</sub> level), and ophiolitic plagiogranites. Defant and Drummond (1990) referred to some specific Cenozoic high-Al TTD as adakites. The table above indicates that the high-Al TTD/adakite contain lower Y, Yb and higher Sr, Sr/Y, Zr/Y, La/Yb relative to the other TTD subtypes. This compositional signature for the high-Al TTD/adakite

results from stabilizing garnet (grt), hornblende (hbl), and clinopyroxene (cpx) at the site of partial melting and general lack of plagioclase (pl) in a hbl eclogite to eclogite restite. In comparison to high-Al TTD/adakite, andesite-dacite-rhyolite suites from continental (CARC) and island (IARC) arcs contains higher Y, Yb and lower Sr, Sr/Y, Zr/Y, La/Yb due to the lack of grt and presence of pl during magma genesis.

Experimental studies have shown that high-Al TTD/adakite major element compositions can be produced by high-pressure (> 15 - 16 kbar, > 50 km depth) partial melting of basalt leaving grt + cpx + hbl restite. We have suggested that the partial melting of subducted oceanic crust at 23 - 26 kbar (75 - 85 km depth) and 700-800°C (9°C km<sup>-1</sup> geotherm) may define the minimal physical conditions for slab melting. This *P-T* regime coincides with a number of potential dehydration reactions in the slab, such as clinohumite, paragonite, zoisite, serpentine, tremolite, talc+phengite. Recently, Thompson and Ellis (1994) have shown that at 800°C and 26 kbar partial dehydration melting of a basaltic source could follow, zoisite + hbl + quartz = cpx + pyrope + high-Al TTD melt.

Martin (1993) has suggested that the widespread Archean high-Al TTD is the product of slab dehydration melting under hbl eclogite conditions associated with an elevated geothermal gradient. Thus, a potentially higher slab geotherm may have been responsible for the voluminous high-Al TTD produced in the Archean. Cenozoic adakite localities are commonly associated with subduction of young (< 25 Ma), hot oceanic crust. Approximately 20% of the modern ocean floor is comprised of Miocene or younger crust, implying that adakite generation may not be as rare as originally thought. Viable alternative or supporting tectonic effects that may enhance slab melting include highly oblique convergence and resultant slow subduction and incipient subduction into pristine hot mantle. An alternative hypothesis to slab melting for high-Al TTD/adakite genesis would involve partial melting over-thickened continental arc crust. The CARC compositions exhibit elevated Cs and U values relative to high-Al TTD/adakite due to incorporation of or derivation from continental crust. Alternatively, the high-Al TTD and Cenozoic adakite, in particular, exhibit elevated Ni and Mg# relative to CARC and IARC due to minor (5-10%) mantle - adakite mixing. Localities that best exemplify mantle - adakite mixing include: Setouchi belt, Japan (sanukitoids); Baja California (bajaites); Adak Island, Aleutians; Komandorsky Island, western Aleutians; and

northern Kamchatka. Given our recent detailed studies in northern Kamchatka, we will use this locality as a case example for slab melting and adakite - mantle mixing.

- Defant, M.J. and Drummond, M.S., 1990. Derivation of some modern arc magmas by melting of young subducted lithosphere. *Nature*, **347**, 662-665.
- Martin, H., 1993. The mechanics of petrogenesis of the Archean continental crust—comparison with modern processes. *Lithos*, **30**, 373-388.
- Thompson, A.B. and Ellis, D.J., 1994. CaO + MgO + Al<sub>2</sub>O<sub>3</sub> + SiO<sub>2</sub> + H<sub>2</sub>O to 35 kb: amphibole, talc and zoisite dehydration and melting reactions in the silica-excess part of the system and their possible significance in subduction zones, amphibolite melting, and magma fractionation. *Am. J. Sci.*, **294**, 1229-1289.

### **Tismana (Neoproterozoic) Granitoid Pluton from the Danubian Basement (South Carpathians - Romania): A Geochemical Approach**

<sup>1</sup>Duchesne, J.C., <sup>2</sup>Berza, T.,

<sup>3</sup>Liegeois, J.P. and <sup>2</sup>Tatu, M.

<sup>1</sup>University of Liege, Belgium

<sup>2</sup>Geological Institute of Romania, Bucharest, Romania

<sup>3</sup>Royal Museum of Central Africa, Tervuren, Belgium

The Tismana Massif holds a special position between the granitoid bodies associated with the crystalline schists from the basement of South Carpathian's lower Alpine units - the Danubian Nappes. So, from the 15 major plutons known here, only Tismana and a smaller twin display geochemical, mineralogical, petrographical and structural patterns pointing to a different origin than the crustal anatexis generally advocated for this igneous province. The Tismana Massif is exposed on 300 km<sup>2</sup> at the southern border of the western South Carpathians, but below Mesozoic and Cenozoic covers its area must be at least double. The body is emplaced in a high temperature - low pressure metamorphosed sedimentary sequence. Both at small and medium scale, the contacts of the body are concordant with the structural elements of the surrounding crystalline schists. No apophyses or proper migmatites do exist and only a few roof pendants were mapped. The age of the Tismana massif is, from geological relations, certainly pre-Silurian. Twenty K-Ar ages range between 90 and 540 Ma, reflecting Alpine overprinting related to nappe tectonics. An Ar-Ar plateau age of c. 593 Ma (R.D.

Dallmeyer, personal communication, 1994) and a U-Pb age of 567 ± 3 Ma (Liegeois *et al.*, 1995) were interpreted as dating the intrusion of the pluton.

The Tismana granitoid body is made up of porphyritic granites, which cover around 80% of the exposed area, and equigranular darker granitoids, grading from granodiorites to diorite-gabbros; hectometric pods of peridotite are also present. The areal distribution of the equigranular granitoids is asymmetric in the uncovered area: they are dominant near the western border, common in the central area and are missing in the southern part. There is also a southwards directed trend in the reduction of both the size of the lenses (from kilometric to centimetric) and of the grain size of the rocks (from 1 - 4 mm to 0.3 - 0.5 mm). The smallest bodies of equigranular granitoids can be described as mafic microgranular enclaves and are generally disposed in swarms. The MME have either rounded contours, when they are enclosed in hybrids, or planar borders, when they are hosted by porphyritic granites. The position of both the borders of the enclaves and of the foliations expressed by biotite flakes in the MME and by K-feldspar megacrysts in granites are parallel, producing a few symmetrical folds.

The MME evidence the process of magma mingling and can be trapped either by hybrid rocks, or by porphyritic granite. The presence of porphyritic granodiorite, containing both centimetrically spaced K-feldspar megacrysts, typical for the granites, and of amphibole ± clinopyroxene, minerals characteristic for the equigranular granitoids, was frequently observed as metrical transition zones between the two main lithologies. Even in the "clean" porphyritic granite, there are hectometrical zones where amphibole is added to biotite and plagioclase is richer in anorthite. These aspects point to the existence of large scale mixing (hybridization) in the Tismana pluton. Tismana displays an alkali-calcic trend in Peacock diagram, with the intersection near the alkaline field. Potash content is increasing from 2% to 4% in the 48 - 52% SiO<sub>2</sub> range and from 4% to 6% in the 52 to 70% SiO<sub>2</sub> range. The slight increase of K<sub>2</sub>O from 52% SiO<sub>2</sub> upwards reflects the higher increase of K-feldspar in respect with concomitant decrease of biotite. The Tismana trend lies entirely within the shoshonitic or alkaline field. In the (Zr + Nb + Ce + Y) vs. (K<sub>2</sub>O + (Na<sub>2</sub>O/CaO)) diagram, Tismana has A-type affinities, shown only by trace elements due to relatively low Na<sub>2</sub>O abundances (2 - 3% for the whole silica range). This points to a clear potassic character (K<sub>2</sub>O/Na<sub>2</sub>O ratio up to 2) for the massif. The geochemical data show that the genesis of this massif has

been greatly controlled by fractional crystallization and mixing processes leading to a composite series (following Rossi and Cocherie, 1991).

Liegeois, J.P., Berza, T., Tatu, M. and Duchesne, J.C., 1995. The Neoproterozoic Pan-African basement from the Alpine Lower Danubian nappe system (South Carpathians, Romania). *Precamb. Res.*, in press.

Neubauer, F., Mocanu, V. and Fritz, H., 1994.  $^{40}\text{Ar}/^{39}\text{Ar}$  mineral ages for the pre-Alpine and Alpine evolution of nappe complexes in the southern Carpathians. *Romanian J. Tect. Region. Geol.*, **75**, 77-86.

Rossi, P. and Cocherie, A., 1991. Genesis of a Variscan batholith. Field, petrological and mineralogical evidence from the Corsica-Sardinia batholith. In Freeman, R., Huch, M. and Mueller, S. (eds), *The European Geotraverse*, 319-346.

## Late Variscan Amphibole-Bearing Granitoids in Lusatia (Northern Part of Bohemian Massif) as Melting Products of Metasomatically Overprinted Mafic Lower Crustal Rocks

<sup>1</sup>Eidam, J. and <sup>1,2</sup>Hammer, J.

<sup>1</sup>FR Geowissenschaften, Universität Greifswald,  
Jahn-Str. 17a, 17489 Greifswald, Germany

<sup>2</sup>Geochemisches Institut, Universität Göttingen,  
Goldschmidt-Str. 1, 37077 Göttingen, Germany

The Lusatian Anticlinal Zone (LAZ; Southeast Germany; Eastern Saxothuringicum) is composed of Cadomian and Late Variscan granitoids and anchimetamorphic Brioverian greywacke-pelite successions (Kröner *et al.*, 1994). Variscan granitoid magmatism played rather a subordinate role in LAZ when compared with the adjacent Saxothuringian regions (Erzgebirge). The LAZ represents a tectonic block, which was already stabilized in the Cadomian era. Younger magmatic activity (early Variscan and Mesozoic mafic dykes, late Variscan granitoids) are related to mobile fault zones bounding the Cadomian Granodiorite Complex.

The late Variscan granitoids were dated by single zircon evaporation method ( $304 \pm 14$  Ma; Kröner *et al.*, 1994). They range in modal composition from quartz diorites through tonalites and granodiorites to monzogranites. Occurrences of weakly postmagmatically altered ( $\delta^{18}\text{O}_{\text{Q-Fsp}} = 0.6 - 1.0$  ‰) granitoids with  $\text{SiO}_2$  content down to 60.2 wt % are atypical for the eastern part of Saxothuringian Zone. The metaluminous rocks with

increasing molar  $\text{Al}_2\text{O}_3/(\text{CaO} + \text{Na}_2\text{O} + \text{K}_2\text{O})$  ratios at increasing  $\text{SiO}_2$  content are petrographically characterized by occurrences of magnesio-hornblende (up to 8 vol %) and plagioclase cores with up to 56 mol % anorthite. Relatively high Ca and Sr contents in Lusatian rocks correspond to values of I-type granites. High  $(\text{La}/\text{Yb})_{\text{N}}$  ratios from 5 to 20 and negative Eu-anomalies in chondrite-normalized REE patterns indicate restitic garnet and plagioclase in their source rocks.

In comparison to average granodiorite the Lusatian granodiorites (with MgO content between 1.6 and 2.3 wt %) and monzogranites (1.5 up to 2.3 wt % MgO) are characterized by high concentrations of Ba, Ce, Hf, K, Li, Nb, Pb, Rb, REE, Sr, Ta, Th, U and Zr. Enrichments of these elements are caused either by high contents in source rocks or by specific conditions of partial melting. Most probably are metasomatic overprints of upper mantle rocks above a subduction zone and element mobilization from upper mantle wedge into lower crustal mafic source rocks by dehydrated fluids from the subducted oceanic crust.

According to results of partial melting experiments of mafic lower crustal rocks (*e.g.* Springer, 1992; Wolf and Wyllie, 1991, 1994) and to calculation of source rock composition using the batch melting model (Shaw, 1970) the Lusatian granitoids represent melting products of metasomatically overprinted mafic lower crustal rocks at  $T = 900\text{-}950^\circ\text{C}$ ,  $a_{\text{H}_2\text{O}} < 0.5$ ,  $P = 10\text{-}15$  kbar and various degrees of partial melting (15-20 % for monzogranites; 20 % for granodiorites and 30 % for quartz diorites). This is documented also by relatively low  $\delta^{18}\text{O}$  whole rock values (quartz diorites, 7.1-7.3 ‰; granodiorites, 7.6-7.8 ‰; monzogranites, 8.1-10.3 ‰). The homogeneous Sr and Nd isotopic compositions ( $(^{87}\text{Sr}/^{86}\text{Sr})_i = 0.7055 - 0.7063$ ;  $\epsilon_{\text{Nd}}(304 \text{ Ma})$  of -3.1 - -3.3 for quartz diorites; -2.3 - -2.5 for granodiorites and -1.6 - -4.4 for monzogranites) correspond to mafic source rocks and homogenized effect of metasomatic fluids.

Geophysical data, like gravimetric and magnetic anomalies, suggest a larger distribution of this granitoid type in marginal zones of the Cadomian Lusatian Granodiorite Complex.

Kröner, A., Hegner, E., Hammer, J., Haase, G., Bielicki, K.-H., Krauss, M. and Eidam, J., 1994. Geochronology and Nd-Sr systematics of Lusatian granitoids: significance for the evolution of the Variscan orogen in east-central Europe. *Geol. Rundsch.*, **83**, 357-376.

Shaw, D.M., 1970. Trace element fractionation during anatexis. *Geochim. Cosmochim. Acta*, **34**, 237-243.

- Springer, W., 1992. *Entstehung granitoider Magmen durch partille Aufschmelzung basischer Unterkruste: Eine experimentelle Studie*. Unpubl. Diss., Universität Köln, 116 pp.
- Wolf, M.B. and Wyllie, P.J., 1991. Dehydration melting of solid amphibolite at 10 kbar: textural development, liquid interconnectivity and applications to the segregation of magmas. *Mineral. Petrol.*, **44**, 151-179.
- Wolf, M.B. and Wyllie, P.J., 1994. Dehydration melting of amphibolite at 10 kbar: the effects of temperature and time. *Contrib. Mineral. Petrol.*, **115**, 369-383.

## Zircon Inheritance in an S-type Granite and its Microgranitoid Enclaves, Lachlan Fold Belt, Australia

Elburg, Marlina A.

*Department of Earth Sciences, Monash University, Clayton 3168, Australia*

Microgranitoid enclaves (ME) in granites have been alternatively interpreted as restite, chilled margins of the granite itself, and chilled globules of a more mafic magma. For ME in the S-type Wilson's Promontory Batholith (WPB), Lachlan Fold Belt, Australia, the chilled margin interpretation is least tenable because of significant differences in initial isotopic composition between ME and host granite. Field and petrographic evidence points towards a magma mingling origin for the ME. To further assess this interpretation, zircons from the host granites and enclaves were dated by the SHRIMP ion microprobe. The host was expected to be rich in inherited zircons, in keeping with its S-type geochemical signature. Restitic enclaves (which should be dominantly high-grade metasediments) might be expected to contain a larger proportion of inherited zircons than the host. However, if enclaves represent chilled globules of a mafic magma, inheritance might be expected to be less prominent, although mixing with the host magma might have introduced older zircons.

Zirconium contents of the granites decrease with decreasing whole rock  $\text{FeO}^T$  content. Zr concentrations in ME vary from 250 to 730 ppm irrespective of whole rock  $\text{FeO}^T$  content. Zircons from the granitic samples are generally euhedral and large (up to 200 microns). Inheritance is not as prominent as expected, despite attempts to specifically target "cored" crystals. Only 8 out of 69 analyses gave ages older than the granite crystallization age of 395 Ma. Zircons in ME are generally small and

anhedral. In thin section many zircons can be seen to have needle-like shapes, but these may have been broken during separation of the crystals. These small crystals typically yield ages around 395 Ma, although their small size makes reliable SHRIMP dating difficult.

Two enclaves (bulk Zr contents 570 and 280 ppm respectively) with quartz and plagioclase megacrysts contain few large zircons, of which a significant proportion contains inherited cores. Some of these have thin overgrowths of magmatic zircon; others have not developed overgrowths. A megacryst-poor enclave with high Zr contents (730 ppm) contains very few euhedral zircons; all other zircons are small and anhedral. No dates indicating inheritance were found.

Dates given by inherited zircons of granites and ME are similar. A "young" cluster gives ages of 500-650 Ma; three analyses give 1100-1200 Ma ages, two 1500-1600 Ma. An age population of 750-830 Ma (3 analyses) is present only in the granite, whereas an enclave contains a 2700 Ma old core.

The small grain size, anhedral shape and apparent magmatic crystallization ages of most zircons in the ME is in accordance with these enclaves representing globules of a chilled mafic magma. The larger zircons which show inheritance are thought to have been derived from the granitic magma, like the quartz and plagioclase megacrysts. The higher proportion of inherited cores in the large zircons from megacryst-bearing ME, compared to those in the host granites, may reflect the timing of mixing between granitic and enclave magma. This may have taken place when relatively few zircons had crystallised from the granitic magma. All inherited zircons were already present in the granite magma, and their relative over-representation at the time of magma mixing has been translated into the "large" zircon population of the ME.

Small zircons which are typical of the ME tend to be lost during separation, mounting and polishing prior to SHRIMP analysis, and are often too small to be analysed by SHRIMP. This, together with the introduction of inherited zircons from the granitic magma during mixing, can easily lead to a serious sampling bias and an overestimation of inherited (restitic) crystals in enclaves.

The age groups for zircons analysed in this study are similar to those recognised by Williams *et al.* (1990) for I and S-type granites in the NE part of the Lachlan Fold Belt. Compared to these S-type granites the WPB is relatively poor in inherited zircons. It also has less negative  $\epsilon_{\text{Nd}}$  values compared to other Lachlan Fold Belt

S-type granites (-4 versus < -6). This could suggest a larger role for juvenile mantle derived melts in the petrogenesis of the WPB. The microgranitoid enclaves may represent heavily contaminated globules of this mafic magma.

Williams, I.S., Compston, W., Chappell, B.W., Crook, K.A.W. and Chen, Y.D., 1990. Untangling the sources of granites by dating inherited zircons. *Geol. Soc. Aust. Abstr.*, 27, 112.

### **Could Some Regional Metamorphism be Induced by Flowing of Magma? The Case of Hercynian Metamorphic Domes and Plutonic Intrusions of the Eastern Pyrenees**

Enrique, P.

*Departament de Geoquímica, Petrologia i  
Prospecció Geològica, Facultat de Geologia,  
Universitat de Barcelona, Zona Universitària de  
Pedralbes, 08028-Barcelona, Spain*

The Hercynian regional metamorphism in the Pyrenees is characterized by tightly concentric isograds around metamorphic domes. The intensity of metamorphism increases rapidly from low-grade (chlorite-muscovite) zones to high-grade (sillimanite and anatexis) zones, giving rise to typical low-*P* and high-*T* metamorphism. This metamorphism postdates the main orogenic deformation but is synchronous to a second group of less intense tectonic phases. Stephanian sediments lie unconformable over folded Namurian deposits, which narrowly constrains the timing of deformation, metamorphism and plutonic emplacement.

In addition to the old dome cores (Lower Palaeozoic and Neoproterozoic schists and orthogneiss) and the younger Silurian to Westphalian synforms located between them, about 20% of the area consists of large calc-alkaline plutonic intrusions (up to 600 km<sup>2</sup>) which produce a contact metamorphic aureole in the Palaeozoic host rocks. Intrusions clearly cut the main Hercynian folds and foliations but they are not usually significantly deformed. The abundant apophyses and xenoliths of the enclosing rocks near the contacts suggest a moderate or high fraction of melt in the magmas during their emplacement.

A volcanic calc-alkaline suite, ranging from basaltic andesites to rhyolites, is interbedded in the post-orogenic

Stephano-Permian sequence. Thick layers of basaltic magma underlying each metamorphic dome, in an extensional context, have been postulated by Wickham and Oxburgh (1987) to account the high thermal gradients observed. Nevertheless there are some features that should be taken into consideration: a) existence of small stocks and dykes of calc-alkaline plutonic rocks associated with migmatites inside the thermal domes (*e.g.* Cap de Creus), these rocks range in composition from quartz-hornblende gabbros and diorites to leucogranites, and they display several degrees of mixing with anatectic melts; b) the stocks are slightly older than the perianatectic pegmatites; c) a subvertical foliation is present in these plutonic rocks, and to a lesser extent in the pegmatites, which was produced by the late-Hercynian compressive phases; d) the overlap in time of the calc-alkaline magmatism and low-*P* - high-*T* metamorphism.

Therefore, it would appear probable that the source of heat for this metamorphism was the huge volume of calc-alkaline magmas that fed the upper crustal batholiths and, perhaps, volcanism. The small, compositionally expanded, calc-alkaline stocks might represent the last fractions of magma trapped in the conduits on their way to the upper levels of the crust. These magmas may have crystallized only when magmatic activity, and, consequently, temperature, decreased. Therefore, the intensity of metamorphism cannot be explained by present-day relict volumes of magma in high grade metamorphic zones since almost all of it would have been squeezed out by the late compressive phases.

If this hypothesis is correct the isograds must have a subvertical arrangement (following more or less cylindrical or conic surfaces) and the extent of the metamorphism would be limited around the magmatic feeders. On the other hand, the whole metamorphic area would have a lower density than the cold surrounding rocks, which might have originated the domes by diapiric ascent. Finally, the compositional zoning and temporal sequence, from dioritic to leucogranitic, observed in many plutons of the area, might have been originated by progressive contamination of the deep andesitic magmas by pegmatitic and granitic anatectic melts during their ascent through the narrow conduits.

Wickham, S.M. and Oxburgh, E.R., 1987. Low-pressure regional metamorphism in the Pyrenees and its implications for the thermal evolution of rifted continental crust. *Trans. Roy. Soc. London*, A231, 219-242.

## Amphibole-Rich Clots in Calc-Alkalic Granitoids and in Their Mafic Microgranular Enclaves from Two Foldbelts, NE Brazil

<sup>1</sup>Ferreira, V.P., <sup>1</sup>Sial, A.N.,

<sup>2</sup>Fallick, A.E. and <sup>3</sup>Cruz, M.J.M.

<sup>1</sup>*Nucleus for Granite Studies (NEG), Dept. Geol. UFPE,  
P.O. Box 7852, Recife, 50732-970, Brazil*

<sup>2</sup>*Scottish Universities Research and Reactor Centre,  
East Kilbride, Glasgow, G75 0QU, Scotland*

<sup>3</sup>*Department of Geology, UFBA, Salvador,  
Bahia, 40170-290, Brazil*

Metaluminous granodiorite/tonalite plutons (Conceição-type) intruded low-grade metaturbidites of the Cachoeirinha-Salgueiro Foldbelt (CSF) in the central states of Paraíba and Pernambuco and metasediments of the Macururé Group (Coronel João Sá-type) in the Sergipano Foldbelt (MSF, states of Sergipe and Bahia) further south, around 620 Ma ago. Amphibole-rich polycrystalline clots (ARC), subrounded to angular, from millimetric size up to 20 cm long, are relatively common in these plutons. They are found within microgranular diorite/tonalite enclaves or in their granodiorite hosts. ARC from five plutons in the CSF and from two in the MSF have been studied in detail.

Clots hosted by the granodiorites are usually angular, have granoblastic texture, being composed essentially of zoned amphibole, which has patchy actinolite cores and magnesian hornblende margins, in polygonal packing where grains display near-120° triple junctions (type I ARC). Other phases present are interstitial biotite, Ca-clinopyroxene, sphene and apatite. Clots are usually armored by an external layer of hornblende and biotite, crystallized from the host magma. Type II ARC (amphibole cumulates) and type III ARC (pseudomorphs after clinopyroxene-rich restites or early-crystallized clinopyroxene aggregates) are less common and were observed only in Conceição-type granitoids.

In a (Na + Ca + K) vs Si diagram, compositions for most amphibole cores in type I ARC in the CSF (*e.g.* Boa Ventura pluton) plot in the metamorphic field, suggesting ARC are of metamorphic origin. Compositions of amphibole margins from either the clots or from the granodiorite/tonalite hosts plot in the field common to metamorphic and igneous amphiboles.

Although these plutons are oxidized I-type granitoids, those from the Conceição-type ones display quartz-cor-

rected whole-rock  $\delta^{18}\text{O}$  values typical for S-type granites (+11 to +13‰<sub>SMOW</sub>). Amphibole-rich clots are usually 1.5‰ lower than their hosts (+10 to +11.5‰<sub>SMOW</sub>). Values of  $(^{87}\text{Sr}/^{86}\text{Sr})_i$  for plutons and their microgranular mafic enclaves is 0.70598 in the CSF.  $\epsilon_{\text{Nd}}(0.6 \text{ Ga})$  varies from -2.0 - -1.0 (Van Schmus *et al.*, in press) and  $\delta^{34}\text{S}$  from +1.0 to +9.0‰ CDT for the ARC host plutons.

Whole-rock D/H values for granodiorite hosts, mafic microgranular enclaves and ARC vary from -69 to -114‰<sub>SMOW</sub> (with no correlation with H<sub>2</sub>O), covering a significant proportion of the  $\delta\text{D}$  variation for most terrestrial rocks. The  $\delta\text{D}$  variation is much broader than that for the  $\delta^{18}\text{O}$ .

Basalts probably filled a major rift and floored the furrow (at 1.0-1.4 Ga, as indicated by Nd  $t_{\text{DM}}$  model age in ARC granodiorite hosts; Van Schmus *et al.*, in press), that later accommodated CSF marine turbidites. Partial fusion of this basaltic floor, hydrothermally altered at low temperature, generated the calc-alkalic ARC-host magmas. Type I ARC represent fragments or restites of such a fusion. Temperatures obtained for this type in the CSF (670-690°C) are lower than those for host granodiorites (700-850°C), as expected if they are fragments from the source.

If the source for the CSF magmas is a low temperature-altered oceanic crust, as supported by oxygen isotopes, one would expect  $\delta\text{D}$  values above -70‰, not below as attested. In one pluton, however, a very homogenous behavior of  $\delta^{18}\text{O}$  (average +11.8‰  $\pm$  0.2, for 5 analyses) show a broad variation of  $\delta\text{D}$  values. Such observation attests that H and O isotopes probably had decoupled behaviors. Actinolite pseudomorphs after clinopyroxene in some ARC resulted from reaction between clinopyroxene and hydrogen, which requires extraneous hydrogen to be incorporated into the magma, perhaps causing a wide  $\delta\text{D}$  isotopic range.

Van Schmus, W.R., Brito Neves, B.B. de, Hackspacher, P. and Babinski, M., 1995. U-Pb and Sm-Nd geochronologic studies of eastern Borborema province, northeastern Brazil: initial conclusions. *J. South Amer. Earth Sci.*, in press.

## Hercynian Evolution from Calc-Alkaline to Peraluminous A-Type Leucogranites, Catalonian Coastal Ranges, NE Spain

<sup>1</sup>Ferres, M., <sup>2</sup>Enrique, P.,

<sup>1</sup>Delaloye, M. and <sup>2</sup>Sole, J.

<sup>1</sup>Department de Mineralogie, 13 Rue des Maraichers,  
1211 Geneve-4, Switzerland

<sup>2</sup>Facultat de Geologia, Zona Universitaria de Pedralbes,  
08028-Barcelona, Spain

A fragment of the Hercynian Orogen is exposed over 2000 km<sup>2</sup> in the Catalonian Coastal Ranges. Magmatism evolved from a predominantly high-K calc-alkaline association to minor peraluminous A-type granites. Three types of high-silica (74 - 77 wt % SiO<sub>2</sub>) biotite-leucogranites can be distinguished: 1) late plutonic calc-alkaline differentiates; 2) peraluminous A-type leucogranites post-dating the calc-alkaline magmatism; and, 3) an intermediate between types 1 and 2. The latter may represent a transition between calc-alkaline and peraluminous A-type granitoids.

*High-K calc-alkaline association.* Coarse to fine grained plutons of different shapes and sizes form a composite batholith of 1500 km<sup>2</sup>. Granodiorite is the most common rock type followed by granites and tonalites. The evolving plutonic sequence starts with more basic rocks represented by a few diorites, gabbros and hornblendites and ends with leucogranites of type 1. This magmatic evolution is also expressed in systematic changes in the biotite composition trending from phlogopite toward siderophyllite, with F content varying from 5 to 10% OH substitution. In addition to ubiquitous biotite, hornblende occurs in some granodiorites or less differentiated rocks. Major and trace element patterns of whole-rock analyses show linear trends for diorites to leucogranites indicating that they may be related by relatively simple differentiation processes.

K-Ar, <sup>40</sup>Ar/<sup>39</sup>Ar and Rb-Sr data give cooling ages from about 300 to 270 Ma for the whole suite. Values for (<sup>87</sup>Sr/<sup>86</sup>Sr)<sub>i</sub> range from 0.711 for acidic and intermediate rocks to 0.709 for gabbros. These values suggest an important crustal component. A NE-SW calc-alkaline dioritic to granitic dyke-swarm intruded the calc-alkaline plutonic sequence. The dykes show well-developed chilled margins indicating already cooled host-rocks.

*Peraluminous A-type leucogranites.* Slightly peraluminous A-type leucogranites crop out in the batholith

over an area of about 70 km<sup>2</sup>. These consist of major coarse to fine grained intrusions, and several small, very fine grained stocks. The latter post-date the calc-alkaline dyke swarm and contain miarolitic cavities plus granophyric intergrowths indicating a shallow level of emplacement. All these leucogranites are cut by associated granophyric and felsitic dykes with spherulitic textures indicating a devitrification of rhyolitic glass matrices. Biotite (the only mafic mineral) has a composition close to annite, with high F contents (up to 25% OH substitution). Plagioclase of albite to oligoclase composition and perthite are present in similar amounts (about 30%) of the modal composition. Whole-rock analyses show low CaO content (<0.5 wt %), a depletion in Ba, and high Ga concentrations peraluminous A-type leucogranites plot as WPG in the Y-Nb diagram after Pearce *et al.* (1984). Their REE concentrations are low with a strong negative Eu anomaly.

*Intermediate biotite-leucogranites.* These consist of several medium to fine grained intrusions with miarolitic cavities.

They occur widespread in the batholith covering areas of about several meters to 10 km<sup>2</sup>. They are slightly peraluminous. Biotite composition is intermediate between siderophyllite and annite, with F contents up to 15% OH substitution. Whole-rock major and trace element analyses show features of both leucogranite types 1 and 2. Namely, high CaO contents (>0.5 wt %) and low Ga concentrations (14 - 17 ppm) but Ba depletion, low REE concentrations with strong negative Eu anomaly, and they plot as WPG. Timing of their emplacement is unclear.

According to the chemistry, leucogranites of type 3 may represent a transition from calc-alkaline 2 to peraluminous A-type 1 granites. Work underway is focused on establishing the timing and petrogenetic links between these three types of leucogranites. The lack of peralkaline granites already suggests an incomplete development (or a non-preservation) of the alkaline event that typically follows calc-alkaline activity, notably in the neighbouring Hercynian Island of Corsica.

Pearce J.A., Harris, N.B.W. and Tindle, A.G., 1984. Trace element discrimination diagrams for the tectonic interpretation of granitic rocks. *J. Petrol.*, **25**, 956-983.

## Granitoids from Oceanic to Continental Environments: The Example of the Urals (Russia)

<sup>1</sup>Fershtater, G.B. and <sup>2</sup>Bea, F.

<sup>1</sup>*Institute of Geology and Geochemistry,  
Ekaterinburg, Russia*

<sup>2</sup>*Department of Mineralogy and Petrology,  
Campus Fuentenueva, University of Granada,  
18002 Granada, Spain*

Granitoid magmatism of the Ural mobile belt reflects main features of its tectonic structure and evolution. All geodynamic settings from oceanic to continental collision experienced by the Urals have their own magmatic events.

The following megablocks in the W-E cross-section of the Ural mobile belt have been distinguished: 1) passive continental margin; 2) All-Ural suture with oceanic type of the crust; 3) and 4), NW and SE island-arc - continental megablocks with the following zones: island - arc (a), active continental margin (b) and continental (c); and, 5) Trans-Ural megablock as a transition zone to Kazakh structures.

The magmatism of these zones is different in age and composition. The suture megablock is the area of ultramafic-mafic magmatism of middle-late Ordovician (harzburgite-type ophiolites) and early Devonian (lherzolite-type ophiolites) age which is accompanied by oceanic type diorites and plagiogranites.

Magmatism of the island arc zones is represented by differentiated gabbro-granitoid and comagmatic basalt-rhyolite rock series of Silurian age in NW megablock and of middle-late Devonian age in the SE megablock. They are low-K tholeiitic at the early stage and K-Na calc-alkaline to subalkaline at the late stage of evolution. All granitoids in oceanic and island arc zones have basic in composition magmatic source. Some of them are produced by fractionation of basic magma, some have an anatectic origin. The last are very poor in all incompatible rare elements and have the positive Eu anomaly.

In continental marginal zone of the NW megablock two types of granitic rocks can be observed. Late Silurian-Middle Devonian magmatic rocks belong to calc-alkaline gabbro-granitic rock series with different K contents increasing from older to younger series. Early Carboniferous tonalite-granodiorite plutons mark the subduction of oceanic and island arc crust under the Eastern continent. They have clear geochemical lateral

zonation very similar to that in modern island arc. Good correlation between contents of K, Rb, Ba, Ga, Th, U, Mo, Nb, LREE, in granodiorites on the one hand, and the distance from suture being the track of paleosubduction zone, on the other hand, shows that it was the subduction that controlled the continental crust thickness and granite composition in continental marginal zone. The common geochemical feature of the Ural above-subduction granitoids is the absence of Eu anomaly, probably caused by high water contents in the initial magma and therefore early crystallization of allanite, controlling REE behaviour.

In continental zones granitic magmatism is the most widely distributed. The early stage of magmatism fixing the beginning of collision is represented by different types of tonalite-granodiorite rock series derived from andesitic magma. They have the same age as above-mentioned continental margin orogenic rock series being close to them in composition. At the late stage of collision (late Carboniferous-Permian) anatectic granites appear. In their formation one can see three main episodes: migmatitic (synchronous with the main stage of regional amphibolite stage metamorphism), granitic and leucogranitic. In vertical cross-section the rocks of these three episodes are placed from the bottom (migmatite roots) upwards. In the NW megablock granites have  $(^{87}\text{Sr}/^{86}\text{Sr})_i = 0.712$ . The source rocks for them were Archean and Low Proterozoic metamorphic rocks of the basement of the Urals. In the South Urals anatectic crustal derived granites have the mantle  $^{87}\text{Sr}/^{86}\text{Sr}$  ratio = 0.704463. It means that source material for anatexis was represented by products of erosion of island arc magmatic rocks and therefore South continental zone of the Urals was probably formed in the process of its development.

The change of type of magmatic rock series, zoning in composition and age of the rocks in the W-E cross-section of the Urals reflect the sequence of geological events in the Urals mobile belt evolution from oceanic to continental environments.

This work was supported by RFFR grant 95-05-142-80.

## Non-linear Dynamics and the Distribution and Compositions of Enclaves in Granitoid Magmas

<sup>1</sup>Flinders, James and <sup>2</sup>Clemens, John D.

<sup>1</sup>*Department of Geology, The University, Manchester, M13 9PL, UK*

<sup>2</sup>*School of Geological Sciences, Kingston University, Kingston-upon-Thames, KT1 2EE, Surrey, UK*

Physics attempts to quantify the non-linear, real world by the solution of equations that have been constructed principally on the basis that they are capable of solution. A hundred years ago, scientists were aware that deterministic systems can behave in unpredictable ways but, in order to learn anything about these complex systems, with numerous degrees of freedom, variables and parameters, they had to simplify their analyses. Simplification of imperfect information still dominates the analysis of complex natural systems. The equations that most nearly represent how a chaotic natural system behaves are insoluble. Thus, it is assumed that, because the higher-order discarded terms are small (which is true), the difference between the solution of the linearized and the "true" equation must also be small (which is not necessarily true). It is assumed that the discarded terms are unimportant. This is dangerous practice because the importance of such terms is both unknown and unknowable. Linear equations are poor descriptors of nature, and are incapable of predicting the evolution of any natural system beyond very narrow time limits. If only linearized equations are used, then a self-propagating self-censorship is established, producing innumerable triumphs of linear analysis that are far removed from reality.

Some real chaotic systems have mostly predictable time evolutions, albeit with some noise that cannot be quantified beyond a certain limiting period. Although chaos is inherent in the system, the characteristic time period for non-linear dynamics to become the dominating factor is long enough to enable mathematical models to give usable results (*e.g.* planetary motion [several millions of years] and weather forecasting [several days]). Unfortunately, however, the relationship between most real systems and their models remains obscure. Such models, whilst intrinsically interesting, are unable to answer many questions posed by natural systems, since sensitive dependence on initial conditions makes them inaccessible to analysis or prediction beyond a very short time interval.

The onset of hydrodynamic turbulence and convection in high-viscosity magmas, and mingling and mixing of partially miscible magmas are examples of natural chaotic systems.

Patterns produced by folding and stretching provide visual analogues of the deterministic chaos within a dynamic fluid system, where two initially spatially juxtaposed points may be driven arbitrarily and exponentially far apart. It is impossible to predict or calculate the time evolution vectors of points within partially miscible fluids. However, the creation of interfacial area and the reduction of length scales produces reduced striation thickness and eventual disaggregation of a lower viscosity component. The amount of break-up is much less within "islands", associated with periodic elliptical points that hinder efficient mixing, than it is within "horseshoes", associated with periodic hyperbolic points that promote efficient mixing due to chaotic flow.

We show some examples of the widely different morphologies of small, intermediate to mafic magma bodies suspended within felsic magmas, and conclude that these represent different stages in the temporal evolution of a fluid system driven by non-linear dynamics.

Microgranitoid enclaves display a chaotic distribution of their Nd isotope systematics. This could be modelled as: several individual coeval magma fractions modified by internal differentiation and/or diffusion; a single magma whose composition has been modified by chaotic stretching and folding during mixing; the result of late-stage coalescence of enclaves; or a combination of these. The first of these possibilities may be capable of detailed analysis and solution, the others are not.

Since we have no way of deciding between the alternative models, this could mean that the study of the compositions and distributions of such enclaves will yield no data that can adequately constrain their origin, original composition or their role in petrogenetic processes operating in a granitoid magma. The study of enclaves in granitoids might therefore be an irresolvable, time-consuming, petrological *cul-de-sac*.

Ottino, J. M., 1989. The Mixing of Fluids. *Sci. Am.*, **260**, 40-49.

Ottino, J. M., Leong C. W., Rising H. and Swanson P. D., 1988. Morphological structures produced by mixing in chaotic flows. *Nature*, **333**, 419-425.

Ruelle, D., 1994. Where can one hope to profitably apply the ideas of chaos? *Physics Today*, **47**, 24-30.

## Granites and Microgranitoid Enclaves: The Importance of Cumulates

Flood, R.H. and Shaw, S.E.

*Centre for Petrology and Lithospheric Studies,  
School of Earth Sciences, Macquarie University,  
NSW 2109, Australia*

Many models presently used to account for the range of granite compositions within individual plutons involve either magma mixing or restite separation. Yet the traditional view of magma chamber crystallization (Turner, 1981) involves formation of crystal-rich cumulates along the sides and floor of the magma chamber and the accumulation of complementary residual melts near the roof of the pluton. Much of the chemical variation in both granite plutons and microgranitoid enclaves that most granites contain, can be explained using a cumulate model.

We accept that chemical and textural zoning in many granitic plutons is the result of the crystallization of water undersaturated magmas, with most crystallization taking place as cumulates along the sides and floor of the developing pluton. Recent papers that demonstrate that granitic magma can be transported very rapidly along dykes means that the volume of magma present at any time within the magma chamber may be only a small fraction of the final pluton volume but if this is so, expansion of the pluton must be possible without necessarily deforming wall rocks or early-formed cumulates.

Whatever the emplacement mechanism of granite magma, crystallization of relatively anhydrous cumulates will eventually produce residual magmas near the roof that are water saturated. With the crystallization of these magmas, excess water will escape episodically as vapour generated overpressure fractures the roof thus inducing pressure quench crystallization in the upper parts of the magma chamber. Water vapour collecting along the roof of the magma chamber during venting may prevent the magma from nucleating on the solid roof of the pluton. Under these pressure quench conditions, nucleation may well form around pre-quench phenocrysts. Build up of heat will also slow the growth of what initially are aggregates (rafts) of crystals, and for rafts of crystals too small to sink, this may limit the crystallization to the minerals on the liquidus. We suggest that in some hornblende-biotite I-type plutons, this would produce small microgranitoid enclaves rich in hornblende. Rafts that grow larger, perhaps by the amalgamation of several smaller rafts of crystals are able to sink and leave behind the hot depleted

magma produced by quench crystallization. The continued growth of these crystal rafts as they sink will form microgranitoid enclaves that are cumulates as a consequence of being depleted in the near solidus minerals of the host magma (typically K-feldspar and/or quartz). The extent to which the compositional zoning in the minerals of microgranitoid enclaves reflects different magma compositions, crystallization under different water pressure and crystallization under quench conditions needs to be more fully evaluated but we believe that crystallization in a quench environment is an important part of the explanation. The variety of microgranitoid enclaves in swarms and the common association of a small proportion of wall-rock xenoliths support the view that most concentrations of microgranitoid enclaves are "death assemblages" formed away from the site of crystallization.

Microgranitoid enclaves that are not in isotopic equilibrium with the host pluton indicates that they formed from different (but we would argue, commonly only slightly different) magmas. Typically the isotopic composition of the enclaves overlaps that of the host pluton but the enclaves are less evolved. The pressure quench cumulate model of enclave formation requires that magma at depths in the magma chamber where the microgranitoid enclaves collect is commonly isotopically more evolved than magma near the roof. This difference may result from the addition of a small melt component from stopped blocks that have partially melted as they sank in the magma.

Turner, J.S., 1980. A fluid-dynamical model of differentiation and layering in magma chambers. *Nature*, **285**, 213-215.

## Significance of Magmatic Epidote in the Zeljin Pluton, Serbia

<sup>1</sup>Forizs, I., <sup>2</sup>Vukov, M. and <sup>2</sup>Jovic, V.

*<sup>1</sup>Laboratory for Geochemical Research  
of the Hungarian Academy of Sciences,  
1112 Budapest, Budaorsi ut 45, Hungary*

*<sup>2</sup>Faculty of Mining and Geology, University of Belgrade,  
Djusina 7, 11000 Belgrade, Yugoslavia*

Magmatic epidote (mEP) can be a good indicator for the pressure, temperature and original water content of a granitoid body. A lot of work has been done to determine the stability field of mEP, but the borders of this field are uncertain even now. This paper contributes to the descrip-

tion and explanation of the texture, and pressure of formation of magmatic epidote in the Zeljin pluton, Serbia (Yugoslavia).

The Zeljin pluton is an I-type granitoid body of Miocene age (24-22 Ma), lies in the Inner Dinarides and belongs to the Late Alpine granitoid zone. The mineral assemblage of the granitoid rock is hornblende, biotite, plagioclase, quartz, epidote, titanite, orthoclase, magnetite, and accessory apatite, zircon and some rare minerals. Secondary minerals are mainly chlorite, some titanite and rarely epidote.

Two geobarometers have been applied to determine the pressure of solidification. One is the Al-in-hornblende barometer, which has been criticized since the moment it was published first by Hammarstrom and Zen (1986). The average Al content of rim of hornblende is 2.12 atom per formula unit. It indicates 7.2 kbar pressure using the formula  $P (\pm 1 \text{ kbar}) = -4.76 + 5.64 \cdot \text{Al}$  (Hollister *et al.*, 1987). The calibration of this barometer has been improved recently, but in this case there is no big difference in the calculated pressure. To determining the pressure we use rim compositions of hornblende, which crystallized at the lowest temperature. A part of the hornblende is resorbed and has epidote precipitated during the narrow temperature interval where hornblende and epidote coexist (Naney, 1983). So the epidote and the rim of hornblende crystallized at the same conditions. The other barometer we have applied to these rocks is the biotite-amphibole thermobarometer (Perchuk and Fedkin, 1976), which gives conditions of  $T = 700^\circ\text{C} - (650^\circ\text{C})$ , total  $P = 7 \text{ kbar}$ .

Epidote crystals up to 2 mm are euhedral against biotite, and the same crystals have highly embayed, wormy contacts with plagioclase, quartz and K-feldspar. There is textural evidence that the epidote precipitated after resorption of hornblende. Rounded hornblendes are enclosed in epidote, which is the textural criterion for magmatic epidote described by Zen and Hammarstrom (1984). Some epidotes have zoned allanitic cores due to light rare earth element contents. Generally the epidote crystals are homogeneous, rarely showing a slight zonation caused by LREE. Their compositions range between 26% - 28% pistacite content. Quartz inclusions are the most frequent with some apatite and zircon in epidote. Synchronously with or after the crystallization of epidote, biotite surrounded a part of some epidote crystals. At a later stage of differentiation epidote would have become unstable against the residual melt in the rock and a part of it was resorbed, while plagioclase, orthoclase and quartz formed.

This is our interpretation for the highly embayed, wormy contact between epidote and plagioclase, orthoclase and quartz. Where an epidote crystal was surrounded by biotite, it was protected from resorption and so its euhedral form has remained. The stable oxygen isotope composition of the epidote is  $5.2 \pm 0.1 \text{ ‰}$  vs. SMOW indicating magmatic origin.

Magmatic epidote (mEP) of two kinds of textural characteristics (euhedral and wormy) can be found in the Zeljin pluton, Serbia. It formed under conditions of about 7 kbar pressure and  $675^\circ\text{C}$  temperature in equilibrium with melt. Probably as a result of ascent, at lower  $P$ - $T$  conditions the mEP became unstable with the melt and a part of it resorbed. At the last stage plagioclase, K-feldspar and quartz formed showing wormy contact with magmatic epidote.

- Hammarstrom, J.M. and Zen, E-an, 1986. Aluminum in hornblende: An empirical igneous geobarometer. *Am. Mineral.*, **71**, 1297-1313.
- Hollister, L.S., Grissom, G.C., Peters, E.K., Stowel, H.H., and Sisson, V.B., 1987, Confirmation of the empirical correlation of Al in hornblende with pressure of solidification of calc-alkaline plutons. *Am. Mineral.*, **72**, 231-239.
- Naney, M.T., 1983. Phase equilibria of rock-forming ferromagnesian silicates in granitic systems. *Am. J. Sci.*, **283**, 993-1033.
- Perchuk, L.L. and Fedkin, V.V., 1976. Temperature and gas regime in granitoid formation. *Thermodynamic Regime of Metamorphism*. Nauka Publishers, Leningrad, USSR (in Russian).
- Zen, E-an and Hammarstrom, J.M., 1984. Magmatic epidote and its petrologic significance. *Geology*, **12**, 515-518.

## Extreme Compositional Variability in Granitic Monazites

Förster, H.-J. and Rhede, D.  
*GeoForschungsZentrum Potsdam,*  
14473 Potsdam, Germany

Electron microprobe analyses of more than 800 monazites from geochemically diverse Hercynian granites of the Erzgebirge (Förster and Tischendorf, 1994) and Fichtelgebirge (Germany) revealed broad compositional variabilities and extraordinary non-essential element enrichments (Th, Ca, Si, U, Y) and LREE depletions not previously reported for granitic rocks. Particularly in multi-phase plutons, both monazites and other accessory phases show strong compositional differences at a variety of scales (Förster, 1993). Monazites ranging in size from a few microns to more than 200  $\mu\text{m}$  may exhibit delicate

zonation patterns; however, the zonation is often complex and non-monotonic. Monazite displays contrasting compositions with respect to the abundance of non-essential elements and their substitution reactions between metaluminous and peraluminous granites in the studied area. Evolution trends of monazite composition and whole-rock geochemistry in composite plutons are not always consistent, except for the ubiquitous trend of LREE depletion with magmatic differentiation.

Monazites from a strongly peraluminous, multi-phase pluton composed of Li-Fe mica- and topaz-bearing monzotopy syenogranites high in F, Li, Rb, Cs, Sn and  $P_2O_5$  (Eibenstock massif, W Erzgebirge), are distinguished by an extremely broad range in terms of Th (3 - 40.8 wt %), U (<0.05 - 4.6 wt %), Ca (0.7 - 7.1 wt %), and Y (0.6 - 4.1 wt %) concentrations. The strongest enrichment in these elements is found in monazites from late differentiates which have remarkably low total LREE (11 ppm), Th (4.4 ppm) and Y (7.2 ppm) whole-rock contents. Substitution of the REEs by thorium and uranium is extensive; the mole fraction of the isomorphous cheralite molecule  $(Th,U,Ca)PO_4$  varies between 0.09 and 0.81 indicating that the REEs do not always predominate. Even at the thin-section scale, the cheralite mole fraction may vary over a range of more than 50%, expressing that only part of the monazites is actually in equilibrium with the host-granite REE composition. Huttonite  $(Th,U)SiO_4$  substitution is generally insignificant. With ongoing magmatic differentiation, the monazite La/Nd ratio decreases from 1.4 to 0.5 corresponding to the observed progressive flattening of the whole-rock LREE pattern. Nd content does not exceed 10.2 wt %. Monazite HREE abundances (sum Gd-Er: 0.9 - 3.7 wt %) and patterns vary non-systematically. Monazites from the geochemically similar G4 granite in the Fichtelgebirge, currently interpreted as a single intrusion, closely resemble those of the Eibenstock composite pluton (Th: 7.3 - 35.6 wt %; U: 0.1 - 6.3 wt %; Ca: 1 - 6.3 wt %; Y: 0.6 - 3.1 wt %; La/Nd: 1.3 - 0.7; sum Gd-Tb: 1.5 - 4.1 wt %).

By comparison, the monazites from metaluminous to slightly peraluminous biotite monzogranites low in F, Li and  $P_2O_5$ , exemplified by the multi-phase Kirchberg massif (W Erzgebirge), display a more restricted compositional span with respect to Th (1.3 - 18.3 wt %), U (<0.05 - 2.3 wt %), and Y (0.2 - 3.5 wt %) concentrations. They are usually characterized by a high degree of huttonite substitution reaching 20 mol %. Local extreme Th abundances up to 40 wt % may represent fine monazite-thorite intergrowths. Relative to monazites from the Eibenstock

pluton, the range in the La/Nd ratio (2.7 - 0.8) is even more pronounced.

Particularly impressive are the compositional characteristics of the monazites from the various, geochemically distinct fine-grained aplitic dikes which cross-cut the Kirchberg pluton. Both the absolute elemental abundances as well as the shape of the REE patterns show a strong compositional diversity within and between the individual aplites (Th: 2 - 24.7 wt %; Y: 0.3 - 2.8 wt %, La/Nd: 1.4 - 0.4, sum Gd-Tb: 1.0 - 4.5 wt %). Compared with the host pluton, unusual features include local extreme enrichment in cheralite component (45 mol %), Nd (max. 14.6 wt %), Sm (4.6 wt %), and Gd (3 wt %). Nd-rich monazites possessing relatively shallow and steep HREE profiles occur within the same thin section.

The most outstanding composition (Th: 0.14 - 0.4 wt %; Nd: 17.6 - 18.5 wt %; La/Nd: 0.3; Dy and heavier REE below the electron microprobe analysis detection limit) was found in a large, anhedral monazite from a fine-grained biotite monzogranite of Schlema-Alberoda (W Erzgebirge). This monazite formed presumably a very late-crystallizing phase.

The abnormal variability and evolution of monazite compositions in the studied granite plutons must reflect strong spatial and temporal changes in melt composition during progressive differentiation and highlight the operation of different processes as described by Wark and Miller (1993). The great extent of non-essential element substitutions requires further experimental studies on monazite stability relations in terms of miscibility with huttonite and cheralite.

- Förster, H.-J., 1993. Th-Y-REE-bearing accessory minerals in Hercynian granites of the Erzgebirge (Ore Mountains), Germany. *Geol. Soc. Am. Abstr. Prog.*, **25**, 42-43.
- Förster, H.-J. and Tischendorf, G., 1994. Evolution of the Hercynian granite magmatism in the Erzgebirge metallogenic provinces. *Mineral. Mag.*, **58A**, 284-285.
- Wark, D.A. and Miller, C.F., 1993. Accessory mineral behavior during differentiation of a granite suite: monazite, xenotime, and zircon in the Sweetwater Wash pluton, southeastern California. *Chem. Geol.*, **110**, 49-67.

**Geochronology of the Idaho-Bitterroot  
Batholith and Bitterroot Dome:  
An Example of Magmatism  
Preceding and Contemporaneous  
with Core Complex Extension**

<sup>1</sup>Foster, D.A. and <sup>2</sup>Fanning, C.M.

<sup>1</sup>*Victorian Institute of Earth and Planetary Sciences,  
School of Earth Sciences, La Trobe University,  
Bundoora, Victoria 3083, Australia*

<sup>2</sup>*Research School of Earth Sciences, The Australian  
National University, Canberra, ACT 0200, Australia*

Granitic plutonism and extension are broadly contemporaneous in many metamorphic core complexes. However, the relationship between magmatism and extension is rarely unambiguous, because in many cases it is not clear whether magmatism caused or was the product of extension. Furthermore, the apparent lack of synkinematic plutons in some core complexes has led to the suggestion that there is no relationship between magmatism and extension. Both of these problems are exacerbated by insufficient high precision geochronologic and thermochronologic data.

The Idaho-Bitterroot batholith, Montana and Idaho, forms the infrastructure for most of the Bitterroot Dome metamorphic core complex and thus is an ideal area for assessing the relationships between magmatism and extension. Previous U/Pb zircon and monazite studies of main-phase granitoids from the Bitterroot batholith give a range of lower discordia intercepts from ~73 to 48 Ma, with the youngest ages obtained from granite within the Bitterroot mylonite. These studies reveal complex inherited zircon populations and some radiogenic Pb-loss, so the significance of lower intercept ages is unclear for some samples. We have analyzed zircon from 6 samples of Bitterroot batholith granite using the SHRIMP ion microprobe. Three mylonitic granite samples from the Bitterroot mylonite in Lost Horse Canyon give a weighted mean <sup>206</sup>Pb/<sup>238</sup>U age of 54 ± 1 Ma. A protomylonitic granite from the central part of the Bitterroot Dome also gives a <sup>206</sup>Pb/<sup>238</sup>U age of 53 ± 1 Ma. Mylonitic megacrystic granite from Sweathouse Canyon yields an age of 65 ± 1 Ma. Finally, a granite sample from the Lochsa Canyon, in the central Bitterroot batholith, gives 57 ± 1 Ma. Inherited zircon from these samples ranges in age from 1460 to 1820 Ma. Paleoproterozoic crust dominates the source region of the Bitterroot batholith because the

majority of the inherited grains formed between 1750 and 1800 Ma.

These SHRIMP U-Pb zircon crystallization ages are consistent with the conventional zircon and monazite ages, though with higher precision and tighter range. Hornblende <sup>40</sup>Ar/<sup>39</sup>Ar ages for synplutonic mafic dikes in the central Bitterroot batholith also suggest crystallization of the main-phase plutons between 57 and 53 Ma. New and previously published <sup>40</sup>Ar/<sup>39</sup>Ar and K/Ar apparent ages of biotite and muscovite from the Lochsa area and the western and central Bitterroot Dome are 50 - 48 Ma. Younger mica ages (46 - 43 Ma) are restricted to the vicinity of the mylonite zone. These results indicate that the cessation of main-phase magmatism migrated east with time, and that most of the plutons in the Bitterroot Dome were intruded during the Paleocene and early Eocene. If the ~48 Ma conventional ages actually record crystallization, these younger granites appear to occur only in and adjacent to the Bitterroot mylonite.

Emplacement of magma during the period 65 to about 50 Ma reduced the strength of the crust in the Bitterroot batholith region. When the regional tectonic setting changed from compressional to extensional at ~50 Ma, mid-crustal plutonism was localized in what is now the Bitterroot Dome. Extensional deformation was focussed in the Bitterroot Dome, and formed the thick mylonite zone as a consequence of rheological contrasts with cooler areas to the east and west. The progression of granite crystallization ages and <sup>40</sup>Ar/<sup>39</sup>Ar cooling ages from west to east are consistent with top-to-the-east shear indicators in the mylonite zone. Thermochronology indicates that the western part of the Bitterroot Dome was below ~350°C at about the same time as the last stage of granite emplacement and metamorphism in the east. Therefore, the transition from mylonitization to brittle deformation to inactivity of the shear zone was progressive from west to east across the Dome from ~48 - 44 Ma. This explains the previously enigmatic occurrence of amphibolite facies ductile deformation in the eastern part of the Dome coincident with epizonal syenogranite magmatism along the western border.

## Pluton Emplacement Mechanisms: A View from the Roof

Fowler, T. K. Jr., Paterson, S.R.,  
Crossland, A. and Yoshinobu, A.

*Department, of Earth Sciences,  
University of Southern California,  
Los Angeles, CA 90089-0740, USA*

Exposures from tilted plutons and regions of steep topography reveal that the upper portions of many plutons in continental arcs are piston-shaped in three dimensions, being elliptical in plan view with steeply-dipping walls that abruptly roll over into gently-dipping or domal roofs. Such pluton roof exposures allow powerful tests of emplacement mechanisms that simply are not available from more commonly exposed map-plane sections through pluton walls. For example, lateral extensional models predict that host rocks above the pluton roof must be either strongly extended, structurally detached, or both. On the other hand, diapir models predict intense, roof-parallel flattening strains. At the roof, one can view directly the effects of doming, ring faulting, and cauldron subsidence. Because pluton roofs are directly in the path of magma ascent, they may represent a "process zone" preserving early portions of the ascent and emplacement history.

We have mapped partially preserved roofs and walls of ten plutons: the Mt. Powell batholith, MT; the Guadalupe, Castle Creek, Emerald Lake, Mitchell Peak and Hall Canyon plutons, CA; the Yerington batholith, NV; the Mt. Stuart batholith, WA; and the Chita and Agua Negra plutons, San Juan Province, Argentina. Estimated emplacement depths range from 2 to 10 kilometers, whereas host rock types include fine- to coarse-grained clastic rocks, calcisilicate, carbonate and volcanic rocks, schist, granite and granodiorite, offering a varied panorama of emplacement conditions.

Observed pluton/host rock relations share many traits in common. Pluton contacts are irregular, step-like (cm to 100 m) and discordantly truncate host-rock structure and fabric at all scales. With respect to the host rocks, intrusive contacts are brittle fractures, although thin section analysis indicates some grain-scale modification by near- and/or sub-solidus processes. Adjacent to roofs, host rocks show only weak emplacement-related ductile strains (< few %). Margin-parallel dikes are locally common. Emplacement-related faulting is uncommon and/or of small displacement (generally < 10 m). Host rocks above the

pluton roofs are non- to weakly-extended and are not detached. Roof lifting is relatively minor (generally < 200 m). At Yerington, Guadalupe and Mt. Stuart, narrow (10s to 100s m) deformed aureoles occur along the pluton walls and are characterized by moderate contact-normal host rock ductile shortening (few to several 10s %). The overall pluton/host structural relationship is similar to that produced by an ice-cream scoop; the contact represents a "surface of truncation" along which host rock material has been removed. Although not all arc plutons exhibit these relationships, a variety of published geological and geophysical data suggest that such three-dimensionally discordant plutons are common in the upper crust of arcs.

Within the plutons, spatially complex compositional zoning and fabric geometries show little relationship to host rock structure. Some of the plutons show large-scale (> 100s m) vertical zonation. Locally, roof contacts have served as ponding sites for late aplite, pegmatite and schlieren. Magmatic foliation patterns vary from concentric and contact-parallel, to planar and contact-oblique, to chaotic, to isotropic. In some cases, oblique foliations only deflect into contact-parallelism within a few cm of the contact. Host-rock xenoliths in the plutons occur from hand-sample to 100s of meters in size, but are rarely abundant.

Pluton emplacement destroys structural information; late, brittle processes eliminate kinematic evidence and host-rock material is "lost". Late magmatic and tectonic processes may overprint emplacement-related magmatic fabrics. Nevertheless, the data permit the following conclusions: 1) most host-rock material removed during emplacement has not been displaced upwards or laterally, and thus, must have been displaced downwards; 2) stoping is the final dominant emplacement process, however it may obliterate evidence for earlier downward host-rock displacement (*e.g.* downfolding, hot-Stokes flow); and, 3) pluton magmatic fabrics form extremely late and late-stage host rock and pluton strains are commonly mechanically decoupled.

**Sr-Nd Isotopic Record of Multi-Stage Interactions Between Mantle-Derived Magmas and Crustal Components in a Collision Context: Ultramafic-Granitoid Association from Vivero, NW Spain**

<sup>1</sup>Galan, Gumer, <sup>2</sup>Pin, Christian  
and <sup>2</sup>Duthou, Jean-Louis

<sup>1</sup>*Departamento de Geología,  
Universidad Autónoma de Barcelona,  
Edificio C(S) 08193 Bellaterra-Barcelona, Spain*

<sup>2</sup>*Département de Géologie, URA 10 CNRS,  
Université Blaise Pascal, 5 Rue Kessler,  
63038 Clermont-Ferrand, France*

One of the main characteristics of the Hercynian orogen is the abundance of orogenic granites. A pure crustal origin is widely accepted for the aluminous leucogranites but a mantle contribution is often invoked for granitoids of calc-alkaline affinity. However, the involvement of mantle-derived magmas in these granitoids is often controversial since 1) most available isotopic and other geochemical data favor crustal sources of meta-igneous and/or metasedimentary type, 2) isotopic compositions of basic-intermediate rocks associated with them cannot be usually related to a depleted mantle. In some few examples of the Hercynian orogen, basic-intermediate rocks related to calc-alkaline granitoids include olivine-amphibole bearing ultramafic rocks (*i.e.* cortlandtites) which provide further insight into the mantle contribution to the composition of these granitoids and into the interaction processes between mantle-derived magmas and crustal components.

The Vivero granitic body is situated at the north-western part of the Iberian Hercynides and displays such an association of ultramafic through melanocratic and calc-alkaline granitoids. These are syntectonic granitoids intruded into the middle crust soon after the Hercynian collision (*c.* 330 Ma). Ultramafic rocks are cumulates of peridotite, pyroxenite and hornblendite type. Melano-mesocratic rocks are biotite-amphibole diorites, quartz-diorites and tonalites. Calc-alkaline granitoids comprise fewer melanocratic amphibole-biotite tonalites, biotite granodiorites and monzonitic granites.

Petrological, geochemical data and radiogenic isotopes serve to evaluate (i) the interaction processes operating between mantle-derived magmas and crustal components, and (ii) the nature of the involved sources. Scattered

values for major and trace elements and heterogeneity for Sr-Nd isotope results preclude a common origin for the association as a whole, and even for each rock type.  $\epsilon_{Nd}$  and  $(^{87}Sr/^{86}Sr)_i$  of ultramafic-mesocratic rocks ( $\epsilon_{Nd} = 0.0 - -3.8$ ;  $(^{87}Sr/^{86}Sr)_i = 0.7058 - 0.7080$ ) overlap those of granitoids ( $\epsilon_{Nd} = -1.9 - -6.0$ ;  $(^{87}Sr/^{86}Sr)_i = 0.7061 - 0.7082$ ) but granitoids follow a divergent evolutionary trend with respect to the former rocks. Positive correlation between the degree of differentiation and the degree of contamination for melano-mesocratic rocks supports an origin from a tholeiitic basalt contaminated by a wall-rock assimilation (WRA) process, in a first stage, during ascent to the middle crust. Such a process followed by *in situ* fractional crystallization and interaction with <sup>87</sup>Sr-enriched fluids would also account for the ultramafic cumulates. Among the granitoids,  $\epsilon_{Nd}$  decreases while  $(^{87}Sr/^{86}Sr)_i$  increases from tonalites through granodiorites and monzonitic granites reflecting an increasing contribution of crustal components. A dominant AFC process, including two-component mixing, would account for the divergent evolutionary trend of these granites. This AFC process would contaminate the mafic magmas at deeper crust levels producing hybrid tonalites and related MME-type enclaves. In a second stage, the tonalitic hybrid magmas intruded the ultramafic-mesocratic rocks and were followed by granodiorites and monzogranites. The monzogranites are interpreted as pure crustal melts; their HREE fractionated pattern ( $(Gd/Yb)_N = 4 - 5$ ) suggests equilibrium with a garnet-rich residuum. Intermediate granodiorites would result from mixing between tonalites and monzogranitic magmas. The isotopic composition of the monzonitic granites favors a moderate time-integrated Rb/Sr protolith such as metasediments of greywacke type and/or intermediate-felsic meta-igneous not exposed at present. Taking into account the isotopic characteristics of ultramafic-mesocratic rocks and the operating contamination processes, the mafic end-member would have been extracted from mildly depleted domains of the lithospheric mantle. Partial melting of these fertile domains could have been triggered along shear zones of lithospheric scale during or soon after the Hercynian collision.

## Amphibole Mineral Chemistry of the Anorogenic Robertson River Igneous Suite, Blue Ridge Province, Virginia

Gray, Karen J.

*U.S. Geological Survey, MS 954 National Center,  
Reston VA 22092*

The late Proterozoic Robertson River Igneous Suite (RRIS) is part of a compositionally distinct group of intrusives in the central and southern Appalachians exposed in the core of the Blue Ridge Anticlinorium. The elongate batholith intruded high-grade middle Proterozoic (1.2 - 0.9 Ga) gneisses into the Robertson River rift zone, which trends N25°E and cuts across the Blue Ridge Anticlinorium from southeast to northwest. The RRIS is the largest known body preserving evidence of the plutonic and hypabyssal felsic magmatism associated with the initial stages of the late Proterozoic rifting event that led to the development of the Iapetus Ocean. It is composed of eight units that extend over 100 km, listed below from oldest (735 Ma) to youngest (702 Ma): 1) Rivanna Granite; 2) Laurel Mills Granite; 3) White Oak Alkali Feldspar Granite; 4) Arrington Mountain Alkali Feldspar Granite; 5) Cobbler Mountain Alkali Feldspar Quartz Syenite; 6) Hitt Mountain Alkali Feldspar Syenite; 7) Amissville Alkali Feldspar Granite; and, 8) Battle Mountain Alkali Feldspar Granite-Felsite complex. Catoctin Formation (600-570 Ma) greenstone dikes, which were associated with subsequent stages of the rifting event, intruded the RRIS. The RRIS and the Catoctin Formation indicate that there were two distinct extensional stages, an earlier stage that resulted in extensive felsic A-type magmatism and a later stage that produced predominantly basalt with minor rhyolite. All metaluminous units (except the Rivanna Granite) contain zoned amphiboles and have early primary textures; the Laurel Mills Granite exhibits synneusis texture. The mildly peralkaline (A.I. = 1) Amissville Granite contains evidence for an intersertal primary amphibole, as well as a subsolidus/hydrothermal amphibole. The alkaline/peralkaline units (Amissville Granite, Battle Mountain Granite/Felsite) which are chemically similar to the Younger Granites of Nigeria (A.I.  $\geq$  1, Ga/Al  $\geq$  6), contain riebeckite and aegirine or aegirine-augite. The metaluminous rocks (all except the Amissville and Battle Mountain granites) contain calcic amphiboles and are similar in bulk composition to anorogenic rocks from other localities worldwide (for example the Topsails-

St. Lawrence complex in Newfoundland). All RRIS units contain high abundances of high field strength elements (Nb, Y, Zr, Ga, and Zn) and all contain fluorite (except the Laurel Mills Granite). The peralkaline rocks, characterized by higher SiO<sub>2</sub> (~ 76 wt %), correlate with the higher SiO<sub>2</sub> contents of riebeckite amphiboles, whereas the metaluminous rocks exhibit a range in bulk rock SiO<sub>2</sub> (59 - 74 wt %) that is not reflected in the SiO<sub>2</sub> range of the amphiboles.

Detailed amphibole chemistry on seven units (no amphibole in the Rivanna Granite) allows identification of complex zoning and great variation within a single grain, as well as some variation between different localities within some units. The range of amphibole compositions for all metaluminous units is generally controlled by the edenite substitution and a combination of the Fe-, Ti-, or Al-tschermakite substitutions and a Na + Ti for Ca + Al substitution. The analyzed amphiboles are so Fe-rich that their compositional differences can best be illustrated in plots which compare Ti, Mn, Al, and Mg. In comparison to other alkaline suites, the amphiboles of the RRIS are unique in their high iron contents over the entire compositional range from calcic to sodic. Compositions of alkali and plagioclase feldspars and Fe-Ti oxides suggest that these minerals re-equilibrated during greenschist facies metamorphism. Late-stage magmatic and/or subsolidus reactions partially affected the hastingsitic to ferro-edenitic amphiboles and resulted in crystallization of biotite and later stilpnomelane. In spite of these postmagmatic and metamorphic reactions, the remaining amphiboles retain an igneous chemical signature (Si < 7.3 cations) and complex zonation.

Experimental data indicate that magnesio-hastingsite is stable below 1000°C at an oxygen fugacity of 10<sup>-11</sup> bars at the QFM buffer, hastingsite is stable at 600°C at an oxygen fugacity of ~ 10<sup>-19</sup> bars at the QFM buffer, and that ferro-pargasite has a stability field very similar to hastingsite. These experimental data generally are applicable to the range of calcic amphiboles in the RRIS; however, the high iron contents indicates that the temperature would be in the lower range. The evolutionary trend in the bulk chemistry as indicated by the range in SiO<sub>2</sub> (59 - 76 wt %) is not reflected in the compositions of the calcic amphiboles. The change in amphibole composition from calcic to sodic is abrupt and represents a sudden change in temperature (lower) and oxygen fugacity and alkalinity (higher). The rocks bearing sodic amphibole were emplaced about 8 Ma after the last metaluminous unit, and then the magmatism in the area ceased.

## Shoshonitic Granitoids of the Borborema Province, NE Brazil

Guimarães, I.P. and Da Silva Filho, A.F.  
*DGEO - CT, UFPE CEP 50732-970,*  
*Cidade Universitária, Recife PE, Brazil*

The Borborema Province (BP) has been interpreted by Van Schmus *et al.* (1994) as the central part of a major Pan-African/Brasiliano orogenic belt, that formed during the collision of the Sao Francisco(SFC)-Congo-Kasai Cratons and the Sao Luis/West Africa Craton. The BP is divided into three domains: Paleoproterozoic to Archean Rio Piranhas and Caldas Brandão Massifs; Paleoproterozoic to Archean SFC basement to the South; and a domain, which contains a large amount of Mesoproterozoic fold belts and small amount of reworked Paleoproterozoic to Archean blocks.

The shoshonitic granitoids in the BP have a particular distribution. They have always been described close to the contacts between the Mesoproterozoic Fold Belts and the Paleoproterozoic-Archean blocks. The Rb-Sr data available, point out to an age of 600Ma for them.

The shoshonitic granitoids can be divided into two groups: 1) oversaturated (OG), such as Curituba and Serra do Catu Complexes (North boundary of the Sergipano Fold Belt), Solidão and Teixeira Complexes (NE Boundary of the Pajeu-Paraíba Fold Belt (PPFB); Sial and Ferreira, 1988), Floresta area (SW boundary of PPFB; Valgueiro *et al.*, 1992); and, 2) saturated (SG), such as Bom Jardim and Toritama Complexes (SE boundary of the PPFB; Guimarães, 1989), Terra Nova Complex (S boundary of the Pianco Alto Brigida Fold Belt, Silva Filho *et al.*, 1993), and Quixada and Prado Complexes (NW boundary of the Serido Fold Belt, Galindo *et al.*, 1992).

The OG are monzo- to syenogranites containing small enclaves, which are mainly amphibole clots. The SG are monzonites and syenites which contain large amount of mafic enclaves, with composition similar to the less evolved major facies. Low angle foliations recorded in some SG complexes, point out intrusions related to tangential tectonism (Guimarães, 1989). The more mafic major facies of the SG show very high MgO (5 - 7 wt %), Cr (200 - 500 ppm) and Ni (100 - 250 ppm) which point to a mantle contribution in the genesis of these rocks.

Both groups are peraluminous to metaluminous and show high contents of Sr, Ba, LREE, medium content of Rb and Zr, low content of TiO<sub>2</sub>, P<sub>2</sub>O<sub>5</sub> and Nb and, K<sub>2</sub>O/N<sub>2</sub>O ratios >1. These chemical characteristics,

associated with the ubiquitous presence of calcic amphibole (Mg-hornblende to edenite), clinopyroxene showing no Fe-enrichment trend and K-feldspar surrounded by plagioclase, fit with those of shoshonitic rocks associations (Morrison, 1980). The calc-alkali ratio - SiO<sub>2</sub> trends for the shoshonitic granitoids of the BP are similar to that of New Guinea Continental Arc (Brown, 1982).

Shoshonitic rocks are produced above a steepening subduction zone when a flip in the direction of subduction occurs and uplift and block faulting occur within the arc (Morrison, 1980). The distribution in space and time of the shoshonitic granitoids within the BP, suggest that: the Archean to Paleoproterozoic blocks probably represent (or behaved as) continental microplates during the Pan-African collisional event in the BP, and an age of 600 Ma is a good estimation for the end of the compressive regime within the BP. The Shoshonitic magmatism the tectonic model (Caby, 1987; Guimarães, 1989; Caby *et al.* 1991; Jardim de Sá, 1994) in which collision of continental microplates and arc took place during the Brasiliano orogeny (850 to 600 Ma), followed by transcurrent intracontinental reworking

- Brown, G.C., 1982. Calc-alkaline intrusive rocks: their diversity, evolution and relation to volcanic arcs. In Thorpe, R. (ed), *Andesites*, J. Wiley and Sons, p. 437-461.
- Caby, R., 1987. The Pan-African belt of West Africa from the Sahara desert to the Gulf of Benin. In Schaer, J. and Rodgers, J. (eds), *The Anatomy of Mountain Ranges*, Princeton University Press, p. 129-170.
- Caby, R., Sial, A., Arthaud, M. and Vouchez, A., 1991. Crustal evolution and the Brasiliano Orogeny in northeast Brazil. In Dallmeyer, R. and Lecorche, J. (eds), *The West African Orogen and Circum-Atlantic Correlatives*, p. 373-397.
- Galindo, A.C., Dall'agnol, R., McCreath, I., Leterrier, J., 1993. Química mineral de anfíbolios e biotitas de alguns granitoides Brasileiros do oeste do Rio Grande do Norte, nordeste Brasil. *MAGMA-Academia Brasileira de Ciências, Rio de Janeiro, Brasil, Extended Abstracts*, 66-68.
- Guimaraes, I., 1989. *The petrologic evolution and tectonic association of the Bom Jardim Complex, Pernambuco State, NE Brazil*. PhD thesis, University of London, 424 p.
- Jardim de Sa, E.F., 1994. *A Faixa Seridó (Providência da Broborema, NE do Brasil) e seu significado geodinâmico na cadeia Brasileira/Pan-Africana*. Doctor Thesis, Universidade de Brasília, 803 p.
- Morrison, G., 1980. Characteristics and tectonic setting of the shoshonite rock association. *Lithos*, 13, 97-10.
- Sial, A. and Ferreira, V., 1988. Brasiliano age peralkaline plutonic rocks of the central structural domain, NE Brazil. *Rend. Soc. Italiana.*, 43-2, 307-342.
- Silva Filho, A.F., Guimaraes, I.P. and Thompson, R. 1993. Shoshonitic and ultrapotassic Proterozoic intrusive suites in the Cachoeirinha-Salgueiro Fold Belt, NE Brazil: a transition from collisional to post-

collisional magmatism. *Precambrian. Res.*, **62**, 323-342.

Valgueiro, C., Ferreira, V., Sial, A., Sa, L., 1992. Rochas shoshoníticas e peralcalinas a noroeste de Floresta, Pernambuco. *37 Cong. Bras. Geo., SBG, São Paulo-SP, Extended Abstracts*, **2**, 69.

Van Schmus, W., Brito Neves, B.B. and Babinski, M., 1994. Mesoproterozoic crustal domains in the Borborema Province: Evidence from U/Pb and Sm/Nd geochronology. *38 Cong. Bras. Geo., SBG, Camboriu-SC, Extended Abstracts*, **1**, 403-404.

## Miocene Rapakivi-Like Granites of Southern Newberry Mountains, Nevada, USA: Comparison to the Proterozoic Rapakivi Granites of Finland

<sup>1</sup>Haapala, I., <sup>1</sup>Rämö, O.T. and <sup>2</sup>Volborth, A.

<sup>1</sup>Department of Geology, P.O. Box 11,  
FIN-00014 University of Helsinki, Finland

<sup>2</sup>Montana College of Mineral Science and Technology,  
Butte, MT 59701, USA

Rapakivi granites occur on all continents and are commonly characterized by a Proterozoic age (1.75 to 1.0 Ga, with a few exceptions), bimodal magmatic association, extensional tectonic setting, A-type geochemical and mineralogical characteristics, dominantly crustal source, and Sn-W-Be-Zn mineralization associated with topaz-bearing late-stage intrusive phases. All these features are well-documented in southern Finland and adjacent Russian Karelia where 1.65 to 1.54 Ga rapakivi granite plutons intrude Paleoproterozoic or Archean metamorphic crust (Rämö and Haapala, 1995).

The Tertiary extension-related magmatic association of the southwestern United States (Basin and Range Province) shows marked similarities, but also some dissimilarities, with the Proterozoic rapakivi magmatism of Finland. In both areas, extensional tectonics is indicated by swarms of parallel rhyolite and basalt dikes, normal and listric faulting, and by thinning of the crust (Gans *et al.*, 1989; Haapala and Rämö, 1992; Korja and Heikkinen, 1995). The synextensional bimodal magmatism of the Basin and Range Province comprises basalts and rhyolites, in lesser amount plutonic equivalents, whereas in Finland the plutonic members prevail. In both areas, the felsic igneous rocks show commonly A-type or within plate granite characteristics. The Be and Sn deposits locally associated with the Tertiary topaz rhyolites of southwestern U.S.A. are probably volcanic - subvolcanic analogues of the greisen and skarn-type Sn-Be-W-Zn mineralization related

to the topaz-bearing granites of the Finnish and Russian Karelian rapakivi complexes.

The Miocene Spirit Mountain pluton (SMP; Howard *et al.*, 1994) in the southern Newberry Mountains, southern Nevada, is one of the few epizonal-subvolcanic synextensional granite plutons of the southern Basin and Range Province. Numerous NNW-trending dikes composed of rhyolite or basalt or their mingling products transect the pluton and the surrounding, mainly Proterozoic, crust. SMP is mainly composed of various textural types of light-coloured biotite-bearing or two-mica granites; hornblende is rarely present. Overall, the Finnish rapakivi granites are more mafic, often showing hornblende as a typical mafic silicate. Titanite and magnetite are characteristic accessory minerals of SMP, whereas in the Finnish rapakivi granites ilmenite and anatase are the Ti-bearing accessory minerals. Some of the alkali feldspar crystals in SMP are mantled by plagioclase; in Finland, plagioclase-mantled alkali feldspar ovoids are typical in the larger rapakivi granite batholiths.

The SiO<sub>2</sub> content of the SMP granites ranges from 66.6 to 77.4 wt %, (Na<sub>2</sub>O + K<sub>2</sub>O) from 7.5 to 9.6 wt %, and molecular Al<sub>2</sub>O<sub>3</sub>/(CaO + K<sub>2</sub>O + Na<sub>2</sub>O) from 0.98 to 1.04; these values coincide with those measured for the Finnish rapakivi granites. A-type and within plate granite characteristics of the granites of SMP are not so well expressed as in the case of the Finnish rapakivi granites; some of the former plot into the field of volcanic arc granites or fractionated granites. FeO<sup>T</sup>/(FeO<sup>T</sup> + MgO) varies in SMP granites from 0.74 to 0.90, whereas in the Finnish rapakivis it is usually between 0.85 and 1.00 (average 0.92). The F content (0.03 to 0.09 wt %) of the SMP granites is very low compared to the average of 0.35 wt % F in the rapakivi granites of Finland.

Nd isotopic data on the Precambrian country rocks of SMP ( $\epsilon_{Nd}(1.4 \text{ Ga})$  c. - 3.5,  $t_{DM}$  1.93 - 2.03 Ga) show that they conform to the evolution of the Paleoproterozoic Mojave province (*cf.* Gleason *et al.*, 1994). The Nd isotopic composition of the granites of SMP ( $\epsilon_{Nd}(15 \text{ Ma})$  - 9.6 - - 11.6,  $t_{DM}$  1.14 to 1.34 Ga) is indicative of a substantially younger source. This contrasts with the Finnish rapakivi granites that have been interpreted to have derived from the Paleoproterozoic crust hosting the granites (Haapala and Rämö, 1992).

Gans, P.B., Mahood, G.A. and Schermer, E.R., 1989. Synextensional magmatism in the Basin and Range Province: A case study from the eastern Great Basin. *Geol. Soc. Am. Spec. Paper*, **223**, 53 p.

Gleason, J.D., Miller, C.F., Wooden, J.L. and Bennet, V.C., 1994. Petrogenesis of the highly potassic 1.42 Ga Barrell Spring pluton,

- southeastern California, with implications for mid-Proterozoic magma genesis in the southwestern USA. *Contrib. Mineral. Petrol.*, **118**, 182-197.
- Haapala, I. and Rämö, O.T., 1992. Tectonic setting and origin of the Proterozoic rapakivi granites of southeastern Fennoscandia. *Trans. Royal Soc. Edinburgh: Earth Sci.*, **83**, 165-171.
- Howard, K.A., John, B.E., Davis, G.A., Anderson, J.L., and Gans, P.B., 1994. A guide to Miocene Extension and magmatism in the Lower Colorado River Region, Nevada, Arizona, and California. *U.S. Geological Survey, Open-File Report 94-246*, 54 p.
- Korja, A. and Heikkinen, P.A., 1995. Proterozoic extensional tectonics of the central Fennoscandian Shield: Results from the Baltic and Bothnian Echoes from the Lithosphere experiment. *Tectonics*, **14**, 504-517.
- Rämö, O.T. and Haapala, I., 1995. One hundred years of rapakivi granite. *Mineral. Petrol.*, **52**, 129-185.

## Geochemistry and Petrogenesis of Lusatian Cadomian Granitoids (Northern Margin of Bohemian Massif)

<sup>1,2</sup>Hammer, J. and <sup>1</sup>Eidam, J.

<sup>1</sup>*FR Geowissenschaften, Universität Greifswald,  
Jahn-Str. 17a, 17489 Greifswald, Germany*

<sup>2</sup>*Geochemisches Institut, Universität Göttingen,  
Goldschmidt-Str. 1, 37077 Göttingen, Germany*

Within the Lusatian Anticlinal Zone (LAZ; Southeast Germany, Eastern Saxothuringicum) Cadomian ( $587 \pm 17$  Ma to  $542 \pm 9$  Ma) and subordinate late Variscan ( $304 \pm 14$  Ma) granitoids occur (Kröner *et al.*, 1994). As documented by microscopic observations and low differences in  $\delta^{18}\text{O}$  values of coexisting quartz and feldspars, the Cadomian granitoids of the western part of LAZ are only weakly overprinted by Caledonian and Variscan metamorphism and hydrothermal activity. Most probably, the intensive Caledonian tectogenesis along the western margin of East-European platform in connection with the closure of the Tornquist Ocean (Oliver *et al.*, 1993; Oliver and Kelley, 1993) has slowly affected only slightly the LAZ rocks.

Traditionally, based on macroscopic observations, three main petrographic rock types have been distinguished within the Cadomian Lusatian Granodiorite Complex (LGC): two-mica granodiorites (tmgd), muscovite-bearing biotite granodiorites (mbgd) and biotite granodiorites (bgd). According to the Streckeisen classification, the rocks represent predominantly granodiorites and tonalites. Rarely, small stocks of monzogranites/ syeno-granites

occur as the youngest intrusive phases. The rock association displays a large range of chemical compositions, reaching  $\text{SiO}_2$  contents between 64 and 77 wt %. Concentrations of such elements as Ba, La, Hf, Rb, Sr, Th and Zr are nearly constant over the whole compositional range of LGC. This means that fractional crystallization did not greatly modify the compositions of granitoid magmas and modifications of whole rock chemistry are interpreted to have been caused by restite unmixing.

There are clearly differences in geochemical characteristics between tmgd and bgd, with the mbgd as a transitional rock type. The tmgd broadly fits the classical definition of S-type granites (metasedimentary inclusions; high occurrences of rounded inherited zircons; peraluminous whole-rock chemistry; particularly high modal proportions of cordierite, garnet, sillimanite, monazite/xenotime, muscovite; low Ca and Sr contents;  $(^{87}\text{Sr}/^{86}\text{Sr})_i = 0.7067 - 0.7101$ ;  $\epsilon_{\text{Nd}} = -8.8 - -4.9$ ;  $\delta^{18}\text{O}$  whole rock values of 9.0 - 10.5 ‰ and  $\delta^{34}\text{S} < 0$ ). The bgd are clearly richer in  $\text{CaO}$ ,  $\text{TiO}_2$  and  $\text{P}_2\text{O}_5$  than the tmgd. Particularly low  $\delta^{18}\text{O}$  values (7.5 - 9.5 ‰), mostly metaluminous whole-rock chemistry,  $(^{87}\text{Sr}/^{86}\text{Sr})_i$  between 0.7041 and 0.7063;  $\epsilon_{\text{Nd}} = -6.7 - -2.1$  and high anorthite content in plagioclase cores (up to 55 mol % An) are not compatible with derivation from metasedimentary source rocks.

Calculated source rock composition for the bgd (on the basis of 30 % restite-free partial melt and 70 % restite) corresponds to the average chemistry of tonalites. In comparison to worldwide averages of tonalite (K.H. Wedepohl, personal communication, 1994) the source rocks of bgd are richer in  $\text{TiO}_2$ ,  $\text{K}_2\text{O}$ , Cs, Cr, Ni, Hf, Nb, Zr, REE and poorer in CaO. Most probably, partial melting processes occur in a heterogeneously composed intermediate to mafic lower crust with Nd model ages between 1.13 and 1.86 Ga. Melting may be attributed to tectonothermal activity in the hanging wall of a subduction zone and may be induced by subduction-related, mantle-derived underplated mafic magma. Coincidence of Cadomian granitoids and of the gravimetric anomaly of Bernsdorf-Kamenz can be used as an argument for intrusion of large amounts of mafic melts from the mantle. Mixing processes between mantle-derived mafic magmas and lower crustal granitoid melts are possible. Increasing  $(^{87}\text{Sr}/^{86}\text{Sr})_i$  and decreasing  $\epsilon_{\text{Nd}}$  in the mbgd and tmgd in comparison to the bgd may be interpreted either as due to an increasing contribution of reworked metasedimentary source rocks or by relatively independent melting processes in metasediments, probably in higher crustal horizons.

The geological evolution in LAZ region is comparable with the late Proterozoic/early Palaeozoic tectonomagmatic development of Northern Armorican Massif (Brown and D'Lemos, 1991) and with Cadomian orogenic activity in other circum-Atlantic, late pre-Cambrian Gondwanan marginal terranes, including southern portions of the Iberian Massif (Ochsner *et al.*, 1993) and various sectors of North African orogens (Nance *et al.*, 1991).

- Brown, M. and D'Lemos, R.S., 1991. The Cadomian granites of Mancellia, northeast Armorican Massif of France: relationship to the St. Malo migmatite belt, petrogenesis and tectonic setting. *Precambrian Res.*, **51**, 393-427.
- Kröner, A., Hegner, E., Hammer, J., Haase, G., Bielicki, K.-H., Krauss, M. and Eidam, J., 1994. Geochronology and Nd-Sr systematics of Lusatian granitoids: significance for the evolution of the Variscan orogen in east-central Europe. *Geol. Rundsch.*, **83**, 357-376.
- Nance, R.D., Murphy, J.B. and Strachan, R.A., 1991. Late Proterozoic tectonostratigraphic evolution of the Avalonian and Cadomian terranes. *Precambrian Res.*, **53**, 41-78.
- Ochsner, A., Schäfer, H.-J., Gebauer, D. and Friedl, G., 1993. The timing and nature of the Cadomian geodynamic evolution within the Ossa Morena Zone (SW Spain) on the basis of new U-Pb dating of various intrusive rocks. *Terra abstracts, supplement 1 to Terra nova*, **5**, 320.
- Oliver, G.J.H., Corfu, F. and Krough, T.E., 1993. U-Pb ages from SW Poland: Evidence for a Caledonian suture zone between Baltica and Gondwana. *J. Geol. Soc. London*, **150**, 355-369.
- Oliver, G.J.H. and Kelley, S., 1993.  $^{40}\text{Ar}/^{39}\text{Ar}$  fusion ages from the Polish Sudetes: Variscan tectonothermal reworking of Caledonian protoliths. *N. Jb. Geol. Paläont. Mh.*, 321-334.

## ORAL PRESENTATION

### Hydrodynamics of Magmatic and Meteoric Fluids in the Vicinity of Granite Plutons

Hanson, R. Brooks

*Science, 1333 H Street, N.W.,  
Washington, DC 20005, USA*

During emplacement and cooling of granitic magmas in the crust, fluid production from magma and wall rocks, thermal expansion of fluid, thermal and chemical buoyancy, topography, and thermal and mechanical deformation of rocks all interact to drive fluid flow. Mixing of fluids with rocks and other fluids produces ore deposits and alters rocks, and variation of fluid pressure, particularly related to degassing of a magma leading to hydrofract-

uring, is a dominant control on permeability. Numerical models that account for the dynamics of these basic processes following emplacement of a granitic magma in the upper crust reveal the evolution of the hydrothermal system. In general, the hydrothermal system evolves from lithostatic fluid pressures and expulsion of internally generated magmatic and metamorphic fluids to hydrostatic fluid pressures and circulation of externally derived (meteoric) fluids with time; high permeability, low rates of fluid production, and shallow depth accelerate the transition. The relative importance of these processes and thus the locations where distinct fluids mix or react with rocks to produce ore deposits depends most on 1) permeability and its evolution, and 2) the history of fluid generation, particularly from the magma (figure). Fluid production in the magma and wallrocks is the dominant mechanism elevating fluid pressures to lithostatic values. For granitic intrusions, about 3 to 5 times as much magmatic fluids are produced as metamorphic fluids. Permeabilities of <1 microdarcy are required for generation of lithostatic pressures for reasonable rates of fluid production in granites with dimensions of several kilometers. Lower permeabilities, <0.1 microdarcy are required around small systems or stocks. Such low permeabilities are unlikely to be maintained once thermal fracturing ensues; the resulting drop in fluid pressure allows rapid influx of meteoric fluids. The tight interaction of fluid production and permeability in controlling fluid pressures means that near the surface and around small stocks dramatic changes in fluid pressure, flow regime, permeability, and interaction of rocks with magmatic and meteoric fluids are likely.

Buoyancy, and the strong pressure gradient from lithostatic pressures in the intrusion to near-hydrostatic parts closer to the surface drive magmatic fluids upward. The continued production of magmatic fluids from the interior of the chamber as the magma crystallizes further isolates magmatic fluids from wallrocks. Near the surface, topography and hydrothermal circulation can act to transport magmatic fluids laterally. At depth, in the metamorphic aureole, elevated fluid pressures in the aureole induced by metamorphic fluid production and low permeabilities hinder lateral influx of magmatic fluids. Extensive lateral flow of magmatic fluids at depth requires creation and maintenance of a laterally enhanced permeability, sublithostatic fluid pressures in the aureole - produced either by low rates of metamorphic devolatilization or high permeability (>1 microdarcy) - and early release of fluids from the magma (figure). Extensive lateral flow thus becomes unlikely with increas-

ing depth. Together, these patterns are consistent with the distribution and evolution of skarns and hydrothermal ore deposits around granitic magmas.

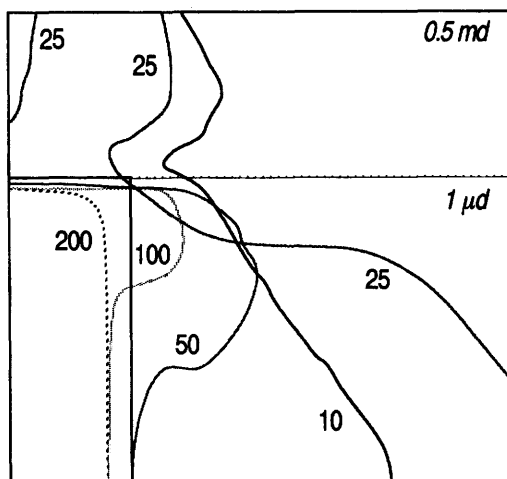


Figure: Evolution of the boundary between magmatic fluids and predominantly meteoric fluids (and some residual pore fluids) around a granitic intrusion in a model (numbers give time in 1000 years after emplacement). The magma, on the left, contained 5% water by weight, which was released linearly with cooling in this model. The intrusion was 4 km wide and was emplaced at 800°C at a depth of 5.5 km. There was no metamorphic fluid production; low fluid pressures in wallrocks allowed extensive lateral influx of magmatic fluids. Upper crustal layer has a permeability of 0.5 millidarcy; lower layer has a permeability of 1 microdarcy.

## Experimental Study of the Distribution of H<sub>2</sub>O Between Cordierite and Peraluminous Melt, and its Bearing on the Generation and Evolution of Migmatites and Granites

Harley, S.L. and Carrington, D.  
*Department of Geology and Geophysics,  
 University of Edinburgh, Edinburgh, Scotland*

The occurrence of cordierite in migmatites and S-type granitoids testifies to its significance in melt generation and crystallization under upper-crustal conditions. As cordierite is able to incorporate both CO<sub>2</sub> and H<sub>2</sub>O within its structure it is potentially an indicator of the proportions and contents of these volatile species in any coexisting fluid or melt. Specifically, the volatile contents of melts present in high-grade metamorphism may be estimated using cordierite as a monitor providing the distribution of H<sub>2</sub>O between melt and coexisting cordierite,  $D_w [=H_2O_{\text{melt}} / H_2O_{\text{Crd}}]$ , is known.

Estimates of  $D_w$  for H<sub>2</sub>O-saturated conditions, derived from maximum solubility data for Mg-cordierite (Mirwald *et al.*, 1979) and granitic melts (Holtz and Johannes, 1994), are in the range 5 - 7. Experiments aimed at defining  $D_w$  for melt-cordierite over a range of melt H<sub>2</sub>O contents from saturated (*i.e.* cordierite + melt + vapour) to highly undersaturated have been conducted at 5.0 kbar and 800-1000°C, and at 900°C for a range of pressures. Several cordierite-melt pairs have been run in an internally-heated gas apparatus at identical pressure-temperature conditions but with differing bulk H<sub>2</sub>O. Natural cordierite ( $X_{\text{Mg}} = 0.66$ ) and a gel of peraluminous granite composition have been equilibrated, forward experiments involving evacuated (volatile-free) cordierite and reversals using H<sub>2</sub>O-saturated cordierite. H<sub>2</sub>O contents in product cordierite and melt have been determined using SIMS, with <sup>1</sup>H/<sup>30</sup>Si isotopic ratios converted to wt % H<sub>2</sub>O through calibration curves derived from standards.

These reversed experiments demonstrate that cordierite in equilibrium with melt can have a range of H<sub>2</sub>O contents at a single *P-T* condition. Hence, volatile-undersaturated cordierite coexists with H<sub>2</sub>O-undersaturated melt. For example, at 5.0 kbar and 900°C cordierite varies from 0.5 wt % to 1.8 wt % H<sub>2</sub>O, the latter saturation value being in good agreement with extrapolations from Mirwald *et al.* (1979). Under these *P-T* conditions the melts vary from a minimum of 2 wt % H<sub>2</sub>O to maximum H<sub>2</sub>O contents (10

wt %) that agree well with previous solubility studies (Holtz and Johannes, 1994).  $D_w$  is near-constant with a value between 3.5 - 4.5 for melt  $H_2O$  contents of less than 5 - 6 wt %. At melt  $H_2O$  contents above this critical range  $D_w$  increases up to 6 - 7 at saturation, a behaviour ascribed to melt  $H_2O$ -solubility mechanism effects.  $D_w$  at saturation also increases with temperature. Experiments using starting cordierites with differing  $X_{Mg}$  show that  $D_w$  is independent of this parameter.

These experimental results can be used to infer the volatile contents of the fugitive melts that formerly equilibrated with cordierite in migmatites and granites. SIMS analysis of cordierites in patch leucosomes from several terranes (e.g. Arunta Complex, Cooma, Rauer Group, Kerala, Madagascar, Willyama) reveals low  $H_2O$  and  $CO_2$  contents of 0.6 - 1.2 wt % and 0.1 - 0.7 wt % respectively (Harley, 1994). Melt  $H_2O$  contents calculated from low- $CO_2$  cordierites using the experimental  $D_w$  data are in the range 2.8 - 4.4 wt %, consistent with generation of the migmatites through dehydration-melting reactions involving biotite ( $\pm$  sillimanite). Cordierite has also been used to compare migmatites and S-type granitoids in selected terranes. At Mt. Stafford in the Arunta Complex,  $CO_2$ -poor cordierites in segregated S-type granite leucosomes are clearly distinct in their volatiles from cordierites in locally-developed patch migmatites, which contain mixed  $H_2O$ - $CO_2$  fluids. It appears that extensive melting in this terrane has been triggered by the influx of fluids probably derived from subjacent crystallising plutons. Cordierites in other S-type granites and pegmatites are also  $H_2O$ -rich and close to volatile-saturated and signify formation either during wet melting or from a melt approaching saturation in  $H_2O$ .

Harley, S.L., 1994. Cordierite as a sensor of fluid and melt distribution in crustal metamorphism. *Mineral. Mag.*, 58A, 374-375.

Holtz, F. and Johannes, W., 1994. Maximum and minimum water contents of granitic melts: implications for chemical and physical properties of ascending magmas. *Lithos*, 32, 149-159.

Mirwald, P.W., Maresch, W.V. and Schreyer, W., 1979. Der Wassergehalt von Mg-Corderierit zwischen 500°C und 800°C sowie 0.5 und 11 kbar. *Fortschr. Mineralogie*, 57, 101-102.

## A Detailed Sr-Pb Isotope Study of the Naivasha Comendites, Kenya

Heumann, A., Davies, G.R. and Staudigel, H.  
*Faculteit der Aardwetenschappen, Vrije Universiteit,  
 Amsterdam, The Netherlands*

Quantification of the time scales over which silicic magmatic systems evolve is crucial to the understanding of how fast batches of silicic magma are produced and how long they survive in magma chambers prior to eruption. Recent comendites of the bimodal Naivasha (Olkaria) volcanic complex in the Kenya Rift Valley have elevated Rb/Sr ratios (Sr = 1.3 - 2 ppm; Rb = 521 - 819 ppm) that potentially allows the resolution of time differences on the order of 1 ka by conventional Sr isotope determination. For our study we used pristine obsidian glasses and minerals from the most chemically evolved comendites, which comprise two out of seven chemostratigraphic groups with distinct trace element and isotope systematics (Group III and VI, the latter being morphologically the younger). Individual lava groups have total eruptive volumes of <5 cubic km. Ar-Ar isotope dating of sanidines from both groups cannot resolve an age and hence implies young eruption ages of <10 ka. This conclusion is supported by Carbon-14 ages from overlying lake sediments.

The comenditic glasses have relatively radiogenic Sr isotope ratios between 0.707355 and 0.707950. Rb-Sr glass isochrons define ages older than the eruption ages. The data do not define mixing relationships on diagrams of Sr isotopes against  $1/Sr$  content. The Pb isotope ratios of glasses from an individual group are indistinguishable but there is a small difference between Group III and IV ( $^{206}Pb/^{204}Pb$  of 19.87 and 19.73). These data establish that the Sr isochrons are not a consequence of mixing and suggest magma production at 50 ka for the morphological younger Group VI and 20 ka for the older Group III. In order for an isochron to be preserved in a magma chamber, the magmas of each group must form rapidly relative to the error in the isochron age (10 and 5 ka respectively). Subsequent to formation, mixing within the magma chamber must be limited, because homogenisation of Rb/Sr will destroy an isochron relationship. Crustal contribution from wall rocks can also be ruled out since it would change the Rb-Sr systematics of the magma due to the low Sr contents of the comendites. Together, these data imply that the comenditic magmas had long residence times of up to 40 ka.

Over time the Rb-Sr systematics of a mineral in a magma chamber will reflect a combination of the growth of radiogenic Sr and diffusive re-equilibration with the surrounding melt. The Sr diffusion coefficient of K-feldspar are low such that  $\ll 1\%$  of the Sr in the feldspar will be exchanged with the host magma over a time period of 50 ka. An amphibole separate from Group VI has Sr isotope systematics that lie on the 20 ka isochron possibly implying that this phase remained an isotopically closed system in magma chamber for about 20 ka. The Pb and Sr systematics of the feldspars, however, are not consistent with growth from the magma and subsequent long residence times. Euhedral grains from Group VI have Sr isotope ratios that plot above the Group VI glass isochron and this implies that either, they crystallized at  $\sim 13$  ka or they have a xenocrystic origin. Feldspars from Group III have different morphologies, some samples contain euhedral grains while others are rounded and appear resorbed. Sr isotope ratios are very variable, up to 0.727. The feldspars also have very variable Pb isotope ratios ( $^{206}\text{Pb}/^{204}\text{Pb}$  from 19.7 to 20.2) which suggests that they are either xenocrystic or restitic in origin. The regional basement is Archaean and has very unradiogenic Pb isotope ratios ( $^{206}\text{Pb}/^{204}\text{Pb} = 17.0$ ) so we are able to conclude that the feldspars are derived from the Miocene to Recent volcanics that form the majority of the upper 6 km of the Rift Valley. The important conclusion from this study is that phenocrysts in an individual magma batch may have multiple sources and in order to use the Sr isotope systems for age information other isotope systems (Pb-Nd-Th) are required to prove minerals are cogenetic with the host magma.

## Geochemical Constraints on Magma Sources of Mesozoic Continental Arc Plutonic Complexes, Andean Plate Boundary Zone, North Chile

<sup>1,2</sup>Hodkinson, D., <sup>1</sup>Krogstad, E.J.  
and <sup>1</sup>Brown, M.

<sup>1</sup>*Department of Geology, University of Maryland  
at College Park, MD 20742, USA*

<sup>2</sup>*Now at: Department of Geosciences,  
University of Arizona, Tucson, AZ 85721, USA*

During the late Triassic, Jurassic and early Cretaceous, an extensional magmatic arc was formed in the Andean Margin of North Chile. The crust into which arc magmas were emplaced is composed of Upper Paleozoic metasedimentary rocks, part of an accretionary complex, intruded by plutonic complexes of a broad Permian-Triassic magmatic arc. Plutons were emplaced at ramps within a hinterland-propagating extensional duplex, likely fed by dikes that transferred magma through the crust (Grocott *et al.*, 1994). We present geochemical data, including Nd and Pb isotope data, for one Early Jurassic plutonic complex, and Nd isotope data for one Early Cretaceous plutonic complex. These data allow assessment of source components and temporal change in magma sources during the evolution of this extensional continental margin.

The Caldera-Pajonales Plutonic Complex (CPPC) is part of the Early Jurassic magmatic arc. The Complex is composed of hornblende-biotite-two pyroxene gabbros, with subvertical pre-full-crystallization fabric and magmatic layering, clinopyroxene-hornblende diorites, hornblende-biotite tonalites and granodiorites, and microgranites. It has yielded  $^{40}\text{Ar}/^{39}\text{Ar}$  hornblende plateau isotope correlation ages in the range *c.* 194 to *c.* 188 Ma, and a  $^{40}\text{Ar}/^{39}\text{Ar}$  plateau age on hornfels muscovite adjacent to the complex of *c.* 194 Ma (Dallmeyer *et al.*, 1995); for modelling isotope evolution we take the age of the complex to be *c.* 190 Ma. Whole-rock geochemical data demonstrate calc-alkaline affinity of the complex, with characteristic features such as relative depletion in Ta, Nb, P and Ti and relative enrichment in Rb, Th, K and LREE. Although REE abundances are variable, and a gabbro sample exhibits a small positive Eu anomaly, tonalite/granodiorite and microgranite samples from the CPPC exhibit negative Eu anomalies consistent with an

evolution that includes fractional crystallization of plagioclase. Normalized HREE values suggest hornblende is stable in the source rather than garnet. Ten samples, selected to cover the range of bulk rock compositions within the CPPC, have been analyzed for Nd isotopic compositions. The samples exhibit a range of  $\epsilon_{Nd}(190)$  from *c.* +6 to *c.* -3 without covariation with  $f(\text{Sm}/\text{Nd})$ . These data require a minimum of three reservoir components to satisfy the range of values within the complex (see figure below), as follows: depleted mantle ("DM"); short-term LREE-enriched mantle or juvenile crust ("EM"); and, *c.* 1 Ga continental crust ("CC").

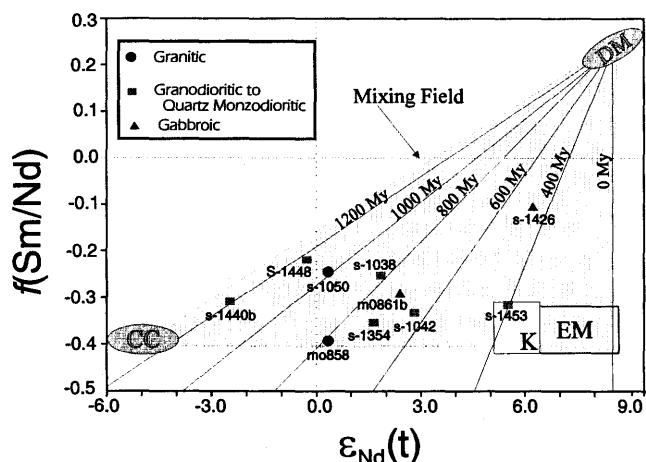


Figure:  $f(\text{Sm}/\text{Nd})$  vs.  $\epsilon_{Nd}(t)$  for ten samples from the Early Jurassic Caldera-Pajonales Plutonic Complex. "DM" is depleted mantle, "EM" is short-term LREE-enriched mantle or juvenile crust, and, "CC" is *c.* 1 Ga continental crust; K is the field defined by six samples from the Early Cretaceous Las Tazas Plutonic Complex.

The age of the continental crust component is consistent with basement ages inferred from published U-Pb zircon (inheritance) and Rb-Sr isotopic studies of other plutonic complexes in the region. Whole-rock Pb compositions of samples from the CPPC have a large spread,  $>0.1$ , in inferred  $^{207}\text{Pb}/^{204}\text{Pb}$ . Rocks with  $\epsilon_{Nd}$  from *c.* +6 to -0.3 have  $^{207}\text{Pb}/^{204}\text{Pb}$  near or below the Stacey-Kramers and Doe-Zartman (orogene) growth curves, except one granite ( $\epsilon_{Nd} = +0.3$ ) that lies well above the curves. The lowest  $^{207}\text{Pb}/^{204}\text{Pb}$  samples have both the highest and lowest  $\epsilon_{Nd}$  ( $t_{DM} = 400$  and 1200 Ma). Metasedimentary country rocks have strongly negative  $\epsilon_{Nd}$  (-9.5), but  $^{207}\text{Pb}/^{204}\text{Pb}$  above the growth curves. These data require a minimum of two crustal sources: one high  $^{207}\text{Pb}/^{204}\text{Pb}$  and the other low

$^{207}\text{Pb}/^{204}\text{Pb}$ . Separation of these two sources must have occurred by at least the middle Proterozoic, to explain how their  $^{207}\text{Pb}/^{204}\text{Pb}$  can be so different. The isotopic composition of the low  $^{207}\text{Pb}/^{204}\text{Pb}$  source resembles that of distinctive eastern Laurentian Pb. Such a correlation would be consistent with recent tectonic models for South America that would give this area a Laurentian basement by the middle Paleozoic. The high  $^{207}\text{Pb}/^{204}\text{Pb}$ , low  $\epsilon_{Nd}$ , crustal source from which the metasediments were derived may have had an Archean component. These Pb data are not amenable to simple interpretation with standard Pb growth curves, requiring instead a recognition of the isotopic variations that occur within the region, and within the individual plutonic complexes.

Six samples from the early Early Cretaceous Las Tazas plutonic complex, which occurs inboard to the east from the CPPC, have  $\epsilon_{Nd}(130) = +5.1$  to  $+6.4$  and  $f(\text{Sm}/\text{Nd}) = -0.30$  to  $-0.41$ . The magmatic source(s) of these samples is similar to the LREE-enriched mantle or juvenile crust component ("EM") required by the Nd data from the CPPC (see figure above). In contrast to the Early Jurassic magmatic arc, no older crust is suggested to have been involved in the Early Cretaceous magmatism.

Dallmeyer, R.D., Brown, M., Grocott, J., Taylor, G.K. and Treloar, P.J., 1995. Mesozoic Magmatic and Tectonic Events Within the Andean Plate Boundary Zone, 26°-27°30'S, North Chile: Constraints from  $^{40}\text{Ar}/^{39}\text{Ar}$  Mineral Ages, in review.

Grocott J., Brown, M., Dallmeyer, R.D., Taylor, G.K. and P.J. Treloar, 1994. Mechanisms of continental growth in extensional arcs: An example from the Andean Plate Boundary Zone, *Geology*, 22, 391-394.

## ORAL PRESENTATION

### Insights From Igneous Reaction Space: A Holistic Approach to Granite Crystallization

Hogan, J.P.

*School of Geology and Geophysics,  
University of Oklahoma, Norman, OK 73019, USA*

Petrologic investigations of granite commonly reveal multiple periods of mineral growth punctuated by resorption as well as compositional heterogeneity within constituent minerals. Such reaction textures and compositional variability are indicative of complex crystallization histories which ultimately must reflect changes in intensive

parameters during petrogenesis and solidification of these melts. Traditional petrologic tools, such as comparison with experimentally determined phase diagrams or Schreinemaker's analysis, are effective for analyzing relationships among reduced subsets of the crystallizing assemblage. In contrast *Reaction Space* (Thompson, 1982) provides a holistic approach that can simultaneously model mineral reaction relationships, compositional variations, and changes in intensive variables for the complete mineral assemblage during crystallization. A general reaction space is presented for crystallization of peraluminous biotite-muscovite-garnet granites using the Northport pluton Maine, USA as an example.

Distinct periods of crystallization, resorption,  $\pm$  renewed crystallization for biotite, muscovite, garnet and feldspar in Northport granite are recognized from petrography and compositional differences. Compositional variation in these minerals can be correlated with relative position in the order of crystallization and are critical to constructing permissible crystallization paths within the reaction space. The following observations were used in the reaction space analysis of the Northport pluton. Plagioclase glomerocrysts, formed during the reaction  $Pl + melt \rightarrow Ksp + melt$  (e.g., Hogan, 1993), was used to subdivide crystallization into an earlier (Ksp absent) and later (Ksp present) periods. Earlier and later crystallization was modeled by separate reaction space volumes in order to facilitate visual representation. The initial melt composition is represented by whole rock compositions and later adjusted for fractional crystallization. Early crystallizing garnets are typically euhedral, 0.2 - 0.75 mm in size, unzoned to reversely zoned, with rare inclusions of oxide, zircon, or monazite and are preserved as "armored" inclusions in plagioclase. These garnets react with the melt and replaced by crystallization of biotite and muscovite. Late crystallizing garnets are euhedral to anhedral, 0.15 - 1.50 mm, display both reverse and normal zonation (even within the same crystal), and contain inclusions of muscovite, biotite, alkali - feldspar, and quartz. Compositional zonation in garnet corresponds to changes in the crystallizing assemblage. Earlier and later periods of muscovite crystallization separated by a period of resorption, are also recognized. Anhedral embayed muscovite partially rimmed by quartz included in alkali-feldspar is interpreted as evidence for resorption.  $Fm^{2+}Si^4Al_1^{IV}Al_1^{VI}$  and  $Fm^{2+}Ti^4Al_2^{VI}$  components ( $Fm^{2+} = Fe, Mg, Mn$ ) in muscovite systematically decrease with progressive crystallization. A hiatus in this compositional trend is interpreted to correspond to the period of non-crystallization and resorption. Biotite

exhibits similar compositional changes with crystallization and is absent from the final crystallizing assemblage which yielded minor muscovite-garnet granite.

The following general insights concerning crystallization of peraluminous granites can be made from the topology of the linearly independent set of reactions that define this reaction space and the reconstructed crystallization path of the Northport granite: 1) there is no one unique reaction that produces or consumes aluminous minerals such as garnet; 2) mineral phases can alternate as reactants or products in different reactions accounting for textures indicating multiple periods of crystallization separated by resorption; 3) increasing  $f_{H_2O}$  favors crystallization of biotite and muscovite at the expense of garnet yielding biotite-muscovite granites; and, 4) garnet-forming and biotite-consuming reactions near the solidus can give rise to muscovite-garnet granites, without necessarily requiring an increase in Mn activity.

Hogan, J.P., 1993, Monomineralic glomerocrysts: Textural evidence for mineral resorption during crystallization of igneous rocks. *J. Geol.*, **101**, 531-540.

Hogan, J.P. and Dickenson, M.P., 1986, Application of reaction space to the crystallization of muscovite - biotite  $\pm$  garnet granites: *Geol. Soc. Amer. Abstr. Progs.*, **18**, 638.

Thompson, J.B., Jr., 1982, Reaction Space: An algebraic and geometric approach. In Ferry, J.M. (ed) *Characterization of Metamorphism through Mineral Equilibria*, Reviews in Mineralogy 10, Mineralogical Society of America, Washington, D.C., p. 33-52.

## Petrogenesis of A-type Sheet-Granites from an Ancient Rift

<sup>1</sup>Hogan, J.P., <sup>1</sup>Gilbert, M.C., <sup>1</sup>Price, J.D. and <sup>2</sup>Wright, J.E.

<sup>1</sup>*School of Geology and Geophysics, University of Oklahoma, Norman, OK 73019, USA*

<sup>2</sup>*Department of Geology and Geophysics, Rice University, Houston, TX 77005, USA*

The Southern Oklahoma Aulacogen (SOA) is one of several aulacogens that formed in the North American craton during breakup of the Laurentian Supercontinent in late Proterozoic to Cambrian time. Lithospheric extension was accompanied by voluminous bimodal igneous activity that can be subdivided into two distinct magmatic episodes separated by a period of uplift and erosion (Fig. 1). Evidence for coeval mafic and felsic magmatism within the

rift is scarce and spatially restricted. Late Precambrian-Cambrian layered anorthositic gabbro intruded by small (<10 km<sup>2</sup>) plutons of hydrous gabbro (primary biotite+amphibole) forms an extensive substrate (>1000 km<sup>2</sup>, 3-4 km thick) to the rift. Unconformably deposited on this gabbroic floor is a voluminous sequence (~44,000 km<sup>2</sup>, ~1.4 km thick) of middle-late Cambrian subaerial A-type rhyolite flows with minor tuffs and agglomerates. Intrusive into the base of this volcanic pile are a series of ~coeval thin (~0.5 km thick) but laterally extensive (~20-55 km in length) A-type granite sheets of which the Mount Scott Granite sheet is typical. Numerous basaltic dikes and rare porphyritic "rhyolite" dikes represent the final stages of rift-related igneous activity.

Felsic igneous rocks associated with the SOA are clearly A-type. Plutonic rocks are typically leucocratic alkali-feldspar amphibole-biotite granites. Both hypersolvus and subsolvus granites are present. Zircon, titanite, ilmenite and magnetite occur as accessory minerals. The presence of magmatic fluorite is indicative of high fluorine contents for the melt. They are characterized by high SiO<sub>2</sub> (71 - 78 wt %), low CaO (<1.5 wt %) and are meta-luminous to weakly peraluminous and subalkaline. They are enriched in Ba (e.g., Mount Scott, 799 - 1180 ppm), high field strength elements (e.g., Mount Scott, Zr, 415 - 554 ppm) and have high Ga/Al ratios with minor/trace element abundance that have a "within-plate" signature. The granites crystallized from high temperature (T<sub>zr</sub> ~900 - 950°C), H<sub>2</sub>O-poor magmas emplaced non-explosively at low pressures (10<sup>2</sup> bar range) high in the crust beneath an ~coeval volcanic pile.

Geochemical characteristics of SOA A-type granite/rhyolite are in marked contrast with typical crustal melts and require derivation from mantle-like sources with minor crustal involvement. The absence of a Ta-Nb anomaly and Yb/Ta, Y/Nb and Ce/Nb ratios of the granites are more typical of Ocean Island Basalt (Fig. 2). In addition low initial <sup>87</sup>Sr/<sup>86</sup>Sr (0.7030 - 0.7043) and positive ε<sub>Nd</sub> (+3.3 - +3.7) for Mount Scott Granite indicate a primitive source. Initial <sup>87</sup>Sr/<sup>86</sup>Sr (0.7033 - 0.7041) and positive ε<sub>Nd</sub> (+2.8 - +4.3) for Late Diabase Dikes are indistinguishable from the granite/rhyolite suggesting a closely related origin for rift-related mafic and felsic rocks. The extreme scarcity of igneous rocks of intermediate composition and lack of a significant Eu anomaly in Mount Scott Granite or phenocryst-poor rhyolite argues against derivation of these felsic liquids by extended fractional crystallization of basaltic magma. We suggest A-type felsic melts of the SOA formed by partial melting at depth of mafic rocks

that were intruded early during the initial stages of rifting. The large volume of mafic and felsic igneous rocks, both with primitive sources, associated with the SOA indicate a substantial amount of new material can be added to the crust during lithospheric extension and should have important consequences for modeling the time-integrated geochemical evolution of crust and mantle reservoirs.

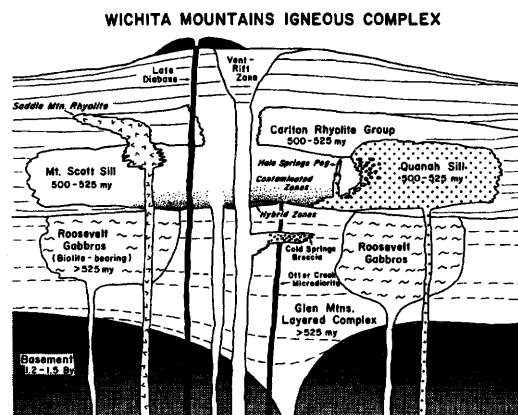


Figure 1. Schematic Cross-section of Cambrian Igneous Stratigraphy for the SOA.

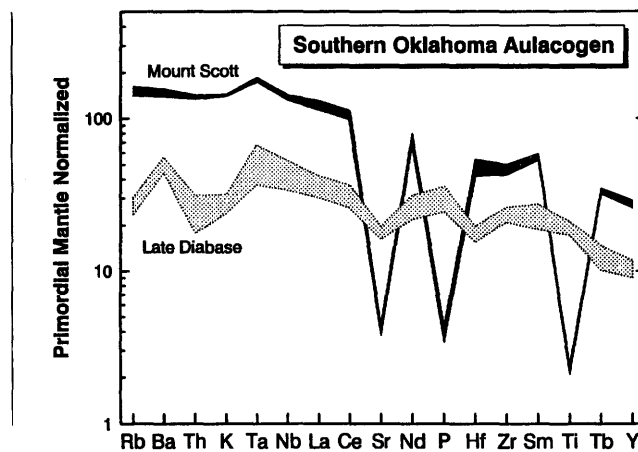


Figure 2. Comparative "Spidergram" for Mount Scott Granite and Late Diabase, SOA

## ORAL PRESENTATION

### Effects of Dissolved C-O-H Species on Chemical and Physical Properties of Ascending Granitic Magmas

Holtz, Francois and Scaillet, Bruno

*Centre de Recherche sur la  
Synthese et la Chimie des Mineraux,  
CNRS, 1A, rue de la Ferrollerie,  
45071 Orléans Cedex 02, France*

The most abundant volatile species dissolved in common granitic melts belong to the system C-O-H (apart from highly differentiated melts). Pressure is known to influence strongly the solubility of volatile species in aluminosilicate melts. However, both individual (H-O, C-O) and combined effects of dissolved volatiles on physical and chemical properties of ascending magmas are still not well constrained. New experimental data show that previous available experimental datasets and calculation models are not always suited to predict physical (viscosity) and chemical properties (phase relations) of ascending magmas.

The viscosity of hydrous granitic melts is commonly calculated using the empirical model of Shaw (1972). New experimental data for haplogranitic compositions with 0 to 8 wt % water show significant discrepancies with calculated viscosities. For the investigated haplogranitic composition  $Qz_{28}Ab_{38}Or_{34}$  (normative proportions) the model overestimates the viscosity by up to 1.5 log units at low water contents ( $< 2$  wt %  $H_2O$ ) while it underestimates the viscosity at high water contents (less than 1 log unit). In addition, the predicted increase in viscosity with increasing Qz content is not verified for compositions that contain less than 30% normative Qz. The viscosity of  $Qz_{28}Ab_{38}Or_{34}$  and Ab melts is not significantly different (for water contents higher than 2 wt %  $H_2O$ ). Viscosity measurements also were carried out on a natural peraluminous leucogranitic composition. A comparison with the experimental data obtained for a metaluminous obsidian (Shaw, 1963) shows that the excess of aluminium has no significant effect on the viscosity.

Water solubility was shown to increase significantly up to 3-4 kbar by Oxtoby and Hamilton (1978). At higher pressure, the water solubility was found to remain almost constant. This last finding has to be reconsidered in the light of new experimental data showing that water solubility still increases strongly up to at least 8 kbar (typical

increase for a haplogranitic composition from 3 to 8 kbar is +1.3 wt %  $H_2O$ / kbar). In addition, water solubility in haplogranitic (quartzofeldspathic) melts is almost constant for a given Na/K ratio in the compositional range  $Qz_0$  to  $Qz_{35}$  (normative proportions), while at higher Qz contents water solubility decreases. This observation, together with viscosity data, suggest that two incorporation mechanisms of water are involved in granitic melts. A "feldspar- $H_2O$ " mechanism is dominantly involved in melts with less than 30-35% normative Qz, explaining the same effect of water on properties of Ab and  $Qz_{28}Ab_{38}Or_{34}$  melts. At higher Qz contents, the interplay between a "feldspar- $H_2O$ " and a " $SiO_2$ - $H_2O$ " solubility mechanisms must be taken into account. It is worth pointing out that different water solubility mechanisms in haplogranitic melts are not taken into account in current solubility models used to predict phase relations under both  $H_2O$ -saturated and -undersaturated conditions (e.g., Burnham and Nekavsil, 1986). In addition, important parameters such as the alkali effect (Na/K) or redox conditions are not included in these models.

Phase relations carried out on a metaluminous granite under different oxygen fugacities (NNO + 0.5 and FMQ - 0.5) and  $a_{H_2O}$ , coexisting with a C-O-H fluid phase, show that  $f_{O_2}$  has a strong influence on the stability of both iron-bearing (e.g., amphibole, biotite, oxides) and iron-free (tectosilicates) phases. Under reduced conditions (FMQ - 0.5) the thermal stabilities of all major phases are depressed by c. 40-50°C relative to oxidized conditions (NNO + 0.5). The solidus is however not affected by changes in redox conditions. Therefore, at fixed temperature and melt water content, the melt fraction is lower under reduced conditions than under oxidized ones. One major implication is that physical properties, such as the viscosity, of granitic magmas undergoing oxidation change significantly due to the decrease in melt fraction. In particular, the redox state may control in part the emplacement level of magmas.

Burnham, C.W. and Nekavsil, H., 1986. Equilibrium properties of granite pegmatite magmas. *Am. Mineral.*, **71**, 239-263.

Oxtoby, S. and Hamilton, D.L., 1978. The discrete association of water with  $Na_2O$  and  $SiO_2$  in NaAl silicate melts. *Contrib. Mineral. Petrol.*, **66**, 185-188.

Shaw, H.R., 1972. Viscosities of magmatic silicate liquids: an empirical method of prediction. *Am. J. Sci.*, **272**, 870-893.

Shaw, H.R., 1963. Obsidian- $H_2O$  viscosities at 1000 and 2000 bars in the temperature range 700-900°C. *J. Geophys. Res.*, **68**, 6337-6343.

## Comparative Granitoid Geochemistry and Lateral Repetition of Magmatic Arcs

<sup>1</sup>Horak, Jana M. and <sup>2</sup>Gibbons, Wes

<sup>1</sup>*Department of Geology,  
National Museum of Wales,  
Cardiff, Wales, CF1 3NP, UK*

<sup>2</sup>*Department of Earth Sciences,  
University of Wales Cardiff, P.O. Box 914,  
Cardiff, Wales, CF1 3YE, UK*

Lateral repetition of magmatic arc and forearc sequences during oblique plate convergence is a well documented phenomenon. Initiation of this process in a young arc, such as Sumatra, may lead to substantial strike slip dispersal and consequent juxtaposition of coeval, but originally widely separated arc segments, such as the Salinian sliver of the Sierra Nevada arc in California. In older orogens the recognition of such dispersed slivers may be obscured by modifications of primary geochemical signatures, tectonic overprinting and poor exposure. An excellent example of the problems associated with interpretation of ancient arc-related slivers is provided by the Neoproterozoic rocks of Southern Britain. Here a poorly exposed magmatic arc complex [Avalonia] is suspected of being riddled with intra-arc strike slip faults. The margin of this arc (exposed in Anglesey, Wales) preserves blueschists within a steep sinistral ductile fault zone, beyond which are further exposures of granitoid rocks (Coedana Granite). Previous interpretations of the rocks outboard of this ductile fault zone have suggested that they are suspect terranes with a non-Avalonian affinity.

Granitoid geochemistry has been used as a tool in terrane characterisation in several published studies (*e.g.* Barr, 1990) either to compare directly the chemical signature of juxtaposed granitoid intrusions or to determine the nature of basement terranes by granites derived from them. To more closely determine the affinity of the granitoid component of the rocks outboard of the blueschist belt on Anglesey, a study was undertaken on the Coedana Granite, which proved to be an evolved mildly peraluminous, calc-alkaline, arc-related, biotite monzogranite pluton. It has three main facies, of which the most evolved (leucomonzogranite) is spessartine garnet-bearing. Various of geochemical parameters such as a trend of increasing  $P_2O_5$  with fractionation and  $\epsilon_{Nd}$  values of - 3.6 to 6.1 (at 600 Ma) suggest that the granite was

derived from a metaluminous crustal source with a crustal residency age of 1.3-1.5 Ga., rather than from the adjacent metapelitic migmatites as proposed by some previous workers.

A U-Pb zircon age of  $604 \pm 4$  Ma for the Coedana Granite falls within the main phase of Avalonian arc magmatism as defined by O'Brien *et al.* (1992). These data indicate that the outboard Coedana Granite rocks belong to the Avalonian. Furthermore they are associated with marine siliciclastic metasediments containing abundant arc material and a chaotic melange unit bearing Coedana Granite clasts. The Coedana Granite and the arc plutonic complexes inboard of the ductile fault zone are exactly coeval in age and have similar Sm-Nd isotopic signatures (*e.g.* 1.3-1.5 Ga for the Coedana Granite compared to 1.2-1.6 Ga for the most NW expression of the Avalonian arc in Southern Britain), however, no direct correlation between the Coedana Granite and any specific plutons in the Avalonian of Southern Britain can be made. It is concluded that the Coedana Granite was derived from Avalonian lower crust closely resembling that in Southern Britain, but has been transported along the edge of the arc by sinistral faulting. The distance travelled by this forearc sliver, fortuitously preserved within the younger Caledonian Orogen, is unknown, but is likely to be considerable.

Barr, S. M., 1990. Granitoid geochemistry and terrane characterisation: an example from the northern Appalachian Orogen. *Geol. J.*, **25**, 295-304.

O'Brien S.J., O'Driscoll, C.F., Tucker, R.D. and Dunning, G.R., 1992. Four-fold subdivision of the Late Precambrian magmatic record of the Avalon Zone type area (east Newfoundland): nature and significance. *GAC-MAC Prog. Abst.*, **17**, A85.

## Late Neoproterozoic A-Type Granites and Rhyolites Associated with Rift-Related Clastic Rocks Within the Grenvillian Basement of Virginia

<sup>1</sup>Hutson, F.E. and <sup>2</sup>Tollo, R.P.

<sup>1</sup>*Department of Geological Sciences,*

*University of Texas, Austin, TX 78712, USA*

<sup>2</sup>*Department of Geology, George Washington University,  
Washington, DC 20052, USA*

Integrated sedimentologic and petrologic studies of late Neoproterozoic clastic sediments and anorogenic granitoids and rhyolites exposed within 1.1-1.0 Ga basement rocks of the Blue Ridge anticlinorium (BRA) of central Virginia demonstrate a clear tectonic relationship between anorogenic igneous activity and rift basin sedimentation. A combination of field, petrographic, geochemical, and isotopic data have enabled us to determine the spatial and temporal relationship of rift-related plutonism, volcanism, and sedimentation.

Late Neoproterozoic metasedimentary rocks of the Mechum River Formation (MRF) nonconformably overlie basement rocks of Grenvillian age and *c.* 0.73 Ga anorogenic granitoids of the Robertson River Igneous Suite (RRIS). The MRF and RRIS are temporally correlative with rift sequences exposed throughout the southern Appalachians and, on a much larger scale, to sequences exposed on all margins of Laurentia. These sedimentary and igneous rocks are interpreted as part of a *c.* 0.7 Ga extensional event which preceded a *c.* 0.6 Ga rift event that led to opening of the Iapetus Ocean.

The MRF is composed of conglomerates, sandstones, and mudstones that are variably deformed and metamorphosed under upper greenschist facies conditions. The metasediments are exposed in a 100 km long by 0.5-3 km wide belt that has been down-faulted into the core of the BRA. The MRF experienced the effects of multiple Paleozoic tectonic events; nevertheless, it retains identifiable features associated with many modern rift basins. These include areal dimensions, grain size trends, facies patterns, lithologic associations, and structural style. For example, the present length and structurally restored width of the MRF outcrop belt is broadly equivalent in dimensions to many East African rift basins. Additional evidence includes increasing grain size toward the margins of the MRF belt and depositional environments that range

from alluvial fan to lacustrine. A major identifying characteristic of many but not all rift basins is the presence of magmatic rocks, commonly volcanics, which are associated with the sediments. Prior to our studies, volcanic rocks had not been found within the MRF and the relationship of the *c.* 0.73 Ga anorogenic granites of the RRIS to the MRF sediments was unclear.

Field, petrographic, and geochemical studies of rocks from the RRIS, MRF, and a limited number of samples from the Grenvillian basement enabled us to identify the source of some clasts within conglomerates of the MRF and demonstrate that rocks previously mapped as MRF clastic rocks are felsic volcanic rocks. Clast count data indicate a large proportion of the clasts are composed of relatively undeformed granitoids, which is in direct contrast to the lithologic character of the presently exposed Grenvillian basement that is dominated by orthogneisses. Point count data from the clasts overlap data from the RRIS but these data are not clearly distinguishable from some Grenvillian granitoids. However, elevated concentrations of high field strength elements (HFSE) and light rare earth elements (LREE) were found for clasts that are similar in petrography to units of the RRIS. This same pattern of geochemical enrichment is typical of the RRIS. In addition, a local nonconformable relationship was recognized between a specific unit (U-Pb zircon age of 729 Ma) of the RRIS and the MRF. Clasts from this unit are present within the basal portion of the MRF above the nonconformity. The combined field, petrographic, and geochemical evidence strongly supports the derivation of many of the MRF clasts from the RRIS. A detailed study of a MRF sub-basin that contains rocks previously mapped as sediments revealed the presence of rhyolites and associated volcanoclastic rocks. The evidence of a volcanic origin for these presumed clastic rocks includes: 1) the presence of euhedral grains of feldspar and quartz, volcanic rock fragments, and spherulites contained within a very fine-grained, white matrix and 2.) whole-rock geochemical data that display highly elevated concentrations in HFSE and LREE. These rhyolites can be clearly distinguished from sedimentary rocks, including samples of the MRF. More importantly, there is a strong geochemical correlation between these rhyolites and nearby mildly peralkaline subvolcanic rocks (U-Pb zircon age of 702 Ma) of the RRIS.

U-Pb isotopic dating of specific units of the RRIS combined with the data outlined above, make it possible to demonstrate a direct link between anorogenic magmatism and rift-related sedimentation. In addition, we are able to

constrain the maximum depositional age of the MRF to 0.73 Ga and further demonstrate that sedimentation and volcanism were occurring at 0.7 Ga. These integrated studies provide a unique perspective on the coeval relationship of anorogenic plutonism/volcanism and extension-related sedimentation.

### A Mechanism for the Segregation and Collection of Crustal Melts

Jackson, M.D., Cheadle, M.J.  
and Atherton, M.P.

*Department of Earth Sciences,  
University of Liverpool,  
Jane Herdman Laboratories, PO Box 147,  
Brownlow St., Liverpool, L69 3BX, UK*

Partial melting of the lower crust can be caused by the intrusion of mantle-derived basalt, which acts as a heat source. Melting begins along grain boundaries and on grain faces, quickly forming an interconnected network of melt. Initially, the distribution of melt will range from a maximum next to the heat source, to zero at the position of the solidus isotherm. As melt migrates upwards, and the source region heats up, both the spatial distribution of melt and the position of the solidus isotherm change with time. Porosity falls to zero at the solidus isotherm, so melt migrating along grain edges cannot move beyond this point. If melt moves through an anastomosing network of small fractures, these fractures may propagate beyond the solidus isotherm, but the melt will quickly freeze in the cold region above. So effectively, the solidus isotherm acts like a "lid" on the top of the source region. Intuitively, if the melt migrates upwards faster than the "lid" migrates upwards, then melt will pond beneath the lid at the top of the source region.

We present a dynamic model of the physical processes which govern crustal melting, to test this intuitive hypothesis. We assume that the lower crust is heated by the intrusion of sills of mantle-derived basalt, and that melt migrates by buoyancy driven porous flow and compaction of the matrix. The effect of melt moving along grain boundaries, or through a fracture network, is simulated by varying the permeability function. Both porous flow networks and small fracture networks are efficient heat

exchangers, so the melt is always in thermal equilibrium with the matrix. Hence the temperature at any point is described by one temperature variable. The basalt heat source is represented in the model as a "hot plate" at the spatial origin, which is switched on at time  $t = 0$ . The boundary condition on flow is that melt velocity = matrix velocity = 0 at the spatial origin. With these initial and boundary conditions, the 1-D equations that govern heat transport, melting, and resulting gravity-driven porous flow and compaction are solved numerically.

We have applied this model to the generation of granitic melts from a basaltic protolith. Our results suggest that, with a maximum of 50 vol % melting at the hot plate, buoyant melt migrates upwards faster than the solidus isotherm. The melt collects below the solidus isotherm, increasing the porosity to >50% near the top of the source region, and decreasing the porosity to <10% at the base of the source region. The high porosity region, effectively a "melt lens", is of the order 1km thick and forms in <1Ma; a realistic timescale for a crustal melting event. As melt moves up through the source region it constantly thermally re-equilibrates with cooler matrix. Consequently, the melt in the "lens" near the top of the source region has thermally equilibrated with relatively cool matrix, and its composition reflects this; *i.e.* the melt in the lens has a composition corresponding to a 20% melt of the protolith, but volumetrically occupies >50% of the host. Our results therefore differ from those of Fountain *et al.* (1989), primarily because we take into account the equilibration of melt and matrix temperatures as each move. We envisage that it is this melt, in the pool at the top of the source region, which is free to ascend to upper crustal levels and is emplaced to form a pluton.

Fountain, J.C., Hodge, D.S. and Shaw, R.P., 1989. Melt segregation in anatectic granites: A thermomechanical model. *J. Volc. Geotherm. Res.*, 39, 279-296.

## Interaction of Tectonic-Related Strain Fields During Pluton Construction; Argyll Suite, SW Grampian Highlands, Scotland

<sup>1</sup>Jacques, J.M. and <sup>2</sup>Reavy, R.J.

<sup>1</sup>*Department of Geological Sciences, University of Durham, South Road, Durham, DH1 3LE, UK*

<sup>2</sup>*Department of Geology, University College Cork, Eire*

Within the Argyll Suite, SW Grampian Highlands, integration of data show that these plutons have been emplaced into crust within which it is possible to distinguish tectonically induced strain fields, established by the interaction of shear zones, from strain fields associated with pluton expansion. The imposition of strain fields by NE-SW-trending shear zones and faults related to the Caledonian transpressional collision are recognised as being distinct from strain fields imposed by an intersecting set of NW-SE-trending pre-Caledonian crustal lineaments which were reactivated during Caledonian orogenesis. The combination of data, such as the overall shape, distribution of intrusive phases, fabric intensities, strain distribution and local emplacement phenomena, can be used to determine the dominant controlling structure during pluton construction, relative to depth of crystallization. This fundamental distinction has led to the recognition that pluton construction at relative depths of approximately 10 km or greater is dominantly controlled by NW-SE-trending structures, whereas pluton emplacement near to the free surface and up to approximately 6 km in depth is dominantly controlled by NE-SW-trending faults and shear zones.

It is envisaged that transpressive motion along the Caledonian NE-SW-trending shear zones is transferred to non-transpressive motion at lower crustal levels, the possible transfer zone corresponding to the upper detachment surface which bounds the lower crustal reflectivity zone (LCRZ). It is suggested that the lower crust inherits the dominant structural characteristics of the crust above, producing within the LCRZ a series of blocks bounded by anastomosing shear zones. Within the LCRZ it is foreseen that non-transpressive deformation is regionally dominant, allowing the rotation and interaction of the low strain mega-augen, leading to the development of a structural framework which may help to explain the location of anatectic zones, siting and type of ascent pathways and subsequent emplacement phenomena in orogenic belts.

## Evolution of Granites and Continental Crust by Dehydration-Melting of Amphibolites and Tonalites

<sup>1</sup>Johannes, Wilhelm and <sup>2</sup>Singh, Jagmohan

<sup>1</sup>*University of Hannover, 30167 Hannover, Germany*

<sup>2</sup>*G.N.D. University, Amritsar 143005, India*

Granitic rocks constitute a major proportion of the upper continental crust, and granite magmatism is an important phenomenon in the crustal differentiation leading to a granulitic lower and granitic upper continental crust. The evolution of the continental crust may have begun with the generation of a thick pile of basaltic material including amphibolites, granulites and eclogites. This first episode is mantle related and is followed by three intracrustal processes: 1) generation of tonalitic magmas by partial melting of amphibolites, eclogites, etc.; 2) subduction, overthrusting, etc. of tonalites and their sedimentary equivalents; and, 3) formation of I-type and S-type granitic magmas by dehydration-melting of tonalites, metagreywackes, etc. This model is based on geochemical characteristics of upper mantle and crustal rocks (Wedepohl, 1991).

Tonalitic magmas may be mainly generated by dehydration-melting of amphibolites. This process is often believed to take place at high *P-T* conditions. However, Wyllie and Wolf (1993) demonstrated that dehydration-melting of amphibolites may begin already at 650°C at high pressures (above 10 kbar) and at >900°C below 10 kbar. Our investigations below pressures of 10 kbar yielded beginning of dehydration-melting temperatures as low as 850°C. The compositions of the partial melts are identical to those of natural tonalites. Garnet forms at 10 kbar (at 900°C) and indicates that generation of tonalitic melts depleted in HREE, typical for most Archean trondhjemites and tonalites, can be an intracrustal process. The composition of partial melts seems to be mainly controlled by the composition of the parent rock.

Dehydration-melting of tonalite (quartz-plagioclase-biotite assemblages), depending upon the composition of biotite, begins between 710 and 760°C. Orthopyroxene, clinopyroxene, potassium feldspar and anorthite-rich plagioclase are the main residual products. The composition of melt ranges from granitic to granodioritic, and is controlled by the degree of partial melting (increasing with *T*) and the starting composition.

Thus, the dehydration-melting of amphibolites leads to an increase of SiO<sub>2</sub>, Na<sub>2</sub>O and K<sub>2</sub>O in the melt and FeO, MgO and CaO in the residual minerals. Dehydration-melting of tonalites contributes to a further increase of Na<sub>2</sub>O and K<sub>2</sub>O in the melt and concentration of FeO, MgO and CaO in the residuum. The increase in SiO<sub>2</sub> here is less pronounced. The experimental investigations support the model of evolution of the continental crust into a granitic upper and granulitic lower crust by dehydration-melting of amphibolites and tonalites.

Wedepohl, K.H., 1991. Chemical composition and fractionation of the continental crust. *Geol. Rundsch.*, **80**, 207-223.

Wyllie, P.J. and Wolf, M.B., 1993. Amphibolite dehydration-melting: Sorting out the solidus. In Prichard, H.M., Alabaster, T., Harris, N.B.W. and Neary, C.R. (eds), *Magmatic Processes and Plate Tectonics*. Geol. Soc. London Spec. Publ., **76**, 405-416.

### Evidence for Magmatic Fracturing and Small-Scale Melt Segregation During Late Stage Pluton Emplacement

<sup>1</sup>John, Barbara E., <sup>2</sup>Stunitz, Holger and <sup>3</sup>Blundy, Jonathan D.

<sup>1</sup>*Department of Geology and Geophysics, University of Wyoming, Laramie, WY 82071, USA*

<sup>2</sup>*Geologisches-Paleontologisches Institut, Universität Basel, Basel, Switzerland*

<sup>3</sup>*Department of Geology, University of Bristol, BS8 1RJ, Bristol, UK*

Geologic evidence for the generation, segregation, ascent and emplacement of silicic magmas is fragmentary at best. Experiments and/or natural examples documenting the processes of silicic melt segregation during emplacement are rarely observed. Superb natural examples of residual melt distribution in a silicic magmatic system are preserved in the southern Adamello Massif, Italy, and provide insight into the processes of magmatic fracturing and melt segregation.

Hydrous, calc-alkaline magmas that crystallized to form plutonic rocks ranging in composition from quartz diorite, through tonalite to granodiorite, crop out in the Lago della Vacca Suite, southern Adamello Massif. The suite is exposed as a small (~10 km<sup>2</sup>), compositionally and temporally zoned pluton, emplaced at ~3.5 kbar pressure. Textural evidence for melt segregation associated

with emplacement of the suite correlates with the intensity of foliation development and 3-D enclave strain estimates determined in the field. The most intensely foliated rocks occur in the older marginal units, as anastomosing, sinuous circumferential zones that wrap around lenses of less intensely foliated granitoid. These zones vary in width from millimeters to hundreds of meters, and extend for tens to hundreds of meters along strike. Contacts between the zones of intense deformation and their host are remarkably abrupt without strain gradient or intermediate grain size development, and are observed on the scale of < 1-2 mm. This relationship implies an extremely steep strain gradient across the contact, resulting from migration and accumulation of interstitial melt in small dike-like features. Amphibole-plagioclase thermometry indicates deformation temperatures in the magmatic or "submagmatic" state (~780 - 650°C).

The deformed marginal units are finer-grained with documented increases in magmatic deformation. Macroscopically, these zones show a strong shape preferred orientation of plagioclase and hornblende parallel to their margins. Mafic enclaves in these zones have oblate shapes whose aspect ratios correspond to shortening values in the adjacent country rocks. Zones of the most intense foliation development are typically very fine grained (subequant grains ≤50 μm), and have a strong crystallographic preferred orientation of hornblende and plagioclase.

Microscopic evidence for melt migration and segregation comes from these zones of intense foliation and fine grain size, and comprises intra- and intercrystalline fractures and veinlets cutting marginal units of the suite. In regions of small volume melt segregation, and relatively low measured flattening strains, fringing discrete grains (≤ 50 μm) of plagioclase and quartz are dispersed along grain boundaries. Angular intragranular cracks (20-30 μm wide) cutting oriented, zoned plagioclase grains are filled either with slightly more sodic plagioclase or quartz. With an increase in volume percent melt, both intra- and intergranular fractures coalesce to form through-going veinlets or anastomosing bands of fine-grained material. The veinlets are filled with non-eutectic composition melt, comprising the same mineralogy as their host; biotite often has a greater modal abundance (often at the expense of amphibole), and plagioclase a homogenous composition. Their texture is "aplitic", with polygonal boundaries between grains that are free of chemical zoning and optical strain.

Documented shape fabrics and measured enclave strains indicate substantial shortening normal to the walls of the

veinlets while they were still in the magmatic state. Deformation was clearly concentrated in the zones of weakness, that is the veinlets of segregated melt. We suggest that deformation of the older, marginal units of the Lago della Vacca Suite was associated with non-hydrostatic stress (*i.e.* intrusion of subsequent magma pulses), which led to deformation assisted melt segregation, a potentially important deformation process in late stage pluton emplacement.

#### ORAL PRESENTATION

### **New Approaches to Crustal Evolution Studies and the Origin of Granitoids Through the Lu-Hf and Re-Os Isotope Systems**

<sup>1</sup>Johnson, Clark M., <sup>1</sup>Barovich, Karin, M. and <sup>2</sup>Shirey, Steven B.

<sup>1</sup>*Department of Geology and Geophysics, University of Wisconsin, Madison, WI 53706, USA*

<sup>2</sup>*Department of Terrestrial Magnetism, Carnegie Institution of Washington, Washington DC, USA*

Several decades of Sr, Nd, and Pb isotope studies of granitoid rocks have highlighted the diverse origins of crustal igneous terranes, have supported models for crustal melting and differentiation of mafic magmas, and quantified the proportions of crust and mantle inputs to crustal magmatic systems. Recent Nd isotope work on Western North America Cordilleran batholiths and volcanic fields have identified large mantle-derived basalt fluxes that may accompany magmatism that is associated with orogenic and extensional terranes. These basalt fluxes result in significant hybridization of ancient crust and can constitute addition of new crust at depth. Such processes are difficult to identify using Sr and Pb isotope ratios due to large uncertainties in the Sr isotope compositions of the crust and the minimal Pb flux from the mantle during injection of basaltic magmas into the crust. Geophysical and crustal xenolith studies indicate that the lower crust beneath the Cordillera may be mafic and garnet-rich, reflecting high-pressure crystallization of mafic magmas and/or metamorphism. Mafic, garnet-rich lower crust has Lu/Hf and Re/Os ratios that are distinct from those of

silicic crust, or mafic crust at intermediate to shallow depths (non-garnet bearing), and therefore Hf and Os isotope ratios offer a new opportunity to evaluate the depth, chemical composition, and mineralogy of this type of crust if it is involved in granitoid petrogenesis.

Because garnet is highly influential in Lu/Hf partitioning during melting or metasomatic processes in the mantle and crust, distinct Hf isotope compositions may be produced that are dependent upon the role of garnet and thus the depth and extent of melting in the crust. Orogenic Proterozoic and Archean granitoids have distinctly non-radiogenic Hf isotope compositions as compared to "enriched" (low  $\epsilon_{Nd}$ ) sub-oceanic or sub-continental mantle. This indicates derivation from depleted garnet peridotite or garnet-bearing lower crust that was directly derived from the mantle with minimal prior residence in the crust. Granitoids that have these unique Nd-Hf isotope variations represent the only known Hf isotope mass balance to the depleted mantle that has radiogenic Nd and Hf isotope compositions (*i.e.* high  $\epsilon_{Hf}$  MORB). In contrast, mid-Proterozoic anorogenic granitoids from Western North America have anomalously radiogenic Hf isotope compositions for their non-radiogenic Nd isotope ratios that are likely to reflect intra-crustal melting and garnet growth during earlier, orogenically-related crustal hybridization and metamorphism. Although Sr, Nd, and Pb isotope compositions of the anorogenic granitoids indicate a major crustal component, these isotope systems cannot place constraints on the mineralogy of the deep crust that was involved in the genesis of the rocks.

Although most work on terrestrial samples using the Re-Os isotope system has focused on mantle-derived rocks, new work on Proterozoic granitoids from the Penokean orogenic belt in the north-central USA and the Mesozoic Sierra Nevada batholith indicates that the Re-Os isotope system promises to provide important insights into evolution of the continental crust. Re/Os ratios of mafic rocks are well known to be exceptionally high, which has led to the assumption that most continental crust has highly radiogenic Os isotope compositions and very low Os contents; these characteristics would be formidable obstacles to obtaining meaningful initial Os isotope ratios in ancient crustal rocks. New work on oxide minerals in granitoids indicate that Os contents in these minerals are enriched by up to several orders of magnitude relative to whole rocks and that they have relatively low Re/Os ratios, allowing precise calculation of initial Os isotope compositions. Moreover, Re/Os ratios apparently decrease strongly in oxide minerals from silicic rocks, suggesting

that silicic Precambrian continental crust may have relatively non-radiogenic Os isotope compositions. Such a conclusion contrasts with previous estimates for the average Os isotope composition of the continental crust based on oceanic sediments, which are highly radiogenic. Future work lies in combining Nd, Hf, and Os isotope studies on granitoid rocks as a probe of the mineralogy and bulk chemical composition of the crust involved in generation of silicic crustal magma systems.

### **Anatectic Melt Generation and Migration in a Shear Zone Associated with a Lower Crustal Mafic Intrusion, Ivrea-Verbano Zone, Italy**

Kalakay, Thomas J. and Snoke, Arthur W.

*Department of Geology and Geophysics,  
University of Wyoming, Laramie, WY 82071-3006, USA*

The Ivrea-Verbano zone, northern Italy, is a sample of lower continental crust that was upthrust and exhumed during the Alpine orogeny. Uplift and tilting has resulted in a natural cross-section that exposes metasedimentary and metabasic rocks that were intruded at lower crustal levels in the late Paleozoic by a heterogeneous mafic to intermediate igneous complex. Amphibolite- to granulite-facies metamorphism, widespread anatexis, and intense deformation accompanied the underplating or intraplating of mantle-derived mafic magmas.

Detailed geologic mapping indicates that the contact between the igneous complex and its wallrocks is a deformed, intrusive contact. A kilometer-scale zone of intense, high-temperature deformation, traced for at least 20 km, is localized in the wallrocks. This amphibolite-grade shear zone, now steeply dipping, is characterized by highly strained pelitic paragneiss, scattered mafic and calcareous layers, and locally abundant leucosome. Shear zone fabrics include: transposition of earlier foliation(s), isoclinal folding, and widespread boudinage of competent layers. Qualitative assessment of strain intensity across the shear zone suggests a strain increase toward the intrusive contact. A mineral lineation, interpreted to have developed during magmatic emplacement, is defined by north-east-plunging bundles of sillimanite. In thin-section, the strongly oriented sillimanite is intergrown with other peak metamorphic phases such as garnet. Individual garnet

grains have an elongate shape-fabric subparallel to the sillimanite bundles. Crystal-plastic mylonitic fabrics are scarce, isolated, and overprint the high-temperature, crystalloblastic fabrics. The coincident timing of wallrock deformation with magmatic emplacement is indicated by cross-cutting mafic dikes that are deformed in the aureole.

Sense-of-shear data indicate an overall oblique-sinistral, non-coaxial deformation in their present steep orientation. Mesoscopic shear-sense indicators include: asymmetric mafic boudins, shear folds, and rotated mafic enclaves. At the micro-scale, asymmetric pressure shadows around garnet demonstrate sinistral shear and are therefore consistent with the mesoscopic features. Within leucosome-rich portions of the shear zone, there are equal numbers of rotated enclaves for either sense of shear. This suggests that kinematic interpretation may be difficult in regions where overall rock viscosities have been substantially lowered by large melt volumes present during deformation.

Metasedimentary wallrocks are mostly stromatic migmatites with leucosomes occurring both as discontinuous lenses and in more continuous sheets interlayered with biotite + garnet-rich selvages. Lithologic banding occurs on a centimeter to decimeter scale. Melting and deformation were coeval as evidenced by leucosome (frozen melt) concentrations found in boudin necks and extensional shear fractures.

Leucosome concentrations vary within the shear zone. However, a consistent gradient exists with lowest (<20%) leucosome concentrations at or near the contact. Highest concentrations (>45%, with local concentrations >65%) exist some 1-1.5 km away from the contact, coincident with the outermost limit of shear zone fabrics. Near the highly deformed interface with the pluton, wallrocks rich in garnet and sillimanite are interpreted as restites from which melt has been extracted. Leucosome compositions from the structurally higher, melt-rich zone, do not always reflect a minimum melt composition of the rocks in which they reside. This suggests that the melts have migrated from the point of generation to their present position, by vertical melt migration within the shear zone, and that it was the melts that migrated and not the melting zone.

North of the Mastellone River, the eastern contact of the mafic complex curves westward into a large antiform, forming the flank or "sidewall" of the intrusion. In this region, the intense non-coaxial strain, characteristic of the eastern contact zone, grades into a domain of relatively low strain. For a distance of up to 2 km from the contact, the wallrocks are characterized by alterations of

quartzo-feldspathic leucosome with garnet- and sillimanite-rich gneiss. In the field, leucocratic layers commonly display coarse-grained igneous textures and locally comprise greater than 60% of a total outcrop. Based on the compositions of the leucosomes and those of the surrounding granulite-facies country rocks, it is not likely that these rocks represent locally-derived melts. Instead, they may correspond with crustal melts generated along the eastern contact. If so, the "sidewall" region may be viewed as a large pressure shadow or dilational zone adjacent to the intrusion. Such a low-pressure domain, positioned next to a melt-filled, low-angle shear zone, would result in a sub-horizontally oriented pressure gradient driving layer-parallel migration of melts within the shear zone.

### Neogene Granitoids in North Fossa Magna, Central Japan

Kawano, Yoshinobu  
*Department of Geology,  
Faculty of Education,  
Saga University, Honjo 1,  
Saga 840, Japan*

The Fossa Magna is one of the green tuff regions in Japan; it exposes the contact between the Northeast and Southwest Japan Arcs, which are different geological units. In this area, many Neogene granitoid rocks occur. These granitoids are characterized by low  $K_2O/Na_2O$  ratios and low tin contents, and were considered to have been derived from an upper mantle source (Ishihara *et al.*, 1976). However, granitoids in the South Fossa Magna have been investigated in detail, whereas those in the North Fossa Magna have not. New geochemical and isotopic data for granitoids in the North Fossa Magna will be discussed.

The granitoids of the North Fossa Magna are divided into three groups; Utsukushigahara-Kirigamine (UK), Susaka-Ueda (SU) and Makihata-Tanigawa (MT) which locate from southwest to northeast in the North Fossa Magna region. They consist of quartz diorite, tonalite and granodiorite. K-Ar biotite and fission track zircon ages of the UK range from 8.5 Ma to 13.5 Ma (Kawano and Ueda, 1966; Shibata *et al.*, 1976; Koshimizu and Yamagishi, 1987) and those of the MT from 3.1 Ma to 5.9

Ma (Kawano and Ueda, 1966; Ganzawa and Kubota, 1987; Kawano *et al.*, 1992). Radiometric ages for the SU are not determined. However, ages of intrusion are inferred from stratigraphic sequence, they may be the same as those of the UK.

A/CNK ratios of the UK, SU and MT are from 0.79 to 1.03, 0.62 to 1.01 and 0.71 to 1.09, respectively, and  $(^{87}Sr/^{86}Sr)_i$  of the UK, SU and MT are from 0.7035 to 0.7056, 0.7041 to 0.7046 and 0.7044 to 0.7047, respectively. These values suggest that granitoids are mostly classified as metaluminous rocks that belong to the I- or M-type granitoids, and it has been considered that source magmas were not affected by crustal material. Furthermore, on the  $\epsilon_{Sr} - \epsilon_{Nd}$  diagram, granitoids in the North Fossa Magna plot in the field of Tertiary volcanic rocks (basalt and andesite) of the Northeast Japan Arc. It appears from these data that source magmas for granitoids in the North Fossa Magna are derived by partial melting of subducted oceanic crust or fractional crystallization of basalt.

In comparison with Cretaceous granitoids in Northeast Japan, Neogene granitoids in North Fossa Magna are widely exposed. This may be due to a close association with the tectonic situation, the contact between the Northeast and Southwest Japan Arcs; the tectonic setting that caused generation of the source magmas will be discussed.

- Ganzawa, Y. and Kubota, Y., 1987. Geological setting of the Tanigawa-quartz diorite and its cooling history. *Abst. 94th Ann. Mtg. Geol. Soc. Japan*, **194**.
- Ishihara, S., Kanaya, H. and Terashima, S., 1976. Genesis of the Neogene granitoids in the Fossa Magna Region in Japan. *Ocean Sci.*, **8**, 19-24.
- Kawano, Y. and Ueda, Y., 1966. K-Ar dating of the igneous rocks in Japan (IV)- Granitic rocks in northeast Japan. *Jour. Min. Petr. Econ. Geol.*, **56**, 191-211.
- Kawano, Y., Shibata, K., Uchiumi, S. and Ohira, H., 1992. K-Ar age of the Tanigawadake Pliocene plutonic body, North Fossa Magna, central Japan. *Jour. Min. Petr. Econ. Geol.*, **87**, 221-225.
- Koshimizu, S. and Yamagishi, I., 1987. Fission track dating of the Neogene intrusive rocks in the northern Fossa Magna, central Japan. *Jour. Geol. Soc. Japan*, **93**, 773-776.
- Shibata, K., Aoki, M., Kawachi, S., Yamazaki, T. and Kobayashi, T., 1976. Description and K-Ar age of pegmatite in the Tertiary quartzdiorite from Wada-mura, Nagano Prefecture, central Japan. *Bull. Geol. Surv. Japan*, **27**, 509-516.

## Crust-Mantle Interaction at Bingie Bingie Point: Implications for I-Type Granite Petrogenesis in the Lachlan Fold Belt

Keay, Sue and Collins, Bill

*Geology Department, University of Newcastle,  
NSW 2308, Australia*

The Moruya Suite was used by White and Chappell (1977) as the type example of an I-type minimum melt granitoid exhibiting restite-controlled chemical variation. It is well exposed at Bingie Bingie Point on the coast of eastern Australia, and represents the most primitive end-member of the Sr-Nd granitoid spectrum in the Lachlan Fold Belt (LFB) (McCulloch and Woodhead, 1993).

Excellent mingling relations between Moruya Suite tonalites and contemporaneous diorite-gabbros of the Bingie Suite are visible at Bingie Bingie Point. Transitional, 10 metre-wide contacts between the two intrusive bodies comprise abundant (> 80%) pillows of diorite in tonalite, preserving striking evidence of *in situ* microgranular enclave formation. The enclaves are lobate, commonly with crenulate margins, and some have chilled contacts. Others show evidence of spalling and/or net-veining by the host tonalite magma. The proportion of enclaves decreases markedly only a few hundred metres away from these contacts, becoming sparse over several kilometres to background levels (< 5 vol %) throughout the Moruya Suite.

Fine-grained, hornblende-bearing microdiorite dykes of similar composition to the gabbroids intrude the tonalite and display sharp contacts. In one area a microdiorite dyke terminates in the tonalite as a spray of enclaves, but elsewhere the dyke disaggregated into blocks similar to those formed by chocolate tablet boudinage. These features indicate intrusion of the gabbroids and their associated dykes late in the solidification history of the tonalite.

The gabbroids form a sublinear chemical array between hornblende and plagioclase, reflecting a two-component fractionation/accumulation system. The granitoids define a different chemical trend, which can be extended to encompass the compositions of those gabbroids which have not undergone significant fractionation. The microgranular enclave compositions plot in a triangle between the chemical trends of the two suites, indicating chemical hybridism.

Nd model ages for the tonalite are Neoproterozoic (600-700 Ma), the microdiorite dykes have younger model ages (350-500 Ma), with enclaves and gabbroids overlapping both ranges. The diverse rock-types displayed at Bingie Bingie Point form a Sr-Nd isotopic array with tonalite and juvenile mantle of basaltic composition as end-members. These results suggest that the Moruya Suite was derived by partial melting of 600-700 Ma old, basaltic lower crust, which mixed with mantle-derived, hydrous basaltic magmas represented by the microdiorite dykes. The enclaves are interpreted as reflecting upper crustal mingling of hybrid magmas, which formed by deeper crustal mixing between Bingie Suite magmas of variable composition and the Moruya Suite.

Field, chemical and isotopic evidence from the gabbroids, granitoids and enclaves at Bingie Bingie Point suggests that the Moruya Suite is a product of crust-mantle interaction. The data indicate that the enclaves can not be restite and casts serious doubts about the validity of applying the restite model to explain the evolution of I-type granitoids. Instead, the Sr-Nd isotopic array encompasses the isotopically primitive granitoids of the LFB indicating that crust-mantle mixing was significant in granite petrogenesis in the Lachlan Fold Belt.

McCulloch, M.T. and Woodhead, J.D., 1993. Lead isotopic evidence for deep crustal-scale fluid transport during granite petrogenesis. *Geochim. Cosmochim. Acta*, **57**, 659-674

White, A.J.R. and Chappell, B.W., 1977. Ultrametamorphism and granitoid genesis. *Tectonophysics*, **43**, 7-22.

## Rb-Sr and Sm-Nd Study of the São Rafael Batholith, Rio Grande do Norte, Northeast Brazil

<sup>1</sup>Ketcham, D.H., <sup>1</sup>Long, L.E. and <sup>2</sup>Sial, A.N.

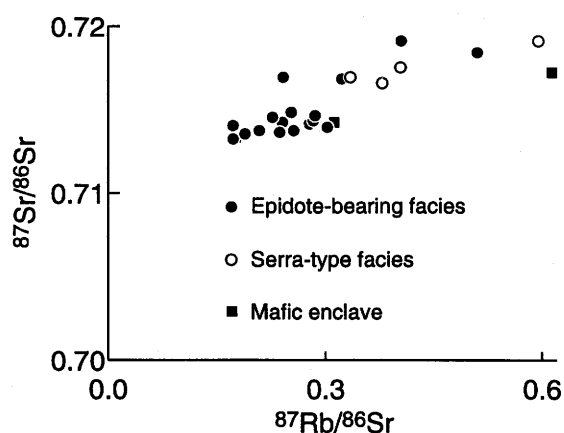
<sup>1</sup>*Department of Geological Sciences,  
University of Texas, Austin, Texas 78712, USA*

<sup>2</sup>*Department of Geology, Federal University  
Pernambuco, Recife, PE 50732-970, Brazil*

During the Brasiliano (Pan-African) orogeny from 7 to 5.5 Ga, the Borborema geologic province in northeast Brazil was intruded by more than 80 granitoid bodies, one of them the primary epidote-bearing São Rafael Batholith located in the Seridó foldbelt. This unfoliated quartz monzonite pluton is thought to be of very late Brasiliano

age, perhaps between 6 and 5.5 Ga based on regional considerations and local field relations.

Twenty-four samples were analyzed isotopically, including 4 from a subtly different sub-facies of the pluton ("Serra-type"), and 2 mafic enclaves. In general, the rocks have high Sr ( $655 \pm 175$  ppm) and low Rb ( $61 \pm 9$  ppm), with consequent low enrichment in radiogenic Sr. Three mineral-whole rock isochrons provide cooling ages of  $0.49 \pm 0.01$  Ga, consistent with the inferred age of emplacement. Data of 18 main-facies whole rocks plot as an amorphous "blob" on a Rb-Sr isochron diagram.



Inhomogeneous initial Sr ratios preclude the determination of a Rb-Sr age of crystallization. Somewhat more systematic data from the Serra-type samples suggest an age of about 0.6 Ga. Sr ratios of epidote-bearing facies rocks, projected back to 0.6 Ga, are high ( $0.713 \pm 0.001$ ), pointing to an ancient radiogenic crustal source.

Six whole-rock samples provide a Sm-Nd isochron apparent age of about 1.1 Ga, which is inconsistent with field evidence for late Brasiliano emplacement. Anomalous Sm-Nd data indicate that initial  $^{143}\text{Nd}/^{144}\text{Nd}$  ratios were also inhomogeneous, just as Sr initial ratios were. Strongly negative values of  $\epsilon_{\text{Nd}}(0.6 \text{ Ga})$  of  $-18$  -  $-21$  imply a source relatively enriched in Nd, a characteristic of continental crust. Crust-formation ages calculated with reference to the depleted mantle curve are consistent with minimum values of  $2.7 \pm 0.3$  Ga.

Limpid euhedral zircon crystals are optically faintly zoned, suggesting multi-stage growth. Extremely discordant U-Pb data of entire-crystal fractions are consistent with presence of an inherited component with 2 Ga minimum age.

A precise age of emplacement of the São Rafael pluton is yet undetermined. U-Pb data, negative  $\epsilon_{\text{Nd}}(0.6 \text{ Ga})$ , Sm-Nd depleted-mantle model ages, and high initial Sr (0.6 Ga) all suggest that the source rock was ancient continental crust. Poorly understood Precambrian basement in northeastern Brazil has been complexly reworked, and there is independent evidence for relict Archean crust in the region.

The only "normal" isotope data from São Rafael are sharply delimited whole-rock  $\delta^{18}\text{O}_{\text{SMOW}} = +7.8$  to  $+8.1\%$ , and consistent mineral cooling ages of about 0.49 Ga. Formed at about 0.6 Ga (?) by partial melting of Archean crust, the São Rafael magma mixed sufficiently to attain a distinctively uniform physical appearance and chemical-mineralogical composition, but its parent-daughter isotope systems failed to homogenize isotopically. Thus, the São Rafael batholith consists neither of simply remobilized source rock nor of completely re-equilibrated material.

### Origin of the Shir-Kuh Granite, South-West Yazd, Central Iran

Khalili, M.

*Department of Geology, University of Isfahan,  
Isfahan, Iran*

Within the Shir-Kuh batholith four granite types have been identified by means of field observations, mineralogy, and major and trace element geochemistry. Monzogranite covers the major part of the batholith area, and is assumed to be the dominant granite unit. These granites are characterized chemically by  $\text{SiO}_2$  (66 - 70 %),  $\text{Al}_2\text{O}_3$  (14 - 15 %),  $\text{Na}_2\text{O}$  (2 - 3.82 %),  $\text{K}_2\text{O}$  (3.5 - 4 %), and  $\text{CaO}$  (2 - 3 %). The second unit, composed of mafic granodiorite grading into monzogranite and tonalite is probably an earlier consolidated portion of the main unit. These rocks are recognized by abundant biotite, plagioclase and some accessories (apatite, zircon and rutile). Chemically, they are lower in  $\text{SiO}_2$ , and higher in  $\text{Al}_2\text{O}_3$  relative to the monzogranite rocks. However, these two units display large overlaps for most major and trace elements. The youngest intrusive units are leucogranitic and trondhjemitic rocks that generally are characterized by decreased  $\text{Al}_2\text{O}_3$  (12 - 13 %), high  $\text{SiO}_2$  (74 - 78 %), and minor  $\text{CaO}$  (0.3 -

0.5 %) concentrations. In comparison with other units, Rb is high and Sr is much lower in the leucogranites.

All of the Shir-Kuh granitoids are S-type granites according to their Ni/Mg ratio, ASI  $((Al_2O_3)/(CaO + Na_2O + K_2O)) = 1.1 - 2.7$ , and presence of muscovite and their lack of hornblende. The strongly peraluminous character of the Shir-Kuh granitoids is shown by high normative corundum and high molar A/CNK; which is reflected by the occasional presence of garnet and cordierite. In the Rb versus (Y + Nb) discrimination diagram, most data plot close to or within the field of syn-COLG, and in the Nb versus Y discrimination diagram within the VAG - syn-COLG field. Hence, the Shir-Kuh granitic melts were presumably derived from metasedimentary crustal sources during the collisional tectonic regime of the Late Kimmerian orogenesis.

Judging from many of the major and some of the trace element plots, these granites are interpreted to be cogenetic with the leucogranitic rocks derived from monzogranitic melts by crystal fractionation involving mafic minerals, plagioclase and some accessory phases.

### Hercynian Granitic Rocks of the Western Carpathians: Products of Crustal Reactivation

<sup>1</sup>Kohút, M., <sup>2</sup>Kotov, A.B., <sup>2</sup>Salnikova, E.B.,  
<sup>2</sup>Kovach, V.P. and <sup>1</sup>Michalko, J.

<sup>1</sup>*Dionýz Štúr Institute of Geology,  
Bratislava, Slovakia*

<sup>2</sup>*Institute of Precambrian Geology and Geochronology,  
St. Petersburg, Russian Federation*

Granitic rocks form numerous plutons in the Western Carpathians (WC). The majority of the granitoid plutons are metaluminous to peraluminous and are composed of several rock types ranging from tonalite to leucocratic granite. Silica contents of granitic rocks vary in the range c. 60 - 75 wt %, documenting the increase of alkalinity from the tonalites to the leucogranites. The prevalence of Na<sub>2</sub>O over K<sub>2</sub>O is a common geochemical feature, except in the porphyritic granite of "Prašiva" type, in which K<sub>2</sub>O > Na<sub>2</sub>O. Carpathians granitoids represent low- to high-potassium calc-alkaline (trondhjemite and monzonite) series of magmatic rocks. Biotite is the dominant Fe-Mg mafic mineral, and hornblende occurs only rarely in the

WC granitoids. Accessory minerals (magnetite + allanite, and monazite + ilmenite) show in some plutons (Tribeč) dichotomy and/or antagonism, which permits distinguishing two principal granite groups (Petrik and Broska, 1994). The occurrence of the mafic microgranular enclaves (MME) in the magnetite-bearing granites and presence of the host (metamorphic) rocks xenoliths in the magnetite-free granites support this division in the Western Carpathians. In some plutons (the Tatry Mts., the Malá Fatra Mts.) one can observe both enclaves and xenoliths in one place. REE are typically LREE enriched in the WC granitoids. Chondrite-normalized patterns of the REE exhibit no or slight negative Eu anomalies and uniform nonfractionated distribution trends for various granite types. (<sup>87</sup>Sr/<sup>86</sup>Sr)<sub>i</sub> in the granites are low (0.703 - 0.708), suggesting a mixed lower crustal and mantle component and/or Rb-poor crustal source. Rarely is (<sup>87</sup>Sr/<sup>86</sup>Sr)<sub>i</sub> higher than 0.715 documenting crustal origin only. Rb/Sr = 0.1 - 0.5 for common tonalite - granite types, but for some leucogranites extending from 0.6 to 2.5; ε<sub>Nd</sub>(0) = 50 - 130 and 150 - 250, respectively. The ε<sub>Nd</sub>(0) values vary from -2.3 to -9.4 and are comparable with data of Liew and Hofmann (1988). Apparent crustal residence ages indicated by the Nd model ages (t<sub>DM</sub> = 1.1 - 3.8 Ga and t<sub>DM</sub> = 1.1 - 1.7 Ga) support the authors concept that Hercynian Europe comprises mainly recycled Proterozoic components with significant new Paleozoic addition. The crustal contribution to the WC granitoids is essential and exhibit a Neodymium Crustal Index (DePaolo *et al.*, 1992), NCI, of 0.49 - 1 (majority 0.6 - 0.8).

All geochemical features suggest that the WC Hercynian granitoids are analogous to VAG (CAG) granites related to the subduction processes. However, during the late Devonian and early Carboniferous, metamorphic, sedimentary and structural data rule out this scenario as similar to almost everywhere in Europe and suggest continental collision processes. These collisional processes with overthrusting of the deep crustal nappes were juxtaposed with crustal reactivation and granitoid production. Field evidence together with *P-T-t* paths (generally clockwise) suggest in the Tatra Mts. tectonic inversion of metamorphism, documented by thrusting of hotter, higher-metamorphosed slab (migmatites, gneisses, amphibolites) over cooler parautochthon (mica schists). A comparable situation occurs in the Malá Fatra Mts. and in the Nízke Tatry Mts. During the climax of the Hercynian collisional tectonic event (350-340 Ma) older igneous material was partially melted in the Western Carpathians. The new anatectic granitic rocks inherited VAG geochemi-

cal characteristics from older (Caledonian or Panafrican-Cadomian?) igneous rocks. Nowadays these granitoids show a low degree of magma fractionation and represent common products of the crustal reactivation and remagmatization.

DePaolo, D.J., Perry, F.V. and Baldrige, S.W., 1992. Crustal versus mantle sources of granitic magmas: a two-parameter model based on Nd isotopic studies. *Trans. Royal Soc. Edinburgh: Earth Sci.*, **83**, 439-446.

Liew, T.C. and Hofmann, A.W., 1988. Precambrian crustal components, plutonic associations, plate environment of the Hercynian Fold Belt of central Europe: Indications from a Nd and Sr isotopic study. *Contrib. Mineral. Petrol.*, **98**, 129-138.

Petrík, I. and Broska, I., 1994. Petrology of two granite types from the Tribeč Mountains, Western Carpathians: an example of allanite (+ magnetite) versus monazite dichotomy. *Geol. J.*, **29**, 59-78.

### Remnants of Lower Crustal Mineral Assemblages in Granitoid Rocks: Examples from the South Bohemian Pluton, Austria

Koller, F. and Kloetzli, U.S.  
*University of Vienna, Austria*

The South Bohemian pluton is formed by a complex, 6000 km<sup>2</sup> sized batholith and belongs to the granitic intrusives of the Variscan orogeny in Central Europe. The late-syntectonic to post-tectonic magmatites were intruded into the polymetamorphic pre-Variscan basement rocks of the Southern Bohemian Massif. The widespread coarse-grained granitoids of the Weinsberg Granite and the more easterly situated Rastenberger Granodiorite exhibit K-feldspar megacrysts up to 20 cm in length. The granitoids show a metaluminous to slightly peraluminous I-type composition. Sr- and Nd-isotope investigations seem to prove that no mantle component or only a strongly suppressed mantle component, contributed to the magma generation.

Dark colored varieties of the Weinsberg granite are found in the vicinity of Sarleinsbach over an area of 10 - 15 km<sup>2</sup>. These rocks show a close structural relationships to the normal type of Weinsberg Granite but a distinct quartz- monzonitic composition. The variation in SiO<sub>2</sub> resembles closely the composition of the diorites found in the South Bohemian Pluton although significantly lower MgO, CaO and Cr, and higher K<sub>2</sub>O, Zr and Ba concentrations are observed. Overall, an evolutionary trend to the

normal Weinsberg Granite can be observed. In these rocks, two different mineral assemblages, which are not in mutual equilibrium, are found. The definitely younger one is clearly of magmatic origin (quartz - oligoclase - orthoclase - biotite - ilmenite), having crystallized from a granitic magma at pressure of about 3 - 4 kbar. The granitic evolution of these rocks is best demonstrated by the pronounced zonation of the K-feldspar. Noteworthy is the considerable amount of celsian component of ~2 mol % with a normal chemical zonation. More elevated, erratic celsian components of up to 8 mol % are found with no visible correlation to magmatic zonation. This is thought to represent relicts of old K-feldspar. The formation of the granitic mineral assemblage took place at 355 ± 8 Ma (zircon Pb/Pb). The older, equigranular mineral assemblage is formed by plagioclase - orthopyroxene - clinopyroxene ± ferrous tschermakite ± alkali feldspar (plagioclase with An >40 mol %, X<sub>Mg</sub> for Opx 0.35 - 0.42, X<sub>Mg</sub> for Cpx 0.50 - 0.54). A symplectic reaction zone with quartz and biotite is found between the two mineral assemblages, defining the breakdown reaction Opx + Kfs + H<sub>2</sub>O + Bt + Qtz. Pyroxene is replaced by amphibole and, with continuing breakdown, by biotite. The first breakdown of pyroxene occurs without the interaction of a melt. Only in a later stage of breakdown, the reaction took place with the participation of a granitic magma. In the older, pyroxene bearing mineral assemblage granulite facies metamorphic conditions are found with pressures around 8 kbar and equilibrium temperature of 755 ± 26°C (two-pyroxene- thermometer). Single zircon ages of 529 ± 22 Ma provide good evidence, that this charnockitic relict assemblage is of Cadomian age.

In the Rastenberger Granodiorite (~40 km<sup>2</sup>) Precambrian zircons with ages around 623 ± 22 Ma were found. The growth of these zircons is thought to have taken place during a magmatic or a high grade metamorphic event. In monzonitic to dioritic enclaves, partly also with large K-feldspars, remnants of relictic Cpx (X<sub>Mg</sub> between 0.82 - 0.67) are found. The Cpx is normally replaced by amphibole. Biotite inclusions within the cpx provide some evidence, that the Cpx enclaves form relicts of a prograde, high-grade metamorphic rock at pressure ≥6 kbar, according to the Ca-tschermakitic substitution in Cpx. Dating of zircons in large K-feldspar megacryst and in the finer grained matrix has shown a marked age difference between the two occurrences: a) in the K-feldspar, ages around 353 ± 9 Ma and the 623 ± 22 Ma age are found; and b) in the matrix, additionally an age group of 338 ± 2 Ma is present, which is formed primarily by zircons

with distinct different typology than found in the other age groups. The age of  $338 \pm 2$  Ma is thought to represent the time of intrusion of the granodiorite magma. At least parts of the K-feldspar megacrysts were not formed during the 338 Ma event but distinctly earlier.

The preliminary results lead to the assumption that in both investigated complexes at least some of large K-feldspar crystals and/or parts of the mineral assemblages and/or the above mentioned enclaves were possibly formed in a lower crustal level with distinct higher pressure than present in the granite melt system.

### **Emplacement of the Abukuma Pluton, Northeast Japan, Inferred from the Subsurface Distribution of Gabbroic Xenoblocks and Structure of the Wall-Rocks**

**Kubo, Kazuya**

*Geological Survey of Japan, 1-1-3 Higashi,  
Tsukuba, Ibaraki 305, Japan*

The Abukuma pluton is a large-scale Cretaceous granitic intrusion located in the northeast Japan. It is 160 km long with a width of 50 km, trending in a NNW - SSE direction. Eastern and western margins of the Abukuma pluton are bounded by left-lateral shear zones. Many small-scale gabbroic masses are exposed aligned, showing the S-shaped trend in the Abukuma pluton.

Based on the petrologic and gravitational studies, three-dimensional structures of the gabbroic masses and the uppermost part of Abukuma pluton, and structure of sedimentary wall-rocks were described. Results are as follows. (1) The Abukuma pluton was intruded into a zone between the upper sedimentary rocks and the lower regional metamorphic rocks. (2) Before the emplacement of the granitic pluton, the metamorphic wall-rocks were under the condition of left-lateral shear stress and deformed. After the emplacement, the same condition occurred, resulting in two shear zones bounding the eastern and western ends of the pluton. This physical condition may produce the enough space for the emplacement of the pluton. (3) Linearly aligned basic plutonism represented by the distribution of gabbroic masses occurred before the granitic plutonism. This basic plutonism may corresponds to the root zone of the pre-Cretaceous volcanic front.

### **Geochemical Constraints of Enclaves and Pre-Himalayan Champawat Granitoids of Kumaun Lesser Himalaya, India**

**Kumar, Santosh**

*Department of Geology, Banaras Hindu University,  
Varanasi-221 005, U.P., India*

The Champawat granitoids (CG) ( $560 \pm 20$  Ma) occur as an elongated body roughly trending east-west close to the Main Boundary Fault (MBF), and have intruded into Precambrian metapelite country rocks. On the basis of mode of occurrence, distribution, shape, size, colour index and microtexture, the enclaves hosted in CG can broadly be classified as country rock xenoliths, surmicaceous (dark coloured Bt-schist) enclaves (SE), limited mobilized mafic (Cpx-Hbd-Bt) enclaves (MME) and less abundant ( $\leq 1$  vol % on exposed level) light and dark colored igneous looking fine-grained microgranitoid enclave (ME).

The CG show leucocratic (Bt-poor) and mesocratic (Bt-rich) medium- to coarse-grained hypidiomorphic textures and belong to granodiorite-granite-adamellite calc-alkaline medium-K series with Bt ( $\pm$ Hbd $\pm$ Ms)-Kf-Pl-Qtz and minor amount of zircon, Fe-Ti oxides, rutile, sphene and apatite. The ME (up to 0.5 m across) occur as rounded, ellipsoidal, discoidal, stretched and elongated shapes with occasional mineral foliation, which are suggestive of magma mingling and flow within the CG. The ME bear fine-grained porphyritic and non-porphyritic hypidiomorphic textures with dominant quartz, plagioclase and biotite, although K-feldspar is uncommon. The ME belong to the calc-alkaline - trondhjemite (quartz diorite to tonalite) low-K series.

The CG broadly can be characterized as S-type (peraluminous; high  $\text{SiO}_2 = 65 - 75$  wt %; mol A/CNK  $> 1.1$ ;  $\text{K}_2\text{O}/\text{Na}_2\text{O} > 1.0$ ;  $\text{Na}_2\text{O} < 3.2$  wt %;  $\text{Fe}_2\text{O}_3/\text{FeO} < 1.0$ ; normative corundum  $> 1.0\%$ ; elevated ( $^{87}\text{Sr}/^{86}\text{Sr}$ )  $> 0.709$ ). Moreover, CG also have limited affinity with A-type (anorogenic) granitoids (occurrence of tourmaline pegmatite; selective enrichment of Sc, V, Th, U, Sr, Ba and Pb relative to alkaline magma) and H-type (hybrid) granitoids (occurrence of enclaves; patchy zoned plagioclase; K-feldspar megacrysts and Bt ( $\pm$  Hbd) - Grt assemblage). The MME, restricted to the Khark region, are nepheline normative and enriched in Th, U, Nb, Y and LREE which are more akin to an alkaline rock. The ME, however, show relatively higher content of Sc, V, Cr, Ni, Co, Cu, Zn, Ga, Rb, Y, Nb and Cs compared to those of

the host CG, whereas Pb, Th and U are lower in the CG than in the ME, suggesting the more basic composition of ME than the CG.

On the basis of HFSE, REE-patterns,  $La_N/Yb_N$  and  $Eu_N/Eu^*$ , the ME can be grouped into three which are more likely resulted by an internal differentiation controlled by fractional crystallization of a moderately LREE-enriched ME without significant Eu-anomaly ( $Eu_N/Eu^* = 0.92$ ) giving rise to ME having partial cumulate with +ve Eu-anomaly ( $Eu_N/Eu^* = 1.28$  and  $1.30$ ) and subsequently evolved ME with -ve Eu-anomaly ( $Eu_N/Eu^* = 0.24$  to  $0.64$ ). The LREE patterns, however, may correspond to bulk crust ( $Eu_N/Eu^* = 0.97$ ), lower continental crust ( $Eu_N/Eu^* = 1.12$ ) and upper continental crust ( $Eu_N/Eu^* = 0.63$ ) respectively, demonstrating the crustal evolution phenomena, but the HREE patterns contradict the view. The CG show the different REE patterns with -ve Eu-anomaly ( $Eu_N/Eu^* = 0.28$  to  $0.59$ ) and relatively enriched LREE patterns compared to those of the ME, implying that the CG have either already experienced the feldspar fractionation or derived from feldspar depleted source. Comparing the chondrite normalized REE patterns of individual pairs of ME and respective host CG suggest their local partial equilibrium, although the ME still maintains a separate entity. The higher Th and U contents of the CG than the ME suggest the evolved nature of the CG but incomparable to those of upper and lower continental crust, respectively. Hence, the ME neither represents the cognate enclave of the host CG nor the older tonalitic crust.

The ORG (Ocean Ridge Granite) normalized LILE and HFSE patterns of ME and CG are typical of calc-alkaline granitoid plutons. Some of the equivocal LILE concentration of the ME and the host CG can be attributed to equilibrium but cannot be characteristics of a common source. The major cations and HFSE (Nb, Y, Ta and Yb) discriminate the CG largely as syn-collisional granites whereas a majority of the ME and a few of the CG show affinity with within-plate granite. The diverse nature of the ME and the host CG is not surprising and appears to be a common coeval bimodal (mafic/basic and felsic) magma association in an orogenic belt. The ME represents the mingled and undercooled (hybrid) magma into the host CG leading to chemical exchange through volatile transfer. The lower mass fraction ( $\leq 1\%$ ) and cessation of basic ME magma injection into the CG promoted the mingling and inhibited the homogenization, however, the felsic melt (CG) continued to produce anatectic crustal melt increasing the large volume of the CG.

## **Petrology and Geochemistry of a Calcic, Peraluminous and Ferrous Granitoid Pluton: the Mitsuhashi Granite in the Ryoke Belt, Southwest Japan**

Kutsukake, Toshio

*Aichi University, Toyohashi, 441 Japan*

The Mitsuhashi Granite pluton, 8 x 8 km in extent, was emplaced within the Ryoke metamorphic rocks. It belongs to the younger Ryoke granitoids, which constitute a continental-margin magmatic arc of Cretaceous age in Pacific Asia before the opening of the Japan Sea. This pluton yields a radiometric age of *c.* 80 Ma.

The main rock types are coarse-grained hornblende-biotite tonalite and low- $K_2O$  granodiorite, with subordinate quartz diorite which bears cummingtonite or almandine garnet. At the margin of the pluton, wallrock assimilation produced garnet-biotite granite and granodiorite. Geochemically the rocks are unusually calcic (alkali-lime index = 65), peraluminous and low-potassic, and also have characteristically high Fe/Mg ratios. In the AFM-diagram the mafic enclaves and intermediate rock types plot in the tholeiite field. They have moderate (*c.* 450 ppm) Sr and low (< 50 ppm) Rb concentrations.

Mineralogic equilibria show that crystallization took place at a depth of *c.* 20 km. Absence of clinopyroxene, expected to crystallize from the whole-rock chemistry, and the early crystallization of hornblende suggest a high water-vapour pressure condition. Very low ferric/ferrous ratios, absence of magnetite and occurrence of almandine garnet coexisting with hornblende imply a low oxygen fugacity. Trace element variations and REE patterns indicate strong plagioclase and moderate hornblende fractionation. Modal and geochemical variations are modelled principally by varying the ratios of cumulus plagioclase and inter-cumulus liquid, which precipitated quartz and alkali feldspar.

Although the high  $X_{ALK}$  values ( $> 1.30$ ) of the Mitsuhashi granite appear to relate to S-type granite in Pitcher's geotectonic classification of granites, the petrographic features suggest that it is I-type. A high  $(^{87}Sr/^{86}Sr)_i$  ( $> 0.708$ ) indicates its source to be mafic rocks of old continental lower crust beneath the Ryoke Belt.

## Geochemistry and Evolution of the 1.89-1.81 Ga Granitoids in the Tampere- Hämeenlinna Area, Southern Finland

Lahtinen, Raimo

*Geological Survey of Finland,  
SF-02150 Espoo, Finland*

The study area is situated in southern Finland, in the central part of the Fennoscandian shield. The region lies entirely within the Paleoproterozoic Svecofennian domain and a number of distinct, broadly E-W trending tectonic units have been recognized, each having distinctive magmatic and metamorphic signatures. The northernmost unit is the Central Finland Granitoid Complex (CFGC) with the Tampere Schist Belt occurring along its southern margin. A thrust separates these from the Mica gneiss-migmatite Belt (MB) to the south which is characterized by tonalitic LPHT migmatites and abundant granitoids. An inferred suture in the southern part of the MB separates it from the Hämeenlinna Schist Belt (HSB) which, together with the Microcline granite Complex (MC), form the southernmost sub-areas in this study.

Granitoids in the study area have syn-tectonic (1.89-1.88 Ga) to late- to post-tectonic ages (1.88-1.86 Ga) in the CFGC, MB, and HSB. The gneissic granitoids in the MC belong to these age groups, but the dominant microcline granites belong to a SW-NE trending belt of 1.84-1.81 Ga granites and granitic LPHT migmatites, and 1.81-1.79 Ga granitoids related to the 1.86-1.84 Ga collision and subsequent collapse.

Syn-tectonic granitoids are dominated by high-K calc-alkaline metaluminous to slightly peraluminous granodiorites with abundant mafic enclaves and local comingling features producing hybrid rocks. At least three end-members in different proportions are needed to account for the observed compositional variations; arc related calc-alkaline magma, WPB-affinity tholeiitic magma and crustal-derived partial melt. The complex interaction and mixing relations between different end-members complicates the situation, but melting of a mafic-intermediate source in the presence of a vapour phase is proposed for the silicic granodiorites, with an additional sedimentary component in the MB.

Late- to post-tectonic granites in the CFGC coincide with a regional magnetic high and are divided into high-K and very high-K groups. Mafic enclaves and comingling features are rare. The silicic high-K granites are slightly

peraluminous and have low combined FeO + MgO + TiO<sub>2</sub> (< 3%) and high FeO/MgO. Vapour-phase absent melting of a tonalitic to granodioritic source is proposed. The very high-K granites are porphyritic to coarse-grained rocks with local rapakivi-like textures. They have a wide range of silica contents and are slightly peraluminous, alkaline to nearly alkaline rocks with high FeO/MgO. The intermediate variants have high Zr, Ba, K/Rb and Nb/Th indicating an affinity with WPB in the CFGC. The lack of rocks in the silica range 54-66% favors high temperature (high Zr) vapour-phase absent melting. The more silicic granites have lower Ba, higher Rb and F, and variable Th, Y and Zr. Although two feldspar fractionation can explain some features, the participation of more of the crustal component is also probable.

The abundant MB high-K granitoids are of tholeiitic affinity and at least partly belong to the 1.88-1.86 Ga stage. They comprise quartz diorites to predominantly porphyritic granodiorites with both mafic and intermediate mafic enclaves. They are peraluminous over a wide silica range with high S, Te, As, Bi and local graphite derived from the assimilated sedimentary component. These granitoids have high TiO<sub>2</sub>, P<sub>2</sub>O<sub>5</sub>, Ba, Nb, Y, Zr and La and they follow trends from WPB to strongly peraluminous granodiorites. The high Th/U ratios in the intermediate granodiorites show that the assimilation/interaction with sediments have occurred under disequilibrium conditions, leaving restitic zircon.

Late pegmatite dykes and small granite bodies within the MB schists and migmatites are peraluminous S-type granites. S-type microcline granites (1.84-1.81 Ga) and granitic migmatites in the MC have lower level of Au, As, Bi, Sb and Cs compared to similar rocks in the MB indicating the loss of fluid phase before the onset of vapour-phase absent melting in the sedimentary source. Low Ba indicates the occurrence of K-feldspar in the source residue.

Thrusting of hydrous rocks and the ponding of water-rich subduction related magmas in the lower and middle crust during crustal thickening and subsequent magmatic underplating (WPB magmas) produced vapour-phase present melting and migmatization at 1.89-1.88 Ga. The continuous magmatic activity and high heat flow from the mantle, combined with more anhydrous conditions, promoted vapour-phase absent melting at higher temperatures at 1.88-1.86 Ga. The prolonged high heat flow and anhydrous source rocks (escaped fluid phase) contributed to large scale vapour-phase absent

melting in the middle crust forming the 1.84-1.81 Ga granites and migmatites.

### **S-type Granites of the Hillgrove Plutonic Suite, New England Batholith, Eastern Australia: Products of Partial Melting of an Intermediate Greywacke Source**

Landenberger, B. and Collins, W.J.

*Department of Geology, University of Newcastle,  
Callaghan, New South Wales, Australia*

Late Carboniferous S-type granites of the Hillgrove Plutonic Suite (New England Batholith, eastern Australia) were emplaced into the Devonian - Carboniferous subduction - accretion complex of the southern New England Fold Belt. The suite was largely generated by partial melting of the accretionary prism during late Carboniferous arc migration. Volumetrically minor, primitive arc tholeiites (gabbros) also intruded the accretion complex at this time, and are considered to have been part of the heat source responsible for partial melting and local high-*T*/low-*P* metamorphism.

The suite is isotopically primitive ( $(^{87}\text{Sr}/^{86}\text{Sr})_i = 0.7040 - 0.7065$ ,  $\epsilon_{\text{Nd}} = -1 - +4$ ) compared to most S-types suites world-wide, and some members of the suite have a bulk rock chemistry which is transitional between I- and S-types. Compositionally the suite ranges from 67 - 77%  $\text{SiO}_2$ , is mildly peraluminous (ASI 1.00 - 1.15), and is relatively high in  $\text{Na}_2\text{O}$  (3 - 4 %) compared to most S-types. These differences are attributed to the chemical and isotopic immaturity of the source rocks involved in magma generation, and to minor contamination processes.

A wide variety of potential S-type granite source rocks were available for melting in the subduction - accretion complex. These include pelites ( $(^{87}\text{Sr}/^{86}\text{Sr})_i = 0.7080 - 0.7170$ ,  $\epsilon_{\text{Nd}} = -2 - -8$ ), metabasalts ( $(^{87}\text{Sr}/^{86}\text{Sr})_i = 0.7045 - 0.7080$ ,  $\epsilon_{\text{Nd}} = +6 - +4.5$ ), and a range of mafic to felsic greywackes ( $(^{87}\text{Sr}/^{86}\text{Sr})_i = 0.7042 - 0.7080$ ,  $\epsilon_{\text{Nd}} = +6 - -3$ ). Only the greywackes of intermediate composition ( $\sim 65\% \text{SiO}_2$ ) overlap with the isotopic composition of the granitoids. Major and trace element modelling indicate that the parental magmas (68 - 70 %  $\text{SiO}_2$ ) of the bulk of the suite, were produced by  $\sim 48\%$  partial melting of a dominantly intermediate greywacke source, via dehydration partial melting reactions involving biotite breakdown.

The isotopic and chemical variability within the mafic granites of Hillgrove Suite demands that two additional magma sources have contributed to some members the suite. The most isotopically and chemically primitive granites ( $(^{87}\text{Sr}/^{86}\text{Sr})_i = 0.7040$ ,  $\epsilon_{\text{Nd}} = +4.0$ ), which form  $\sim 5\%$  of the Hillgrove Suite, have a bulk chemistry which deviates from the main trend of the suite, with higher  $\text{CaO}$ ,  $\text{Al}_2\text{O}_3$ ,  $\text{TiO}_2$  and lower  $\text{K}_2\text{O}$ ,  $\text{FeO}$  contents. These granites plot on an isotopic mixing curve between intermediate greywacke ( $(^{87}\text{Sr}/^{86}\text{Sr})_i = 0.7048 - 0.7070$ ,  $\epsilon_{\text{Nd}} = +2 - -1$ ) and the coeval gabbros ( $(^{87}\text{Sr}/^{86}\text{Sr})_i = 0.7027$ ,  $\epsilon_{\text{Nd}} = +9.5$ ). Accordingly, mantle-derived magmas are considered to have been a contributor to the most primitive granites. Another possible minor magma source are the seawater-altered metabasalts, which are common in the deeper parts of the accretion complex. These metabasalts are likely to have undergone small degrees of partial melting (via amphibole breakdown), contributing a minor melt component to the primary S-types, causing an isotopic shift towards higher  $\epsilon_{\text{Nd}}$  and higher  $(^{87}\text{Sr}/^{86}\text{Sr})_i$ .

### **Himalaya and Karakorum Leucogranites: A Comparison**

LeFort, Patrick

*Géodynamique des Chaînes Alpines (EPR 69, CNRS),  
Institut Dolomieu, Grenoble 38031, France*

Two remarkable collision belts in South-Asia contain leucogranites of similar age: Himalaya and Karakorum. But the two groups strongly differ by the characteristics of their setting, extent and volume, petrofabrics, chemistry of trace elements and isotope systematics. Each group also presents a typical lateral variation within the orogenic unit. The study of the determining parameters underlines the fundamental parts played by the acquisition of the temperature in the source region, the nature and the abundance of the melting fluids, and the composition of the protolith, in the production of the melt. The global tectonic setting is directly responsible for the (segregation?), mode of ascent, and level of emplacement of the leucogranitic bodies. The timing may vary in a given mountain belt and even be repeated as shown in the Nanga Parbat and Hunza regions of the Himalaya and Karakorum, respectively. The very different geodynamic framework of the two belts is clearly

reflected in the singularity of the production and emplacement of the two types of leucogranite.

### Oxygen Isotope Mapping of Young Anatectic Migmatites From the Nanga Parbat Massif, Pakistan

<sup>1</sup>Leslie, Karen, <sup>1</sup>Mattey, David  
and <sup>2</sup>Harris, Nigel

<sup>1</sup>Geology Department, Royal Holloway College,  
University of London, Egham, Surrey, TW20 0EX, UK

<sup>2</sup>Department of Earth Sciences, Open University,  
Walton Hall, Milton Keynes, MK7 6AA, UK

Rapid uplift of the Nanga Parbat-Haramosh Massif (NPHM) has exposed an unusually young suite of anatectic migmatites and leucogranites. Field and geochemical data show that anatexis of pelitic and semipelitic sillimanite grade gneisses was coeval with rapid exhumation of the NPHM over the past 10 Ma (Zeitler *et al.*, 1993). Two phases of melting have been recognized, an earlier phase resulting in sheets and small plutons of leucogranites, followed by cordierite-bearing granitic pods and veins. Structurally, the youngest magmatism is found in the interior of the massif, at least 5 km from unequivocal exhumation structures. These cross-cut all units within the massif and petrographic studies suggest that the younger cordierite granite pods result from biotite breakdown in metasedimentary gneisses forming peritectic cordierite and granite melt. Preliminary thermobarometric studies of the metapelites indicate conditions of  $P = 3.5 \pm 0.5$  kbar,  $T = 690 \pm 40^\circ\text{C}$  (Whittington and Harris, 1995).

Chamberlain *et al.* (1995) have reported evidence of hydrothermal activity in the area and identified  $\delta^{18}\text{O}$  depleted gneisses and migmatites and marked oxygen isotope disequilibrium between mineral pairs that is indicative of fluid infiltration on a regional scale. Local chemical and isotopic equilibria between melt and restites, normally vulnerable to the effects of later metamorphic reequilibration, may preserve evidence of the mechanism and kinetics of melt formation. The high uplift rates within this area (up to  $7 \text{ mm yr}^{-1}$ ) and inferred rapid cooling rates ( $> 100^\circ\text{C Ma}^{-1}$ ) minimize the effects of post-anatectic metamorphic reequilibration and provides an ideal opportunity to examine in detail the kinetics of melting and the role of fluids during anatexis.

Samples displaying melt-restite relationships have been selected for detailed oxygen isotope mapping by laser fluorination techniques at Royal Holloway College, University of London. Preliminary mapping has been undertaken on a centimeter scale by separating grains for analysis from domains sawn from leucocratic and melanocratic horizons. Oxygen isotope data were obtained using a Nd-YAG laser fluorination system (Mattey and Macpherson, 1993) employing a fluxing technique for quartz and aluminosilicates (precision  $\sim 0.2$  ‰ compared to  $< 0.1$  ‰ for the normal analysis of ferromagnesian minerals). The  $\delta^{18}\text{O}$  of NBS 28 quartz is  $9.62 \pm 0.15$  ‰,  $n=14$ ) using the fluxing technique. Quartz from all samples possesses  $\delta^{18}\text{O}$  values that are typical of metasediments and range from 10‰ to 14‰. Quartz-biotite and quartz-feldspar mineral fractionations are variable but generally record temperatures in the range 550-650°C. Minerals from migmatites can be heterogeneous with  $\delta^{18}\text{O}$  values showing up to 1‰ variation on a hand specimen scale. The preliminary data suggest that  $\delta^{18}\text{O}$  heterogeneity resides in biotite-rich restite zones, whereas melt layers are isotopically more homogenous.

Oxygen isotopic data confirm the existence of isotope disequilibrium phenomena on a variety of scales. A migmatitic gneiss from a locality near Fairy Meadows possesses extreme oxygen isotope disequilibrium of over 10‰ between quartz and biotite, consistent with exchange with a low  $\delta^{18}\text{O}$  fluid (Chamberlain *et al.*, 1995). Quartz-biotite and quartz-feldspar mineral fractionations for the gneisses are variable but generally record peak metamorphic temperatures; oxygen isotope temperatures for the young cordierite migmatites seem to be in agreement with preliminary thermobarometric studies of the metapelites. The data obtained so far confirm that some gneisses have interacted with low  $\delta^{18}\text{O}$  fluids, but significant isotopic heterogeneity on a cm scale suggests local disequilibrium may also be related to the process of melt formation and extraction. Detailed oxygen-isotope mapping of leucosome-restite relationships and selected cordierite granites is underway to determine the geometry and magnitude of equilibrium on an intergranular scale. These data will be used to determine the extent to which early formed granitic melts are in isotopic equilibrium with source and restite materials and constrain the cause and timing of disequilibrium among mineral pairs in these rocks.

Chamberlain, C. P., Zeitler, P.K., Barnett, D.E., Winslow, D., Poulson, S.R., Leahy, T. and Hammer, J., 1995. Active hydrothermal systems during the recent uplift of Nanga Parbat, Pakistan Himalaya. *J. Geophys. Res.*, **100**, 439-453.

- Mattey, D. and Macpherson, C., 1993. High-precision oxygen isotope microanalysis of ferromagnesian minerals by laser fluorination. *Chem. Geol.*, **105**, 305-318.
- Whittington, A., and Harris, N., 1995. *Abs.*, 8th Himalayan Conf., ETH, Zurich
- Zeitler, P.K. and Chamberlain, C.P., 1993. Synchronous anatexis, metamorphism, and rapid denudation at Nanga Parbat (Pakistan Himalaya). *Geology*, **21**, 347-350.

## Origin of Syenite Magmas in Anorogenic Granitoid Series: Field, Geochemical and Experimental Data from East Central Asia

<sup>1</sup>Litvinovsky, B.A., <sup>2</sup>Wickham, S.M.,

<sup>1</sup>Zanvilevich, A.N. and <sup>2</sup>Newton, R.C.

<sup>1</sup>Russian Academy of Sciences, Ulan-Ude 670047, Russia

<sup>2</sup>Department of the Geophysical Sciences,

University of Chicago, Chicago, IL 60637, USA

Syenites and quartz syenites are generally abundant in anorogenic (A-type) granitoid series. Usually, syenites are far exceeded in volume by granites, which is probably why their origin attracts less attention. However, in some areas it can be shown that syenitic magmas are parental to the whole syenite-granite series, so the origin of syenites can be considered as a key to the origin of A-type granitoid magmas. We approached the syenite problem by making a petrogenetic study of Late Paleozoic alkaline and peralkaline granitoid series in East Central Asia. Here a complex system of long-lived granitoid belts is superimposed on a vast region of about 5000 by 2000 km. The largest of these belts (the Mongolian-Transbaikalian) stretches for > 2000 km. Within this belt four successive syenite-granite series have been formed over about 200 Ma, from the Devonian to the Triassic. Each series comprises several hundreds of individual plutons, the largest of them as big as 3000 km<sup>2</sup>. In the Devonian, the tectonic setting of the belt was a broad area of diffuse postcollisional extension; beginning from the Early Permian, it evolved as a transcontinental rift zone.

The following important features are characteristic of the syenite-granite series. 1) Both syenites and granites of each of the four suites are very similar in mineralogy and composition along the length and across the width of the entire belt, over distances of thousands of kilometers; the uniformity of individual suites contrasts with clear differences between suites. 2) In terms of <sup>18</sup>O/<sup>16</sup>O and <sup>87</sup>Sr/<sup>86</sup>Sr, the magmas become progressively more mantle-like with

time. Magmatic  $\delta^{18}\text{O}$  values of granites and syenites decrease from  $\sim +9$  in the Devonian suite to  $\sim +6$  in the youngest Permo-Triassic suite. 3) In plutons of all suites coeval mafic igneous rocks are present, in each case mainly associated with the earlier syenitic intrusive phase. 4) Both in granitoids and in the coeval mafic rocks, there is a progressive increase in the abundance of alkalis and high-field strength elements with time. 5) There is clear textural evidence for the mingling and mixing of mafic magmas with coexisting silicic liquids, leading to the generation of hybrid monzonitic magmas. 6) Mineralogical and chemical evidence suggests that syenite magmas were produced by crystallization-differentiation of hybrid monzonite.

These data provide strong constraints on the origin of syenite magma. In addition, two more pieces of evidence should be taken into consideration. The first, is our new experimental results demonstrating that partial melting of typical mid- to deep-crustal acid-intermediate rocks (charnockite-enderbite) cannot form syenite liquid, even at very high pressure (15, 20 and 25 kbar); in all our runs (exhibiting < 5% to > 50% melting), the melt composition was rather similar to that of average A-type granite. The second is evidence for a very high (about 1000°C) temperature for some of the A-type silicic magmas from Transbaikalia, obtained by study of melt microinclusions in quartz and sanidine phenocrysts from the volcanic counterparts to some of the granitoids. Taking into account the enormous dimensions of the K-rich granitoid belts, these high temperatures suggest that the generation of the silicic magmas (especially the syenites) took place at deep crustal levels and probably involved significant quantities of high-temperature mafic magma.

These data clearly suggest that both crust- and mantle-derived magmas were involved in the petrogenesis of the syenites, and by implication the entire anorogenic granitoid suite in Transbaikalia. The essence of our proposed crustal-scale hybridization model is as follows. Potassium-rich alkali basalt magma underplated and intruded the lower crust causing extensive melting of lower and mid-crustal material; this resulted in the production of voluminous K-rich silicic melts. Juxtaposition and interlayering of silicic and basaltic magmas inevitably caused mixing and the formation of hybrid monzonitic magmas of intermediate composition. Crystal/liquid fractionation of this hybrid magma caused the formation of 50 - 60 wt % syenitic residual liquid. Further differentiation of syenite magmas led to the production of the K-rich granites which

form the other major lithological component of this anorogenic granitoid province.

## ORAL PRESENTATION

### Pegmatites

London, David

*School of Geology and Geophysics,  
University of Oklahoma, Norman, OK 73019, USA*

Nearing the end of a century of study, advances have been made in understanding the internal features of pegmatites, but less on their ultimate origins and zonation within a given group. This paper constitutes a review and summary of recent investigations.

*Compositions.* The vast majority of pegmatites are granitic in composition, with affinities to *S*-, *I*-, and *A*-type sources. As a generality, *S*-types have a characteristic trace-element (TE) signature enrichment of Li-Cs-Ta; *A*-types carry a Nb-Y-F TE signature; *I*-types may carry either TE suite, and crossovers among source types are common. Pegmatites inherit the geochemical signature of the granitic source, but TE abundances and ratios are extensively modified by differentiation among pegmatite bodies. Pegmatites derived from *S*-type sources fractionate toward strongly peraluminous compositions.

*Relations to granites.* Links between pegmatite groups and larger masses of granite have been confirmed by field and TE chemistry. Pegmatite dikes emanate from the cupolas of granites and manifest no entrained phenocrysts. Pegmatite magmas appear to represent crystal-free liquids derived from the most fractionated magmas that accumulate at the tops of larger plutonic bodies.

*Zonation within groups.* The chemical zonation of pegmatite groups resembles the chemical zonation of rhyolites that is inverted by eruption; both apparently stem from zoned magma chambers. Pegmatite dikes span large gradients in *P* and *T*; refinement within this gradient by crystal fractionation probably dominates the chemical zoning patterns.

*Zonation within individual bodies.* The textural and chemical zonation within individual pegmatites is most consistent with sequential crystallization, essentially from margins to (not necessarily central) pools of residual melt, rather than simultaneous crystallization of all marginal and internal units. The process originates from pronounced

undercooling of magma and low crystal nucleation rates in volatile-bearing siliceous melts; textural transition from granite to pegmatite marks the point of *T-X* conditions where crystal nucleation is highly suppressed, but growth rates are not. The more these processes operate (together), then the more sharply zoned the pegmatite mineralogy, and the more unidirectional the mineral fabric (comb, graphic, and radial growth habits dominate).

*P-T conditions.* Phase relations among the Li-aluminosilicates (petalite, spodumene, eucryptite, and  $\beta$ -phases) represent the most widely applicable petrogenetic grid. Liquidus and solidus *T* can only be inferred from estimates of bulk chemistry, but recent inclusion and experimental studies put solidi near 450°C for the most fractionated pegmatites.

*Advances in mineralogy.* Much new data on crystal chemistry and zonation trends have been obtained for feldspars, micas, phosphates, complex oxides, tourmaline, and Cs-, Be-, and LiAl-silicates. These data have industrial as well as geologic applications. Mapping patterns of chemical zonation within a single phase has led to improved understanding of crystallization sequence within individual bodies.

*Internal subsolidus alteration.* A myriad of secondary phase assemblages result from initially alkaline followed by acidic vapor (*sensu lato*) - solid reactions. Reaction fronts are most intense at the boundaries between zones or even between giant crystals. Alkalis, alkaline earths, F, and P tend to be redistributed during subsolidus alteration, but not high field-strength elements (*e.g.*, Ti-Nb-Ta-Sn).

*Pegmatite-wallrock interactions.* Metasomatic reactions between pegmatite-derived vapor and host rocks have provided insight into the timing and chemistry of pegmatite vapor exsolution. Wallrock alteration spatially mimics pegmatite zonation; all primary internal zones are crystallized prior to vapor loss from pegmatite. A large mass fraction of rare alkalis, B, and F are lost from pegmatites and partly conserved by reactions in hosts. The chemical signature of wallrock alteration provides useful clues for exploration of internal zones, but few if any pegmatite mining activities have been initiated solely on the basis of the chemistry of wallrock metasomatism.

*Experimentation.* Petrologic experiments under a wide range of conditions have added immensely to the understanding of likely processes in pegmatites. Most chemical, zonal, and textural features of pegmatites have been replicated experimentally. The effects of added components of Li, B, F, and P in addition to H<sub>2</sub>O on granite phase relations have been elucidated. High silica contents

plus these added components flux pegmatite melts to low temperatures, inhibit crystal nucleation, enhance element diffusion, forestall vapor saturation, and cause melt fractionation to initially peraluminous and eventually alkaline, silica-depleted melt compositions. Pegmatites associated with basic and alkaline rocks may be less common than granitic ones because the (less polymerized) liquid compositions of basic and alkaline magmas do not inhibit crystal nucleation and equilibration with melt, as is widespread in granitic systems.

### The Phosphorus Cycle in Peraluminous Granitic Magmas

<sup>1</sup>London, David, <sup>1</sup>Wolf, Michael B.,

<sup>1</sup>Morgan, G.B. VI, and <sup>2</sup>Gallego, Marcos

<sup>1</sup>*School of Geology and Geophysics,*

*University of Oklahoma, Norman, OK 73019, USA*

<sup>2</sup>*Nuevo Baztan, 28809 Alcala de Henares, Madrid, Spain*

A distinctive feature of (mostly S-type) peraluminous granites, pegmatites, and rhyolites and their hydrothermal aureoles is an elevated P content compared to metaluminous and peraluminous I- or A-types. Whole-rock (WR) values  $> 0.2$  wt %  $P_2O_5$  are typical, and concentrations  $> 0.5$  wt % are common.

*Reactions at the source.* Apatite (Ap) and monazite (Mnz) are likely sources of P in metasedimentary protoliths. The solubility of Ap increases linearly with ASI (molar  $Al_2O_3 / M_2O + MO$ ) of melt from 0.1 wt % at ASI = 1 to 0.7 wt %  $P_2O_5$  at ASI = 1.3. First-formed hydrous melts ( $Ms + Ab + Qtz + H_2O = L + Als$ ) possess an ASI between 1.3 - 1.4, so that melts may contain up to 0.7 wt %  $P_2O_5$  contributed by Ap. The solubility of Ap increases with  $T$ , but for peraluminous magmas, initial low- $T$  melting is likely to exhaust P in the source. The solubility of Ap is an activity product; increasing Ca or F decrease the P content of melt at Ap saturation. REE (and Sr)-rich Ap melts incongruently to  $Mnz + P$  (and Sr)-rich melt; variations in Mnz solubility with ASI, if they occur, are below detection by electron microprobe analysis.

*Magmatic crystal fractionation.* S-type granites are low in Ca, and the crystallization of Pl decreases the Ca:P of melt below that of Ap stoichiometry; this in part limits Ap saturation. In the absence of Ap, equilibrium among Bt, Fe-Mg-Mn (FM) phosphate (FMP, e.g., triplite), and melt

buffers P in peraluminous melt near 0.7 - 0.8 wt %  $P_2O_5$ . The central facies of the S-type Albuquerque batholith, Spain, contains Bt-FMP assemblages at WR  $P_2O_5$  of 0.79 wt %.

P is nearly compatible in alkali feldspars (Af) via the exchange  $AlPSi_2$ ; this substitution is not extensive in other silicates. As S-type melts fractionate toward increasing ASI (1.3 - 1.4), P partitions increasingly into Af. The partition coefficient,  $D_p^{Af/m}$ , increases from 0.3 at ASI = 1 to 1.0 at ASI = 1.35. Thus, as ASI increases, the Af become important reservoirs of P. In total, melt concentrations of P increase, but more slowly than for other more incompatible fluxing components (e.g., F, B).

The combination of the experimental  $D_p^{Af/m}$  with WR ASI provides a means of monitoring the P content of melt at various stages of Af crystallization. For the central facies of the Albuquerque granite, this method yields a calculated 0.8 wt %  $P_2O_5$ . Natural Af contain up to 2.6 wt %  $P_2O_5$  (marginal layered aplite with WR  $P_2O_5 = 1.15$  wt %, Albuquerque batholith) in rocks with WR ASI = 1.31; these values record P contents of melt well above the Bt-FMP and the Ap saturation limits (Bt and Ap are absent) and reveal the extent to which P is not conserved in WR.

*Effects on liquidus relations.* Increasing P drives melt compositions away from Qtz along an Or isopleth ( $Or_{28}$  at 200 MPa[ $H_2O$ ]). The association in melt of P with Al initially augments melt fractionation toward increasing ASI, though the limiting ASI of melt is 1.3 - 1.4 regardless of the P content or the Al-saturating phase (Ms, Als, C, Spl, etc.). Melt may eventually fractionate toward alkaline, sodic, and silica-depleted (but Qtz-saturated) compositions by the creation of an  $NaPO_3$  component of melt. The solidus of the metaluminous haplogranite granite system (Ab-Or-Qtz- $H_2O$ ) plus P is unknown, but lies near or below 500°C at 200 MPa( $H_2O$ ). P may increase the solubility limits of  $H_2O$  in melt.

*Late-stage reactions in melt.* Evolved S-type magmas commonly attain saturation in the lithium aluminosilicates (spodumene, petalite and eucryptite in granites and pegmatites,  $\beta$ -phases in some rhyolites) and the phosphates montebrasite-amblygonite [ $LiAlPO_4(OH,F)$ ]; these are related by reactions such as  $LiAlSi_4O_{10}$  (petalite) +  $PO_2(OH) = LiAlPO_4(OH)$  (montebrasite) + 4  $SiO_2$ . This P-buffering equilibrium is presently under investigation.

*Melt - vapor relations.* P is substantially nonvolatile:  $D_p^{vapor/melt}$  varies from 0.3 for peraluminous to  $< 0.1$  for metaluminous compositions. Only in alkaline compositions does P become soluble in vapor as  $NaPO_3$ .

*Subsolidus reactions.* P appears to be incompatible in micas and clays, so that sericitic or argillic alteration of Af liberates P. Thus, magmas and WR do not hold their P for two reasons: 1) the  $\text{NaPO}_3$  component in residual melt or magmatic vapor is highly soluble and, 2) alteration of Af is pervasive in many S-type granites (*e.g.*, kaolin deposits of the UK, France). Hydrothermal veins containing a myriad of secondary phosphates manifest the near- to subsolidus flood of P from igneous Af and phosphates to endogenic or exomorphic hydrothermal aureoles.

*Ore deposits.* P represents a likely ligand for high field-strength elements in melt or aqueous vapor. Preliminary experiments indicate that P enhances the solubilities of Sn (cassiterite) and Ta (manganotantalite) in melt, though the solubilities of these ore minerals are high even in simple haplogranitic melts. There is also evidence for stable W-P aqueous complexes, which may promote the formation of hydrothermal W-P deposits (*e.g.*, Panasquiera, Portugal).

### **Some Pampean Pre-Taconic and Taconic (Famatinian) Granites of Southwestern South America**

<sup>1</sup>López de Luchi, M.G. and <sup>2</sup>Dalla Salda, L.H.

<sup>1</sup>*Centro de Investigaciones en Recursos Geológicos,  
J. Ramírez de Velasco 847,  
1414 Buenos Aires,  
Argentina*

<sup>2</sup>*Centro de Investigaciones Geológicas,  
Calle 1 n 644, 1900 La Plata,  
Argentina*

Late Cambrian to Devonian granitoids are conspicuous rocks in the Famatinian Orogen, today the Pampean Ranges in Central Argentina. This orogen is considered as a Taconic collisional belt, developed by the interaction of Laurentia and South America, following the break-up of Rodinia. A precollisional subduction Andino-type regime along the Cambrian South American active margin produced the Pampean granitoids. Taconian granitoids are collisional rocks usually named as Famatinian granitoids. These plutonites may be used as tracers of the geodynamic evolution of the orogenic belt.

Three groups of granitoids are distinguished on the basis of their geochemical signatures, ages and their relationships to deformational events: 1) Pre-Taconic (Pampean); 2) Taconic (Famatinian); and, 3) Late Taconic (Acadian ?) granitoids. The Pre-Taconic Group rocks (mostly 520-460 Ma) are represented by batholiths and minor plutons showing slightly discordant to concordant contacts, moderate to strong deformation, extensive mylonitization and recrystallization. Granitoids are mainly biotite and biotite-hornblende tonalites and granodiorites with minor monzogranites, gabbros and diorites. Calcic to calc-alkaline, metaluminous to moderately peraluminous compositions are typical. Sequences have a magmatic arc signature with differences arisen from their relative geological setting and erosion level.

The Taconic Group rocks (mostly 460-420 Ma) are concordant plutons associated with migmatites and pegmatites or minor bodies intruded in the Pre-Taconic granitoids. They are chiefly biotite-muscovite monzogranites with minor syenogranites and granodiorites with metasedimentary xenolites. Apatite, garnet, cordierite and epidote are common accessories. Calc-alkaline to alkali-calcic peraluminous compositions are the rule. All of them share a collisional signature, that means crustal protoliths and a restricted compositional range.

The Late Taconic Group rocks (mostly 420-360 Ma) are batholithic-sized plutons of syenogranitic composition. A NNE fault controlled emplacement and contact aureoles are characteristic. These rocks are alkali-calcic, peraluminous to slightly peralkaline, MgO poor crustal granites. Geotectonic diagrams show their collisional to late tectonic affinities. The youngest plutons may also be related to the Acadian tectonic event.

These three groups might suggest a similar geotectonic setting to the contemporaneous granitoids in the Appalachian orogen.

This paper is a contribution to IGCP Projects 376, 345 and 319.

## ORAL PRESENTATION

**Intrusive Degassing at the  
Magma/Wallrock Interface**

Lowenstern, Jacob B.

U.S. Geological Survey, M.S. 910,  
Menlo Park, CA 94025, USA

Evidence from a wide variety of sources indicates that most erupted rhyolites contained 3 to 7 wt % dissolved H<sub>2</sub>O prior to their eruption. As yet, there is no substantive evidence that granitic magmas contain less H<sub>2</sub>O than their volcanic counterparts. The presence of sulfur and CO<sub>2</sub> in rhyolitic magmas requires that they, and by analogy granitic magmas, are vapor-saturated at crustal depths less than 10-12 km. For example, a granitic magma at 750°C, containing 5 wt % H<sub>2</sub>O and 1000 ppm CO<sub>2</sub> would be saturated with vapor at any pressure less than about 300 MPa (~10 km). At that pressure, the equilibrium vapor would contain ~60 mol % H<sub>2</sub>O, the rest being CO<sub>2</sub>. Ascent to the shallow depths at which ore-forming porphyries are emplaced (3 to 4 km) must involve further magma vesiculation, with the vapor becoming more H<sub>2</sub>O-rich as decompression progresses. Upon reaching a depth of 3 km, the magma would contain ~10% vesicles by volume. The combined processes of magma convection, Stokes bubble ascent and percolation should allow exsolved fluid to coalesce at the roof of the magma reservoir, prior to intermittent fluid-loss events associated with fracturing of wallrock. Granites rarely if ever contain evidence for the former presence of tens of vol % of exsolved fluid, implying that mechanisms exist for magma to degas.

One piece of evidence for the former presence of exsolved fluid at the magma/wallrock interface is comb-layering and other types of coarse-grained textures composed of quartz and alkali feldspar. These textures are found near the tops of Mo porphyries, W-skarns, and Cu porphyries (Shannon *et al.*, 1982). Layers of coarse-grained "pegmatitic" quartz alternate with fine-grained aplites that often contain b-form (high-temperature) quartz, interpreted to be early-grown magmatic phenocrysts. The coarse layers contain a-form quartz, which grows at temperature less than 600°C at 100 MPa. I suggest two possibilities for growth of the low-temperature quartz form: 1) the magma solidus temperature was reduced 125° below that of the H<sub>2</sub>O-saturated haplogranite system; or,

2) the crystals grew from a hydrothermal fluid in equilibrium (and in contact) with a supercooled silicate liquid.

The first scenario could occur if the solidus temperature were lowered by addition of F, B, Li, or some other flux. However, this should force the melt toward more albitic compositions, whereas the bulk compositions of most comb-layered rocks (including the aplite interlayers) have very little normative or modal albite/plagioclase. Potentially, an albite-rich melt could crystallize coarse-grained quartz and orthoclase due to surface-energetic effects; *i.e.*, the addition of B, Li, F, etc. could poison albite nucleation and growth. This would result in a residual liquid extremely rich in albite-component. Residual liquid formed in such a manner would have to escape the system without crystallizing or causing sodic alteration, as there is no evidence for either albite-rich pods or sodic metasomatism in or near the comb-layered rocks.

Instead, comb-layering may form at the interface between supercooled magma and exsolved magmatic fluid, similar to the suggestions of Kirkham and Sinclair (1988). Heat loss due to conduction, exsolution of volatiles, and adiabatic ascent of melt/fluid mixtures will all cause cooling of the magma during its intrusion as a high-level porphyry. Because crystallization rates for degassed silicic magmas are extremely slow, they can remain at subsolidus temperatures for years without solidifying. Pockets of exsolved fluids that accumulate at the roof of the intrusion would be expected to form crystals larger and more well-formed than those from coexisting supercooled melt. Increases in fluid pressure would fracture the wallrock, thereby quenching adjacent silicate melt to form aplite, and altering wallrocks by released magmatic fluids. Fracture sealing and accumulation of magmatic fluid would re-initiate growth of the comb layering.

Kirkham, R.V. and Sinclair, W.D., 1988. Comb quartz layers in felsic intrusions and their relationship to porphyry deposits. In Taylor, R.P. and Strong, D.F. (eds), *Can. Inst. Mining Metal. Sp. Iss.*, 39, 50-71.  
Shannon, J.R., Walker, B.M., Carten, R.B. and Geraghty, E.P., 1982. Unidirectional solidification textures and their significance in determining relative ages of intrusions at the Henderson Mine, Colorado. *Geology*, 10, 293-297.

## Some Thermal Constraints on Crustal Assimilation in Calc-Alkaline Batholiths

Matile, Lusius, Thompson, Alan Bruce  
and Ulmer, Peter

*Departement fur Erdwissenschaften, ETH Zurich,  
CH-8092 Zurich, Switzerland*

Simple thermal models constrain the extent of assimilation of adjacent rocks by an ascending magma, independently of geochemical considerations. We have examined the degree of melting of crustal materials of differing fertility by a rising hydrous mantle magma, halted at various crustal depths. Fractional crystallization causes the melt to evolve from gabbro to tonalite-granodiorite and is accompanied by increasing water content in the progressively smaller melt volumes. A pseudobinary phase-diagram for fractional crystallization has been constructed along a pseudocotectic line, based on geochemical modeling of calc-alkaline rock suites and experimental data of liquidus temperatures. The AFC-process has been modelled by mixing of assimilate and slightly supercooled basic melt with subsequent crystallization until the hybrid melt reached the liquidus composition corresponding to the lowered temperature. The heat balance involves heating up and partial melting of assimilate, cooling down and crystallization of the basic melt. Not included in the heat balance was the time dependent conductive heatflux to the country rock and the heat of mixing of the two melts.

The composition of the assimilated melt mainly affects the ratio of the assimilated mass to the crystallized mass. Approximately the same amount of granodioritic and granitic melt can be assimilated but after mixing with granite less crystallization of the mantle magma is possible than after mixing with a granodioritic melt (because the composition of the "hybrid" liquid is shifted much closer to the liquidus composition). The influence of the composition of the country rock on the degree of melting is very critical for the possible amount of assimilation.

Because the liquidus is much flatter (*e.g.* large change in composition for small change in temperature) in the fractionation range gabbro-tonalite, than for more differentiated compositions, greater amounts of heat of crystallization are released at high temperature at the beginning of the AFC-process. On the other hand much more energy is required to heat up the assimilate to the high temperatures of the gabbro liquidus than to temperatures of the granodiorite liquidus and, hence, more assimilation is

possible in the intermediate than in the undifferentiated fractionation range. This conclusion is in apparent contradiction to much geochemical evidence, which suggests that the principal contamination of calc-alkaline rock suites occurs at the beginning of the AFC-process. This means either that if assimilation has occurred in the generation of calc alkaline magmas, then the primary magmas contributing heat to the assimilation are high-Mg melts, *e.g.* picritic or boninitic, or that other physical factors such as rheology of mixing control the extent of assimilation for intermediate to evolved compositions.

It is true that assimilation of adjacent rocks could be easier if they were already at temperatures above their solidi, but then it is likely that they would have already lost their low-melting fractions. The ambient temperature of the crust controls the amount of assimilation and the ratio of assimilation to crystallization, obviously both have the greatest values at high temperatures (*e.g.* at the base of the crust). In reality the effect of the ambient temperature is even bigger, as the neglected conductive heat flux to the country rock increases with decreasing ambient temperature.

The approaches developed here enable us to begin to address the fundamental problems of the relation of size and shape of magma bodies to the melt-temperature evolution during cooling at specific crustal depths, and also to the tectonic environment permitting intrusion.

## Isotopic Constraints on Petrogenesis of the Jurassic Eagle Mountain Intrusion, Southeastern California

<sup>1</sup>Mayo, David P., <sup>1</sup>Anderson, J. Lawford  
and <sup>2</sup>Wooden, Joseph L.

<sup>1</sup>*Department of Earth Sciences, University of Southern California, Los Angeles, CA 90089-0740, USA*

<sup>2</sup>*U.S. Geological Survey, 345 Middlefield Rd., Menlo Park, CA 94025, USA*

The 165 Ma Eagle Mountain intrusion is a metaluminous, calc-alkaline pluton intruding Proterozoic crystalline rocks and Paleozoic supracrustal rocks. The heterogeneous main phase of the intrusion grades compositionally from diorite through tonalite and granodiorite to monzogranite, and is intruded by small leucogranite bodies. Thermobarometric calculations

indicate main phase emplacement at about 2.5 kbar and solidus temperatures between 700° and 750°C. Main phase rocks, in spite of diverse bulk compositions (52 to 68 wt % SiO<sub>2</sub>), have relatively uniform (<sup>87</sup>Sr/<sup>86</sup>Sr)<sub>i</sub> (0.7083 to 0.7094), ε<sub>Nd</sub>(165) (-8.9 - -9.8), and feldspar Pb ratios (<sup>206</sup>Pb/<sup>204</sup>Pb = 18.8, <sup>207</sup>Pb/<sup>204</sup>Pb = 15.7, and <sup>208</sup>Pb/<sup>204</sup>Pb = 39.1).

In coordinates of ε<sub>Nd</sub> vs. <sup>87</sup>Sr/<sup>86</sup>Sr, the Eagle Mountain intrusion and other Jurassic plutons in southeastern California (data from Miller and Wooden, 1994, and Young, 1992) form a curve extending from the evolved end of the mantle array (ε<sub>Nd</sub> = -7.0, <sup>87</sup>Sr/<sup>86</sup>Sr = 0.7065) into a field defined by Proterozoic country rocks (ε<sub>Nd</sub> < -15, <sup>87</sup>Sr/<sup>86</sup>Sr > 0.71) exposed in the region. In spite of similar bulk compositions, each individual Jurassic intrusion occupies a relatively limited segment of the Sr-Nd curve. All of the Jurassic intrusions have similar feldspar Pb isotopic compositions that resemble Proterozoic country rocks.

The Sr and Nd data require the involvement of more than one isotopic reservoir in the petrogenesis of the Eagle Mountain intrusion, and elemental compositions require the source to be relatively mafic and Sr-rich. Variably enriched mantle components and Proterozoic country rocks were used as endmembers to fit mixing and AFC curves to the Sr-Nd array defined by the Jurassic plutons, with solutions specifically anchored to the Eagle Mountain intrusion. Although these models are non-mechanistic, they do provide some constraints on the primitive endmember composition and the amount of crustal recycling recorded in the intrusion. The Eagle Mountain data can be reproduced by mixing 81 to 93 % enriched mantle component (ε<sub>Nd</sub> = -7.0, Nd = 25 - 29 ppm, <sup>87</sup>Sr/<sup>86</sup>Sr = 0.7065, Sr = 665 - 749 ppm) with 19 to 7 % Proterozoic crust (ε<sub>Nd</sub> = -17.5, Nd = 45 - 125 ppm, <sup>87</sup>Sr/<sup>86</sup>Sr = 0.72 - 0.83, Sr = 145 - 425 ppm), or by mixing 60 to 86 % bulk earth-like mantle component (ε<sub>Nd</sub> = 0.0, Nd = 27 - 24 ppm, <sup>87</sup>Sr/<sup>86</sup>Sr = 0.7043, Sr = 680 - 947 ppm) with 40 to 14 % Proterozoic crust (ε<sub>Nd</sub> = -17.5, Nd = 45 - 125 ppm, <sup>87</sup>Sr/<sup>86</sup>Sr = 0.72 - 0.75, Sr = 185 - 425 ppm). A MORB-like depleted mantle component can be ruled out because of the high Sr concentrations (> 690 ppm) required by the data. AFC calculations (r = 0.4, D<sub>Sr</sub> = 1, D<sub>Nd</sub> = 0.35) require 9 to 23 % crystallization of an enriched mantle component or 19 to 41 % crystallization of a bulk earth-like component during assimilation of Proterozoic crust to reproduce the Eagle Mountain data.

The Sr and Nd data indicate that most of the "new" crust added as magma in the Eagle Mountain intrusion was juvenile, and probably derived from relatively enriched mantle. This conclusion is masked in the Pb data, where the isotopic compositions of mantle-crust mixtures or mantle-derived magmas that have assimilated crustal rocks are strongly levered toward Pb-rich crust. The small isotopic variations observed within the Eagle Mountain intrusion are interpreted as 1) reflections of small endmember compositional heterogeneities or 2) minor local assimilation during emplacement. These results are consistent with Miller and Wooden's (1994) hypothesis that mantle-derived magmas intruded the crust during the Jurassic and were strongly contaminated to form hybridized lower crust.

Miller, C.F. and Wooden, J.L., 1994. Anatexis, hybridization and the modification of ancient crust: Mesozoic plutonism in the Old Woman Mountains area, California. *Lithos*, 32, 111-133.

### **Sheet-like Assembly of the Jackass Lakes Pluton, Central Sierra Nevada, California: Multiple Mode Emplacement**

McNulty, Brendan A., Tong, Weixing and Tobisch, Othmar T.

*Earth Sciences Department, University of California, Santa Cruz, CA 95064, USA*

The Jackass Lakes pluton/wall rock system, central Sierra Nevada, California, presents an exceptional case study of the many physical processes that may operate during the emplacement of magma. Pervasive N- to NNW-striking structural and petrologic fabrics in the pluton/wall rock system indicate that the pluton formed via in-situ assembly of a shallow magma chamber fed by mafic and felsic injections. These N- to NNW-striking fabrics include: 1) the pluton's straight eastern and western contacts; 2) mafic microgranular enclave swarms, synplutonic dioritic dikes, and aplitic and coarse-grained granodioritic dikes within the pluton; 3) leucogranitic to granodioritic dikes which cut the country rock; 4) magmatic foliation in the pluton and dikes; 5) narrow elongate volcanic septa and pluton/wall rock interfingering from the meter- to kilometer-scale; and, 6) solid state foliation in the septa and marginal wall rock.

Disrupted synplutonic dikes and mafic microgranular enclave swarms within the pluton document intrusion and mingling of mafic and felsic magma at the final emplacement site. We infer the orientation, distribution and nature of syn-plutonic dikes and enclave swarms (*e.g.* their presence or absence in long linear belts) to represent the former presence of mafic and possibly felsic NNW-oriented magma feeder conduits. Pluton/wall rock interfingering east of the pluton may represent an arrested nascent stage of the magma chamber. Within the pluton, transverse east-to-west fluctuations in magmatic strain and fabric intensity, and in enclave population (presence/absence), further support the presence of linear, although somewhat cryptic, NNW-striking magmatic belts. Cryptic sheeting, or the coalescence of sheets, may be the result of compositionally and thermally indistinct magma pulses, and/or a rapid intrusion rate. U-Pb zircon dating from different parts of the pluton indicates that assembly via multiple pulse injection occurred during the time frame  $\sim 97.1 \pm 0.7$  -  $\sim 98.5 \pm 0.3$  Ma. We propose that fracture initiation for magma sheet emplacement was generated within a weak dextral tectonic regime that produced N- to NNW-striking tension gashes.

The Jackass Lakes pluton is a classic example of multiple physical processes acting together to accommodate the emplacement of magma. The wall rock exhibits rheological criteria for both fracture and ductile flow, and therefore we propose a hybrid emplacement model involving viscoelastic behavior of the wall rock (*cf.* Rubin, 1993). Evidence of brittle wall rock behavior includes the presence of dikes (implied fractures), formation of the overlying and roughly penecontemporaneous Minarets Caldera (Peck, 1980; Fiske and Tobisch, 1994), and stoping in the subvolcanic part of the magma chamber. Evidence for ductile wall rock behavior includes well-developed solid state fabrics, strongly flattened volcanic clasts and ptymatically folded dikes emanating from the pluton. Although we document that emplacement of the pluton was facilitated by multiple processes, the bulk of the evidence strongly suggests that episodic magma transport via fracture(s) was the primary mechanism through which it was assembled.

Fiske, R. S. and Tobisch, O. T., 1994. Middle Cretaceous volcanic rocks in the Minarets Caldera, east-central Sierra Nevada, California. *Geol. Soc. Am. Bull.*, **106**, 582-593.

Peck, D., 1980. Geologic map of the Merced Peak quadrangle, central Sierra Nevada, California. U.S.G.S. Geol. Quad. Map GQ-1531.

Rubin, A. M., 1993. Dikes vs. diapirs in viscoelastic rock. *Earth and Planet. Sci. Lett.*, **117**, 653-670.

## Plutonism in a Rapidly Evolving Continental Rift System, Eldorado Mountains, Southern Nevada

<sup>1</sup>Miller, C.F., <sup>1</sup>Patrick, D.W., <sup>2</sup>Miller, J.S., <sup>3</sup>Heizler, M.T., <sup>4</sup>Wooden, J.L., <sup>5</sup>Hook, S.J., <sup>1</sup>Unkefer, J., <sup>1</sup>Lee, Y.F.S. and <sup>1</sup>Falkner, C.M.

<sup>1</sup>Department of Geology, Vanderbilt University, Nashville, TN 37235, USA

<sup>2</sup>Department of Geology, University of North Carolina, Chapel Hill, NC 27599-3315, USA

<sup>3</sup>New Mexico Geochronology Research Lab, New Mexico Institute of Mining and Technology, Socorro, NM 87801, USA

<sup>4</sup>US Geological Survey, Menlo Park, CA 94025, USA

<sup>5</sup>Jet Propulsion Laboratory, California Institute of Technology, Pasadena, CA 91109, USA

Middle Miocene intrusive activity in the Eldorado Mountains spanned a brief but eventful period, beginning during early stages of tectonism that preceded rifting and terminating during waning extension. In the northern part of the range, an 18.5-13 Ma sequence of mafic, intermediate, and felsic volcanic rocks is imbricated by rotated normal faults. To the south, deeper levels of the Miocene crust are exposed. Hypabyssal to mid-crustal plutons and numerous dikes intrude Proterozoic basement and Mesozoic granites and comprise more than 60% of the subvolcanic crust. The plutons were emplaced between 16.2 and 15.7 Ma and therefore preceded peak extension (*cf.* Gans *et al.*, 1994). Much smaller volumes of magma were emplaced as dikes through 14.2 Ma, spanning the interval of peak extension.

Six plutons with a total area of  $\sim 180$  km<sup>2</sup> are exposed beneath the volcanic sequence. They include, from north to south (<sup>40</sup>Ar/<sup>39</sup>Ar ages): 1) Keyhole Canyon, 15.5 Ma, very felsic (granite-leucogranite); 2) Nelson, 16.2 Ma (with a 15.8 Ma lobe), dominantly intermediate (quartz monzodiorite, quartz monzonite); 3) Aztec Wash, 15.7 Ma, bimodal (granite, diorite); 4) Searchlight, 16.2 Ma, bimodal; 5) Rockefeller Mine, not yet well dated (U-Pb zircon lower intercept confirms mid-Miocene age; appears to be cut by Searchlight), intermediate (granodiorite, quartz monzodiorite); and, 6) Copper Mountain, undated, felsic (granite, leucogranite). Dikes range in age from synchronous with Nelson pluton to 14.2 Ma. Earlier dikes are mostly intermediate; those synchronous with Aztec

Wash pluton include both mafic and felsic; and post-Aztec Wash dikes are mostly mafic. Fabrics and hornblende barometry suggest that all intrusive rocks except the Rockefeller Mine pluton are hypabyssal, emplaced at < 5 km. The fabric of the Rockefeller Mine pluton, which was emplaced at ~ 10 km, reflects much slower cooling and syn- to post-magmatic ductile deformation.

With the exception of the Nelson pluton, the plutons are consistent with the regional pattern of northward younging of magmatic activity in the Colorado River region. The Nelson pluton is also anomalous in its emplacement style: it intruded in dike-on-dike fashion along an E-W active fault. This fault can be interpreted as either a sinistral strike-slip fault or a rotated, down-to-the-north dip-slip fault; neither interpretation is consistent with the E-W extension that occurred slightly later. N-S dike orientations and structures within plutons (*e.g.* N-S oriented mafic injections into felsic magma chambers) elsewhere in the Eldorado Mountains document the E-W extension that characterizes rifting here. The Keyhole Canyon and Nelson plutons and volcanic strata to the north were imbricated and tilted steeply eastward along rotating N-S normal faults; Aztec Wash pluton remained largely intact and untilted; and the Searchlight, Rockefeller Mine, and probably Copper Mountain plutons were tilted westward. Structures in the relatively deep-seated Rockefeller Mine pluton suggest that it was undergoing E-W stretching during and immediately after emplacement, and that it underwent subsequent rapid unroofing, probably during westward tilting.

The Keyhole Canyon, Aztec Wash, and Searchlight plutons are bimodal, dominated by granite (~ 72 wt % SiO<sub>2</sub>) and mafic trachyandesite (~ 54 wt % SiO<sub>2</sub>) with spectacular mingling textures but limited mixing. Olivine-rich cumulates from the trachyandesite in Aztec Wash pluton have as little as 44 wt % SiO<sub>2</sub> and up to 22 wt % MgO. Aztec Wash pluton experienced repeated injections of both felsic and mafic magma; what we interpret to be the lower portion of the magma chamber is dominated by mafic rock, and the upper portion is uniformly granite. The Nelson and Rockefeller Mine plutons also span a broad compositional range (~ 50-70 wt % SiO<sub>2</sub>), but they are dominantly intermediate (~ 57-65 wt % SiO<sub>2</sub>).

Although all intrusives are enriched in K and all incompatible trace elements, as expected for rift-related magmas, they are calc-alkaline and plot with arc-related rocks on discrimination plots. We suspect that this geochemical signature reflects the ancient lithospheric crust and mantle beneath southern Nevada rather than the extant

tectonic setting. Lead isotopic compositions of mafic to felsic rocks match the distinctive range of ancient regional (Mojave Province) crust and inferred lithospheric mantle (high <sup>208</sup>Pb/<sup>204</sup>Pb (~ 39); high <sup>207</sup>Pb/<sup>204</sup>Pb (~ 15.58) relative to <sup>206</sup>Pb/<sup>204</sup>Pb (~ 18.2)). Initial ε<sub>Nd</sub> and (<sup>87</sup>Sr/<sup>86</sup>Sr)<sub>i</sub> span a range that lies between the composition of regional crust and that of depleted mantle (-5 to -11, 0.7075 - 0.7105). The isotopic compositions correlate well with composition among the bimodal plutons (more felsic rocks are more evolved isotopically). Higher incompatible element concentrations in mafic than in felsic rocks is not explained by mixing between depleted mantle-derived melts and crust; rather, a source for the mafic magmas in ancient enriched mantle is suggested (*cf.* Ormerod *et al.*, 1988; Farmer *et al.*, 1989; Beard and Glazner, 1995). Additional complexities in sources are indicated by compositions of late mafic dikes, which are among the most isotopically evolved, and samples from the Nelson pluton, which are displaced toward higher ε<sub>Nd</sub> at a given <sup>87</sup>Sr/<sup>86</sup>Sr compared to the main trend.

The Nelson pluton intruded while the crust was undergoing tectonic activation, but before the onset of active E-W rifting. Its early appearance and intermediate composition are consistent with generalizations by Gans *et al.* (1989) about tectonomagmatic sequences in the Basin and Range. The other plutons constitute a major, rapid addition to the upper crust synchronous with the onset of rapid extension, suggesting the possibility that they accommodated extension and facilitated collapse of the overlying uppermost crust (*cf.* Gans *et al.*, 1989). However, there is no direct evidence that they facilitated such a collapse: they predate by several hundred thousand years imbrication of the volcanic sequence that is exposed to the north.

- Beard, B.L. and Glazner, A.F., 1995. Trace element and Sr and Nd isotopic composition of mantle xenoliths from the Big Pine volcanic field, California. *J. Geophys. Res.*, **100**, 4169-4179.
- Farmer, G.L., Perry, F.V., Semken, S., Crowe, B., Curtis, D. and DePaolo, D.J., 1989. Isotopic evidence on the structure and origin of subcontinental lithospheric mantle in southern Nevada. *J. Geophys. Res.*, **94**, 7885-7898.
- Gans, P.B., Mahood, G.A. and Schermer, E.R., 1989. Synextensional magmatism in the Basin and Range Province: A case study from the eastern Great Basin. *Geol. Soc. Am. Spec. Paper*, **223**, 53 p.
- Ormerod, D.S., Hawkesworth, C.J., Rogers, N.W., Leeman, W.P. and Menzies, M.A., 1988. Tectonic and magmatic transition in the Western Great Basin, USA. *Nature*, **333**, 349-353.

## Construction of Mid-Crustal Magma Chambers During Regional Contraction, North Cascades, Washington

<sup>1</sup>Miller, Robert B. and <sup>2</sup>Paterson, Scott R.

<sup>1</sup>*Department of Geology, San Jose State University, San Jose, CA 95192-0102, USA*

<sup>2</sup>*Department of Earth Sciences, University of Southern California, Los Angeles, CA 90089, USA*

Many recent models for pluton emplacement emphasize extension as a dominant space-making mechanism, either in dilational jogs within strike-slip zones or in normal fault systems. Conversely, the mid-crustal levels of many active arcs are constructed while undergoing contraction, and magma emplacement during contraction is well-documented in several ancient arcs. One such arc is the > 1500-km-long Coast Belt of the North American Cordillera. Cretaceous plutonism in the south-east extension of this belt, the Cascades core, was synchronous with amphibolite-facies metamorphism and major crustal shortening. Markedly different styles of syn-contraction emplacement are illustrated by relatively elliptical 96-90 Ma plutons and deeper, sheet-like, 75-65 Ma plutons. These observations raise the question of how magmas were emplaced during contraction.

The 96-93 Ma Mt. Stuart batholith forms two main bodies, the largest of which is ~ 50 x 20 km, and crystallized at 2-4 kbar. Petrological variations in this dominantly tonalitic intrusion define complex internal zoning, elliptically shaped internal bodies, dikes and petrographic banding. Structural and petrologic data suggest that the batholith was constructed from small to moderate sized (100s to 1000s m<sup>3</sup>) batches of fractionated and in places mingled magmas that were emplaced as crystal poor melts (< 50% crystals). The igneous structures described above are overprinted by magmatic foliation and lineation, which define small- and large-scale folds, batholith-scale sigmoidal patterns, and lobate margin-parallel patterns. These patterns reflect simultaneously operating body forces and regional deformation.

Space was made during emplacement by multiple country-rock material-transfer processes that include: 1) regional folding and faulting during SW-NE contraction; 2) regional horizontal NW-SE extension; 3) vertical and horizontal ductile flow in a narrow (0.1 to 0.2 body radii) structural and thermal aureole that accounts for ≤ 30% of the space, and possibly by stretching of roof rocks; 4)

possibly large-scale stoping and minor assimilation; and, 5) minor fracturing associated with dike injection.

A zone of 75-65 Ma, sheet-like plutons that crystallized at 6-8 kbar lies NE of the Mt. Stuart batholith. Regional structures in these plutons and country rocks indicate that NE-SW contraction with a component of SW-directed flow and NW-SE subhorizontal extension occurred during emplacement. We have mapped the dominantly tonalitic, Entiat and Cardinal Peak plutons, which are highly elongate (length:width > 10:1) and contain widespread internal sheets that range from > 2 km wide and > 6 km long to ~ 10 cm wide and decimeters long. The compositionally heterogeneous north-west ends of these plutons consist of hundreds of sharply bounded sheets that range from hornblende to granodiorite. To the SE the Cardinal Peak pluton consists of more homogeneous tonalite bounded by meter- to decameter-long rafts of country rock and slightly more mafic intrusive rocks. In the Entiat pluton, sheets are also less distinct to the SE and are marked by differences in texture and modal abundances. Sheets mainly strike NW and dip steeply, but in places are folded around N-S to NW-SE plunging axes. Thus, lateral compositional and structural changes in these chambers are as large as vertical changes proposed in other chambers.

Well-developed magmatic foliation and lineation in both plutons are parallel to or crosscut sheets, bands and pluton contacts, define large and small-scale folds, and along with axes of folded sheets have similar orientations to regional country rock structures. Magmatic structures thus formed after construction of the magma chamber by injection of multiple sheets and during regional folding.

Both the sheet-like and Mt. Stuart plutons are elongate perpendicular to the regional contraction direction, presumably at high angles to the far-field  $\sigma_1$  axis. This is puzzling for the sheeted plutons, as the widespread rafts imply that sheets were repeatedly injected along fractures somewhat analogous to a crack-seal process.

We conclude that regional contraction strongly influenced magma chamber dynamics of the sheet-like bodies by controlling chamber construction (sheeting), lateral compositional variations, later flow (and thus strain) during crystallization, and subsolidus deformation. In contrast, the effects of regional contraction on construction of the Mt. Stuart batholith are less obvious and contraction mainly served as a relatively minor (< 20%) space-making mechanism. These differences may reflect the shallower crustal level (7-13 km) of the Mt. Stuart versus the sheeted plutons (20-25 km), and the sizes of individual batches of

magma. The emplacement of all three plutons was apparently not strongly controlled by fault zones, in contrast to models for other plutons emplaced during contraction.

### **The Ardara Pluton, Co Donegal, NW Ireland: A Straightforward Example of a Ballooning Pluton**

Molyneux, S.J. and Hutton, D.H.W.

*Department of Geological Sciences, University of Durham, South Road, Durham, DH1 3LE, UK*

The Ardara pluton occurs at the SW margin of the Donegal Batholith, NW Ireland and is a 2/3 stage sub-circular pluton, with a concordant aureole of deformed and thermally metamorphosed Neoproterozoic meta-sedimentary rocks. This pluton has been the subject of extensive study in recent years, it has variously been interpreted as: an intrusive diapir (Akaad, 1956a, 1956b); a ballooning pluton (Berger and Pitcher, 1972; Holder, 1979); a pluton combining ballooning and stoping (Vernon and Paterson, 1993).

The project has involved a remapping and reexamination of the granitic phases and the contact features, measurement of strain from mafic enclave sizes and Fry crystal spacing, together with timing and kinematic indicators from pre-full crystallization (PFC); and solid state fabrics. In particular, the Fry method has been extensively applied to the pluton, in order to examine the strained distributions of different mineral phases, using the grain size normalised method. Fry strains are consistent with (initial-shape-adjusted) mafic enclave strains, allowing extension of strain analysis into areas of low mafic enclave density.

The general conclusions are: a) the pluton appears to have been emplaced from a point offset to the south west of its centre, expanding in concordance with the country rocks, preferentially in a northwards direction; b) during emplacement, deformation was confined almost entirely to the magmatic state, solid state deformation occurring only at the northern rim of the pluton in a metres-wide region; c) there is no evidence that the pervasive fabric within the pluton was formed by an superimposed regional strain, except in the tail where it is crossed by the Main Donegal Granite shear zone; d) mafic enclaves and Fry spacing show that strains are flattening in nature ( $K < 1$ ), a

feature consistent with a balloon model for emplacement; e) kinematic indicators associated with PFC fabrics are consistent with emplacement directed towards the north, the regional shear zone to the south perhaps acting as a barrier to emplacement.

Northward directed ballooning is consistent with earlier structural work in the aureole (Meneilly, 1982), which showed circumferential stretching around the northern part of the pluton together with local enhancement of the regional D4 deformation. Such ballooning in a preferred direction is seen in other well-known plutons around the world *e.g.* Flamanville, France and Criffell, Scotland.

Akaad, M.K., 1956a. The Northern Aureole of the Ardara Pluton, Co. Donegal. *Geol. Mag.*, **93**, 337-392.

Akaad, M.K., 1956b. The Ardara granite diapir of Co. Donegal, Ireland. *Quart. J. Geol. Soc.*, **112**, 263-287.

Berger, G. and Pitcher, W.S., 1972. Examples of diapiric intrusion. In Pitcher, W.S. and Berger, A.R. (eds), *The Donegal Granites, a Study in Emplacement and Unroofing*, J. Wiley and Sons. Chapter 8.

Holder, R.A., 1979. An emplacement mechanism for post-tectonic Granites and its implications for the geochemical features. In Atherton, M.P. and Tarney, J. (eds.), *Origins of Batholiths, Geochemical Features*, Shiva Publishing Limited, p. 117-126.

Meneilly, A.W., 1982. Regional structure and syn-tectonic granite intrusion in the Dalradian of the Gweebarra Bay area, Donegal. *J. Geol. Soc. London*, **139**, 633-646.

Vernon, R.H. and Paterson, S.R., 1993. The Ardara pluton: deflating an expanded intrusion. *Lithos*, **31**, 17-32.

### **Accumulation of Rare Earth and High Field Strength Elements in Peralkaline Granitoids: The Galiñeiro Pluton, NW Spain**

Montero, Pilar G.

*Department of Mineralogy and Petrology, Campus Fuentenueva, University of Granada, 18002 Granada, Spain*

The Galiñeiro Pluton is a composite body formed by A-type peralkaline granitoids with very high contents of rare earth and high field strength elements. Rb-Sr (whole-rock) and U-Pb (zircons) isotopic dating suggest an age of 460 Ma, with later recrystallization at 320 Ma during the peak of Hercynian metamorphism. The Galiñeiro Pluton is formed by three rock types: amphibole-biotite orthogneisses, riebeckite-aegirine orthogneisses, and metasomatic rocks. Amphibole-biotite orthogneisses have quartz + oligoclase + microcline + biotite + hastingsitic

hornblende as major minerals, and zircon, titanite, apatite and fluorite as accessories. Riebeckite-aegirine orthogneisses have microcline + albite + riebeckite-arfvedsonite + aegirine  $\pm$  annitic biotite as main minerals. The accessory mineral assemblage is composed of zircon, magnetite, ilmenite, fluorite, astrophyllite, titanite, pyrite, chalcopyrite, sphalerite, and an overabundance of REE-saturated minerals such as fergusonite, samarskite, aeschynite, unknown Yb- and Y- silicates and niobotantalites, bastnaesite, allanite, monazite, xenotime, thorite, and uraninite, which appear either as single crystals or, more frequently, forming aggregates with complex intergrowths. Metasomatic rocks — customarily called "radioactive gneisses" — are composed by quartz + albite + microcline + low-Al biotite  $\pm$  gruneritic amphibole, with no riebeckite or aegirine. They have the same accessory mineral assemblage as riebeckite-aegirine orthogneisses, but the abundance of REE-saturated minerals is much higher.

Amphibole-biotite gneisses have mol  $(\text{Na}_2\text{O} + \text{K}_2\text{O})/\text{Al}_2\text{O}_3 \sim 0.8$ ,  $\text{Fe}/(\text{Fe} + \text{Mg}) \sim 0.68$ ,  $(\text{Na}_2\text{O} + \text{K}_2\text{O}) \sim 8.5$  wt % and  $(\text{Na}_2\text{O}/\text{K}_2\text{O}) \sim 1.13$ . Riebeckite-aegirine orthogneisses have very low Al and Ca contents, mol.  $(\text{Na}_2\text{O} + \text{K}_2\text{O})/\text{Al}_2\text{O}_3 \geq 1$ ,  $\text{Fe}/(\text{Fe} + \text{Mg}) \sim 0.96$ ,  $\text{Na}_2\text{O} + \text{K}_2\text{O} \sim 8$  wt %, and  $\text{Na}_2\text{O}/\text{K}_2\text{O} \sim 1.18$ . Radioactive gneisses have  $(\text{Na}_2\text{O} + \text{K}_2\text{O})/\text{Al}_2\text{O}_3 \sim 0.85$ ,  $\text{Fe}/(\text{Fe} + \text{Mg}) \sim 0.9$ , and low  $\text{K}_2\text{O}$  contents with  $\text{Na}_2\text{O}/\text{K}_2\text{O} \sim 6.5$ . All Galiñero rocks have high REE and HFSE contents, which may occasionally reach economic levels in radioactive gneisses. The average composition of amphibole-biotite rocks is  $\sim 40$  ppm Y, 66 ppm Nb, 10 ppm Ta, 270 ppm Zr, 20 ppm Ga, 3 ppm U, 13 ppm Th, 1850 ppm F, 53 ppm La, 116 ppm Ce, 8 ppm Dy, 4 ppm Yb, with  $\text{La}_N/\text{Lu}_N \sim 14.2$  and  $\text{Eu}^*/\text{Eu} \sim 0.75$ . Riebeckite-aegirine orthogneisses have  $\sim 303$  ppm Y, 350 ppm Nb, 35 ppm Ta, 1500 ppm Zr, 40 ppm Ga, 45 ppm U, 260 ppm Th, 2220 ppm F, 241 ppm La, 495 ppm Ce, 43 ppm Dy, 20 ppm Yb, with  $\text{La}_N/\text{Lu}_N \sim 10.2$  and  $\text{Eu}^*/\text{Eu} \sim 0.11$ . Radioactive gneisses have  $\sim 1790$  ppm Y, 1850 ppm Nb, 155 ppm Ta, 5865 ppm Zr, 45 ppm Ga, 125 ppm U, 826 ppm Th, 6500 ppm F, 482 ppm La, 1444 ppm Ce, 178 ppm Dy, 68 ppm Yb, with  $\text{La}_N/\text{Lu}_N \sim 12.4$  and  $\text{Eu}^*/\text{Eu} \sim 0.15$ . Some peralkaline orthogneisses are extremely enriched in HREE, Y, and Be.

Values of  $\epsilon_{\text{Nd}} \sim +2.2$  and the geochemical features of Galiñero rocks suggest they were produced by differentiation of a mantle-derived magma. Original magmas were already REE and HFSE-rich, likely generated by melting of a strongly metasomatized area of the mantle. These

magmas were emplaced at high crustal levels where they underwent extensive fractionation. Residual melts were enriched in F, which stabilized RE and HFS elements due to the formation of complexes, probably alkali-Zr-fluorides. At the end of magmatic crystallization, a fluid phase rich in REE and HFSE complexes was released, causing intense local metasomatism either on peralkaline or country rocks. The decrease in fluoride activity as a consequence of lower temperatures and the formation of F-rich mica and amphibole produced the breakdown of the fluoride complexes and so the massive precipitation of REE and HFS, forming aggregates of REE-saturated minerals. The magmatic and metasomatic parageneses, due to their richness in F, are easily reactivated by inputs of energy and water, thus causing remobilizations and a total recrystallization during the Hercynian metamorphism, as reflected in U-Pb ages of hydrothermal zircons.

### Melt Inclusion, Matrix Glass and Mineral Compositions From a Zoned S-Type Peraluminous Rhyolite Suite, Morococala Volcanic Field, Bolivia

<sup>1</sup>Morgan, VI, G.B., <sup>1</sup>London, D.  
and <sup>2</sup>Luedke, R.G.

<sup>1</sup>University of Oklahoma, School of Geology  
and Geophysics, Norman, OK 73019, USA

<sup>2</sup>U.S. Geological Survey, National Center MS-959,  
Reston, VA 22092, USA

The Miocene peraluminous tuffs and domal flows of the Morococala volcanic field, Bolivia, record a temporal sequence of early (basal) andalusite  $\pm$  biotite  $\pm$  muscovite rhyolites (AR), middle cordierite + biotite rhyolites (CR), and latest biotite quartz latites (QL). Quartz phenocrysts in all three rock types contain abundant euhedral (negative crystal-shaped) melt inclusions. Melt inclusions in the QL and CR are glassy, whereas those in the AR are typically devitrified; prior to analysis, the solids in the latter inclusions were homogenized to glass in R-41 cold-seal reaction vessels (750°C,  $P_{\text{H}_2\text{O}} = 0.5$  kbar). Melt inclusions are homogeneous within and between two samples of the QL ( $\text{ASI} = 1.15 - 1.23$ ,  $\text{Na}/\text{K} = 0.92 - 1.08$ ,  $\text{F} = 0.21 - 0.29$ ,  $\text{Cl} = 0.15 - 0.19$ ), but have higher Al and Na versus lower Si and Fe than perlitic glass in the matrix of one sample. Similarly, melt inclusion compositions are

fairly homogeneous within and between four samples of the CR (ASI = 1.21 - 1.27, Na/K = 0.80 - 1.09, F = 0.35 - 0.42, Cl = 0.16 - 0.20), and with the exception of slightly higher F, are essentially identical to matrix glasses in all samples. Among four samples of the AR, melt inclusion compositions show considerable scatter both within and between samples (ASI = 1.21 - 1.40, Na/K = 1.05 - 1.80, F = 0.20 - 0.60, Cl = 0.04 - 0.09), even among different inclusions within a single phenocryst. EMPA totals for all the melt inclusions are high (average wt %: QL = 97.4, CR = 97.9, AR = 98.1), suggesting low H<sub>2</sub>O contents. All melt inclusions show lower contents (by 0.5 - 0.1x) of Ca, Mg, and Fe than do their whole rocks.

Sanidine (~Ab<sub>27</sub>) shows oscillatory zonation in barium throughout the QL and CR, but is unzoned in the AR; the molar celsian component of sanidine decreases from 1.4 - 2.2% in the QL, to 0.6% in the CR, and 0.2% in the AR. Plagioclase compositions become more evolved from the QL (cores = An<sub>27-47</sub>Or<sub>2-5</sub>, rims = An<sub>29-31</sub>Or<sub>4</sub>) through the CR (cores = An<sub>34-42</sub>Or<sub>2-3</sub>, rims = An<sub>22</sub>Or<sub>5</sub>), and finally to the AR (cores = An<sub>13-21</sub>Or<sub>4</sub>; rims = An<sub>11-20</sub>Or<sub>4-6</sub>). The Mg# for biotite decreases from QL (0.43 - 0.49), through CR (0.36 - 0.37), to AR (0.22 - 0.32), whereas F contents increase. Biotite displays zonation only in F, and in almost all samples increases sharply from core to rim (wt % averages: QL<sub>core</sub> = 1.16; QL<sub>rim</sub> = 1.74; CR<sub>core</sub> = 1.41; CR<sub>rim</sub> = 1.72; AR<sub>core</sub> = 2.65; AR<sub>rim</sub> = 3.57); a similar increase is noted for F in muscovite from the AR (core = 2.19, rim = 3.65 in wt %). Biotites are unzoned with respect to Cl. The Cl contents of biotites increase slightly from QL (0.21 - 0.25 wt %) to CR (0.25 - 0.26 wt %), but are lower and more variable (0.09 - 0.14 wt %) in the AR. Biotite appears to have become unstable (is altered and/or resorbed) in two of four samples of the AR. Muscovite was identified in only two of four samples of the AR, and its presence does not correlate with the apparent instability of biotite.

The compositions of melt inclusions, matrix glasses, whole-rocks, and phenocrysts are all consistent with the origin of this sequence from a single zoned rhyolitic magma chamber in which the AR represent the apical most evolved portion. Core-rim increases of F in biotite could be explained by increased F activity in melt accompanying either progressive melt fractionation or devolatilization, but a lack of Cl zonation in biotite is inconsistent with the latter. The lower average Cl contents of both melt inclusions and biotite in the AR suggests a greater degree of melt devolatilization in the apical portion of the magma

chamber. Homogeneity of melt inclusions in the QL and CR suggest little lateral heterogeneity within the lower regions of the magma chamber. Melt inclusions within the AR apparently record a quite different scenario for the apical portion of the chamber. Variations in average compositions between individual samples suggest the operation of processes giving rise to heterogeneity at length scales of tens to thousands of meters, and could involve gradients in temperature or volatile contents, or variable degrees of country rock (roof pendant) assimilation. Variability of melt inclusions in individual samples and phenocrysts, and variability in Al contents of quartz phenocrysts also suggest fine-scale disequilibrium in the AR.

### **Kilometer Scale Vertical Translation, Concordancy, and Nonrotation of Porphyroblasts Surrounding the Papoose Flat Pluton: Inclusion Trails and AMS Reveal the Kinematics of Emplacement**

<sup>1</sup>Morgan, Sven, <sup>1</sup>Law, Richard,  
<sup>2</sup>Saint Blanquat de, Michel  
and <sup>2</sup>Bouchez, Jean-Luc

<sup>1</sup>*Department of Geological Sciences, Virginia Tech,  
Blacksburg, VA 24061, USA*

<sup>2</sup>*Laboratoire de Pétrophysique et Tectonique,  
Université Paul Sabatier, 38 Rue des 36 Ponts,  
F-31400 Toulouse, France*

Consistent inclusion trail geometry from andalusite porphyroblasts within the contact aureole of the Papoose Flat pluton reveals that wall rocks were translated vertically out of the Inyo Mt. Anticline during intrusion, and that porphyroblasts have not rotated, with respect to compositional layering, even though the wall rocks have been thinned to less than 10% of their original thickness. Restoring the wall rocks back into the Inyo Mt. anticline, by assuming a vertical motion out of the anticline's southwest dipping limb, returns the planar inclusion trails into a position parallel with the regionally developed slaty cleavage, consistent with our palinspastic restoration, and also explains the orientation of the well developed stretching lineation. Restoring the wall rocks back to the east in a horizontal movement, which is suggested by examination of the map pattern deflection of aureole rocks, produces an

inconsistent inclusion trail geometry from the north side of the pluton to the south side, and does not explain the orientation of the lineation.

The Harkless Formation has been deformed into concordancy with the western margin of the pluton for over 16 km, and defines a domal shape around the pluton at the present level of exposure, dipping away from the pluton on the north, west, and south sides. If the Harkless Formation is "undomed" from concordancy and placed into a planar reference frame, not only do inclusion trails have a constant angular relationship to the foliation, but all inclusion trails become aligned parallel to one another indicating that porphyroblasts grew when the Harkless Formation was originally planar, pre-dating the doming event and present emplacement position of the pluton. Andalusite porphyroblasts exhibit a two stage growth history; an initial period of static growth where andalusite overgrows the regional slaty cleavage (pre-doming/inflation) and a second period of growth synchronous with the extreme attenuation and translation, where inclusion trails curve into the matrix foliation, representing the rotation of the matrix into parallelism with compositional layering.

Our model also simplifies the "space problem" by including wall rock translation in strain/volume analysis. Concordant aureoles cannot be explained by simple, *in situ* shortening, and previous studies of strain in pluton-wall rock systems consistently calculate volumes of granite much greater than wall rock strains can provide space for.

We argue that this space problem arises because translation of wall rocks has not been taken into account. Assuming, 1) a homoclinal structure for the pre-pluton emplacement position within the western limb of the Inyo Mt. anticline, the wall rocks surrounding the western margin of the pluton have been translated approximately 2.4 km vertically in order to attain their present structural position, which is out of place with respect to the homocline. Also assuming that, 2) the 90 % shortening is related to stretching of the aureole rocks around the pluton as the pluton inflated vertically, we calculate the shape of the pluton, and therefore it's area at depth that the surrounding aureole rocks must have translated around in order to account for the 90% thinning. Our volume compatible model predicts a flat bottomed pluton and is inconsistent with diapiric transport.

Detailed AMS and microstructural analysis reveals that magmatic fabrics are parallel to solid state fabrics. In the western portion of the pluton-aureole system, where the pluton has uplifted the furthest out of the southwest

dipping limb of the anticline, the grain shape and AMS lineation is best developed and has a constant trend from the deformed aureole, through the gneissic border of the pluton, and into the magmatic interior. Solid state and magmatic foliation's are subparallel to contacts. The parallelism of solid state and magmatic foliation's indicates that they developed synchronously and are related to the same event.

Our analysis reveals a two stage intrusive history. An initial intrusion, possibly as a sill, statically metamorphosed the Harkless Formation and caused porphyroblasts to overgrow the regionally developed slaty cleavage. A second pulse of magma caused the sill to inflate vertically, translating and attenuating the immediate aureole, which had been thermally weakened. Extreme attenuation of the aureole rocks does not rotate porphyroblasts, allowing them to be used as "fossil directions" (Fyson, 1980). In this model, aureole rocks which have been translated the most vertically, should exhibit the most intense attenuation. The increasing amount of strain in the aureole to the west, where the wall rocks have been translated the most to attain their present structural position, is consistent with the idea that aureole strain is related to the amount of vertical translation. This emplacement model is consistent with the inclusion trail analysis, orientation of the stretching lineation, AMS data, increasing amount of strain to the west, and is volume/strain compatible.

Fyson, W.K., 1980. Fold fabrics and emplacement of an Archean granitoid pluton, Cleft Lake, Northwest Territories. *Can. J. Earth Sci.*, 17, 325-332.

## **Geochemistry and Structural Petrology of the Father Pluton, Abitibi Subprovince, Canada**

Moukhsil, Abdelali

*Sciences de la Terre, Université du Québec à Chicoutimi, Chicoutimi, Québec Canada G7H 2B1*

The NW-SE elongated Father Pluton is a syntectonic intrusion in the Northern Volcanic Zone of the Abitibi Subprovince. The pluton ranges from an early mafic tonalite to a late porphyritic granodiorite phase. Geochemically the rocks are calc-alkaline, meta-aluminous to peraluminous, and related by a process of fractional crystallization involving hornblende, biotite, oligoclase,

apatite, epidote and sphene. The fractionated granodiorites are enriched in sphene and magnetite and show positive Ta anomalies. Rare earth patterns show LREE enrichment compared to HREE. Changes in rare earth abundance and shape of REE patterns with pluton evolution may be correlated to the crystal fractionation. Amphibole fractionation is also suggested by a diminishing Sc content with increasing SiO<sub>2</sub>. Mineral analyses (biotite, hornblende and plagioclase) suggest that the pluton was emplaced at a temperature of 700-800°C and a pressure of 1.6 to 2.9 kbar.

The pluton occurs between a major E-trending fault with a dextral strike-slip component (Doda fault) in the north and several lesser faults in the south. The principal magmatic foliation is oriented NE-SW and is subvertical. A NW-SE foliation is associated with early phases of the pluton and appears to be cut by the principal foliation. The mineral lineation lying in the foliation plane is subhorizontal. Local ductile deformation zones occur parallel to both foliation directions. It is believed that the early foliation reflects mechanical conditions controlling the onset of pluton injection, which subsequently changed to those governing the main emplacement.

Field measurements of foliation and lineation are based on xenolith, phenocryst and mafic mineral alignment. Further detailed laboratory analysis of oriented sections revealed two types of alignment; one characterized by alignment of biotite and hornblende masses, plagioclase and some potassium feldspar phenocrysts, and the other by potassium feldspar phenocrysts, isolated biotite and hornblende grains and some quartz. Analysis on the XZ plane shows a number of kinematic markers, chiefly crystal rotation and tilting indicating a dextral movement.

The two principal foliation directions may be related to subsidiary directions (P and R) of the Doda fault, and the pluton is interpreted to have intruded while this fault was active. Pluton injection was principally subhorizontal, as indicated by the magmatic lineation.

## Sodic Granitoid Magmas Formed by Melting of Mafic Lithosphere: The Separation Point Batholith, New Zealand

Muir, R.J. and Weaver, S.D.

*Department of Geology, University of Canterbury,  
Christchurch, New Zealand*

The Early Cretaceous Separation Point Batholith of the South Island, New Zealand, represents the final magmatic stage of an extensive arc system located on the SW Pacific margin of Gondwana during the Mesozoic. The batholith consists of Na-rich, alkali-calcic diorite to biotite-hornblende monzogranite. The rocks have a distinctive chemistry, atypical of calc-alkaline subduction related granitoids, but comparable with those of adakites and Archaean trondhjemite-tonalite-dacite suites.

All of the granitoids are characterized by high Al<sub>2</sub>O<sub>3</sub> (16 - 23 wt %), high alkalis (Na<sub>2</sub>O + K<sub>2</sub>O = 8 wt %; with Na<sub>2</sub>O/K<sub>2</sub>O = 1.5 - 2.0), high LIL/HFS element ratios, low Y (<20 ppm) and unusually high Sr (typically >1000 ppm). REE abundance patterns are strongly fractionated ((La/Yb)<sub>N</sub> > 20) with negligible Eu anomalies. Low concentrations of the heavy REE (down to 3 x chondritic abundances) suggest that garnet was present in the source region. Primitive Sr ((<sup>87</sup>Sr/<sup>86</sup>Sr)<sub>i</sub> = 0.7042) and Nd isotopic ratios (ε<sub>Nd</sub>(120 Ma) = +1.2 - +1.8) and the absence of inherited zircon, indicate that Separation Point magmas experienced little, if any, interaction with felsic crust. The distinctive chemical and isotopic features of the batholith, including high Na<sub>2</sub>O and Al<sub>2</sub>O<sub>3</sub>, low heavy REE and Y contents together with high Sr/Y ratios, suggest that these rocks were derived from the partial melting of a mafic source with residual garnet and amphibole. The lack of Eu anomalies and the unusually high Sr content preclude significant plagioclase in the source residue. On the basis of this observation, two likely sources for the origin of the Separation Point magmas can be envisaged; young, hot, subducted oceanic lithosphere or newly underplated basaltic crust beneath a thickened continental arc. The latter model is preferred because Separation Point rocks do not possess MORB isotopic characteristics, and cannot be explained as mixtures of MORB-melt and continental crust.

Melting of amphibolitic underplate must have occurred at depths of >40 km (*P* >1.3 GPa) under water undersaturated conditions. This took place either as a

consequence of magmatic underplating and uplift at the base of the thickened arc, or more speculatively, was perhaps triggered by back-arc basin closure. A similar model has recently been proposed for the generation of the Cordillera Blanca Batholith of Peru. We note that in both the Peruvian and New Zealand cases, the adakitic/trondhjemitic - tonalite - dacite magmas were emplaced inboard of older calc-alkaline batholiths.

### REE-Depleted Leucogranites as a Consequence of Disequilibrium Melting of Monazite-bearing Schists, The Black Hills, South Dakota

Nabelek, Peter I. and Glascock, Michael D.

*Department of Geological Sciences and  
MU Research Reactor, University of Missouri,  
Columbia, MO 65203, USA*

The Black Hills, South Dakota, include one of the finest examples of leucogranite-pegmatite complexes generated by partial melting of metasedimentary protoliths. The granites formed as a result of the collision of the Wyoming and Superior Archean cratons 1.7 Ga ago (Redden *et al.*, 1990). The Harney Peak Granite and its satellite intrusions formed by emplacement of hundreds of dikes and sills. They comprises two spatially and isotopically distinct suites. Both can be related to melting of protoliths equivalent to the metasedimentary rocks into which the granites were intruded. The dikes and sills in the core of the Harney Peak granite are two-mica granites with average  $\delta^{18}\text{O}$  value of 11.5 ‰, whereas the peripheral tourmaline granites have relatively elevated  $\delta^{18}\text{O}$  values which average 13.2‰ (Nabelek *et al.*, 1992).  $^{207}\text{Pb}/^{204}\text{Pb}$  ratios in K-feldspars from the core intrusions are higher than in K-feldspars from the peripheral intrusions, with the former indicating a crustal history of the protolith since the Archean and the latter indicating a short Proterozoic history (Krogstad *et al.*, 1993; Walker and Krogstad, this volume). Leucosomes in wall-rocks that have undergone partial melting have compositions similar to the high- $\delta^{18}\text{O}$  granites.

The B and  $\text{TiO}_2$  concentrations in the two suites are for the most part distinct. The peripheral high- $\delta^{18}\text{O}$  granites have high B/ $\text{TiO}_2$  ratios (0.1-30.0) which indicates dehydration-melting of muscovite, the major source for B,

but at temperatures below the breakdown of biotite, the major source for Ti in the protolith metasedimentary rocks. In contrast, the B/ $\text{TiO}_2$  ratios in most (but not all!) samples of the low- $\delta^{18}\text{O}$  suite are low (0.01-0.07), indicating dehydration melting of biotite in the generation of these melts. Dehydration melting temperatures are also indicated by oxygen isotopic equilibration temperatures among minerals in excess of 750°C.

The chondrite-normalized REE patterns in samples with low B/ $\text{TiO}_2$  ratios are LREE-enriched with negative Eu anomalies. The patterns are similar to those in the Archean and Proterozoic metasedimentary rocks in the Black Hills and most crustal sediments. In contrast, the patterns of samples with high B/ $\text{TiO}_2$  ratios are LREE-depleted. LREE depletions, analogous to those in the LREE-depleted granites, are also found in the leucosomes of the migmatites. The LREE-depleted patterns also correlate with very low Th concentrations in the samples. It is proposed that the LREE and Th depletions are the consequence of disequilibrium melting of schists involving monazite. Petrographic observations, back-scatter electron images and X-ray maps of migmatized schists that have undergone small extents of melting without the breakdown of biotite reveal that monazite remained armored by biotite (some also by garnet) in melanosomes. This prevented the equilibration of monazite with the melt. Application of the monazite saturation model of Montel (1993) demonstrates that REE concentrations in the LREE-depleted samples are below those necessary for monazite saturation even at temperatures as low as 600°C. In contrast, REE concentrations in the LREE-enriched granites yield 700-800°C monazite-saturation temperatures that are reasonable for biotite-dehydration melting reactions. The breakdown of biotite permitted the exposure of monazite in the protolith to equilibration with the partial melts, yielding normal crustal REE patterns.

This study demonstrates that LREE-depletion in granites may say little about the relative rates of melt extraction and melt equilibration with accessory minerals in the residue, inasmuch as monazite may remain armored by biotite at melting conditions below biotite breakdown. Instead, the concentrations of LREE's indirectly reflect the different dehydration reactions that can lead to leucogranite melts.

Redden, J.A., Peterman, Z.E., Zartman, R.E., and DeWitt, E., 1990. U-Th-Pb geochronology and preliminary interpretation of Precambrian tectonic events in the Black Hills, South Dakota. In Lewry, J.F. and Stauffer, M.R. (eds), *The Early Proterozoic Trans-Hudson Orogen*, Geol. Assoc. Can. Spec. Paper, 37, 229-251.

- Nabelek, P.I., Russ-Nabelek, C., and Haeusser, G.T., 1992. Stable isotope evidence for the petrogenesis and fluid evolution in the Proterozoic Harney Peak leucogranite, Black Hills, South Dakota. *Geochim. Cosmochim. Acta*, **56**, 403-417.
- Krogstad, E.J., Walker, R.J., Nabelek, P.I., and Russ-Nabelek, C., 1993. Lead isotopic evidence for mixed sources of Proterozoic granites and pegmatites, Black Hills, South Dakota USA. *Geochim. Cosmochim. Acta*, **57**, 4677-4686.
- Montel, J.M., 1993. A model for monazite/melt equilibrium and application to the generation of granitic magmas. *Chem. Geol.*, **110**, 127-146.

## ORAL PRESENTATION

**Cretaceous Granitoids in  
Southwest Japan and  
Their Bearing on  
Crust-Forming Processes in the  
Eastern Eurasian Margin**

Nakajima, Takashi

*Geological Survey of Japan, 1-1-3 Higashi,  
Tsukuba, Ibaraki 305, Japan*

The Cretaceous granitic rocks and associated regional metamorphic rocks in Southwest Japan were formed by a Cordilleran-type orogeny. Southwest Japan was regarded as a hypothetical cross-section of upper to middle crust of the Eurasian continental margin in the Cretaceous, comprising high-level granitoids (called San-yo type) and weakly- to unmetamorphosed accretionary complexes which are exposed on the back-arc side, and low-level (Ryoke type) granitoids with high-grade metamorphites up to migmatitic gneisses on the fore-arc side. This granitic magmatism and metamorphism is an essential part of the crust-forming process at the continental margin. The lowest-level granitoids are foliated concordantly with associated gneisses and migmatites, and higher-level granitoids intrude them cross-cutting those foliations and gneissosities. The lower-level granitoids never intrude into the high-level ones.

All these granitoids are of ilmenite series and predominantly I-type with subordinate amount of garnet- or muscovite-bearing varieties in some Ryoke type ones, but none of them contains cordierite. These mineralogical variations are likely to depend more on their slightly peraluminous chemistry rather than the difference of pressure during crystallization.

Granitoids of both levels have similar cooling ages (given by K-Ar and Rb-Sr biotite ages) and show a systematic along-arc variation of eastward younging but the magmatic ages (given by SHRIMP U-Pb zircon ages) are slightly different between different levels. In the eastern part of Southwest Japan, the granitoids of the both levels give K-Ar biotite ages of approximately 65 Ma, while the magmatic age of high-level granitoids are approximately 70 Ma and are 15 Ma younger than the lower-level ones of nearly 85 Ma. It implies that the formation of the middle crust had started approximately 15 Ma prior to the upper crust. Generally, the Cretaceous granitoids in Southwest Japan have a similar cooling rate of 20-40°C/Ma during cooling from 500°C to 300°C, judging from K-Ar hornblende and biotite ages. This cooling rate is too large to spend 20 Ma from crystallization to 300°C. The middle crust material was kept over 500°C for 15-20 Ma after solidification, presumably foliated and recrystallized at deep beneath, and then it cooled down together with the upper crust to 300°C 6-7 Ma after the formation of the upper crust. The coincidence of cooling history below 500°C of the upper and middle crust might reflect the regional uplift of the crust.

The ( $^{87}\text{Sr}/^{86}\text{Sr}$ )<sub>i</sub> ratios of the Cretaceous granitoids in southwest Japan have an along-arc lateral variation; relatively low (0.705 - 0.708) in the western part and high (0.707 - 0.711) in the eastern part of Southwest Japan. Also their neodymium isotopic ratios have an along-arc variation correlative to the strontium. These isotopic variations could mean that the granitic magma have been generated through the interaction with some crustal materials. The lateral variation patterns of ( $^{87}\text{Sr}/^{86}\text{Sr}$ )<sub>i</sub> of the low-level granitoids and the high-level granitoids are slightly different. The low-level granitoids have higher ( $^{87}\text{Sr}/^{86}\text{Sr}$ )<sub>i</sub> than those of high-level ones in the middle-western part (Chugoku district) but it seems opposite in the eastern part. It may imply that they might have formed by separate magmatic pulses of c. 15 Ma interval, even though they are not independent and are all in a big single geological event.

**Panafrican Stratoid Granites  
of Madagascar:  
A New Post-Collisional  
Alkaline Province**

<sup>1</sup>Nédélec, A., <sup>2</sup>Stephens, W.E.  
and <sup>1</sup>Bouchez, J.L.

<sup>1</sup>*Pétrophysique, URA 67 CNRS,  
Université Paul-Sabatier, Toulouse, France*

<sup>2</sup>*Department of Geology,  
University of St Andrews, Scotland*

A major alkali granite province of late Panafrican age (around 585 Ma) occupies central Madagascar. It takes the form of sheets interlayered in gneissic and migmatitic basement. The thickness of the granitic sheets ranges from < 0.5 m to > 500 m. Their total volume is around one quarter of the c. 7 km-thick outcropping midcrustal section in the studied area (NNW of Antananarivo).

All granitic rocks are metaluminous and display A-type characteristics. Two distinct suites have been recognized: a mildly alkaline suite, including subsolvus granites; and, a strongly alkaline suite, including alkaline hypersolvus granites and quartz-syenites. LILE-enriched monzodioritic enclaves are ubiquitous. The strongly alkaline suite is characterized by higher Fe, Mn, Zr, Zn and REE contents and lower Al, Ca and Sr than the mildly alkaline suite. Major and trace element geochemistry and oxygen isotope data suggest that the mildly alkaline suite was derived from a granodioritic crustal protolith, whereas the strongly alkaline suite was derived from a LILE-enriched mantle source (Nédélec *et al.*, 1995).

A detailed structural study was carried out using the AMS (anisotropy of magnetic susceptibility) technique (Nédélec *et al.*, 1994). The foliations follow a N-S strike and are gently dipping to the west. The lineations trend mostly to the WSW. The structures are mainly magmatic in the granitic rocks and result from a pronounced annealing in the gneisses. In the absence of obvious shear sense indicators in the field, quartz c-axis fabrics display either symmetrical patterns or asymmetrical patterns giving opposite shear senses. It is therefore concluded that the stratoid granites were emplaced under a roughly coaxial strain regime.

Madagascar in its late-Proterozoic configuration was involved in the Panafrican orogeny of eastern Africa.

Emplacement of the stratoid granites was contemporaneous with high-*T* - low-*P* metamorphism. Underplating of a large volume of basic magmas is thought to be responsible for this high geothermal gradient and for partial melting of the continental crust. The late-Panafrican age and the structural and thermal data are consistent with post-collisional extensional tectonics as a result of lithospheric delamination in the Mozambique belt.

Nédélec A., Paquette J.L., Bouchez J.L., Olivier P. and Ralison B., 1994. Stratoid granites of Madagascar: structure and position in the Panafrican orogeny. *Geodinamica Acta*, 7, 48-56.

Nédélec A., Stephens W.E. and Fallick A.E., 1995. The Panafrican stratoid granites of Madagascar: alkaline magmatism in a post-collisional extensional setting. *J. Petrol.*, in press.

**Geochemistry of Granitic Rocks  
and Their Minerals from  
the Kavala Pluton,  
Northern Greece**

<sup>1</sup>Neiva, A.M.R., <sup>2</sup>Christofides, G.,  
<sup>2</sup>Eleftheriadis, G. and <sup>2</sup>Soldatos, T.

<sup>1</sup>*Department of Earth Sciences, Coimbra University,  
3000 Coimbra, Portugal*

<sup>2</sup>*Department of Mineralogy, Petrology,  
Economic Geology, Thessaloniki University,  
GR 5406 Thessaloniki, Greece*

The Kavala pluton mainly is composed of metaluminous granodiorite, with predominance of a medium- to coarse-grained gneissic granodiorite over a coarse-grained granodiorite. Both are cut by aplitic and mafic dykes. Metaluminous diorite and tonalite and metaluminous-to-peraluminous granite occur locally. Diorite, tonalite and part of each granodiorite have magnesian hastingsitic hornblende > Mg-biotite, while other parts of each granodiorite have Mg-biotite > hornblende, and granite contains only Mg-biotite. There are neither mineralogical nor chemical distinctions between the gneissic and the non-gneissic granodiorites. They contain numerous enclaves of metaluminous magnesio-hornblende + Mg-biotite diorite and tonalite. All contain magnetite.

For bulk-rock compositions, variation diagrams of most major and trace elements indicate fractionation trends from diorite to granite, but enclaves fall outside the trends in the diagrams of Al, Fe, Mg, K, V, La, Nb, Rb and Sr/Rb,

and also in diagrams of trace elements of hornblende and biotite, and of Ca and Mn of magmatic epidote (23 - 29 % pistacite content). The variation diagrams of Nb of rocks, Zr, Ce, La, Nd, Rb and Rb/K of hornblende, Ca and Mn of epidote and Mn and Mn/Fe<sup>2+</sup> of allanite indicate that the diorite does not belong to this sequence. This is supported by the fact that its plagioclase has an anorthite content similar to that of tonalite plagioclase, and because its REE pattern is cut in the HREE by the subparallel REE patterns from tonalite to granite. Therefore the sequence is of tonalite, hornblende-biotite granodiorite, biotite-hornblende granodiorite and granite. Least square analysis of major elements and modelling of trace elements indicate that hornblende > biotite granodiorite, biotite > hornblende granodiorite and I-type granite were derived from tonalite magma by fractional crystallization of plagioclase, hornblende, biotite and quartz. However  $K_D$  values  $[(X_{Mg}^{Bt}/X_{Fe}^{Bt})/(X_{Mg}^{Hb}/X_{Fe}^{Hb})]$  are > 1 in diorite, tonalite and granodiorite, higher than normally observed in igneous rocks, but is < 1 in enclaves. So biotite of all rocks, except enclaves, could have been formed by replacement of hornblende, which is interpreted as a magmatic process, because there is increase in F, Rb, Rb/K and decrease in Cr, V, Sc, Nd, Ni, Ni/Fe<sup>2+</sup>, Ni/Mg in biotite of the rock sequence.

Based on hornblende composition, a pressure up to 6 kbar for tonalite and granodiorite and a temperature up to 790°C for tonalite and an average temperature of 750°C for granodiorite were calculated. Based on biotite composition and its equilibrium with alkali feldspar and iron oxides, a pressure of  $f_{O_2} \sim 10^{-13}$  bar for tonalite and granodiorite magmas and  $P_{H_2O} \sim 4$  kbar for tonalite magma and  $\sim 6$  kbar for granodiorite magma were estimated.  $\log (f_{H_2O}/f_{HF})$ ,  $\log (f_{H_2O}/f_{HCl})$  and  $\log (f_{HCl}/f_{HF})$  are similar in tonalite and granodiorite magmas. The tonalite and granodiorite were completely crystallized about 615-505°C (estimated from feldspar compositions).

## ORAL PRESENTATION

### Experimental and Theoretical Constraints on the Differentiation of High Temperature Crustal Magmas

Nekvasil, Hanna, Jensen, Charles and Carroll, William

Department of Earth and Space Sciences,  
State University of New York,  
Stony Brook, NY 11794-2100, USA

Calculated phase equilibria in the granite system (*i.e.*, the system Ab-Or-Qz-An) indicate major differences between the compositional evolution of water-poor, high temperature magmas (*e.g.* trachytic and syenitic liquids) and water-rich magmas (granitic liquids). Such calculated phase relations can provide important insights into possible crystallization trends in regions difficult to determine experimentally. For these trends to be meaningful, however, they must be pinned by experimental data. For high temperature magmas, the effect of water on the cotectic compositions in the bounding binaries of the granite system provides important constraints, since during differentiation high temperature magmas will likely traverse much of the water-undersaturated region towards water-saturation. Experiments were, therefore, conducted to determine the effect of water on the eutectics in the systems An-Or, Ab-Qz and Or-Qz. These data constrain the haplogranite cotectic surface in the system Ab-Or-Qz-H<sub>2</sub>O and the 4-phase surface in the granite-H<sub>2</sub>O system. Because of the importance of determining the effect of water alone, these experiments were designed to determine the location of the anhydrous eutectic and water-saturated eutectic at high enough pressure to permit an enhancement of the effects of water without the use of H<sub>2</sub>O-CO<sub>2</sub> fluids. Nekvasil and Carroll (1993) obtained reversed experimental data in the system An-Or at 11.3 kbar and showed that with increasing water content, the Or content of the melt also increases but to a much lesser extent than that determined by Ai and Green (1989). The new data imply that the maximum Or enrichment (in projection) in the melt as melts evolve along the 4-phase surface (*i.e.*, during the coprecipitation of plagioclase, alkali feldspar, and quartz in the granite-water system) is 10 wt % instead of 20 wt %. These data further imply that coprecipitation of plagioclase and alkali feldspar will result in Or-enrichment of the magma. The extent of

this, however, will decrease with larger bulk water contents and higher bulk Ab contents. Experiments in the system Ab-Qz(-H<sub>2</sub>O) were also conducted under dry and H<sub>2</sub>O-saturated conditions. At 10 kbar there is an unequivocal shift of the eutectic towards Qz with increasing water content. This shift may, however, be as small as 3 wt % (from dry to water-saturated) towards Qz at this pressure. In contrast, experiments in the system Or-Qz indicate a very strong shift of the eutectic towards Qz with increased water content. At 10 kbar this shift is as much as 23 - 25 wt % (from dry to water-saturated conditions). These data imply that unlike the inference of Pichavant *et al.* (1992) the projected quartz + alkali feldspar + L surface in the haplogranite-H<sub>2</sub>O system does not twist in three dimensional space and thus cannot project as a point at the minimum in the water-free haplogranite system. Instead, the surface narrows as the Ab-Qz sideline is approached. This in turn implies that Qz-enrichment of the melt will always occur during precipitation of quartz and feldspar from an H<sub>2</sub>O-undersaturated, H<sub>2</sub>O-unbuffered magma. The more albitic the melt is when it reaches this surface (at the onset of coprecipitation of alkali feldspar and quartz) or when it reaches the 2 feldspar + quartz + L surface in the granite system the less the extent of Qz enrichment. Importantly, it is possible that albitic melts may not show this Qz-enrichment trend if H<sub>2</sub>O-CO<sub>2</sub> fluids are present. Experimental data of Holtz *et al.* (1992), in which the effect of water was determined using H<sub>2</sub>O-CO<sub>2</sub> fluids, indicate that increasing water content in the system Ab-Qz results (in projection) in a decrease in Qz content of the liquid in contrast to the increase seen in the system Or-Qz. The differences between the results with and without CO<sub>2</sub>-bearing fluids suggests that there may be (perhaps unquenchable) alkali carbonate complexing in the fluid which renders the silicate melt peraluminous. In this case, higher CO<sub>2</sub> contents of the vapor (and hence lower water contents) would result in increased peraluminosity. Voigt and Joyce (1991) have shown that increasing peraluminosity shifts the projected quartz-albite eutectic to higher Qz contents. Thus, an increase of the activity of water in H<sub>2</sub>O-CO<sub>2</sub> fluids would result in two competing effects. First, the effect of increased water in the melt would be to shift the eutectic towards Qz. Second, the effect of decreasing CO<sub>2</sub> activity in the fluid would be to decrease the peraluminosity of the melt and shift the eutectic towards the feldspar (Ab or Or). Since the effect of water alone is so small at the Ab + Qz eutectic (and the alkali feldspar quartz + L surface so narrow near the Ab-Qz sideline) CO<sub>2</sub> can readily cause a net shift of the

eutectic away from quartz with increasing activity of water in the fluid. Near the Or-Qz sideline, however, the effect of CO<sub>2</sub> cannot outweigh the effect of water and the shift in eutectic composition with increasing water activity in the presence of a H<sub>2</sub>O-CO<sub>2</sub> fluid remains in the same direction, albeit smaller in magnitude, as for increasing water content alone.

- Ai, Y. and Green, D.H., 1989. Phase relations in the system anorthite-potassium feldspar at 10 kbar with emphasis on their solid solutions. *Mineral. Mag.*, **53**, 337-345.
- Holtz, F., Johannes, W. and Pichavant, M., 1992. Peraluminous granites: the effect of alumina on melt composition and coexisting minerals. *Trans. Royal. Soc. Edinburgh: Earth Sci.*, **83**, 409-416.
- Nekvasil, H. and Carroll, W.J., 1993. Experimental constraints on the high-temperature termination of the anhydrous 2 feldspar + L curve in the feldspar system at 11.3 kbar. *Am. Mineral.*, **78**, 601-606.
- Pichavant, M., Holtz, F. and McMillan, P.F., 1992. Phase relations and compositional dependence of H<sub>2</sub>O solubility in quartz-feldspar melts. *Chem. Geol.*, **96**, 303-319.
- Voigt, D.E and Joyce, D.B., 1991. Depression of the granite minimum by the addition of sillimanite. *EOS Trans. Am. Geophys. Union*, **72**, 304.

## The "Mantle-Like" Component in Felsic Complexes of the Lachlan Fold Belt

Nicholls, Ian and Bagaric, Steve  
*Department of Earth Sciences,  
Monash University,  
Clayton 3168, Australia*

A number of studies of Silurian-Devonian granitic and felsic volcanic rocks of the Lachlan Fold Belt, eastern Australia (most recently *e.g.* Woodhead and McCulloch, 1993) have presented Sr-Nd-Pb isotopic evidence for the involvement of "mantle-like" source components, representing end-members of apparent mixing trajectories to contrasted "crustal" components. The simplest interpretation of these "mantle-like" components is that they reflect the characteristics of mafic magmas which underplated and intruded the crust of the Lachlan Fold Belt (LFB), and which helped provide and transport the heat necessary for crustal melting.

Most LFB felsic complexes which are dominated by hornblende-bearing metaluminous to weakly peraluminous ("I-type") rocks include one or more candidates for representatives of "mantle-like" components. These

typically take the form of mafic-intermediate (gabbro-tonalite) minor plutons, basaltic-andesitic dykes and microgranitoid (microtonalite-microgranodiorite) enclaves within felsic host rocks. Recent detailed studies of the petrography and trace element and isotope geochemistry of these more mafic rock types and their hosts have provided evidence for the nature of processes of granitic magma evolution and emplacement, and also for the characteristics of "mantle-like" components associated with LFB magmatism.

The 405 Ma Swifts Creek hornblende granodiorite pluton, eastern Victoria (Eberz *et al.*, 1990) contains up to 40 vol % of hornblende microtonalite enclaves, with diameters ranging from a few centimetres to tens of metres. These are typically rounded and often have fine-grained, scalloped margins - features which are most compatible with emplacement as globules of a hot fluid crystal-poor magma into a partially crystallized felsic host magma rich in coarse quartz and feldspar crystals. "Trails" of the latter crystals within some enclaves provide strong evidence for physical mingling and incomplete chemical mixing between enclave and host magmas. This interpretation is supported by observed gradations between the trace element and isotopic compositions of enclaves and host, which together define apparent two-component mixing trajectories between "mantle-like" and "crustal" end-members. Enclaves which lack quartz and feldspar megacrysts ( $(^{87}\text{Sr}/^{86}\text{Sr})_i \sim 0.7060$ ;  $\epsilon_{\text{Nd}} \sim -3.5$ ) plot near possible "mantle-like" end-members. Mixing models most compatible with both trace element and isotope systematics, involving "crustal" end-members with  $(^{87}\text{Sr}/^{86}\text{Sr})_i > 0.710$  and  $\epsilon_{\text{Nd}} \sim -9.0$ , indicate a "mantle-like" end-member with  $(^{87}\text{Sr}/^{86}\text{Sr})_i \sim 0.705$  and  $\epsilon_{\text{Nd}} \sim -2.0$ , which has significantly higher incompatible trace element abundances than possible "depleted mantle" components (McCulloch and Chappell, 1982). A component with isotopic and trace element compositions similar to "depleted mantle" requires mixing with unrealistically large proportions of complementary "crustal" components to meet trace element abundance constraints.

The 385 Ma Mt. Stirling-Mt. Buller complex, east-central Victoria, includes the major hornblende-bearing Mt. Stirling Granodiorite, which contains abundant microtonalite enclaves, and several gabbro-diorite stocks. Below the summit of Mt. Buller, at a level near the roof of the pluton, a complex zone of interfingering between the granodiorite and a variably megacrystic, apparently hybrid fine-grained microtonalite phase is exposed. Sr- and Nd-isotopic data for whole rock samples from the

largest gabbroic stock, the microtonalites of the complex zone and enclaves in the granodiorite show a narrow range of isotopically primitive compositions ( $(^{87}\text{Sr}/^{86}\text{Sr})_i = 0.7038-0.7045$ ,  $\epsilon_{\text{Nd}} \sim +4.0 - 4.3$ ). These compositions are more primitive than those of some tonalitic representatives of the 400 Ma "I-type" Bega Batholith ( $(^{87}\text{Sr}/^{86}\text{Sr})_i \sim 0.7041$  and  $\epsilon_{\text{Nd}} \sim +3.0$ , McCulloch and Chappell, 1982; Woodhead and McCulloch, 1993) and they are isotopically almost identical with the "depleted mantle" component used by the former authors. The host Mt. Stirling Granodiorite is only slightly more radiogenic ( $(^{87}\text{Sr}/^{86}\text{Sr})_i \sim 0.7043$  and  $\epsilon_{\text{Nd}} \sim +2.6$ ). This raises the possibility that the entire Mt. Stirling-Mt. Buller gabbro-granodiorite suite was directly related by crystal fractionation to parental basaltic magmas with strong "mantle" signatures, with a significant crustal input (probably due to crustal assimilation/fractional crystallization) apparent only in the large-volume Mt. Stirling Granodiorite. The more mafic members of this suite may therefore give a strong indication of the geochemical characteristics of mantle-derived magmas involved in LFB magmatism, minimally modified by interaction with felsic igneous or metasedimentary material or its partial melts during transport through the crust and magma mingling/mixing during emplacement. Further trace element, isotopic and related model-age data are required to assess this interpretation. Further representatives of "mantle-like" components may be sought amongst Devonian basaltic to high-Mg andesitic dykes which are widespread in the southeastern Lachlan Fold Belt in Victoria. These occurrences include a number of prominent dike "swarms", *e.g.* the Wood's Point, Tabberabbera and Ensay swarms, eastern Victoria. Dikes of this type are often associated with Devonian granitic complexes, but they occur throughout the region, and clearly reflect significant mantle magmatism at or near the time of maximum intensity of granitic batholith emplacement.

Eberz, G.W., Nicholls, I.A., Maas, R., McCulloch, M.T. and Whitford, D.J., 1990. The Nd- and Sr-isotopic composition of I-type microgranitoid enclaves and their host rocks from the Swifts Creek Pluton, southeast Australia. *Chem. Geol.*, **85**, 119-134.

McCulloch, M.T. and Chappell, 1982. Nd isotopic characteristics of S- and I-type granites. *Earth Plan. Sci. Lett.*, **58**, 51-64.

McCulloch, M.T. and Woodhead, J.D., 1993. Lead isotopic evidence for deep crustal-scale fluid transport during granite petrogenesis. *Geochim. Cosmochim. Acta*, **57**, 659-674.

**Petrogenesis of a 1.87 Ga  
Post-Tectonic Granite Suite in the  
Svecofennian of Finland:  
General and Nd Isotope Geochemistry**

<sup>1</sup>Nironen, M. and <sup>2</sup>Rämö, O. Tapani

<sup>1</sup>*Geological Survey of Finland,  
Betonimiehenkuja 4,*

*FIN-02150 Espoo, Finland*

<sup>2</sup>*Department of Geology,*

*P.O. Box 11, FIN-00014*

*University of Helsinki, Finland*

A considerable part of the Paleoproterozoic Svecofennian crust of southern and central Finland is occupied by the 40,000 km<sup>2</sup> Central Finland Granitoid Complex (CFGC) that comprises mainly granites and granodiorites. Most of the granitoids are syntectonic and yield U-Pb zircon ages around 1.89-1.88 Ga, which was the main crust-forming and tectonometamorphic (synorogenic) period in the Svecofennian. On the southern flank of CFGC is a suite of post-tectonic, K-rich granitoids that yield U-Pb zircon ages around 1.87 Ga and have characteristics similar to the 1.65-1.54 Ga anorogenic rapakivi granites further to the south. We report petrographic, general geochemical and Nd isotopic data on the 1.87 Ga granite suite and compare the results to those previously reported for the syntectonic 1.89-1.88 Ga granitoids and the anorogenic 1.65-1.54 Ga rapakivi granites.

The 1.87 Ga granitoids are felsic, weakly to non-foliated, medium- to coarse-grained, and typically porphyritic with angular and rounded K-feldspar megacrysts. At least one of the plutons comprises a bimodal suite of granites and tholeiitic gabbroic rocks. In modal composition, the granitoids vary from quartz monzonite to syenogranite. The main mafic silicate is biotite that typically occurs in the interstices of feldspars; hornblende is occasionally present. The granites in the western part of the suite contain ubiquitous accessory fluorite.

The rocks of the 1.87 Ga suite are weakly peraluminous (molecular Al<sub>2</sub>O<sub>3</sub>/(CaO + Na<sub>2</sub>O + K<sub>2</sub>O) 1.0 to 1.15) whereas the two other groups exhibit a shift from metaluminous to marginally peraluminous compositions with increasing SiO<sub>2</sub>. A characteristic feature of the 1.65-1.54 Ga suite is very high Fe/Mg (up to 50) whereas the 1.89-1.88 Ga granites show uniformly low Fe/Mg (on

the order of 4 to 5); the 1.87 Ga granitoids plot between these extremes and exhibit increasing Fe/Mg with increased SiO<sub>2</sub>. In a P versus Rb diagram the three groups show strong depletion of P with increased Rb conforming to I-type granite evolution. In the tectonomagmatic diagrams (Nb versus Y, Rb versus Y + Nb), the granite suite is transitional between the WPG and VAG fields whereas the rapakivi granites fall in the WPG field. In general, the 1.89-1.88 Ga group shows higher CaO, Na<sub>2</sub>O, and Ba/Rb and lower K<sub>2</sub>O than the 1.65-1.54 Ga rapakivi granites; the 1.87 Ga granites plot between these two extremes. This suggests that the 1.89-1.88 Ga granites were probably derived from a plagioclase-dominated source and the 1.87 Ga and 1.65-1.54 Ga granitoids from a two-feldspar protolith. Moreover, the relatively high zircon contents (up to 600 ppm) in the 1.87 Ga granites point to high-temperature, vapor-absent melting of the source.

On the average, the granitoids of the 1.87 Ga group show a slightly less radiogenic Nd isotopic composition ( $\epsilon_{Nd}(t)$  values range from -1.2 to +0.2) than the granitoids of the 1.89-1.88 Ga group ( $\epsilon_{Nd}(t)$  values -0.9 to +1.2). Comparison of the initial Nd isotopic composition of the 1.87 Ga granitoids to those of the 1.65-1.54 Ga rapakivi granites ( $\epsilon_{Nd}(t)$  c. -1 to -3) indicates, in terms of Nd isotopes, a roughly similar Paleoproterozoic source for the two groups.

The 1.65-1.54 Ga rapakivi granites have been interpreted as the results of vapor-absent melting of an intermediate to acid metaigneous protolith in the lower parts of the cratonized Svecofennian crust. The anatexis probably commenced in response to partial melting in the upper mantle and subsequent mafic underplating, resulting in the emplacement of the rapakivi granites and related mafic rocks in an extensional tectonic setting. The similarities between the 1.87 Ga granitoids and the rapakivi granites suggest that conditions for magmatism in an extensional regime were attained shortly after the 1.89-1.88 Ga synorogenic stage in the southern part of CFGC.

**Midcrustal Pluton Emplacement  
in a Contractional Setting:  
c. 1400 Ma Synkinematic Granites  
of the Southwestern United States**

Nyman, M.W. and Karlstrom, K.E.  
*Department of Earth and Planetary Sciences,  
University of New Mexico,  
Albuquerque, NM 87131, USA*

From a 3-D strain perspective, the "room problem" for syntectonic pluton emplacement is easily solved since any contractional deformation will involve local extension. Recognition of the importance of local extension in contractional settings has been utilized to explain pluton emplacement in transpressional settings, along fault ramps and during reactivation of crustal anisotropies. In some cases, processes such as magma wedging at pressures exceeding mean normal stresses may be required to overcome wall-rock stress during pluton emplacement.

In this paper we present data describing variation of emplacement mechanisms for midcrustal Mesoproterozoic "anorogenic" granite plutons in southwestern U.S. which exemplify the role of local extension within a contractional tectonic setting. Mesoproterozoic magmatic activity from 1500-1300 Ma resulted in emplacement of igneous complexes along the southern margin of Laurentia. In southwestern U.S. this event is marked by emplacement of midcrustal (2-4 kbar) granitic plutons. Previous workers have referred to this event as "anorogenic" citing lack of significant deformation and metamorphism. However, detailed kinematic, structural and metamorphic studies of plutons in AZ and NM indicate that many of these plutons record locally significant deformation and metamorphism. Synmagmatic and high temperature kinematic and structural features associated with widely separate 1400 Ma plutons record a consistent kinematic framework involving contraction, not bulk crustal thinning and extension as implied by earlier models. These plutons and aureoles, therefore, provide a midcrustal record of emplacement mechanisms inboard of a contractional margin.

Although kinematic and structural features are all consistent with northwest-southeast contraction, processes of pluton emplacement for Mesoproterozoic plutons vary across the orogen. In NM, the 1420 Ma Sandia pluton consists of a 5-7 km thick series of northwest-dipping granite sheets which are subparallel with a 1-2 km wide extensional shear zone at the base of the pluton. Fabrics

in the northwest aureole are both cut by the pluton and reactivated during high temperature contact metamorphism. Kinematic and structural data in the pluton and wall rocks are consistent with a 3-D strain field involving subhorizontal southeast-northwest contraction and north-south local extension, which facilitated pluton emplacement. The presence of evolved phases of the Sandia granite within the extensional shear zone attests to the interaction between shear zone deformation and pluton emplacement.

In central AZ, emplacement of 1420 Ma plutons was facilitated by Paleoproterozoic structures, some of which show reactivation during pluton emplacement. The Signal batholith is cut by a northeast-striking contractional shear zone that is parallel with magmatic foliations and moderately southeast-dipping Paleoproterozoic fabrics. Melt-filled shear bands, transition from magmatic to solid state foliation and high temperature K-feldspar microstructures indicate synmagmatic to high temperature deformation. Kinematic elements record southeast-northwest shortening during pluton emplacement. Southeast-directed extensional movement is also recorded along shallow dipping melt-filled shear zones which are both contemporaneous with and postdate contraction. In contrast to the Signal batholith, the Lawler Peak granite has an intrusive contact with only minor evidence for solid state deformation along the western margin. Stringers of Lawler Peak granite intrude parallel to country rock foliation and show varying degrees of boudinage and folding. Magmatic foliation dips steeply and parallel to the Mountain Springs fault, a Paleoproterozoic fault with a component of sinistral strike-slip movement. Orientation of dikes, shear bands in deformed granite and structures and kinematic features in the aureole are consistent with northwest-southeast contraction. The contrast in deformation behavior between the Signal batholith and Lawler Peak granite may reflect preferential synmagmatic reactivation of shallow dipping older fabrics adjacent to the Signal batholith whereas the bulk of strain around the Lawler Peak granite was partitioned into soft wall rocks and along the Mountain Springs fault. Synmagmatic sinistral strike-slip movement along the Mountain Springs fault may have facilitated accumulation of the Lawler Peak granite, consistent with a northeast-southwest extensional component during southeast-northwest contraction.

## Mesozoic-Miocene Granitoid Evolution and Petrogenesis in Southern Chile

<sup>1</sup>Pankhurst, R.J., <sup>2</sup>Weaver, S.D.  
and <sup>3</sup>Herve, F.

<sup>1</sup>*British Antarctic Survey, High Cross,  
Madingley Road, Cambridge CB3 0ET, UK*

<sup>2</sup>*University of Canterbury, Christchurch, New Zealand*

<sup>3</sup>*Universidad de Chile, Santiago, Chile*

The main Cordilleran batholith of Northern Patagonia (44-47°S) consists of Cretaceous granodiorites and leucogranites (90-125 Ma) of typical Andino-type ( $(^{87}\text{Sr}/^{86}\text{Sr})_i = 0.7040 - 0.7045$ ). To the west of this, there is a more extended intrusion history in the Chonos Archipelago. Here, early Cretaceous (125-130 Ma) quartz-rich granites with  $(^{87}\text{Sr}/^{86}\text{Sr})_i$  ratios were emplaced directly into the Palaeozoic-Mesozoic fore-arc accretionary complex. Plutonism then switched to the Cordilleran belt, but subsequently moved back into the archipelago in Eocene (c. 40 Ma) times. Both Early (c. 20 Ma) and Late (c. 10 Ma) Miocene granitoids are closely associated with the Liquine-Ofqui strike-slip fault zone, where small bodies crop out between and around the main branches of the fault. Late Miocene stocks also occur sporadically throughout the Cordilleran belt.

The Miocene rocks are tonalitic to granitic and have major element compositions typical of calc-alkaline I-types; they are strikingly similar to the Cretaceous subduction-related granitoids. At given  $\text{SiO}_2$ , the Miocene rocks tend to have slightly higher Ti,  $\text{Fe}^{3+}$ , P, Na, Zr and K/Rb, but lower Rb. However, they are much more primitive in terms of isotopes, with  $(^{87}\text{Sr}/^{86}\text{Sr})_i$  of 0.7034 - 0.7041 and  $\epsilon_{\text{Nd}}$  of +2.6 to +5.9. These values are similar to those exhibited by Southern Volcanic Zone volcanic rocks and the Miocene granitoids are seen as the first expression of the present subduction-related magmatic regime, which began with a significant switch in the plate convergence angle c. 25 Ma ago. They were most probably generated by remelting of early Tertiary basaltic lavas within the crust - the absence of Yb- and HREE-depletion characteristics indicates that garnet was not involved in their petrogenesis.

The close chemical and lithological comparability between the Miocene and earlier granitoids requires that they were generated by essentially similar processes, i.e. remelting of mafic material within the crust. There is no clear evidence that upper crustal contamination of primitive

magmas was a significant factor. The more evolved isotopic character of the Cordilleran granitoids thus requires that their mafic sources included some that were isotopically mature, and depleted- mantle Nd model ages suggest that mafic crust as old as 1500 Ma was involved.

## ORAL PRESENTATION

### Pluton Emplacement in Arcs: A Crustal-Scale Recycling Process

<sup>1</sup>Paterson, Scott, R., <sup>1</sup>Fowler, T. Kenneth, Jr.  
and <sup>2</sup>Miller, Robert B.

<sup>1</sup>*Department of Earth Sciences,  
University of Southern California,  
Los Angeles, CA 90089, USA*

<sup>2</sup>*Department of Geology, San Jose State University,  
San Jose, CA 95192, USA*

During magma ascent and emplacement, crust must be displaced at a rate equal to the growth or ascent of the magma chamber, emphasizing the mechanically linked nature of this system. We predict that in the county rock multiple material transfer processes (MTPs) will operate during magma chamber growth given the large horizontal, vertical, and temporal gradients in physical conditions. Thus our research has attempted to determine the importance of various MTPs, and whether MTPs largely transport material vertically or horizontally, rather than determine a single model of ascent or emplacement.

We have now mapped partially preserved roofs of 10 plutons with emplacement depths of 2 to 10 km and country rock hosts of plutonic rock, weakly metamorphosed clastic, calcsilicate, carbonate, and volcanic rock, and amphibolite-grade schist and gneiss. During emplacement, these roofs were not, in general, ductilely deformed, detached or extended by faults, or significantly uplifted. Instead, sharp, irregular, discordant contacts are the rule with stoped blocks often preserved immediately below the roof, even in the deeper plutons. Upper portions of these magma chambers are varied, sometimes preserving crests of more evolved magmas or local volatile-rich phases and sometimes complex zones of diking and magma mingling. Magmatic foliations also display a wide variety of patterns and consistently are associated with evidence that they formed after emplacement.

In a few cases we have been able to map roof-wall transitions. At shallow crustal levels steep wall contacts have sharp, discordant, stepped contacts, and sometimes nearby stoped blocks. Around some plutons, a relatively abrupt transition (sometimes within 100s of meters) occurs from discordant, brittle roofs to moderately concordant, ductilely deformed walls with narrow aureoles. We have not found brittle or ductile faults at roof-wall joins. Aureole width and ductile strains in aureoles increase slightly with depth. Igneous layering and magmatic foliations/lineations are common near these wall contacts.

Around shallow to mid-crustal, steep wall contacts (5 to 15 km), deflections of pre-emplacment markers (*e.g.*, bedding, faults, dikes) and ductile strains in narrow aureoles (0.1 to 0.3 body radii) give a complete range of bulk shortening values from 0% to 100% of needed space, but average around 30%, or less, particularly for larger plutons and batholiths. Lack of far-field deflection of these same markers rules out significant horizontal displacement outside the aureoles and requires that any near-field lateral shortening is translated into vertical flow. Lateral variations from ductile to brittle MTPs are sometimes observed, but are difficult to decipher in the outer parts of aureoles. Compositional zoning is common within magma bodies, although this zoning commonly reflects separately evolved pulses that traveled up the same magma plumbing system. Magmatic foliations and lineations largely form after emplacement and reflect strain caused by late magma flow and regional deformation.

Wall rocks near mid- to deep-crustal walls (10-25 km) are extensively deformed, with locally discordant contacts, but the distinction between regional and emplacement-related deformation is less clear. Internal sheeting is increasingly common in these plutons, although elliptical masses are still present. Lateral compositional variations are as large as vertical variations at shallower depths and occur over shorter distances. Magmatic foliations and lineations often reflect regional deformation.

The lack of evidence for horizontal displacement outside the narrow, shallow to mid-crustal aureoles and the lack of lateral or upwards displacement of pluton roofs indicate that during emplacement most country rock is transported downwards in the region now occupied by the magma body and its aureole. The internal sheeting and zoning indicates that during downwards flow of country rock, multiple pulses of magma traveled up the same magma system. Thus, if these relationships are widespread in arcs, then magma emplacement in arcs is the driving mechanism of a crustal-scale recycling process.

## ORAL PRESENTATION

### Effects of Pressure, H<sub>2</sub>O Activity, and Fe/Mg Ratio on the Compositions of Anatectic Melts

<sup>1</sup>Patiño Douce, Alberto E.  
and <sup>2</sup>Beard, James S.

<sup>1</sup>*Department of Geology, University of Georgia,  
Athens, GA 30602, USA*

<sup>2</sup>*Virginia Museum of Natural History,  
Martinsville, VA 24112, USA*

New melting experiments on crustal protoliths (including some with varying amounts of added H<sub>2</sub>O), coupled to a synthesis of previous experimental results, allow us to derive general conclusions about the effects of  $P$ ,  $T$ ,  $a_{\text{H}_2\text{O}}$ , Fe/Mg ratio, and  $f_{\text{O}_2}$  on melting relations and melt compositions during crustal anatexis.

Orthopyroxene and garnet are two of the chief mafic residual phases formed by incongruent melting of biotite-rich protoliths (cordierite becomes important at lower  $P$  and/or in compositions more magnesian than those discussed here). Crystallization of either garnet or orthopyroxene affects the compositions of coexisting melts, and is controlled by several factors besides the obvious one of Al<sub>2</sub>O<sub>3</sub> activity. Thus, in the assemblage biotite + plagioclase + quartz (with no added H<sub>2</sub>O, and at  $f_{\text{O}_2} \leq \text{QFM}$ ) increasing Fe/Mg ratio at constant  $T$  and  $P$ , and increasing  $P$  at constant  $T$  and Fe/Mg, cause garnet to join orthopyroxene in the restitic assemblage, and eventually to replace it entirely as the dominant residual mafic phase. Al and Ca required for garnet crystallization are provided by incongruent breakdown of plagioclase. This in turn raises the Na/K ratio of the melt but has only a minor effect on its SiO<sub>2</sub> content. Increasing  $f_{\text{O}_2}$  suppresses both mafic silicates phases in favor of magnetite, but the effect is stronger on garnet. For example, in an Fe-rich model graywacke at 850°C and 5 kbar, garnet disappears between QFM and Ni-NiO, whereas orthopyroxene is present at  $f_{\text{O}_2} \geq \text{Ni-NiO}$ . Differences in  $f_{\text{O}_2}$  within  $\pm 2$ -3 orders of magnitude of the QFM buffer have only slight effects on melt compositions and melting temperatures, but can have stronger effects on restite assemblages, and hence on trace element characteristics of the melts.

H<sub>2</sub>O-poor melts formed by dehydration-melting of biotite + plagioclase + quartz at  $f_{\text{O}_2} \leq \text{QFM}$ , whether saturated with orthopyroxene or garnet, have SiO<sub>2</sub> > 70

wt % up to  $T$  of at least 1000°C. However, FeO and MgO contents of melts saturated with orthopyroxene + quartz increase more strongly with  $T$  than those of melts saturated with garnet + aluminosilicate + quartz. At constant  $T$  (and  $f_{O_2} \leq QFM$ ), FeO concentrations in silicic melts saturated with either orthopyroxene or garnet ( $\pm$  aluminosilicate) vary inversely with  $P$  and directly with  $a_{H_2O}$ . These relationships are also true in amphibolite-derived melts saturated with orthopyroxene + clinopyroxene. If bulk  $H_2O$  content is fixed (*e.g.*, in the case of dehydration melting), then  $a_{H_2O}$  at constant melt fraction decreases with increasing  $P$ . The effects of  $P$  and  $a_{H_2O}$  on mafic phase saturation act together to cause all dehydration melts to become more leucocratic with increasing  $P$ .

Increasing  $a_{H_2O}$  at constant  $T$  and  $P$  favors congruent dissolution of plagioclase + quartz, which raises both the Na/K and Ca/K ratios of the melt and, depending on the bulk composition of the protolith, may either raise or lower the melt  $SiO_2$  content. Isothermal Ca/Na partitioning between plagioclase and melt is sensitive to both  $P$  and  $a_{H_2O}$ . Increasing  $a_{H_2O}$  at constant  $P$  and  $T$  causes the Ca/Na ratio of melt to decrease relative to that of coexisting plagioclase. Increasing  $P$  at constant  $a_{H_2O}$  and  $T$  has the opposite effect; plagioclase becomes more sodic relative to coexisting melt.

Fe/Mg partitioning between garnet and melt, and between biotite and melt, are strong functions of both  $P$  and  $T$  and, in the case of biotite, insensitive to  $f_{O_2}$ . Our results confirm those of previous workers (Green, 1977; Ellis, 1986) that garnet-melt Fe/Mg partitioning reverses at magmatic temperatures, and the same is also probably true of biotite-melt Fe/Mg partitioning. In contrast, orthopyroxene-melt and clinopyroxene-melt Fe/Mg partitioning appear to be rather insensitive to  $P$  and  $T$ .

These results show that there is no exclusive explanation for the series tonalite-granodiorite-granite. Different magma compositions within this spectrum may reflect different melting temperatures, different source compositions (perhaps differing only in Fe/Mg ratio), different  $H_2O$  activities, or any combination of these factors. For example, melting of a biotite- and plagioclase-rich gneiss (metagraywacke?) at high  $P$  and  $a_{H_2O}$  could produce a granodiorite or tonalite melt and a garnet pyroxenite residue, whereas  $H_2O$ -starved dehydration-melting of the same rock at lower  $P$  would produce a granite melt and a pyroxene granulite (noritic?) residue.

Ellis, D.J., 1986. Garnet-liquid Fe-Mg equilibria and implications for the beginning of melting in the crust and subduction zones. *Am. J. Sci.*, **286**, 765-791.

Green, T.H., 1977. Garnet in silicate liquids and its possible use as a  $P$ - $T$  indicator. *Contrib. Mineral. Petrol.*, **34**, 59-67.

## Recognition and Significance of Mixing in Granites

Pembroke, J.W. and D'Lemos, R.S.

*Geology and Cartography Division,  
Oxford Brookes University, Oxford OX3 0BP, UK*

Models in which plutons are emplaced during extensional space creation require the quasi-continuous injection of magma batches through time as the pluton develops. Evidence for the repeated addition of magmas should therefore be widespread in granites. Sheeted (dike) architectures would only develop if resident magma had largely solidified prior to subsequent injections. Magma addition prior to extensive crystallization would result in mingling and mixing. Some evidence for this style of sequential magma addition is clearly demonstrated by mafic synplutonic dykes and mafic enclaves in granites, where contrasting mineralogies and colors, and large initial thermal contrasts, render features both striking and permanent. However, apart from where obvious internal contacts occur, or gross variations in mode or texture exist, granite plutons are often perceived as homogeneous. Detailed observations of granites from numerous localities reveal subtle heterogeneities and disequilibrium features on a mineral to pluton scale. These features indicate to us that mixing of intruding and resident granite magma within evolving plutons may be a widespread but often overlooked phenomenon due the subtlety of the evidence. We present data from three well exposed case studies in Scotland and the Channel Islands (UK) and from Newfoundland.

Heterogeneities within plutons picked out at outcrop scale range from abrupt boundaries to diffuse, transitional zones defined by gradual changes in mode or texture. These boundaries record intrusive contacts between original magma pulses which have been variably overprinted by post-intrusive processes although some may represent the result of in-situ crystallization processes (*e.g.* crystallization fronts). Plutons examined also exhibit subtle modal heterogeneity on the scale of mms to tens of metres.

Modelling of phase distributions using spatial analysis (SPANS) and Geographic Information System (GIS) software has enabled quantification of heterogeneity. Digitised data for given phases are divided into areas of attraction or cells to create a "voronoi" map.

A simple entropy equation (Shannon Formula) using the relative proportions of each cell provides a numerical expression of the phase distribution. These data allow direct comparison of heterogeneity at different localities or in different samples. Such modelling should enable differentiation between heterogeneities which result from incomplete mixing from those that result from random crystallization processes. Textural heterogeneity, where the same mineral phases exhibit contrasting textural features over short distances, often within the same thin section, is commonly observed. For example, the coexistence of contrasting zonation patterns in plagioclases, or the presence of both phenocrystic and interstitial quartz or alkali feldspar within a single thin section are difficult to reconcile with standard crystallization models and it is more probable that the grains grew at different times and/or in places.

Many, if not most, granites exhibit mineralogical and textural disequilibria. Rapakivi feldspar, cellular feldspars, truncation of growth zoning, acicular apatite, skeletal biotite, embayments and a variety of overgrowths, have been widely reported where magma mixing has been demonstrated (*e.g.* in association with mafic enclaves). However, we have found such obvious disequilibrium textures, and many more subtle features, widely in granites even where there is no mineralogical or geochemical evidence for local mixing with mafic magma, suggesting that mixing between differing granitic magmas has taken place. Interaction between granitic magmas with even small differences in temperature and melt composition can result in a shift from equilibrium conditions and resultant rapid growth, non-growth or resorption features. However, because thermal and chemical differences between the coexisting magmas are small, and subsequent cooling prolonged, the features are not visually striking.

Our field and petrographic observations indicate widespread, albeit subtle, heterogeneity and disequilibrium in granites. While recognising that certain features can result from several processes (*e.g.* in-situ progressive crystallization) we would interpret many as having resulted from mixing between coexisting batches of granite magma during pluton assembly.

## ORAL PRESENTATION

### Granite Ascent: Dykes or Diapirs?

Petford, Nick

*School of Geological Sciences, Kingston University,  
Kingston-Upon-Thames, Surrey KT1 2EE, UK*

Until the last few years, diapirism reigned supreme among granitoid ascent mechanisms. Granitoid masses in a variety of material states, from pure melt through semi-molten crystal mushes to solid rock, were believed to have risen forcefully through the continental crust to their final emplacement levels in a way analogous to salt domes. The structural analogy between granite plutons and salt diapirs, which gained acceptance in the 1930s (Wegmann, 1930) has clearly been an attractive one. Unfortunately, on closer inspection such comparative reasoning appears deeply flawed. Nonetheless the belief in diapiric ascent of granitoid magmas still persists, despite the pessimistic outcomes of thermal models and, at best, ambiguous field evidence. Until very recently, dyke ascent due to active fracture propagation (Clemens and Mawer, 1992), or more passive fault-fracture exploitation (Petford *et al.*, 1993), was dismissed on the grounds that granitic melts were too viscous (due mainly to low intrinsic temperatures and high crystal contents) for dyke-controlled ascent to occur (*eg.* Miller *et al.*, 1988). However, field evidence for the fluidity of granitoid melts is common, and the rejection of dyke transport mechanisms appears to have been based more on received wisdom than hard fact. The realisation that granitic melts generally have viscosities in the range  $10^5$ - $10^7$  Pa s effectively opened the way for the development of dyke ascent models.

Thermal and fluid dynamical models for dyke transport of granitoid magmas have a number of important implications for the geochemistry and emplacement of granites that have yet to be fully explored. For example, rapid ascent rates of  $\sim 10^{-2}$  m s<sup>-1</sup> predicted for granite melts in dykes (*cf.*  $\sim$  m yr<sup>-1</sup> for diapirs) means that granitoid melts may rise adiabatically from their source regions. As a consequence, any restite material present initially in the ascending melt will most probably be resorbed. Thermal balance calculations suggest that adiabatic ascent with a pressure drop of  $\sim 10$  kbar will produce enough heat to resorb approximately 30 wt % restite.

The ascending melts will have little time to assimilate country rock during ascent, and if source extraction is sufficiently rapid, significant magmatic contamination may

occur only at the site of emplacement. However, as predicted pluton filling rates (c.  $10^2$ - $10^4$  years) are orders of magnitude faster than estimated fault opening rates based on plate tectonic motions (Paterson and Tobisch, 1992), there is serious doubt as to whether space can be made fast enough to accommodate large, upper crustal granitic magma "chambers". An important future goal is to reconcile these differences in ascent and emplacement rates with time scales for melt segregation at source. The trinity of ascent, segregation and emplacement still remain to be united.

- Clemens, J.D. and Mawer, C.K., 1992. Granitic magma transport by fracture propagation. *Tectonophysics*, **204**, 339-360.
- Miller, C.F., Watson, E.B. and Harrison, M.T., 1988. Perspectives on the source, segregation and transport of granitoid magmas. *Trans. Royal Soc. Edinburgh: Earth Sci.*, **79**, 135-156.
- Paterson, S.R. and Tobisch, O.T., 1992. Rates of processes in magmatic arcs: implications for the timing and nature of pluton emplacement. *J. Struct. Geol.*, **14**, 291-300.
- Petford, N., Kerr, R.C. and Lister, J.R., 1993. Dyke transport of granitoid magmas. *Geology*, **21**, 845-848.
- Wegmann, C.E., 1930. Über Diapirismus. (Besonders im Grundgebirge). *Bull. Comm. Geol. Finlande*, **92**, 58-76.

### Metal Partitioning from Melts into Vapor and Vapor/Brine Mixtures in Shallow Granitic Systems

Piccoli, Philip M. and Candela, Philip A.  
*Laboratory for Mineral Deposits Research,  
Department of Geology, University of Maryland  
at College Park, MD 20742-4211, USA*

Experimental and computational studies of element partitioning between granitic melts and vapor and vapor±brine are important in our understanding of the mass transfer that occurs in and around crystallizing plutons. Experimental studies provide the necessary data on the equilibria that control melt-vapor and melt-vapor-brine compositions. Theoretical modeling suggests factors that maximize the probability of metal removal from granitic melts, and can also suggest specific tools for evaluating magmatic-hydrothermal ore potential.

We have written an algorithm, MVP (Magmatic Volatile Phases), which can be used to calculate the composition of the magmatic volatile phase(s), vapor or vapor+brine, that are expelled isobarically from granitic

(s.l.) magmas. This phenomenon of crystallization-driven volatile exsolution in plutonic environments has been referred to as second boiling (e.g. Bowen, 1928). Rather than perform simple mass-balance calculations for each element individually, MVP considers the *simultaneous* equilibria (among melt, crystals, and volatile phases including brine) that must be accounted for to model the efficiencies with which ore-metals are removed from magmas into the volatile phases. Briefly, this algorithm calculates the partitioning of elements between melt and volatile phase(s) accounting for crystal-melt partitioning both before and after volatile saturation. Implicitly, the melt composition is modelled as "near minimum", and does not change in major element composition with crystallization. Crystallization is modelled *implicitly* through the use of bulk crystal/melt partition coefficients (D) for each element; Ds are treated as constants throughout magma evolution for most elements. Once the composition of the melt is calculated at volatile saturation (which is equivalent to water saturation in this algorithm: saturation with a CO<sub>2</sub>-free vapor, or a CO<sub>2</sub>-free vapor + brine mixture can be modelled), the composition of successive aliquots of vapor, or vapor+brine can be calculated, until the volatile-saturated melt has crystallized. Both the initial and saturation water concentration (which is a function of pressure) can be set as input parameters. Sufficient data *do not* exist yet for the composition of the brine to be calculated with great accuracy; however, until such data are procured, we believe that our results represent the most rigorous treatment possible at this time, and are illustrative of the effects of brine saturation. The algorithm routinely considers Cu, Mn, Zn, Ca, Mg, Yb, Ce, K, Na, Eu, H (chloride complexed), and Mo, W, and B (non-chloride complexed), and can easily be modified for other elements for which partitioning behavior has been experimentally defined (e.g. Sn<sup>2+</sup>, Sn<sup>4+</sup>, Li, Be, Rb, Sr, Cs, Ba, U, Th and other REE: see Candela and Piccoli, 1995).

The importance of chloride in granite-volatile systems (melt±vapor±brine) has been discussed elsewhere (e.g. Candela and Piccoli, 1995). Phase rule constraints limit the variability in the Cl concentration in melts saturated with both vapor and brine at a given temperature and pressure. Variations in temperature and pressure during vapor+brine saturation are rather restricted, and variations in the Cl concentration of the associated melt phase are apt to be small. For a system of a given major-element composition, the Cl concentration of the coexisting melt, vapor, and brine will be a function of temperature and

pressure only, and will not allow the free variation of an element, as in, *e.g.*, Rayleigh fractionation. Rayleigh fractionation *requires* a system with a variance greater than zero.

Results of this model suggest the following: 1) The probability of mineralization with respect to Cl-complexed ore-metals increases with increasing Cl/H<sub>2</sub>O of the associated magma. As brine can form at relatively at low magmatic Cl/H<sub>2</sub>O, the presence of brine ± vapor-rich inclusions *alone* is not a good indicator of high Cl/H<sub>2</sub>O of the initial melt. The efficiency of removal of metals from a magma into exsolving volatile phases is a function of both the Cl/H<sub>2</sub>O ratio of the magma, and the extent to which the metals are taken up by crystallizing phases. For melts with low initial Cl/H<sub>2</sub>O ratios (0.01), brine saturation occurs relatively late if at all, and overall efficiencies of removal of chloride-complexed metals is low. 2) The Cl/H<sub>2</sub>O ratio in the melt is fixed at a given temperature and pressure when the system is saturated with respect to vapor and brine; further, the *ratio* of vapor to brine, and the composition of these phases remains constant throughout volatile exsolution. The concentration of unbuffered trace elements may vary in the system, and may follow Rayleigh-type fractionation patterns, whereas Cl cannot. Therefore, changes in magmatic Cl concentrations are not necessary consequences of crystal fractionation, even at low pressures. 3) At a given pressure of emplacement, the initial water concentration will determine the timing of volatile saturation. Initial water concentrations can be related to the timing of saturation of a magma with respect to a water-rich phase whether or not the melt is CO<sub>2</sub>-bearing. Other factors, suggested by quantitative modeling, that may increase Cu partitioning into "ore fluids" are: higher  $f_{O_2}$  in mt-saturated systems because of both the destabilization of magmatic sulfides, and the suppression of aqueous FeCl<sub>2</sub>; lower ASI in the melt (for metaluminous to peraluminous compositions) because hydrogen competes with other cations for chloride, and also increases FeCl<sub>2</sub> in mt-saturated systems; and lower Na<sub>2</sub>O and K<sub>2</sub>O in the melt (at a given melt ASI), because of competition for chloride in the volatile phases.

Bowen, N.L., 1928. *The Evolution of Igneous Rocks*. Dover Publications, Inc., New York.

Candela, P.A. and Piccoli, P.M., 1995. Model ore-metal partitioning from melts into vapor and vapor/brine mixtures. In Thompson, J.J.F. (ed), *Granites, Fluids, and Ore Deposits*, Geological Association of Canada Short Course Volume 23, 101-127.

## ORAL PRESENTATION

### Control of Redox State and Sr Isotopic Composition of Magmas: Source or Processes?

Pichavant, M. and Hammouda, T.

*Centre de Recherche sur la Synthèse et la Chimie des Minéraux, CNRS, 1A rue de la Férollerie, 45071 Orléans Cedex 02, France*

That granitic magmas reflect their source regions is now used as a basic underlying assumption in most geochemical studies, and has proven useful in rationalizing many characteristics of granitic rocks. However, the mechanisms by which source rocks control the intensive and compositional parameters of the magmas remain poorly known. In addition, processes that occur at the level of crystallization of the magmas (fractionation, degassing, ...) may modify the geochemical characteristics acquired in the source region. Here, we use recent experimental data obtained at Orléans to challenge the "source rock model" and discuss control of 1) redox states, and 2) Sr isotopic compositions of granitic magmas.

*Redox state.* It has been suggested that the redox state of granitic magmas is controlled by that of the rocks in the source region. However, several other studies have demonstrated that shallow level processes such as degassing or diffusive loss of H<sub>2</sub> can lead to a marked oxidation of the magmas. Experimental studies have been performed in parallel on biotite-muscovite (Manaslu) and tourmaline-muscovite (Gangotri) leucogranites from the High Himalayas. Results under reducing conditions ( $\log f_{O_2} = \text{FMQ} - 0.5$ ) at 4 kbar and variable  $a_{H_2O}$  show that biotite is a near liquidus phase in both magmas. Yet, biotite is nearly absent (except in cores of tourmaline crystals) and reacted out at some stage of evolution of the Gangotri magma. The latter granite is characterized by bulk rock Fe<sub>2</sub>O<sub>3</sub> /FeO values much higher (1.9) than the Manaslu granite (0.2). These results suggest that the Gangotri granite evolved under progressively more oxidizing conditions during crystallization, up to  $f_{O_2}$  values more than 3 log units above the FMQ buffer. Fe<sub>2</sub>O<sub>3</sub> can be efficiently incorporated in muscovite and also possibly in tourmaline. Their crystallization (and also the crystallization of magmatic cassiterite) could be used as mineralogical indications of a magmatic oxidation process. Leucogranite magmas thus provide evidence of a control of redox conditions by

shallow level processes rather than by their source regions. These processes may obliterate the geochemical signature acquired at the source level.

*Sr isotopic composition of partial melts.* Experiments were designed to test mechanisms of isotopic equilibration of Sr during partial melting of a model crustal assemblage made of synthetic mica doped in Sr ( $^{87}\text{Sr}/^{86}\text{Sr} = 4.0$ ) and natural plagioclase ( $^{87}\text{Sr}/^{86}\text{Sr} = 0.70$ ). Glasses and crystals (residual mica and plagioclase, newly-formed plagioclase) were analysed for Sr isotopes and concentrations using an ion microprobe. The Sr data were obtained for experimental conditions corresponding to melting above the critical temperature, *i.e.*, when melting is kinetically controlled by atomic diffusion in the liquid. The experimental liquids are chemically and isotopically zoned as long as the two starting minerals persist in the charge. The residual solids always keep their starting Sr concentration and isotopic composition unchanged. Therefore, Sr in the liquid is controlled by the proportion of phases participating to the melting reaction. Because of the faster melting rate of mica compared to plagioclase, early liquids are characterized by elevated  $^{87}\text{Sr}/^{86}\text{Sr}$  and evolve progressively with time toward lower values of  $^{87}\text{Sr}/^{86}\text{Sr}$ . However, the Sr isotopic composition of the liquid is always higher than that of the bulk starting assemblage, implying that isotopic disequilibrium persists between liquid and residual minerals in the experiments. Under our experimental conditions (*i.e.*, above the critical temperature), crystal dissolution is faster than liquid-crystal equilibration, assumed to be controlled by diffusion in the crystals. For example, total equilibration of Sr isotopes by diffusion between melt and a plagioclase of 1 mm in size would require  $10^4$  years at  $900^\circ\text{C}$ . Such time-scales are in the same range as crustal melting episodes (heat provided by mafic magmas) and processes of magma segregation, extraction and ascent (dikes). In the case of source rocks not previously homogenized during an earlier metamorphic event, partial melts (if formed above the critical temperature) may not necessarily reflect the Sr isotopic composition of source rocks if magma ascent takes place before liquid-crystal homogenization has occurred in the source region.

## ORAL PRESENTATION

### Trace Element and Isotopic Exchange During Acid-Basic Magma Interaction

<sup>1</sup>Poli, G., <sup>2</sup>Davies, G.R. and <sup>2</sup>Tommasini, S.

<sup>1</sup>*Department of Earth Sciences, Perugia, Italy*

<sup>2</sup>*Faculteit der Aardwetenschappen, Vrije Universiteit, Amsterdam, The Netherlands*

Physico-chemical interactions between acid and basic magmas produce diverse magma types and the process is now becoming accepted as an important mechanism in the genesis of composite batholiths. We report studies from two plutonic environments, Elba and Sardinia (Italy), designed to constrain the principal physical processes that control the chemical compositions of mixed lithologies.

The Sardinia-Corsica Batholith is petrologically variable with granodiorite-monzogranite as the dominant lithologies. Gabbroic complexes occur throughout the batholith. Most granitoid lithologies contain evidence of mixing which is manifested by the presence of clots of mafic minerals ( $\sim 0.01$  m), mafic microgranular enclaves (MME,  $< 1$  m) and basic septa (BS,  $> 1$  m). MME often comprise 3-5% of surface outcrop. Interdigitating contacts between the BS and granites indicate that basic and acid magmas were liquid at the same time. Chemical compositions of gabbroic complexes in the batholith indicate formation by amphibole + clinopyroxene + plagioclase fractionation and accumulation. In contrast the centers of the BS have not undergone cumulus processes and probably represent liquids that were parental to the gabbroic complexes. The major and trace element contents of MME with "tonalitic" compositions can be modelled in terms of a process that involves granite contamination and fractional crystallization of amphibole + biotite + plagioclase + apatite and subordinate amounts of titanite and zircon ( $r = 0.3$  in AFC model). MME with "gabbroic" compositions and the margins of the BS have a cumulate geochemical signature. These rocks appear to have lost a liquid phase during crystallization (filter pressing) while undergoing fractional crystallization and assimilation.

Together these field and geochemical observations establish that mixing has involved three physical processes: 1) mechanical magma mingling of basaltic and granitic magmas - this process occurs when there are large temperature and viscosity contrasts between the magmas at an early stage of interaction; 2) contamination of basaltic magmas by granitic magmas (AFC): this process produces

an evolved "basaltic" magma that is thermally equilibrated with the granitic magma; and, 3) filter pressing of residual liquids from the evolved "basaltic" magma: this process may lead to mixing between the evolved "basaltic" liquid and granitic magmas.

In order to better constrain how the above processes work and assess the possible role of diffusive processes in mixing systems we are undertaking a study of a young plutonic system on the island of Elba (Tuscany, Italy). Due to the 6 Ma age of the granitoids, insignificant age correction is required for Sr-Pb-Nd isotopes, hence relatively small isotope variations can be studied. We have sampled a 0.8 m profile across an enclave (0.5m) and host granite and then determined the Sr-Pb isotope composition of plagioclase, K-feldspar and biotite (Nd isotope analyses in progress). At temperatures of *c.* 800°C the Sr isotope diffusion in plagioclase feldspar is relatively slow ( $< 10^{-15} \text{ cm}^2 \text{ s}^{-1}$ ) so that plagioclase may retain the Sr isotope composition of the magma from which they crystallized. In contrast K-feldspar and biotite have diffusion coefficients that are orders of magnitude faster. Consequently these phases will undergo significantly greater degrees of diffusive exchange with any enclosing magma during crystallization and cooling. The Sr and Pb isotope ratios of plagioclase feldspars from the centre of the enclave ( $^{87}\text{Sr}/^{86}\text{Sr} = 0.7116$ ,  $^{208}\text{Pb}/^{204}\text{Pb} = 38.96$ ) are distinct from the granite ( $^{87}\text{Sr}/^{86}\text{Sr} = 0.715$ ,  $^{208}\text{Pb}/^{204}\text{Pb} = 38.89$ ). Plagioclase from the margin of the enclave have isotopic ratios intermediate between the granite and the centre of the enclave. Sr-Pb isotope ratios of the biotite and K-feldspar record smaller isotope differences.

From these preliminary results we conclude that the Sr-Nd-Pb isotope composition of whole rock samples from mixed magmas cannot be used to constrain the extent of bulk mixing during magma interaction. The different diffusion coefficients for Sr-Nd-Pb in each mineral that form a mixed rock is liable to result in different isotopic compositions. Each mineral will therefore have different isotopic ratios and the whole rock isotopic composition will be controlled by the rock mineralogy not the physical extent of magma interaction. Therefore to examine the nature of mixing processes isotopic analyses must be performed on minerals and the effects of diffusion modelled in detail.

## Discordant Cores in Zircons and Granite Genesis

Pupin, Jean-Pierre

*Z.I.R.C., Laboratoire de Pétrologie-Minéralogie,  
Institut de Géologie, Faculté des Sciences,  
Parc Valrose, F-06108 Nice Cedex 2, France  
(and URA CNRS 17-63)*

In magmatic rocks, zircon morphology (morphological or typologic diagram - Pupin 1976, 1980) gives the chronological argument (order of appearance of successive morphological subtypes in a single complete zircon population during a more or less long crystallization period over the magmatic history of the host-rock). The main factors that seem to influence the prismatic and pyramidal relative rate of growth of the crystals are yet considered to be temperature, aluminium-alkali antagonism and more indirectly activity of H<sub>2</sub>O in the magma. This last influences compatible or incompatible behaviour of Zr.

A systematic study of zircon geochemistry in granitic and associated rocks from various origins reveals a clear relationship of geochemical parameters with zircon morphology. Electron microprobe analyses on polished crystals of the different crystallization periods (premagmatic, magmatic and late magmatic = overgrowths) reveal the magmatic history of the rock.

The Y<sub>2</sub>O<sub>3</sub> versus HfO<sub>2</sub> variation diagram in zircons (Pupin 1992, 1994) is used to infer zircon origin and granite petrogenesis. HfO<sub>2</sub> content of zircon magmatic phase is generally  $< 1.2\%$  in mantle derived granites, partly  $< 1.2\%$  (early magmatic phase) in hybrid granites, and usually  $> 1.2\%$  in anatectic granites and migmatites. The importance of the late magmatic zircon crystallization, always enriched in Hf and/or Y, is related to the role of the fluid phase. The diagram OTU using U and Th in zircons shows the dominance of Th in mantle derived crystals, of U in crustal anatectic and late magmatic zircons. Cumulate curves (UO<sub>2</sub>+ThO<sub>2</sub>) underline the role played by the fluid phase in melts with increasing contents of hygromagmatophile elements.

Internal structures of zircon crystals are revealed by defocusing the beam in the electron microprobe (back-scattered electron pictures). They are characterized by a more or less complex zoning (Van Breemen *et al.*, 1986; Varva, 1990, 1994) but also often by discordancies which correspond to fundamental features of magma genesis or later history. Among them, inherited cores from crustal melting in migmatites and anatectic granites are particu-

larly interesting for petrologists and geochronologists. If clearly discordant shaped cores (corroded ones or fragments) are easily detected, they are frequently associated with idiomorphic or sub-idiomorphic cores whose zoning is apparently in continuity with the zoning of the surrounding host-zircon. Chemical discordancies can reveal the presence of such idiomorphic cores and lead to a better interpretation of the chemistry of the different generations of zircon.

A coupled study of morphological data with trace element geochemistry and internal structures leads to interpret the different origins of cores (or nuclei) in zircons. Three fundamental different origins are recognized: 1) relict cores inherited from the protolith that underwent the *crustal partial melting* (migmatites, anatectic granites of crustal origin); 2) cores corresponding to a *more or less late contamination* during the emplacement of the granitic melt; and, 3) cores corresponding to a *mixing/mingling* between two magmas of different origins (crystallizing directly or after remelting). The arguments used to decide each of these different cases are presented and discussed on the basis of some examples. Geochemical and structural data obtained on the cores are used to constrain the nature of the protolith, the contaminant or the hybridized rocks. Morphological data are used to determine at what period this event happened.

The recognition and interpretation of cores in zircons are of a fundamental interest for the understanding of numerous magmatic rocks genesis, especially granitic ones. Zircon is a very powerful tool and the unlimited material offered by zircon populations in granites permits to obtain a lot of available and precise data - which can be separated if polygenic - associated with the primary events of the main magmatic period. The whole rock geochemistry is generally more difficult to be interpreted because inheritance, contamination, mixing/mingling or deuteric phenomena effects are not always easily separated.

Pupin, J.P., 1976. Signification des caractères morphologiques du zircon commun en pétrologie. Base de la méthode typologique. Applications. *Thèse*, Université de Nice, 394 p.

Pupin, J.P., 1980. Zircon and granite morphology. *Contrib. Mineral. Petrol.*, **73**, 207-220.

Pupin, J.P., 1992. Les zircons des granites océaniques et continentaux: couplage typologie-géochimie des éléments en traces. *Bull. Soc. géol. France*, **163**, 495-507.

Pupin, J.P., 1994. Characterization of sources for migmatites and crustal anatectic granites from zircon studies. *C. R. Acad. Sci. Paris*, **319**, 1191-1197.

Van Breeman, O. and Parrish, R.R., 1986. Zircons record ancient geological processes. *Geos*, **15**, 18-21.

Varva, G., 1990. On the kinematics of zircon growth and its petrogenetic significance: a cathodoluminescence study. *Contrib. Mineral. Petrol.*, **117**, 331-344.

## ORAL PRESENTATION

### Monzonite Suites: The Innermost Cordilleran Plutonism of Patagonia

<sup>1</sup>Rapela, C.W. and <sup>2</sup>Pankhurst, R.J.

<sup>1</sup>Universidad Nacional de La Plata, Argentina

<sup>2</sup>British Antarctic Survey, High Cross Madingley Road, Cambridge CB3 0ET, UK

The development of a wide early Mesozoic Cordilleran interior magmatic belt in Patagonia contrasts sharply with the typical Andino-type continental-margin arc that prevailed from Late Jurassic to Tertiary times along the Pacific margin of South America. This extra-Andean province contains Late Triassic - Early Jurassic granitoids in the North Patagonian Massif and the extensive Middle Jurassic Volcanic Province, one of the largest known silicic volcanic fields.

The easternmost exposures of plutonic rocks occur in the Deseado Massif, more than 750 km east of the present oceanic trench, where two Early Jurassic monzonite suites crop out in erosional windows through the Jurassic volcanic rocks. The predominant rocks are hornblende-biotite granitoids, of quartz monzodiorite composition at La Leona and quartz monzonite at La Calandria; both show transitions to biotite monzogranite. Lenses of leucosyenogranite and aplite-monzogranite intrude the main facies in both areas, and are abundant at La Leona. A marginal facies of fine grained gabbro and basic quartz monzodiorite appears only at La Calandria.

These two monzonite suites are metaluminous, ASI increasing from 0.7 to 1.1 as SiO<sub>2</sub> increases from 56 to 72 wt %; only the felsic syenogranites and aplites are marginally peraluminous (ASI = 1.1 - 1.2). Compared with the typical metaluminous Cordilleran tonalite-granite series, they show higher P<sub>2</sub>O<sub>5</sub>, K<sub>2</sub>O, and MgO/FeO<sup>T</sup> ratios, signifying higher-temperature melts. Associated mineralization is of Mo-Cu type.

Lithological and geochemical variations in both districts are the result of extensive, high level, fractional crystallization. Each suite precisely defines a whole-rock Rb-Sr isochron of 203 Ma, and each has a uniform ε<sub>Nd</sub>(t) value.

Internal co-sanguineous differentiation models, using actual modal proportions of essential minerals, closely account for observed trends in Rb, Sr, Ba and Th. REE models require accessory minerals (titanite, apatite and zircon) to be considered. During the early stages, the parent liquids ( $\text{SiO}_2 = 65 - 69 \text{ wt } \%$ ,  $\text{K}_2\text{O} = 3.0 - 3.8\%$ ,  $\text{Rb} = 100 - 150 \text{ ppm}$ ,  $\text{Sr} = 470 - 610 \text{ ppm}$ ,  $(\text{La}/\text{Yb})_N = 16 - 23$ ,  $\text{Eu}/\text{Eu}^* = 0.7 - 1.0$ ) evolved by precipitation of basic plagioclase + hornblende + biotite + quartz + accessory minerals. Ubiquitous microgranular enclaves in both suites ( $\text{SiO}_2 = 60 - 61.5 \text{ wt } \%$ ,  $\text{K}_2\text{O} = 1.7 \text{ wt } \%$ ) represent crystal accumulation, and the gabbros and basic quartz monzodiorites at La Calandria ( $\text{SiO}_2 = 55 - 58 \text{ wt } \%$ ,  $\text{K}_2\text{O} = 0.9 - 1.5 \text{ wt } \%$ ,  $\text{Rb} = 25 - 60 \text{ ppm}$ ,  $\text{Sr} = 800 - 960 \text{ ppm}$ ,  $(\text{La}/\text{Yb})_N = 10$ ,  $\text{Eu}/\text{Eu}^* = 0.95$ ) were also formed by accumulation during this stage. K-feldspar and acid plagioclase dominate crystallization paths in the interval 69 - 76 wt %  $\text{SiO}_2$ , where trends in both suites are similar and show a progressive depletion in Sr, Sc, Zr, MREE and HREE, and concomitant increases in Rb, Th, U, Ta and the negative Eu anomaly. Syenogranites and aplites represent the extreme development of these trends ( $\text{SiO}_2 = 74.5 - 76.5 \text{ wt } \%$ ,  $\text{K}_2\text{O} = 4.7 - 5.2 \text{ wt } \%$ ,  $\text{Rb} = 190 - 240 \text{ ppm}$ ,  $\text{Sr} = 20 - 60 \text{ ppm}$ ,  $(\text{La}/\text{Yb})_N = 26 - 28$ ,  $\text{Eu}/\text{Eu}^* = 0.40 - 0.70$ ). The parent magmas of these suites were derived from melting of more mafic sources, probably deep crust rocks of basaltic composition.

However, there are small but significant differences between the two suites, especially in their isotopic compositions, which suggest independent evolution from similar but not identical parent magmas. The  $(^{87}\text{Sr}/^{86}\text{Sr})_i$  ratios, average  $\epsilon_{\text{Nd}}(203 \text{ Ma})$  and mean depleted-mantle Nd model ages are respectively 0.70487, -0.5 and 950 Ma for La Leona, and 0.70508, -1.5 and 1000 Ma for La Calandria. Both suites are thus isotopically more primitive than the Jurassic silicic volcanic rocks ( $(^{87}\text{Sr}/^{86}\text{Sr})_i$  ratios c. 0.7068 and  $\epsilon_{\text{Nd}}(175 \text{ Ma})$  c. -4.0), which have attributed to partial melting of a mafic lower crust first formed in Grenvillian times (1150-1600 Ma). Sr-Nd isotopic variations within the Triassic-Jurassic extra-Andean province may be generally described by mixing curves, including a hypothetical mafic end-member within the mantle field and a crustal end-member at  $\epsilon_{\text{Sr}} = +75$  and  $\epsilon_{\text{Nd}} = -10$  (much less radiogenic and equivalent, respectively, than the crustal end-member recently proposed for such variations in Jurassic metaluminous-peraluminous granitoids of the Antarctic Peninsula). It is not possible to discriminate between variable mixing between end-member magmas and continuous variation in a zoned crust, although the perfect

homogeneity of the small magma batches represented by the monzonite suites seems to favour the latter interpretation. The unconformable Jurassic volcanic cover of the monzonite outcrops indicates that there was significant uplift in the interval 200-170 Ma, after which a different crustal zone was involved in magma generation.

### **Cordierites in S-type Granites: Restites Following Low Pressure, High Degree Partial Melting of Metapelites**

<sup>1</sup>Rapela, C.W., <sup>2</sup>Pankhurst, R.J.,

<sup>3</sup>Baldo, E. and <sup>4</sup>Saavedra, J.

<sup>1</sup>*Universidad Nacional de La Plata, Argentina*

<sup>2</sup>*British Antarctic Survey, High Cross,  
Madingley Road, Cambridge CB3 0ET, UK*

<sup>3</sup>*Universidad de Cordoba, Argentina*

<sup>4</sup>*Instituto de Recursos Naturales y Agrobiologia,  
Salamanca, Spain*

Large amounts of very pure cordierite rock associated with S-type granites at El Pilon, near Soto in the eastern Sierras Pampeanas, are interpreted as residues from the partial melting of regional phyllites that produced the granite magmas.

The Soto area belongs to the Famatinian orogenic belt, characterized by Lower to Middle Paleozoic granitoids emplaced in a polymetamorphic basement. The cordierites and coeval cordierite-bearing granitoids were emplaced during the second metamorphic event, which reached temperatures high enough to provoke widespread anatexis of the metasedimentary sequences (680-730°C; 4.5-6.7 kbar).

The majority of the outcrop of the El Pilon granite is composed of a sillimanite-cordierite-biotite porphyritic granodiorite or monzogranite ( $\text{SiO}_2 = 69 - 71\%$ ,  $\text{ASI} = 1.26 - 1.38$ ,  $\text{Alk} = 6.7 - 7.2\%$ ,  $\text{Mg}\# = 46 - 49$ ,  $\text{K}/\text{Rb} = 180 - 220$ ,  $(\text{La}/\text{Yb})_N = 8.7 - 10.0$ ). A minor facies consists of Sill-Crd-Bt-Grt medium-grained leucomonzogranite ( $\text{SiO}_2 = 71 - 76\%$ ,  $\text{ASI} = 1.22 - 1.35$ ,  $\text{Alk} = 7.5 - 8.3\%$ ,  $\text{Mg}\# = 25 - 49$ ,  $\text{K}/\text{Rb} = 180 - 315$ ,  $(\text{La}/\text{Yb})_N = 4.1 - 8.5$ ). Four ovoid outcrops of cordierite, each up to 140 m in length, are enclosed within this second, equigranular, phase. They display sharp magmatic-style contacts against both the granite and screen-like exposures of schist (Bt-Qtz-Pl-Kfs), and 0.5

m-wide dykes of massive cordierite (see below) intrude both the latter rock types. Xenoliths of the porphyritic granite are found within both the massive cordierite and the leucogranite, whereas the porphyritic granite itself contains deformed enclaves of the schists.

Two main textural varieties of the cordierites occur - orbicular and massive. The orbicular facies consists of 5-20 cm egg-shaped orbicules, comprising an outer aggregate of polygonal, fresh cordierite with fibrolite between crystals and minor quartz and plagioclase ( $An_{20-26}$ ), and a dark nucleus of oriented biotite, sillimanite, and cordierite. Space between orbicules is occupied by a pale mosaic of quartz, perthitic K-feldspar and plagioclase ( $An_{16-20}$ ). The orbicules typically have  $Al_2O_3 = 28\%$ ,  $Alk = 3\%$ ,  $Mg\# = 63$ , and  $(La/Yb)_N = 5 - 12$ . The massive cordierite approaches pure cordierite (95%), with a composition  $Al_2O_3 = 29 - 31.5\%$ ,  $Alk = 0.5 - 2\%$ ,  $Mg\# = 61 - 68$ ,  $(La/Yb)_N = 3 - 6$ . There is a gradual transition to darker varieties of the massive facies with up to 40% of modal biotite. The cordierite occurs as 1-2 cm crystals set in a groundmass of small crystals (0.3-0.5 cm), both with fibrolite and biotite at the crystal edges. Staurolite appears in the more biotitic varieties, and common accessories are apatite, zircon and tourmaline.

Rb-Sr and Sm-Nd isotope analyses of both granites, cordierite and schist indicate that all these rock-types were genetically linked. In particular, the massive cordierite and equigranular granite analyses together define a single Rb-Sr isochron ( $520 \pm 5$  Ma,  $MSWD = 2.9$ ), with a wide range in Rb/Sr ratios (3-20 in the cordierites due to variation in the modal amount of biotite; 1.5-5.5 in the granite). Three samples of the local schist plot close to the lower end of the same isochron, which has  $(^{87}Sr/^{86}Sr)_i$  of 0.714.  $\epsilon_{Nd}(520 \text{ Ma})$  varies from -5.7 to -6.0 in the cordierites, from -5.1 to -5.5 in the granites, and from -3.0 to -7.7 in schists, suggesting that the metapelites did not undergo complete isotopic re-equilibration during anatexis.

It is suggested that the cordierites and the leucogranite were formed from a large metasedimentary raft in the roof zone of the porphyritic granite, which was itself formed by anatexis of similar source rocks at greater depth. The relict metamorphic minerals in the core of the cordierite orbicules suggest that melting of metapelites was accompanied by a reaction of the kind:



Garnet is absent in both cordierite facies, indicating that melting took place at very low pressure, probably well below 3 kbar. The newly formed Mg-rich cordierite from

this reaction grew as limpid large crystals until Pl and Qtz were exhausted (leaving the Bt-Sill cores of the orbicular facies), while the melt migrated and coalesced nearby forming the equigranular leucocratic facies of the El Pilon granite. The massive cordierite represents an extreme situation where the original composition allowed complete reaction of the products. Water saturation, fluids and high temperature increased the mobility of the massive cordierite so that it become sufficiently ductile to intrude the older, porphyritic, facies of the host granite.

### Estimation of Initial and Saturation Water Contents of Three Mesozoic Granitic Plutons in the North-central Great Basin, Nevada

Ratajeski, K. and Candela, P.A.

*Laboratory for Mineral Deposits Research,  
Department of Geology, University of Maryland  
at College Park, MD 20742, USA*

According to the Magmatic-Hydrothermal Theory for the genesis of granite-related ore mineralization, the ratio of initial melt water content ( $C_{H_2O}^{i,o}$ ) to saturation melt water content ( $C_{H_2O}^{i,s}$ ) influences the timing of volatile phase saturation relative to the crystallization history of the magma, the relative amounts of crystal-compatible and crystal-incompatible ore-forming elements in the exsolved magmatic volatile phases, and the physical mode of egress of magmatic volatiles from the crystallizing magma (Candela, 1991, 1992). Three Mesozoic plutons from the north-central Great Basin in Nevada were studied to determine how well  $C_{H_2O}^{i,o}$  and  $C_{H_2O}^{i,s}$  can be constrained. These plutons are located in Lander and Eureka Counties, NV and include the Jurassic Mill Canyon stock (MCS), the Jurassic McCoy pluton (MP), and the Cretaceous Trenton Canyon pluton (TCP). Selected samples from this study include: MCS-63: a medium-grained biotite granite to granodiorite (68.5 wt %  $SiO_2$ ); MCS-15, a fine- medium-grained, porphyritic biotite-hornblende tonalite (66.4); MP-43, a medium-grained biotite-hornblende granite to granodiorite (66.1); and TCP-41, a medium-grained biotite-hornblende granodiorite (65.1). Rare porphyritic samples (MP-75 and TCP-35) with high phenocryst contents (~70 vol %) were collected from outcrops otherwise similar to hypidiomorphic-equigranular samples MP-43 and TCP-41.

Estimates of  $C_{H_2O}^{l,o}$  were attempted by inferring crystallization sequences from petrographic observations and comparing the inferred sequences with experimentally - determined crystallization paths as depicted on published  $T-X_{H_2O}^{system}$  diagrams for granites and granodiorites at 2 kbar. Except for MCS-63, all samples contain hornblende and texturally-early biotite (based on the presence of euhedral to subhedral biotite inclusions in plagioclase, quartz phenocrysts, and K-feldspar), implying that  $C_{H_2O}^{l,o} > 4$  wt % if Naney's (1983) synthetic granodiorite R5+10M1 is used as a model. However, this conclusion is contradicted by porphyritic samples MP-75 and TCP-35, which contain hornblende phenocrysts but show textural evidence of  $H_2O$ -undersaturated conditions to high crystallinities ( $\sim 70$  vol %) in the form of resorbed quartz and/or K-feldspar phenocrysts. Assuming saturation with a water-rich volatile phase at 70% crystallization, a maximum  $C_{H_2O}^{l,o} \sim 2$  wt % is suggested if Al-in-hornblende geobarometry (presented below) is accurate. MCS-63 has texturally-early biotite but no hornblende, which only suggests that  $C_{H_2O}^{l,o} > 2$  wt % (Naney, 1983).

The Al-in-hornblende geobarometer was used on rocks with the appropriate mineral assemblage, except for titanite. Pressures were calculated with the Johnson and Rutherford (1989) calibration for a sample from the MCS with low ( $\sim 15$  vol %) phenocryst content (high quench temperature), and with the Schmidt (1992) calibration for a sample with high phenocryst content ( $\sim 70$  vol %) from the MP and a hypidiomorphic-equigranular sample from the TCP. Calculated pressures ( $\pm 1\sigma$ ) are  $1.7 \pm 0.6$  kbar for the MCS (12 rims analyzed),  $2.3 \pm 1.0$  kbar for the MP (7 rims), and  $2.9 \pm 1.2$  kbar for the TCP (12 rims). Pressure for the MCS is best constrained, but results generally indicate moderately-shallow emplacement depths for all of the plutons.  $C_{H_2O}^{ls}$  ( $\pm 1\sigma$ ) was estimated from pressure and water solubility data of Holtz *et al.* (1993) as follows:  $5.2 \pm 1.6$  wt %  $H_2O$  (MCS);  $6.3 \pm 2.7$  wt % (MP); and,  $7.3 \pm 3.3$  wt.% (TCP). The uncertainty in the estimates of  $C_{H_2O}^{l,o} / C_{H_2O}^{ls}$  for plutonic rocks of the MCS, MP, and TCP is due to limitations of hornblende barometry, probable alteration of hornblende in the TCP, and by limitations of textural criteria to provide reliable and constrained information on initial water contents. Using these estimates for saturation water concentrations and 2 wt % maxima for  $C_{H_2O}^{l,o}$ , yields  $C_{H_2O}^{l,o} / C_{H_2O}^{ls} < 0.3 \pm 0.1$  for both MP-75 and TCP-35. These low values suggest that these magmas were relatively dry for their inferred level of emplacement (Candela, 1991), which is and are consistent with their lack of significant associated mineralization.

- Candela, P.A., 1991. Physics of aqueous phase evolution in plutonic environments. *Am. Mineral.*, **76**, 1081-1091.
- Candela, P.A., 1992. Controls on ore metal ratios in granite-related ore systems: an experimental and computational approach. *Trans. Royal Soc. Edinburgh: Earth Sci.*, **83**, 317-326.
- Holtz, F., Dingwell, D.B. and Behrens, H., 1993, Effects of F,  $B_2O_3$  and  $P_2O_5$  on the solubility of water in haplogranitic melts compared to natural silicate melts. *Contrib. Mineral. Petrol.*, **113**, 492-501.
- Johnson, M.C. and Rutherford, M.J., 1989, Experimental calibration of the aluminum-in-hornblende geobarometer with application to Long Valley caldera (California) volcanic rocks. *Geology*, **17**, 837-841.
- Naney, M.T., 1983, Phase equilibria of rock-forming ferromagnesian silicates in granitic systems. *Am. J. Sci.*, **283**, 993-1033.
- Schmidt, M.W., 1992. Amphibole composition in tonalite as a function of pressure: an experimental calibration of the Al-in-hornblende barometer. *Contrib. Mineral. Petrol.*, **110**, 304-310.

### Experimental Determination of Rare Earth Element Distribution Between Chloride-Bearing Volatile Phase and Granitic Melt

Reed, Marshall J.

*Laboratory for Mineral Deposits Research,  
Department of Geology, University of Maryland  
at College Park, MD 20742, USA*

Rare earth elements (REE) show systematic variation during most chemical and geologic processes, and the REE distribution patterns of granite-related mineral deposits can be used to monitor the progress of mineralization through the stages of hydrothermal alteration. In this experimental study, the partitioning of rare earth elements between slightly-peraluminous granitic melts and chloride-bearing aqueous phases was investigated at conditions representing a magma chamber crystallizing under lithostatic pressure at a depth of *c.* 7 km in the crust (2 kbar) and 800°C. At these conditions, the aqueous phase is neither a liquid nor a vapor but is supercritical in low- $CO_2$  systems. Anhydrous monzogranite glass (34.0 wt %  $KAlSi_3O_8$ , 31.7 wt %  $NaAlSi_3O_8$ , 7.4 wt %  $CaAl_2Si_2O_8$ , and 26.9 wt %  $SiO_2$ ) was reacted with aqueous chloride solutions containing systematically varied concentrations of  $Na^+$ ,  $K^+$ ,  $H^+$  and ten REE of interest (La, Ce, Nd, Sm, Eu, Gd, Tb, Ho, Yb, and Lu). Starting solutions contained 0.007 to 0.03 *m* REE, 0.44 to 3.5 *m* chloride, and in  $4 \times 10^{-4}$  to 0.8 *m*  $H^+$ . Instrumental neutron activation analysis was used to determine trace-element concentrations (there are few interferences with the rare earth elements). To maintain

a uniformly high accuracy in analyses, the concentrations of the REE were in proportion to their limits of detection. For a sample mass of 30 mg, gamma-ray counting statistics for 3% error limits required concentrations of 500 mg/kg for Gd, Ho, and Nd; 200 mg/kg for Ce and Yb; and 50 mg/kg for La, Sm, Eu, Tb, and Lu.

To assure that samples were representative of run conditions, the experiments were rapid-quenched (800°C to 100°C within 3 seconds) at run pressure. The pH of each quenched solution was determined by dilution to the pH range 1.68 to 4.01, and measurement of samples and standards. Chloride analysis of each quenched solution was made using a digital chloridometer. A sample of each aqueous solution was analyzed for the major elements Na, Al, Si, K, Ca, and Fe by inductively coupled plasma-atomic emission spectrometry. Part of the glass recovered from each experiment was analyzed by electron probe microanalysis, and instrumental neutron activation analysis (INAA) was used to determine the trace element composition of both glass and quenched solution from each experiment.

Equilibrium between granitic melt and the magmatic volatile phase at experimental conditions of 2 kbar and 800°C was examined as a function of the partitioning coefficient of individual elements and as the apparent equilibrium constant for exchange reactions between Na and the other cations. The partition coefficient (D) of an element is the ratio of the concentrations in the two phases (aqueous/melt), for example:

$$D_{La}^{A,M} = \frac{C_{La}^A}{C_{La}^M}$$

but this parameter varies significantly with changes in phase composition and changes in experimental conditions. If the assumption is made that the activity coefficient is constant, or nearly constant, over the range of experimental conditions, then the *apparent* equilibrium constant, K', with respect to sodium can be calculated from the elemental concentration (C) in each phase rather than from the activities:

$$K'_{La,Na}^{A,M} = \frac{(C_{LaCl_3}^A)(C_{Na}^M)^3}{(C_{La}^M)(C_{NaCl}^A)^3}$$

Since this parameter is based on the exchange reaction, it is expected that the variations in the partition coefficient of a rare earth element will be compensated by changes in the

cube of the sodium partition coefficient ( $K'_{Eu,Na}$  calculated with the square of  $D_{Na}$ ). Mean values and 1σ deviations are given for groups of experiments with three different starting solutions to test this assumption:

	1.1 mΣCl 0.05 mH <sup>+</sup>		3.5 mΣCl 0.07 mH <sup>+</sup>		1.1 mΣCl 0.7 mH <sup>+</sup>	
	D	K'	D	K'	D	K'
La	0.037 ±0.0043	0.157 ±0.0047	0.043 ±0.047	0.074 ±0.013	2.02 ±0.28	0.41 ±0.08
Ce	0.032 ±0.0049	0.136 ±0.014	0.39 ±0.043	0.067 ±0.0089	1.97 ±0.32	0.4 ±0.089
Nd	0.022 ±0.0031	0.096 ±0.0091	0.34 ±0.029	0.058 ±0.006	1.96 ±0.3	0.39 ±0.082
Sm	0.021 ±0.0031	0.09 ±0.006	0.28 ±0.037	0.047 ±0.0028	1.61 ±0.29	0.32 ±0.076
Eu	0.033 ±0.0058	0.087 ±0.0098	0.48 ±0.077	0.016 ±0.0168	1.08 ±0.08	0.37 ±0.029
Gd	0.021 ±0.0023	0.089 ±0.0005	0.23 ±0.052	0.039 ±0.0016	1.38 ±0.29	0.28 ±0.073
Tb	0.019 ±0.0028	0.079 ±0.0044	0.21 ±0.033	0.035 ±0.0017	1.23 ±0.2	0.25 ±0.055
Ho	0.017 ±0.003	0.07 ±0.003	0.16 ±0.028	0.033 ±0.0033	0.95 ±0.14	0.19 ±0.039
Yb	0.014 ±0.0016	0.036 ±0.003	0.12 ±0.019	0.021 ±0.0046	0.62 ±0.13	0.13 ±0.031
Lu	0.013 ±0.0015	0.058 ±0.0032	0.11 ±0.02	0.019 ±0.0047	0.53 ±0.093	0.11 ±0.024

Changes in the K' between experiments show there is a more complex relationship between K' and the concentrations than was assumed. The activity coefficients of the components appear to be a function of both Cl<sup>-</sup> and H<sup>+</sup> in solution. The aluminum saturation index (ASI = mole ratio Al/[Na+K+2Ca]) shows a direct response to the H<sup>+</sup> concentration in the starting solutions. For the three groups of experiments, the mean ASI and deviation are: for 1.1 m Cl, 0.05 m H<sup>+</sup>, ASI = 1.02 ± 0.02; for 3.5 m Cl, 0.07 m H<sup>+</sup>, ASI = 1.02 ± 0.03; and for 3.5 m Cl, 0.7 m H<sup>+</sup>, ASI = 1.16 ± 0.04. From these results, it appears that hydrogen ions from the aqueous solution exchange with both sodium and potassium in the melt. Increasing hydrogen ion concentration in the system contributes to greater partitioning of sodium and potassium from the melt into the volatile phase, and this exchange drives the melt toward peraluminosity.

**A Complex Strain and Intrusion Fabric  
Related to Trans-Solidus Deformation:  
The Wolf Mountain Intrusion,  
Llano Uplift, Texas**

Reed, Robert M.

*Department of Geological Sciences,  
University of Texas, Austin, TX 78712, USA*

The Wolf Mountain Intrusion (WMI) is a chevron-shaped (phacolithic) granite body which occupies an upright synform that plunges shallowly to the southeast. The WMI is one of many Proterozoic porphyritic granite intrusions in the Grenvillian Llano Uplift of central Texas that have previously been considered post-orogenic to anorogenic. Deformation during and after the emplacement of the granitic magma has produced a complex internal fabric including foliations with magmatic and tectonic components, multiple diking events, and shearing. This internal fabric is most complex in the hinge region of the intrusion where the history is as follows.

- 1) Intrusion of a magma (coarse-grained porphyritic granite) as a roughly planar mass at or near the contact between the two major lithological units in the uplift.
- 2) Development of a mostly linear magmatic alignment (Smag) of microcline megacrysts and xenoliths.
- 3) Addition of biotite-rich magmatic enclaves, many of which occur in planar swarms suggesting intrusion into the host magma.
- 4) Regional folding (the SE-plunging synform). Folding may have begun earlier, but evidence for deformation is observed after this point.
- 5) Aplitic and pegmatitic dikes, such intrusions continued throughout crystallization.
- 6) A second phase of coarse-grained porphyritic granite with convolute margins is also present. This phase is differentiated by having no mafic enclaves, less biotite, a more reddish color, and more-equant microcline megacrysts. Lack of elongate feldspars gives this phase a less-foliated appearance.
- 7) Intrusion of SE-trending dikes that are later foliated (St). Dikes come in four varieties: aplitic with disseminated biotite, aplitic with planar biotite segregations, phenocrystic granite with a fine-grained matrix, and dikes of the second granitic phase. Much of the foliation (St) in these dikes was formed during solid-state deformation with accompanying recrystallization. The dikes are generally not boudinaged, indicating that they were less competent

than the host granites at the time of deformation. Many dikes are foliated parallel to their margins. However, a significant number; which trend more ESE, have oblique foliations trending SE.

8) Some of these dikes are cut by minor "healed" shears (Ses) with small components of motion (<2.5 m.). Ses development in the granite varies from absent to moderate, indicating Ses formed over a period of time as the granite solidified. These shears come in two orientations, sinistral with ESE trends and dextral with ENE trends. Ses shears seem to form a conjugate pair indicating SW-NE compression, consistent with the axial plane of the main fold.

9) Formation of a SE-trending foliation (St). St foliates earlier dikes and forms zones in the granite meters to tens of meters wide that cut or overprint Smag. St has erased Ses in some places, but is cut by it in others. St has a strong component of solid-state deformation. Quartz and feldspar have undergone high temperature recrystallization. Small xenoliths and elongate magmatic enclaves are oriented subparallel to this foliation where it occurs. St cuts across boundaries between the two porphyritic granite phases. Whereas microfabrics in the main granite are ambiguous, some of the sheared phenocrystic dikes contain sinistral indicators. Displacement of an enclave zone by an St zone also shows apparent sinistral motion.

10) Lastly, intrusion of fine-grained pink granite dikes and bodies. These granite bodies have irregular shapes and poor to non-existent foliation. Dikes with SE and WSW trends radiate from these bodies. WSW-trending unfoliated pegmatites are also common at this stage. Although these dikes are themselves undeformed, the WSW dikes are intruded perpendicular to the inferred compression direction of the folding. This orientation suggests that these dikes are related to the deformation. Some of these dikes also offset earlier features with meter-scale right-lateral offsets, suggesting transtensional intrusion.

The internal structure of the granite is much simpler in the limbs of the intrusion, suggesting concentration of strain in the hinge zone during regional folding of the crystallizing intrusion.

The WMI provides evidence for late synorogenic intrusion of granite in the Llano Uplift, tying what were considered to be "anorogenic" granites to an orogenic event. The WMI also provides an example of the complexities that arise from deformation occurring synchronous with solidification. Deformation is not just concentrated at the pluton margin but within an area in the interior. The localization of deformation in one area with

reduced deformation elsewhere points out the need for caution in labeling a pluton "undeformed" based on an examination of only part of its area.

### The Albite Granites of the Central Eastern Desert (Egypt): The Evolution of a Hot and Dry Granulite-Derived Melt to a Pegmatoid Intrusion

Renno, A.D.

*Institute of Mineralogy, Freiberg University  
of Mining and Technology, Germany*

In the Pan African consolidated basement of the Central Eastern Desert, three albite granite bodies are situated: Nuweibi, Abu Dabbab and Igla. The remarkable features of these granites have interpretation of part of the late- to post-Pan African evolution of this part of the Arabian Nubian Shield. The Abu Dabbab and Nuweibi granites are sheet-like intrusions along preintrusive structures in the wallrocks. The Igla granite forms a stockwork of felsic dikes and mineralized quartz - mica - beryl veins. Clear intrusive contacts, *e.g.*, intrusive breccias, exclude the possible metasomatic formation of these rocks. The present level of erosion is different. The Igla granite is least eroded (only the top of the intrusion is uncovered), the Nuweibi granite has eroded down to the roof zone, and the Abu Dabbab granite has eroded the most. Felsic dikes are closely associated with the granites.

The geochemical characteristics of the peraluminous granites are:  $\text{SiO}_2 > 75\%$ ; molar  $\text{Na}_2\text{O} / \text{K}_2\text{O}$  ratio of  $> 1$ ,  $(\text{Na}_2\text{O} + \text{K}_2\text{O}) > 8\%$ ; extreme low values for CaO (0.1%), MgO (0.02%),  $\text{P}_2\text{O}_5$  (0.01%), and Sr (5 ppm); extreme high values for Ga ( $> 100$  ppm), Ta ( $> 150$  ppm), and Zn ( $> 400$  ppm); moderate values for Li (10 - 100 ppm) and F<sup>-</sup> (400 - 700 ppm); and, Nb/Ta ratio  $< 1$ .

The felsic dikes show big inhomogeneities and patterns that are not typical for magmatic rocks. These rocks cannot be defined as Li-F granites, but as low-phosphorus, low-Ca Ta-granites. The mineralogical composition of the albite - alkali feldspar - quartz - (muscovite) rocks is very monotonous. However, they bear an uncommon assemblage of accessory minerals: orthopyroxene, garnet, gahnite, annite, Mn-Ta minerals, cassiterite and Hf-rich zircons ( $\text{HfO}_2$  10 - 25%). The microstructure of the

rocks ranges from medium grained equigranular over porphyritic (monzonitic feldspar or "snowball-quartz") to felsitic structures (dikes and margins of the intrusions).

The age of the intrusion of the albite granites is  $\sim 590$  Ma. Even though there is no time gap between the postorogenic A-type granites and the albite granites, they are not related. There is also no geochemical evidence for the formation of the albite granites by fractionation of basaltic magmas, as proved by Coleman *et al.* (1992) for the A-type granites related to the Red Sea opening in Saudi Arabia and Yemen.

I suggest the following petrogenetic model. At the base of the lower crust, melting of the (garnet) pyroxene granulites took place at 950 - 1100°C, 10 kbar and  $a_{\text{H}_2\text{O}} < 0.3$  and yielded to Ab-rich melts. Extensional tectonic processes (Greiling *et al.*, 1994) promoted the extraction of the small melt amounts out of the source rock. Due to the relatively low fluorine content in the albite granites, there was no "metasomatic" input of halogen-rich fluids to support the melt generation in the protolith. The quick ascent of the magma did not prevent fractionation processes, but residual garnets are preserved. In the hot and dry haplogranitic melt orthopyroxene, albite, alkali-feldspar, and later quartz and annite crystallized. During the intrusion of the magma in the upper crust, the melt absorbed water from the "wet" wall rocks. This turned the character of the melt into a pegmatoidal melt, which crystallized quickly. In the fine grained albite-quartz (muscovite) matrix typical pegmatite minerals like gahnite, manganotantalite and Hf-rich zircon were formed. The isotopic system of Sr was completely disturbed (measured  $(^{87}\text{Sr}/^{86}\text{Sr})_i \sim 1.1 - 5.1$ ). The felsic dikes, originating from coexisting silicate melts and fluid phases, concluded the magmatic activities. Circulating fluids formed belt-like bodies of amazonitized or sericitized albite granite, marginal greisen bodies and the quartz cap of the Nuweibi granite.

The formation and intrusion of the albite granites was a local process. This process fits into a continuous magmatic evolution of the area from the Red Sea Hills (Sudan) to the Sinai Peninsula (Egypt) in the period from the end of the Pan African accretion to the beginning of the Red Sea rift. The impulses and conditions for this magmatic evolution are not yet completely understood.

Coleman, R.G., DeBari, S. and Peterman, Z., 1992. A-type granite and the Red Sea opening. *Tectonophysics*, **204**, 27-40.

Greiling, R.O., Abdeen, M.M., Dardir, A.A., El Akhal, H., El Ramley, M.F., Kamal El Din, G.M., Osman, A.F., Rashwan, A.A., Rice, A.H.N. and Sadek, M.F., 1994. A structural synthesis of the

Proterozoic Arabian-Nubian Shield in Egypt. *Geol. Rundsch.*, **83**, 484-501.

## ORAL PRESENTATION

### The Perils of AFC Modelling

<sup>1</sup>Roberts, Malcolm P. and <sup>2</sup>Clemens, John D.

<sup>1</sup>*Department of Geology, The University,  
Manchester M13 9PL, UK*

<sup>2</sup>*School of Geological Sciences, Kingston University,  
Kingston-upon-Thames, KT1 2EE, UK*

A major use of whole-rock and isotope geochemical analyses of granitoid rocks is to constrain the nature of magma source regions (protoliths), as well as possible processes by which the magmas evolved. The need to explain elemental variation on bivariate plots has led to the development of mathematical models of processes that may have produced the variation.

Of the published geochemical models, one of the most popular is that of combined wall-rock assimilation and fractional-crystallization (the AFC model of DePaolo, 1981). In this model, mathematical expressions are used to calculate isotopic ratios and elemental compositions of hybrids formed as the assimilating or original magma undergoes fractional crystallization, while simultaneously mixing with another magma or assimilating its wall-rocks (the assimilant). Trace-element and isotope concentrations, obtained from the equations, define curves on bivariate isotope-isotope and isotope-element plots.

This model has been very effective in reproducing trends commonly seen on plots of Nd and Sr isotope data. The governing equations allow assumptions to be made on the ratio ( $r$ ) of the rate of assimilation to the rate of fractional crystallization (an arbitrary fraction) and the bulk distribution coefficient ( $D$ ) for the element under investigation. Choices of the values for  $r$  and  $D$  are typically based on those that produce the best fit to the data set (usually within a broad spectrum of what is considered possible) rather than being grounded in any solid geological, mineralogical or experimental constraints. For such a model to be effective, considerable differences must exist between the elemental and isotopic compositions of the assimilant and the assimilating magma (Powell, 1984).

The reason for the popularity of this model is readily apparent. It is an extremely powerful, yet simple, mathematical formalism that, on the face of it, permits erection of a viable petrogenetic model for essentially any group of related rocks. Herein also lies its Achilles heel, for it *permits* a pattern-matching kind of modelling, essentially unconstrained by the realities of magma physics, geological observation or major-element geochemical data.

Recently, the AFC equations have been extended to allow independent estimation of  $\rho$ , the ratio of the mass of assimilant to the mass of original magma (Aitchison and Forrest, 1994). Thus, a sensitive criterion of model feasibility is that calculated  $\rho$  versus  $r$  curves ought to be the same, within analytical error, for all elements tested. If not, the simple model is invalid.

Modelling of variations among granitoid rocks from the Qu erigut Massif in the Pyrenees, a continental calc-alkaline complex, typical of such bodies world-wide, shows that AFC approaches successfully match the variations in Sr and Nd isotopic systems. However, the models fail, catastrophically, to satisfy any of the *other* major- and trace-element constraints (*e.g.*, SiO<sub>2</sub>, MgO, K<sub>2</sub>O, Rb, Sr, Zr) for the hybrids. Magmas with appropriate Sr and Nd isotope ratios can be produced using an enormous and poorly constrained range of model parameters, but such an approach has little petrogenetic value. Curves generated in this fashion, on bivariate isotope-isotope and isotope-element plots, will *always* form arrays between the two end-member compositions, even if they are genetically unrelated. This is an artefact of the mathematics governing two-component mixing, as used by the AFC equations, and may explain why such modelling commonly makes use of isotope data in preference to major- or trace-element data.

We do not contend that AFC modelling has no role to play in the formulation of petrogenetic hypotheses. However, it should be undertaken with an eye to what is geologically and geochemically reasonable (for values of  $r$ ,  $D$  and  $\rho$ ). If possible, there should be some hard evidence for the existence of the proposed assimilant, and any apparent solution should be tested and evaluated against a number of major- and trace-element constraints, as well as constraints imposed by physics and thermodynamics. Without these precautions, we are in danger of self-delusion.

Aitchison, S. J. and Forrest, A. H., 1994. Quantification of crustal contamination in open magmatic systems. *J. Petrol.*, **35**, 461-488.

- DePaolo, D. J., 1981. Trace element and isotopic effects of combined wallrock assimilation and fractional crystallization. *Earth Planet. Sci. Lett.*, **53**, 189-202.
- Powell, R., 1984. Inversion of the assimilation and fractional crystallization (AFC) equations; characterisation of contaminants from isotope and trace element relationships in volcanic suites. *J. Geol. Soc. London*, **141**, 447-452.

## Are Enclaves Significant in Granite Petrogenesis?

Roberts, Malcolm P. and Clemens, John D.

<sup>1</sup>*Department of Geology, The University, Manchester M13 9PL, UK*

<sup>2</sup>*School of Geological Sciences, Kingston University, Kingston-upon-Thames, Surrey KT1 2EE, UK*

The study of enclaves in granites has long been popular. This is undoubtedly due to the fact that they are a common feature of granitoid rocks, worldwide. Macro- and microscopic textural features of many enclaves suggest that they crystallised from magmas following incorporation into the felsic host. It is these enclaves that attract most interest. There have been various models advanced for the petrogenetic relationships between enclaves and their hosts, with an emphasis on their potential importance in the chemical and mineralogical evolution of the rock body within which they are enclosed. Thus, enclaves are commonly viewed as being of fundamental importance in granitoid petrogenesis.

The Querigut Massif in the French Pyrenees is a much studied Variscan age (285 Ma), metaluminous, calc-alkaline complex renowned for a spectacular mafic-felsic association, including abundant enclaves. The host granitic rocks include hornblende-bearing granodiorites and tonalites ( $(^{87}\text{Sr}/^{86}\text{Sr})_i = 0.709$  to  $0.710$ ;  $\epsilon_{\text{Nd}} = -5.5$  -  $-6.0$ ), monzogranites ( $(^{87}\text{Sr}/^{86}\text{Sr})_i = 0.709$  to  $0.710$ ;  $\epsilon_{\text{Nd}} = -5.5$  -  $-6.0$ ) and biotite granite ( $(^{87}\text{Sr}/^{86}\text{Sr})_i = 0.712$  to  $0.716$ ;  $\epsilon_{\text{Nd}} = -6.0$  -  $-8.0$ ). Associated with these are a number of diorite bodies with olivine hornblende and hornblende cumulates ( $(^{87}\text{Sr}/^{86}\text{Sr})_i = 0.706$  to  $0.710$ ;  $\epsilon_{\text{Nd}} = -1.5$  to  $-6.5$ ). These intermediate and ultramafic rocks are among the least isotopically evolved of the main Querigut suite.

Enclaves are distributed throughout the felsic rocks of the Massif, although they are most abundant within the granodiorites and tonalites. Most have a finer grain-size than their host, and have textures that indicate magmatic

crystallization. They vary widely in the modal abundances of hornblende, plagioclase and biotite phenocrysts. The presence of corroded calcic plagioclase overgrown by more sodic plagioclase rims, suggests that magma-mixing may have been involved in the formation and subsequent modification of some enclaves, although other features such as armoured quartz ocelli are generally absent, and there are alternative explanations for such zoning patterns. Many of the textural and mineralogical features of the enclaves are similar to those of the main diorites. Therefore, it could be hypothesised that the enclaves and the diorites are genetically related, with the enclaves representing dispersed blobs of the same magma that formed the larger diorite intrusions. However, it is particularly important, that there are assemblages of contrasting enclave types within centimetres of each other. Thus, enclave formation by some simple diorite-felsic magma mingling process is difficult to visualise.

The geochemical and isotopic characteristics of the enclaves are of particular interest. On variation diagrams of all kinds, the enclaves do not form coherent arrays between any of the main Querigut magmas. Instead, they show a wide dispersion. This is most apparent for trace-element concentrations, and highlights the impact that simple variations in modal mineralogy can have on compositions. The wide dispersion of enclave data on isotope-isotope plots highlights the polymagmatic character of the Querigut enclaves, that does not fit with any simple, one- or two-magma model for their genesis. For those enclaves that do fall between potential end-members, the data cannot be used to limit their possible origins beyond a minimum of two different models. Another important observation is that some mafic enclaves have Sr and Nd isotopes more crustal than neighbouring intermediate enclaves. This lack of expected parity between enclave mineralogy, geochemistry and isotope characteristics makes interpretation difficult by any of the popular models for the origin and significance of enclaves (*e.g.* mingling, hybridisation, restite-unmixing or crystal accumulation). While, in some cases, they may be comagmatic with their hosts, the bulk of the enclaves seem to be no more than dispersed fragments of unrelated accessory, though broadly cogenetic, magmas caught up in the pluton plumbing system.

Although the presence of enclaves in granitoid rocks is undoubtedly meaningful at some level, there is probably no general statement that can be made about their significance. It seems that the Querigut enclaves are of little significance in the overall petrogenetic evolution of any of

the granitic units. For most of the enclaves, geochemical and isotope data are unable to uniquely constrain their origins. If this is more generally the case, it would seem that, whilst intrinsically interesting, enclave studies may be of very little actual use in unravelling the mysteries of granite petrogenesis.

### **The Plutonic Zone: Significance of the Lower Crust Between the Conrad and Mohorovicic Discontinuities**

Roddick, James A.

*Geological Survey of Canada, 100 West Pender St.,  
Vancouver, B.C., V6B 1R8 Canada*

In most places on all continents the lower crust is markedly seismically reflective and electrically conductive. The combined geophysical effect is most easily accounted for by hydrothermal fluids (saline solutions) resulting from the inevitable breakdown of hydrous minerals. Depth to the top of the zone is less in most Phanerozoic regions (10–20 km), because of higher heat flow, than in the shield regions (20–35 km), and corresponds to the temperature range of 350–400°C. That depth also marks the transition zone where plastic deformation begins to supplant brittle fracture. The principal physical effect of the tenuous hydrothermal fluid (rarely > 1%) is a slight reduction in mass viscosity of the lower crust to perhaps  $10^{18}$  from normal crustal values of about  $10^{23}$ . Structural integrity is preserved, but plastic creep (essentially horizontal) in response to load stress is enabled. The chemical effects, however, are much more profound, and over long periods inevitably rearrange the components of the lower crust and change its texture. This process constitutes plutonism, and its region of activity is best encompassed by the term plutonic zone.

The temperature pattern across the plutonic zone drives metasomatic reactions in the direction of chemically stabilizing the heterogeneous lower crust. In a dry environment the main plutonic minerals are metastable over the normal temperature range of the crust but in the presence of free hydrous fluid they become temperature sensitive. Acting over long periods, plutonism basifies the lower part of the zone, at the expense of the upper part. Plutonism can be halted only by loss of hydrous fluid (into fractures, or into hydrous minerals) or by fusion which

destroys both the hydrous medium and the structural integrity of the affected region.

Substantial volumes of the lower crust are homogenized by plutonism, but mobilization and intrusion as plutons is dependent on stress being great enough to exploit the small viscosity difference between this material and its envelope. Such stress is thought to be commonly transmitted from converging plate margins. Because of horizontal inflow, the Moho does not rise in response to pluton emplacement, which, regionally, is a crustal thinning process.

Can batholithic-size magma chambers exist anywhere in the crust, especially in the lower crust? The mechanism by which a large volume of low viscosity material can support the crust above, is not apparent. Nor is the mechanism intuitive by which such material can be brought up through many kilometers of heterogeneous crust in the shape and size of common plutons. The unmelted envelope is certainly not homogeneous and without irregularities. In such an environment the concentration of enormous stresses at certain points cannot be prevented, or resisted; magma will be forced into relatively narrow fractures, which, if they reach the surface will result in volcanism. Does this mean that the concept of a large magma chambers in the crust is a "veritable warren of untruth, in fact, a scarcely propped vacuity"? Probably, and we fake the rest.

### **A Belt of High-K Plutonic Rocks Related to Crustal Extension: Evidence from the European Variscan**

Rossi, Philippe and Cocherie, Alain  
*BRGM, B.P. 6009, 45060 Orléans, France*

Strongly potassic mafic magmas of calc-alkaline affinity, *i.e.* lamprophyres such as minettes, vogesites, kersantites and spessartites, occur as dyke swarms or sills that intersect country rocks in continental areas. They can be associated with trachydacites and rhyolites, and could be related to crustal extension and heating.

In the Variscan belt of western and central Europe, stocks of ultrapotassic to high-potassic ( $1.5 < K_2O/Na_2O < 3$ ) mafic plutonic rocks commonly are associated with strongly foliated, acidic and K-rich granitoid plutons.

Ultrapotassic mafic rocks were recognized quite early and described with exotic names, such as: vaugnérites in

the Lyonnais Massif, France; stavrites, fraidornites, redzvizites in the Schwarzwald; or mafic durbachites in the Bohemian Massif. Such rocks display several common characteristics throughout the different massifs: "primary minerals" are Cr-diopside to augite clinopyroxene, Ca-plagioclase, Ba-rich K-feldspar, and foxy-red Mg-Ti biotite with rare relics of phlogopitic mica. Ilmenite, generally surrounded by titanite, is the most abundant oxide. Of particular interest is the occurrence of chromium spinel in micaceous aggregates, which could be relics of olivine. Apatite and zircon are the earliest minerals. The chemical composition of such ultra-K to high-K rocks is characterized by a strong enrichment in HFSE elements, and can be compared to that of shoshonite or lamprophyre.

Associated granitoids, ranging in composition from monzonite to monzogranodiorite, show great variety, but generally are medium- to coarse-grained and very commonly mega-K-feldspar bearing. The systematic occurrence of actinolitic hornblende is characteristic of both acidic and mafic rocks, and is interpreted as the result of magmatic crystallization. Such plutonic rocks are quite common and occur as banded-like intrusions, marked by K-feldspar megacrysts, lens- or cigar-shaped enclaves of mafic rock that range from very small to about 1 m in size, and layers of biotite.

Such intrusions occur throughout the European Variscan N-S branch, from Corsica to Central Europe, e.g. the Bohemian massif, as a discontinuous belt of about 1500 km width through some of the external massifs of the Alps (e.g. part of the Belledonne and Aar-Gotthard massifs) and in the north of the French Massif Central, and then in an E-W direction through parts of the Vosges-Schwarzwald massifs into the Central Pluton of the Bohemian Massif.

It has been shown in Corsica that this early plutonism, which postdates continental collision, is of Early Carboniferous age and was emplaced in an amphibolic environment during anatexis of the uplifting basement after a crustal shortening episode.

The ages of different intrusions were investigated along such a mobile belt using the Pb-zircon evaporation method, taking into account that it occurs in both mafic and silicic rocks. The results indicate that most potassic intrusions were emplaced around 340 Ma (e.g. Corsica:  $339 \pm 11$  Ma; the external crystalline massifs of the Alps  $332 \pm 13$  Ma; the Bohemian Massif  $346 \pm 6$  and  $343 \pm 8$  Ma). Other published U-Pb data fully agree with previous these ages.

This high-K magmatism thus took place within a relatively short period within pull-apart structures along a crustal mega-shearzone. This structural feature formed the southern margin of the Variscan orogen and affected the Gondwana palaeo-continent after the crustal-collision processes.

### Contrasting Fe-Enrichment Trends in Calc-Alkaline Granitoid Plutons From Cima d'Asta and Monte Croce, Southern Alps, Italy

<sup>1</sup>Rottura, A., <sup>2</sup>Del Moro, A.,

<sup>3</sup>Caggianelli, A., <sup>4</sup>Bargossi, G.M.,

<sup>1</sup>Gasparotto, G. and <sup>2</sup>Pinarelli, L.

<sup>1</sup>*Dipartimento Scienze Mineralogiche,*

*Università di Bologna, I-40126 Bologna, Italy*

<sup>2</sup>*Istituto di Geocronologia e Geochimica Isotopica*

*C.N.R., I-56100 Pisa, Italy*

<sup>3</sup>*DiTEC, Università della Basilicata,*

*I-85100 Potenza, Italy*

<sup>4</sup>*Istituto di Petrografia e Giacimenti Minerari,*

*I-43100 Parma, Italy*

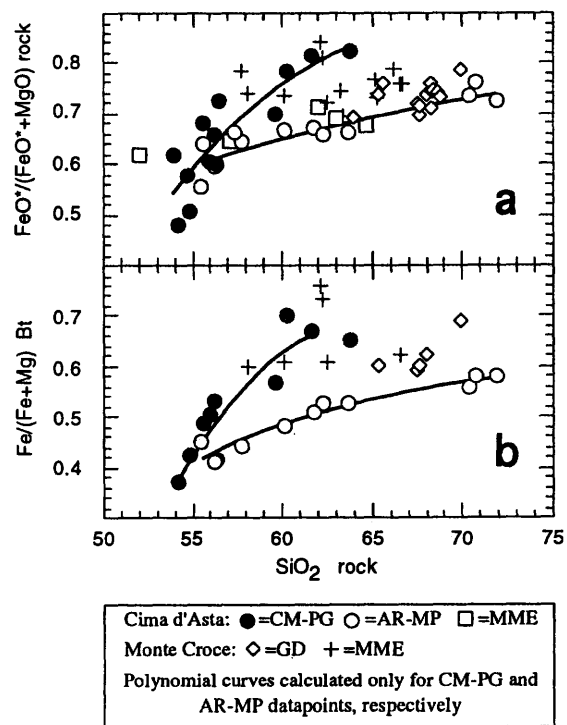
The Cima d'Asta and Monte Croce granitoid intrusions (eastern Southern Alps) belong to a large calc-alkaline ilmenite-bearing volcano-plutonic association of Early Permian age. The granitoids were emplaced at shallow levels at the end of the Hercynian orogeny (274-285 Ma) in a post-collisional (trans)tensional setting.

The Cima d'Asta complex consists of a multipulse main pluton (~ 200 km<sup>2</sup>) made of biotite monzogranites with subordinate biotite ± hornblende tonalites and granodiorites. The Monte Croce pluton (~ 25 km<sup>2</sup>) consists of biotite ± hornblende-bearing granodiorites. Fine-grained intermediate rock types (biotite-hornblende ± pyroxene-bearing quartz norite to melagranodiorite) occur as small satellite bodies (CM, PG, AR, see figure) around the Cima d'Asta main pluton (MP), and as mafic microgranular enclaves (MME) hosted in all the granitoid facies of both plutons. Magma mingling relationships can be observed in both granitoid complexes.

The granitoids form a high-K, metaluminous to subaluminous, calc-alkaline I-type suite, as suggested by: QAP, K<sub>2</sub>O-SiO<sub>2</sub>, AFM, R1-R2 and Na<sub>2</sub>O-K<sub>2</sub>O-CaO diagrams; LREE-enriched patterns ( $Ce_N/Yb_N = 5 - 12$ )

with moderate negative Eu anomalies; LILE enrichment and Nb, Sr, P and Ti negative spikes in the normalized multi-element diagrams. The plutonics have highly variable Sr and Nd isotopic compositions ( $(^{87}\text{Sr}/^{86}\text{Sr})_i$  from 0.7057 to 0.7111;  $\epsilon_{\text{Nd}} = -2.7 - -7.5$ ) indicative of an open system evolution. A single-stage AFC process is ruled out by the lack of increasingly crustal isotopic signatures with rock acidity. Field, petrographic, geochemical and isotopic evidence favors the hypothesis that the granitoid suite originated through complex hybridization and fractionation processes involving both mantle and crustal derived magmas, in accordance with the genetic models inferred for the associated basaltic andesitic to rhyolitic volcanics.

CM and PG rocks, and some MME from the Monte Croce pluton have Fe-rich biotite ( $\text{FeO}^T$  up to 29 wt %) and amphibole (Fe-Ts to Fe-Hbl) compositions, with  $\text{SiO}_2$  rock content ranging between 54 and 64 wt %. Despite their abundance in iron, Fe-Mg minerals have calc-alkaline affinity. However, the above rocks define a steeper Fe-enrichment trend with respect to the other plutonics, similar to a tholeiite-type evolution (Fig. a, b). They also show evidence of chilling, as indicated by the shapes of biotite and amphibole crystals, with length/width ratio up to 30. This suggests that the iron-rich mineral compositions reflect a former chemical feature of the hybrid intermediate mafic magmas, unrelated to any later comingling with the host granitoids. The distinct Fe-enrichment trends indicate that at least two pulses of variably hybridized intermediate magmas were involved in the granitoid genesis. This might reflect the complex nature of the post-orogenic high-K calc-alkaline magmatism of this sector of the eastern Southern Alps and, more generally, of other I-type granitoid suites. The contrasting Fe-enrichment trends could represent the product of: 1) two distinct magma sources; or, 2) two related magma batches which evolved under different redox conditions.



## ORAL PRESENTATION

### Application of Rock Deformation Experiments to Melt Segregation in the Lower Crust

Rushmer, Tracy

*Department of Geology, University of Vermont,  
Burlington, VT 05405-0122, USA*

The Third Hutton Symposium comes during a time of major change in our thinking in regard to melt segregation and melt migration in the lower crust. Current ideas on how the partially molten lower crust behaves, both rheologically and chemically, are just now being incorporated into crustal evolution models. One way in which we have gained further insight into melt segregation has come from the results of several recent experimental studies on rock behaviour during partial melting. Experiments performed on crustal rock cores under both hydrostatic conditions and during deformation have led, in part, to the conclusions that (1) the dihedral angle model which suggests that melt migration is largely or solely controlled by the interfacial energy between melt and mineral cannot dominate melt

segregation processes in the lower crust, and (2) the "critical melt fraction" model which requires granitic melt to remain in the source until melt fractions reach >25 vol % is not a reliable model for melt segregation. The most recent experimental results on crustal rock cores which have helped advance our understanding of melt segregation processes, including the potential geochemical consequences, are discussed below.

Although not all have been able to produce equilibrium textures readily, hydrostatic experiments on cores of amphibolite by Hacker (1990) and Wolf and Wyllie (1995), and on quartz + muscovite cores by Brearley and Rubie (1990) and on quartz aggregates by Laporte (1994), the experiments have provided results for understanding the textures and reaction mechanisms at the beginning of melting. Melt (1-5 vol %) in the amphibolite samples was found both in pools at hbd/plag/qtz triple junctions and along hbd/plag grain boundaries. The melt distribution is initially crystallographically controlled in the hornblende-dominated assemblage, and melt interconnectivity is achieved at low melt fractions. The presence of many diverse and anisotropic minerals in the lower crust, such as hornblende, precludes predicting melt interconnectivity which is a requirement for melt segregation by this model.

Non-hydrostatic or rock deformation experiments on amphibolite by Hacker and Christie (1990) and Rushmer (1995), and on granite by Rutter and Neumann (1995) have shown that melting reactions induced fracture and cataclastic deformation, even in previously ductile rock, and formed pathways for melt migration. As melt fraction increased deformation became viscous and the rock flowed homogeneously. A sharp drop in effective viscosity was not observed. Interpretation of these observations suggests that melt may be able to migrate out of the system by either fracture or flow depending on type of melting reaction (vapor phase-present versus vapor phase-absent), depth of melting reaction (brittle or ductile regime) and strain rate (*e.g.*, see Dell'Angelo and Tullis, 1987), among other factors. This is in contrast to a critical melt fraction model in which viscous melt can only separate from its source at a pre-determined, specific melt fraction interval.

Future work must tie in geochemical data with physical melt segregation models. With ion probe technology and specially designed experiments, we are now able to better measure partitioning of trace and rare earth elements during hydrostatic melting (see current work by Cavallini *et al.*, 1995) and during deformation. Recent ion probe results from the deformed partially molten amphibolite samples show that major trends, such as a depletion in Y

and HREE when garnet is present, are as expected. However, even though local major element chemical equilibrium appears to have been achieved in the melted rock cores, HFSE such as Zr are not fully equilibrated (Rushmer *et al.*, 1994). This suggests that the slow dissolution rates of accessory phases such as apatite and titanite may easily result in extracted melt compositions which have lower abundances of these elements than predicted by partition coefficients. In addition, future melt segregation models must include permeability/porosity changes that occur during melting. The rate of melting may be a major factor in increasing permeability during reaction. These variables need also to be quantified by specific key experiments.

As we continue to update our geochemical and physical models of melt segregation and migration, our overall understanding of the diverse possibilities of granite generation and potential emplacement mechanisms in the Earth's crust will hopefully advance dramatically as well.

- Brearley, A. J. and Rubie, D.C., 1990. Effects of H<sub>2</sub>O on the disequilibrium breakdown of muscovite + quartz. *J. Petrol.*, **31**, 925-956.
- Cavallini, M., Vielzeuf, D., Bottazzi, P., Mazzucchelli, M. and Ottolini, L., 1995. Direct measurements of rare earth contents in partial melts from metapelites. *Terra Abstracts*, **6**, 344-345.
- Dell'Angelo, L.N. and Tullis, J., 1987. Experimental deformation of partially melted granitic aggregates. *J. metamorphic Geol.*, **6**, 495-516.
- Hacker, B., 1990. Amphibolite - facies - to - granulite - facies reactions in experimentally deformed, unpowdered amphibolite. *Am. Mineral.*, **75**, 1349-1361.
- Hacker, B. and Christie, J.M., 1990. Brittle/ductile and plastic/cataclastic transitions in experimentally deformed and metamorphosed amphibolite. In Durham, W., Duba, A., Handin, J. and Wang, H. (eds), *Brittle-Ductile Transitions: The Heard Volume*, Geophysical Monograph Series, AGU, **20**, 127-147.
- Laporte, D., 1994. Wetting behavior of partial melts during crustal anatexis: The distribution of hydrous silicic melts in polycrystalline aggregates of quartz. *Contrib. Mineral. Petrol.*, **116**, 489-499.
- Rushmer, T., 1995. An experimental deformation study of partially molten amphibolite: Application to low melt fraction melt segregation. *J. Geophys. Res.* **100**, in press.
- Rushmer, T., Pearce, J.A., Ottolini, L. and P. Bottazzi, P., 1994. Trace element behavior during slab melting: Experimental evidence. *EOS Trans. Am. Geophys. Union*, **75**, 746.
- Rutter, E., and Neumann, D., 1995. Experimental deformation of partially molten Westerly Granite under fluid-absent conditions, with implications for the extraction of granitic magmas. *J. Geophys. Res.* **100**, in press.
- Wolf, M.B. and Wyllie, P.J., 1995. Liquid segregation parameters from amphibolite dehydration-melting experiments. *J. Geophys. Res.*, **100**, in press.

## Melt Segregation and Melt Geochemistry: What Can Experiments Tell us?

Rushmer, Tracy

*Department of Geology, University of Vermont,  
Burlington, VT 05405-0122, USA*

One of the important directions in the study of crustal evolution is linking theoretical models of granite source regions and melt segregation with the geochemical data extracted from the granites themselves. Recently several studies in granite and leucogranite-bearing terranes such as the Himalaya have shown that the geochemical trace and rare earth element behavior in these granites did not occur as predicted by equilibrium geochemical models. These geochemical data have increased suspicions that melt does not reside long enough in the source region to reach full equilibration. Major questions are now being raised about the tools we use to study granites. In particular, how we can best use the geochemistry data to interpret the nature of the lower crust? One method is to perform partial melting experiments on crustal rocks to better understand the partitioning of trace and rare earth elements during melting, both under hydrostatic conditions and with deformation. Early work on dissolution rates of accessory phases in granitic melt (*e.g.*, Harrison and Watson, 1983) has shown that kinetics will play an important role in the resulting melt trace and rare earth element abundances.

Data have been recently collected from partially molten amphibolite experiments by electron microscope and SIMS. The elements K, Sc, Ti, Cr, Rb, Sr, Y, Zr, Nb, Ba and the REE have been determined in two experiments; one partially melted and deformed at 0.8 GPa, and other at 1.8 GPa (Rushmer *et al.*, 1994). In the 0.8 GPa experiment, analyses were taken of minerals and melt in the coexisting assemblage, clinopyroxene + hornblende + plagioclase + tonalitic melt. The resulting REE pattern of the melt is similar to that of amphibole (*e.g.* La/Sm = 1.7-3.1; Sm/Yb = 0.8-1.1) but with lower absolute abundances due to residual mafic phases and titanite (which is still present in the sample and did not dissolve in the melt, as observed below). At the higher pressure (1.8 GPa), analyses were taken of the mineral and melt assemblage, garnet + clinopyroxene + plagioclase + trondhjemitic melt. The accessory phases, titanite and zoisite were also analyzed. The REE pattern of the trondhjemitic melt is steep (La/Sm = 4.8-7.5; Sm/Yb = 16-20) as expected owing to the presence of garnet, but the high field strength elements (HFSE) have unpredicted bulk

distributions. Mass balance between the experimental charges and the starting composition shows that the abundances of some elements are less than unity for the major residual assemblages in the experiments. This means, theoretically, the melt phase should be enriched in these elements relative to the starting composition, but the data show that the melt is not enriched in important elements, such as the HFSE. This behavior is because the minor phases, in particular titanite, have not completely dissolved and have retained many of the elements which should be in the melt.

During deformation-enhanced melt segregation in the lower crust, trace and rare earth elements might behave very similarly. Data are also currently being collected on partial melts in the felsic system under hydrostatic conditions by Cavallini *et al.*, (1995). Together, these experimental results provide new information which will help in the interpretation of granite geochemical data and assist us in coming to a more complete understanding of the potential geochemical trace and rare earth element abundances and REE patterns produced during melt segregation.

Cavallini, M., Vielzeuf, D., Bottazzi, P., Mazzucchelli, M. and Ottolini, L., 1995. Direct measurements of rare earth contents in partial melts from metapelites. *Terra Abstracts*, **6**, 344-345.

Harrison, T.M. and Watson, E.B., 1983. Kinetics of zircon dissolution and Zr diffusion in granitic melts of variable water content. *Contrib. Mineral. Petrol.*, **84**, 66-74.

Rushmer, T., Pearce, J.A., Ottolini, L. and Bottazzi, P., 1994. Trace element behavior during slab melting: Experimental evidence. *EOS Trans. Am. Geophys. Union*, **75**, 746.

### Geochemical and Nd-Sr Isotopic Composition of Alleghanian Granites of the Southern Appalachians: Origin, Tectonic Setting, and Source Characterization

<sup>1</sup>Samson, S.D., <sup>1</sup>Coler, D.G. and <sup>2</sup>Speer, J.A.

<sup>1</sup>*Department of Earth Sciences, Syracuse University,  
Syracuse, NY 13244-1070, USA*

<sup>2</sup>*Mineralogical Society of America, 1130 17<sup>th</sup> St., N.W.,  
Suite 330, Washington, D.C. 20036, USA*

One of the major manifestations of the late Paleozoic Alleghanian orogenic event was the formation of numerous high potassium (K<sub>2</sub>O ~ 3-4%), metaluminous granites that were emplaced into many of the major lithotectonic

belts in the southern Appalachians. The range in initial  $\epsilon_{\text{Nd}}$  values, depleted mantle model ages, and  $(^{87}\text{Sr}/^{86}\text{Sr})_i$ , respectively, of these granites is -8.2 to -3.4, 940-1020 Ma, and 0.70642 - 0.72798 for the Inner Piedmont; -2.3 to +2.0, 660-1130 Ma and 0.70421 - 0.71035 for the Kiokee belt; -2.7 to +2.4, 660-870 Ma and 0.70353-0.70816 for the Eastern slate belt; -6.7 to +1.9, 690-1140 Ma and 0.70391 - 0.70739 for the Carolina terrane; and, -4.4 to +3.0, 600-1070 Ma and 0.7033 - 0.7078 for the Raleigh belt.

The chemical and isotopic compositions of the granites are most consistent with their formation by anatexis of continental crust, rather than derivation from a depleted mantle source. The pre-Alleghanian rocks of the Carolina terrane, the Raleigh belt, and Eastern slate belt have  $\epsilon_{\text{Nd}}(300 \text{ Ma})$  values indistinguishable from the values of the Alleghanian granites emplaced within these terranes, suggesting that these terranes are a likely source of many of the granites. Some Alleghanian plutons within the Carolina terrane, however, require a more evolved source than the exposed crust of the Carolina terrane. Either the Carolina terrane is isotopically heterogeneous with depth, or more likely, Grenville basement occurs structurally below, or tectonically interleaved within, the terrane. The granites within the Inner Piedmont have higher  $(^{87}\text{Sr}/^{86}\text{Sr})_i$  and lower  $^{143}\text{Nd}/^{144}\text{Nd}$  ratios than most of the other granites, possibly indicating that the Inner Piedmont is not as juvenile as the other major Appalachian terranes.

Although it has been suggested that the granites were generated by east-dipping subduction beneath Laurentia, the lack of Alleghanian plutons with tonalitic to granodioritic compositions, the small volume of the granites, and the absence of geographic trends in major element and isotopic composition across the orogen, makes a subduction origin for the granites extremely unlikely. The chemical and isotopic data are more consistent with the formation of the granites by wholesale melting of continental crust. The evidence for the production of these granites by crustal anatexis, taken together with the observation that they were intruded synchronously with Alleghanian thrusting in the Valley and Ridge Province, suggests strongly that they are collisional in origin. The crustal heating events that produced the granites might have been caused by delamination of the mantle lithosphere during terminal collision of Laurentia and Gondwana, as suggested by Sacks and Secor (1990) and Nelson (1992), or alternatively adequate heating may have occurred by crustal thickening during emplacement of thrust sheets (cf. Patino Douce *et al.*, 1990).

Nelson, K.D., 1992. Are crustal thickness variations in old mountain belts like the Appalachians a consequence of lithospheric delamination? *Geology*, **20**, 498-502.

Patino Douce, A.E., Humphreys, E.D. and Johnston, A.D., 1990. Anatexis and metamorphism in tectonically thickened continental crust exemplified by the Sevier hinterland, western North America. *Earth Planet. Sci. Lett.*, **97**, 290-315.

Sacks, P.E. and Secor, D.T., 1990. Delamination in collisional orogens. *Geology*, **18**, 999-1002.

## ORAL PRESENTATION

### Melt Segregation or Magma Mobility - the Difference Between Migmatites and Granites

Sawyer, E.W.

*Sciences de la Terre, Université du Québec à Chicoutimi, Chicoutimi, Québec, G7H 2B1 Canada*

Melt segregation is the separation of melt from its residuum, whereas magma mobility is the movement of melt plus entrained crystals. For either to occur requires a differential movement between the melt and the residuum, or between the melt plus crystals and some pre-melting reference frame. This can be considered in terms of the velocity of the melt or magma ( $V_m$ ) and the residual solids ( $V_s$ ). Four cases are considered, and their relation to crustal melting is crucial in understanding how granite magmas form.

1)  $V_m = V_s = 0$ . For this end member case the melt fraction and solid residuum remain at the site of melting and there is no melt segregation or magma mobility. Melting under such conditions forms small-scale nebulitic, patch and flecky migmatites and mantle-core structures (melt rims on a core of garnet or orthopyroxene) typical of some granulites. At larger scales  $V_m = V_s = 0$  probably cannot be maintained, unless the melt fraction is very small (less than that required for melt interconnectivity), because deformation and/or melt buoyancy, will generate an instability that initiates melt segregation or magma mobility.

2)  $V_m > V_s = 0$ . Here, the restite remains in place, but the melt fraction moves. This condition applies to those migmatites containing leucosomes (melt) with associated melanosomes (restite), and to some depleted granulites. Estimates of the melt fraction suggest that melt segregation can begin with 5 to 9% melt present, but that in most migmatites 20 to 35% melt is needed. However,

the melt from this type of migmatite (metatexite) is not, in general, the source of granite plutons for two reasons. A) Composition - data from migmatites with leucosomes and melanosomes shows that, regardless of whether they come from the amphibolite or granulite facies, the migmatite melts have lower ( $\text{FeO}^T + \text{MgO}$ ), Zr, Y, and REE, but higher  $\text{SiO}_2$ , than parental granite magmas. The only granites for which migmatite leucosomes are a plausible source are the Manaslu-type leucogranites - a point already made by LeFort. The low ( $\text{FeO}^T + \text{MgO}$ ) of migmatite leucosomes indicates that the segregation process is very effective at separating melt from restite. In contrast, the presence of a significant restite component in many granites implies that granite magmas formed by a different and less efficient segregation process. B) Rheology - the outcrop appearance of metatexite migmatites shows no magma-like flow, *i.e.*, their rheology is that of solid rock and not a magma. Thus, it is difficult to imagine how the restite component can be added to the almost pure melt fraction to make parental granite magmas.

3)  $V_m = V_s > 0$ . This is magma mobility without segregation. Diatexite migmatites that exhibit flow structures, but have compositions identical to their palaeosome, are examples of this behaviour. Magma mobility can occur if there is enough melt to breakdown the matrix framework, such a critical melt fraction (CMF) depends upon many factors, *e.g.*, size and shape of matrix crystals, matrix mineralogy, and on applied stresses, but is typically around 20 to 50% melt. However, there is evidence that mobility can occur with melt fractions below the CMF once sufficient melt has formed to coat the grains, perhaps other deformation mechanisms, such as grain boundary sliding or melt enhanced solution-precipitation processes occur.

4)  $V_m > V_s \geq 0$ . Both the melt and the restite move (magma mobility), but because the melt fraction has the greater velocity melt segregation also occurs; the melting region has the rheology of a magma. Diatexite migmatites are examples of melting under these conditions. In most diatexites the bulk of the restite does not move very far, but a small portion remains in the magma. As with case (3) uncertainty remains as to the proportion of melt required for mobility. Some Opatca Belt diatexites were mobile with only 19% melt, but in most mobility occurred when 34 to 70% melt was present, in agreement with the expected CMF for a leucotonalite source. The rheological and compositional properties of diatexite migmatites and the fact that they occur at the same scale as plutons and

plutonic belts, indicates that this type of migmatite is the connection to granites.

### Melt Segregation or Magma Mobility and the Migmatite-Granite Connection: The Field and Geochemical Evidence

Sawyer, E.W.

*Sciences de la Terre, Université du Québec à Chicoutimi, Chicoutimi, Québec, G7H 2B1 Canada*

The idea that there is a transition through migmatites to granites is an attractive one, but in recent years several contrary opinions have been expressed. Migmatites occupy a fringe position in petrology, they are obviously not regarded as metamorphic rocks in the sense that greenschists or granulites are; probably because they have undergone melting, severe textural modification and material transport. Neither are migmatites treated as igneous rocks because they typically have a lot of unmelted rock and are structurally far more complex than most igneous petrologists like their rocks to be. There are basically two types of migmatite: 1) metatexites where melting is minor and original pre-melting fabrics or layering is preserved largely intact; and, 2) diatexites where the original textures and fabrics have been destroyed and flow structures dominate. Metatexites have been widely studied and typically have small leucosomes that are associated with mafic selvages. Diatexites have not been studied much and exhibit complex leucosome-restite relationships, typically melt and restite show all degrees of separation. When the geochemistry of migmatites and granites is compared several interesting facts emerge. The leucosomes from metatexite migmatites are too  $\text{SiO}_2$ -rich but too poor in  $\text{FeO}^T$ ,  $\text{MgO}$ , Sc, Cr, Zr, Hf, REE, and Y to be considered as the source magma for most granite plutons, the exceptions are the Manaslu-type leucogranites. However, the melt-rich parts of diatexite migmatites overlap considerably the compositional field of granites, and could be suitable sources for granite magmas. The geochemical differences between metatexites and granites implies that segregation process was different - that operating in metatexites being far more efficient than that in granites or diatexites. Consider rheology. Metatexite migmatites preserve pre-migmatization structural integrity, implying a rock-like rheology. In contrast the structure of

both diatexites and granites indicates a magma rheology. Nonetheless the existence of diatexites has been denied by some, simply sweeping this group of rocks into granites as "dirty granites". This is not justified by the field evidence from the Opatica, St Malo, Trois Seigneurs, Ashuanipi, Quetico and Higo migmatite terranes. In some cases diatexite migmatites grade from metatexites, have the same composition as the source (Ashuanipi and Quetico) and are *in situ*. Which means that diatexites are an up-grade progression from metatexites or in heterodox parlance metatexites are the down grade equivalent of "dirty granites". In the Opatica Belt migmatites and granites are observed at their place of formation in 6 kbar rocks and the anatectic products can be traced without break right through the crust to emplacement in 2 kbar rocks. In this case structural and geochemical continuity can be demonstrated across the migmatite-granite transition and to the upper crust. Re-examination of published diatexite data from other terranes shows the same geochemical trends, and in at least two cases where details are provided the same structural continuity also. However, not all diatexites terranes produced significant volumes of granite plutons.

**Effects of  $f_{O_2}$  on Phase Equilibria  
in Granitic Systems.  
Conditions of Stability and  
Compositional Variation of  
Biotite and Amphibole**

Scaillet, Bruno, Pichavant, Michel  
and Dall'Agnol, Roberto

*Centre de Recherche sur la Synthèse et la Chimie des  
Minéraux, CNRS, 1A rue de la Férollerie,  
45071 Orléans Cedex 02, France*

Crystallization experiments have been carried out on a Proterozoic granite of N Brazil of bulk composition (in wt %):  $SiO_2 = 72.1$ ,  $Al_2O_3 = 13.4$ ,  $FeO^T = 3.7$ ,  $MgO = 0.7$ ,  $CaO = 2.2$ ,  $Na_2O = 3.8$ ,  $K_2O = 3.4$ ,  $TiO_2 = 0.8$ . Dry glasses were used as starting products, obtained by two steps of melting at 1400°C of the crushed granite. Experiments were performed at a constant pressure of 3 kbar in two internally heated vessels pressurized with Ar (oxidized) and Ar-H<sub>2</sub> mixtures (reduced). Temperatures ranged from 900 to 700°C. The  $a_{H_2O}$  was controlled by

H<sub>2</sub>O - CO<sub>2</sub> mixtures with fluid/silicate ratios ranging from 10 to 20% ( $X_{(H_2O)_i}$  = starting H<sub>2</sub>O/(H<sub>2</sub>O+CO<sub>2</sub>), between 1 and 0.2). Ag<sub>70</sub>Pd<sub>30</sub> and Au capsules were used. For oxidizing conditions, the  $f_{O_2}$  was fixed by the intrinsic hydrogen fugacity of the vessels, evaluated to be at NNO + 0.5 by using the H<sub>2</sub> sensor technique of Taylor *et al.* (1992). For reduced conditions,  $f_{O_2}$  was fixed around FMQ-0.5 with  $P_{H_2}$  read with a Shaw membrane. Run durations varied between 1023 (700°C) and 166 hours (900°C). After optical inspection, run products were characterized by X-ray and EMPA, SEM techniques. Water contents of quenched glasses were determined with the "by-difference" method using a specific calibration procedure of the EMPA.

The major phases identified are: plagioclase (Pl), alkali feldspar (Af), quartz (Qtz), orthopyroxene (Opx), Ca-rich pyroxene (CaPx), amphibole (Amph), biotite (Bi). Sphene (Sph), magnetite (Mt) and Ti-hematite (Th) are present at NNO + 0.5, while at FMQ - 0.5 only ilmenite (Il) is present. The phase relations obtained under oxidized and reduced conditions have important features in common: 1) Pl is the liquidus tectosilicate phase followed by Qtz and Af at decreasing  $a_{H_2O}$  for a given  $T$ ; 2) Amph is the stable hydrous phase at high water content (melt water content > 4-5 wt %), Bi being stable at low  $f_{O_2}$ , and, 3) the solidus temperature does not change with  $f_{O_2}$ . Differences between the two phase diagrams include: 1) at a given water content, the thermal stabilities of Pl, Qtz, Af, Amph and Opx are depressed by *c.* 40-50°C when  $f_{O_2}$  is reduced; 2) there exists a significant overlap between Bi and Amph stability fields at FMQ - 0.5; 3) Amph is stable down to solidus conditions at FMQ - 0.5, whereas at NNO + 0.5, Amph is never stable at the solidus.

When decreasing  $f_{O_2}$  from NNO + 0.5 to QFM - 0.5 at 700°C, Amph Fe/Fe+Mg ratio increases from 0.36 to 0.71. In contrast, <sup>VI</sup>Al remains constant (1.4 pfu for 23 O), suggesting minor effects of  $T$ ,  $a_{H_2O}$  and  $f_{O_2}$  on this Amph compositional parameter. Bi composition increases in Fe/Fe+Mg from 0.43 (NNO+1.5) to 0.73 (QFM-0.5) at 700°C. Pl composition is strongly dependent on  $T$ ,  $a_{H_2O}$  and  $f_{O_2}$ . At a given  $f_{O_2}$ , An content increases with  $T$ , and decreases with  $a_{H_2O}$ . For a given temperature and  $a_{H_2O}$ , an increase in  $f_{O_2}$  is marked by an increase in the An content. For melt compositions, the major chemical evolution with decreasing  $T$  is characterized in the AFM projection by a shift toward the A apex at increasing F/M ratio, under both redox states investigated. However, at NNO + 0.5, the residual melt composition is more leucocratic than at

FMQ - 0.5, reflecting the higher Fe content of granitic liquids crystallizing under reduced conditions.

This work shows that  $f_{O_2}$  has an extremely important effect on the phase relations of granitic systems by depressing the liquidus temperatures of Pl, Qtz, Af, Amph. Under oxidized conditions, Bi and Amph are mutually exclusive, whereas at low  $f_{O_2}$  they coexist down to solidus conditions. It is important to stress that not only the stability of ferro-magnesian phases are affected but also that of all tectosilicates. In particular, the change in plagioclase composition under fixed  $T - a_{H_2O}$  but variable  $f_{O_2}$ , clearly indicates that activities of Pl forming components are  $f_{O_2}$  dependent. Thus variation in redox state of crystallizing granitic magmas must also be recorded by plagioclase zoning.

Taylor, J.R., Wall, V.J. and Pownceby, M.I., 1992. The calibration and application of accurate redox sensors. *Am. Mineral.*, **77**, 284-295.

## Quantifying Spatial Relationships Between Faults and Plutons

Schmidt, K.L., Paterson, S.R. and Lund, S.P.

*Department of Earth Sciences,  
University of Southern California,  
Los Angeles, CA 90089-0740, USA*

Faults and plutons of similar age commonly occur in the same region. This observation is often used to argue that there is a causative relationship between faults and the generation, ascent, or emplacement of plutons. To establish a causative relationship the following must be demonstrated: 1) a close spatial relationship between faults and plutons; 2) a close geometrical relationship between the shapes and orientations of plutons and the orientations of faults; 3) a close temporal relationship between faults and plutons; 4) that the rates of magma generation, ascent, and emplacement are compatible with rates of fault displacement; and, 5) the specific mechanism(s) by which the magma is generated, ascended, or emplaced. Here we evaluate only the first requirement, that of quantifying the spatial relationship between faults and plutons, paying particular attention to how scale affects the degree of spatial overlap between the two. This is particularly important because the scale at which a close spatial relationship is established may correspond to the scale of the process(es) causing this overlap.

A variety of processes may result in a close spatial relationship between faults and plutons. For example: 1) the ascent and emplacement of plutons may operate independently of faulting, and spatial overlap may be fortuitous; 2) fault systems may develop in crustal regions thermally softened by plutonism, or alternatively plutonism may occur in zones of active deformation due to changes in the stress or thermal structure of the crust; and, 3) individual faults may control the ascent and emplacement of plutons, or alternatively faults may nucleate on plutons.

What then constitutes a close spatial relationship at the scale of individual faults and plutons or at the scale of fault systems and magmatic belts? Our approach to this problem has been to evaluate a set of spatial parameters at different scales that can be statistically analyzed in order to determine random versus nonrandom distributions. Parameters used at the scale of individual faults and plutons include: 1) pluton spacing relative to fault spacing; 2) distance from pluton margin to nearest fault; 3) pluton diameters relative to fault spacing; 4) area covered by plutons relative to the total map area; and, 5) the amount of overlap between separate plutons in nested plutonic complexes. Parameters at the scale of fault systems and magmatic belts include: 1) distance between the centers of mass of fault systems and magmatic belts normalized to the total area of the zones; and, 2) area of the overlapping region between fault systems and magmatic belts normalized to the total area covered by these features. A computer program is used to create artificial maps of faults and plutons and produce statistical histograms for each of the above parameters. Random number generator algorithms allow us to examine a random distribution with respect to any given parameter. The program also generates nonrandom distributions, allowing us to define the characteristics of both random and non-random spatial relationships between faults and plutons. Once these have been examined, we have a statistical means for evaluating the degree of spatial overlap between single faults and plutons or fault systems and magmatic belts using data from geologic maps.

Initial results from analysis of maps of the Cascades Mountains, Washington, British Caledonides, and southern Appalachians indicate that, at the scale of individual faults and plutons (tens of km), little spatial overlap occurs between faults and plutons. For example, in the Cretaceous Cascades arc the average distance from pluton centers to faults is 6.4 km, the largest distance is 16.6 km and the smallest is 0.0 km; fault spacing averages 8.7 km, and pluton spacing averages 7.0 km. However, at the

scale of orogens (hundreds to thousands of km) spatial overlap may occur between active fault systems and active magmatic belts.

### **The Crooks Canyon Intrusive Complex: Bimodal Magmatism in a Proterozoic Island Arc Setting, Central Arizona**

Seaman, S.J. and Williams, M.L.

*Department of Geology and Geography, University of  
Massachusetts, Amherst, MA 01003, USA*

The Crooks Canyon intrusive complex (CCIC) is one of several 1750-1700 Ma apparently arc-related plutonic complexes in central Arizona (DeWitt, 1989; Anderson, 1989). The CCIC is part of the Yavapai province, characterized by mostly juvenile volcanic and plutonic crustal materials (Nelson and DePaolo, 1984; Wooden and DeWitt, 1991), and interpreted to have been accreted to North America during the ~1700 Ma Yavapai orogeny (Bowring and Karlstrom, 1990; Karlstrom and Bowring, 1991). Textural and compositional relationships in the well-exposed CCIC provide an unusual opportunity to assess the influence of infusions of basaltic magma on the evolution of felsic magmas occupying mid-crustal-level magma chambers in island arcs.

The CCIC hosts three types of granodiorite, moderately high-K basalt, an array of chilled magmatic enclave compositions, and a suite of gabbros. The gabbroic suite ranges in composition from high-K to tholeiitic island arc-like basalts and seems to have crystallized prior to the development of the bimodal complex. It is not described further here. The three granodiorites volumetrically dominate the complex. The first is a highly siliceous, fine-grained biotite granodiorite that occurs in the northernmost exposures of the complex. To the south, it becomes coarser grained, less silicic, less potassic, and more aluminous. This coarser grained granodiorite grades to the south into a potassium feldspar megacrystic biotite granodiorite. The megacrystic granodiorite is slightly depleted in both LREE and HREE compared to the fine-grained Crooks Canyon granodiorite. All three of the granodiorites have sharply negative Nb and Ti spikes on trace element abundance diagrams, and have low concentrations of Rb and Y, supporting an island arc ancestry.

The megacrystic granodiorite magma was repeatedly invaded by large volumes of basaltic magma. Several tens of square kilometers of exposure in the central portion of

the CCIC are dominated by complex basaltic/granodioritic magma interaction textures resembling those in the Pleasant Bay magmatic complex of Maine (Wiebe, 1993). Resulting magma mingling textures include the preservation of pipes of silicic magma which buoyantly rose through blankets of basaltic magma, resorption of potassium feldspars in the megacrystic granite near bodies of hot basaltic magma, and the development of hybrid compositions which resulted from mechanical mixing of the basaltic and granodioritic end members.

The largest volumes of basaltic magma occur in the southeastern portion of the northern lobe of the CCIC, and the felsic/mafic magma ratio increases to the north and west, suggesting that the lower reaches of the magma chamber may be preserved to the southeast. The basalt has the LREE-enriched REE pattern of typical high-K calcalkaline basalts of modern island arcs. High Ba/La and low La/Sm ratios support this interpretation. True basaltic (rather than microgranitoid) enclaves, as well as enclaves which are basalt/granodiorite hybrids, are common in the megacrystic granodiorite. On the larger scale, regional variations in the compositions of granodiorite may have resulted from the addition of varying amounts of the high-K basalt to the northernmost, most siliceous Crooks Canyon granodiorite. Simple mixing between the two end members can explain differences in most trace and REE concentrations in the three granodiorites.

The origin of the granodiorites, in view of their moderately peraluminous nature and K/Na near or slightly less than 1, may have resulted from anatexis involving the breakdown of biotite or possibly hornblende (Whitney, 1988). The basalt may represent a contribution to the heat source that facilitated the melt-producing reaction. Local textural complexity and possibly the regional compositional variation in the felsic rocks of the complex resulted from mingling and mixing of the mafic and felsic magma end members.

- Anderson, P., 1989. Stratigraphic framework, volcano-plutonic evolution, and vertical deformation of the Proterozoic volcanic belts of central Arizona. In Jenney, J.P. and Reynolds, S.J. (eds) *Geologic Evolution of Arizona*, Arizona Geological Society Digest 17, 57-148.
- Bowring, S. and Karlstrom, K., 1990. Growth and stabilization of Proterozoic lithosphere in the southwestern United States. *Geology*, 18, 1203-1206.
- DeWitt, E. 1989. Geochemistry and tectonic polarity of early Proterozoic (1700-1750-Ma) plutonic rocks, north-central Arizona. In Jenney, J.P. and Reynolds, S.J., (eds) *Geologic Evolution of Arizona*, Arizona Geological Society Digest 17, 149-163.

- Karlstrom, K., and Bowring, S., 1988. Early Proterozoic assembly of tectonostratigraphic terranes in southwestern North America. *J. Geol.*, **96**, 561-576.
- Karlstrom, K. and Bowring, S., 1991. Styles and timing of Early Proterozoic deformation in Arizona: Constraints on tectonic models. In Karlstrom, K.E. (ed), *Proterozoic Geology and Ore Deposits of Arizona*, Arizona Geological Society Digest **19**, 1-10.
- Nelson, B.K. and DePaolo, D.J., 1984. 1,700-Myr greenstone volcanic succession in southwestern North America and isotopic evolution of Proterozoic mantle. *Nature*, **312**, 143-146.
- Whitney, J., 1988. The origin of granite: The role and source of water in the evolution of granitic magmas. *Geol. Soc. Am. Bull.* **100**, 1886-1897.
- Wiebe, R., 1993. The Pleasant Bay layered gabbro-diorite, coastal Maine: Ponding and crystallization of basaltic injections into a silicic magma chamber. *J. Petrol.* **34**, 461-489.
- Wooden, J. and DeWitt, E., 1991. Pb isotopic evidence for the boundary between the Early Proterozoic Mojave and Central Arizona crystal province in western Arizona. In Karlstrom, K.E. (ed), *Proterozoic Geology and Ore Deposits of Arizona*, Arizona Geological Society Digest **19**, 27-50.

## Sr and Nd Isotope Geochemistry of Mesozoic Plutonic Rocks from Hong Kong: Implications for Granite Petrogenesis, Regional Structure, and Crustal Evolution in SE China

<sup>1</sup>Sewell, R.J. and <sup>2</sup>Darbyshire, D.P.F.

<sup>1</sup>*Hong Kong Geological Survey, 11/F Civil Engineering Building, 101 Princess Margaret Road, Hong Kong*  
<sup>2</sup>*NERC Isotope Geosciences Laboratory, Kingsley Dunham Centre, Nottingham NG12 5GG, UK*

Mesozoic granites of Hong Kong may be grouped into three NE-trending domains on the basis of Sr-Nd isotope and model age characteristics. Plutonic rocks of Zone I in the northwestern part of the Territory have  $\epsilon_{\text{Nd}}(t) < -9$ , Nd depleted-mantle model ages ( $t_{\text{DM}}$ ) of between 1.67 and 2.02 Ga, and  $(^{87}\text{Sr}/^{86}\text{Sr})_i > 0.710$ . They include I-type granites of the Lamma Suite, A-type granites of the Lion Rock Suite subgroup I, and a previously undescribed S-type granite, here defined as the Deep Bay Granite. Granites in the central Zone II exhibit a broad spectrum of isotope characteristics with  $\epsilon_{\text{Nd}}(t)$  values of between -4.2 and -7.0,  $t_{\text{DM}}$  of between 1.30 and 1.51 Ga, and  $(^{87}\text{Sr}/^{86}\text{Sr})_i$  in the range 0.7055 - 0.7152. They include I-type granites of the Lion Rock Suite subgroup II, I-type granite porphyry dykes, syenite stocks and dykes, and A-type granite

dykes and mafic dykes. Granites of Zone III in the southeastern part of the Territory dominantly comprise I-type compositions of the Lion Rock Suite subgroup III. These rocks have  $\epsilon_{\text{Nd}}(t)$  between -5.5 and -6.5,  $t_{\text{DM}}$  of between 1.39 and 1.47 Ga and  $(^{87}\text{Sr}/^{86}\text{Sr})_i$  in the range 0.7071 - 0.7109.

Based on a recent report detailing three episodes of crustal growth at 2.5, Ga, 1.8 Ga and 1.2- 1.4 Ga in Southeast China (Li *et al.*, 1992), the strongly contrasting isotope signatures and model ages between Zone I and Zone III rocks indicate the genetic involvement of late Archaean felsic crust and mid-Proterozoic mafic crust respectively together with a mantle-derived component. The boundary between these two crustal sources representing separate basement terranes is marked by Zone II in which isotope characteristics are more variable and a stronger mantle-derived influence is preserved. It is uncertain when the two basement terranes were juxtaposed.

Comparisons with Sr-Nd isotope data reported for Mesozoic granites from Fujian Province (Huang *et al.*, 1986) show a similar NW-SE geographic isotope zonation. In Fujian, the boundary separating the two isotopically distinct sources is thought to mark the eastern limit of Precambrian crystalline basement. It corresponds to a deep crustal divide conventionally drawn between the South China Fold Belt and the Southeast Maritime Fold Belt. This tectonic lineament is thought to continue south through Guangdong Province to intersect the coast immediately north of Hong Kong. The results presented here suggest that this deep crustal discontinuity transects Hong Kong from northeast to southwest.

Whole-rock geochemistry and Rb-Sr age data for Mesozoic plutonic rocks of Hong Kong indicate a transition from compressional to tensional tectonics. The climax of tensional conditions is marked by the emplacement of bimodal A-type granites within Zone II. These rocks have the strongest mantle signatures, suggesting that the boundary zone provided a pathway for upwelling of mantle-derived magmas which interacted with both Archaean and Mesoproterozoic basement rocks to produce the observed range of compositions.

- Li, X.H., Zhao, Z., Gui, X. and Yu, J., 1992. Sm-Nd and zircon U-Pb isotopic constraints on the age of formation of the Precambrian crust in Southeast China. *Chin. J. Geoch.*, **11**, 111-120.
- Huang, X., Sun, S.H., DePaolo, D.J. and Wu, K.L., 1986. Nd-Sr isotope study of Cretaceous magmatic rocks from Fujian Province. *Acta Petrologica Sinica*, **2**, 50-63.

## Origin of Granites at an Active Plate Margin

<sup>1</sup>Shaw, S.E. and <sup>2</sup>Todd, V.R.

<sup>1</sup>Macquarie University, N.S.W. 2109, Australia

<sup>2</sup>U.S. Geological Survey, U.C. Riverside,  
Riverside, CA 92521, USA

The 1,600-km-long Peninsular Ranges batholith (PRB) of southern California, U.S. and Baja California, Mexico is a major element of the Mesozoic Cordilleran continental margin. The PRB, emplaced across the lithospheric boundary between North America and Pacific oceanic plates in the Jurassic and Cretaceous, is a classic continental-margin arc batholith. The tectonic setting of the magmatic arc at an active plate margin provided a variety of protoliths for granite formation, as reflected in the great diversity of lithologic, geochemical, structural, and geophysical characteristics of PRB plutons. In a 120-km-wide segment of the PRB across San Diego County, Cenozoic tectonism has resulted in approximately 14 km of west-to-east structural relief thus providing a superb section of a batholith emplaced within the middle to upper crust. Emplacement of the batholith was accompanied by synkinematic low-*P*/ high-*T* metamorphism and intra-arc ductile deformation.

Granites of the PRB were emplaced in Jurassic, Early Cretaceous, and mid- to Late Cretaceous pulses above a west-facing subduction zone. The calcic compositions of the granites reflect a strong oceanic source component whereas, geochemical and isotopic characteristics of individual granite suites vary with age and geographic position within the batholith. Middle and Late Jurassic metagranodiorites originated by partial melting at mid-crustal depths within a Triassic-Jurassic turbidite wedge (S-type melts) and also by incorporation of sedimentary material into primitive mafic magma (I-S-type transitional melts). Steep geophysical gradients that bound the Triassic-Jurassic crustal block on the west mark the trace of a regional east-dipping reverse fault, or suture, that extends to mid-crustal depths and juxtaposed the block against Late Jurassic island arc metavolcanic rocks. The Jurassic suture divides the batholith into a western zone of oceanic crust and an eastern zone underlain by continentally derived crust.

Complex spatial and temporal variations among Cretaceous plutons whose compositions range from gabbro to granite reflect source differences west and east of the Jurassic suture as well as changes in the geometry of

Cretaceous convergence. Early Cretaceous I-type granite suites intruded their volcanic cover and older metavolcanic rocks at depths from 1 to 10 km in the western zone. Synintrusive deformation culminated in a ductile shear zone located near the Jurassic suture. Systematic variations in composition and position within the batholith among the Early Cretaceous granite suites indicate that the partial melting of chemically inhomogeneous,  $P_{H_2O}$ -variant older metagneous rocks in the lower crust played a significant role in their origin. Mantle-derived mafic magmas rose through the crust and mingled with granitic melts to form spectacular sheeted gabbro-granite diapirs in the western zone. A mid- to Late Cretaceous eastward shift in the locus of magmatism made available new sources, such as continental basaltic crust, for the voluminous trondhjemitic plutons of the eastern zone. These geochemically distinctive plutons were emplaced at depths of 11 to 15 km after regional deformation had waned.

Common Pb isotopic compositions of feldspars from Jurassic and Cretaceous granites show that Jurassic granites are more radiogenic as are Early Cretaceous granites emplaced east of the suture. Cretaceous granite suites that were emplaced across the suture show enrichments in K, radiogenic Sr, and whole-rock  $\delta^{18}O$  values east of the suture, a reflection of interaction of magmas with thicker, continentally derived crust. Lead isotopic ratios of Early Cretaceous granites of the western zone are too radiogenic for a direct mantle origin and probably reflect derivation from older I-type crustal rocks whose source may have been mantle melts.

## An Assimilation Role in the Crystallization of S-type Tonalite Magma at Granulite Facies Conditions, Hidaka Metamorphic Belt, Hokkaido, Northern Japan

<sup>1</sup>Shimura, Toshiaki and <sup>2</sup>Komatsu, Masayuki

<sup>1</sup>Graduate School of Science & Technology,  
Niigata University, Niigata, 950-21 Japan

<sup>2</sup>Department of Earth Sciences, Ehime University,  
Matsuyama, 790 Japan

The Hidaka Metamorphic Belt (HMB) is a high *dT/dP* type metamorphic belt, and represents a tilted crustal section of a magmatic arc of Tertiary age in Hokkaido, northern Japan (Komatsu *et al.*, 1989). The Belt is

divided into four zones: (I) very low grade metasedimentary rocks; (II) greenschist to lower amphibolite facies rocks; (III) upper amphibolite facies rocks; and, (IV) of granulite facies rocks. Abundant gabbro, diorite and granite are intruded into these metamorphic rocks.

The granitic rocks are mainly tonalitic and granodioritic in composition and classify into peraluminous (S-type) and metaluminous (I-type) granitoids. Both types generally coexist in the same intrusive mass, although S-types by far predominate. The S- and I-type granitic magmas were generated by the crustal anatexis of pelitic granulite and pyroxene amphibolite, respectively, in the lowest crust.

These granitic rocks are grouped into four depth types according to the intrusive metamorphic zones: 1) upper granite - granodiorite in zone I; 2) middle tonalite - granodiorite in zone I and II; 3) lower tonalite in zone III; and, 4) basal tonalite in zone IV. Each type of granitic rocks has a characteristic mineral assemblage and chemical composition that change gradually from higher to lower level types: for S-types these are, 1) muscovite, 2) cordierite  $\pm$  muscovite, 3) garnet + cordierite or garnet + orthopyroxene, and 4) garnet + orthopyroxene  $\pm$  cordierite, including biotite in each type.

In the basal tonalite intruded into granulite facies zone, various types of metamorphic rocks are abundantly included, such as pelitic-psammitic (Grt-Opx-Bt granulite), mafic (amphibolite, Opx-amphibolite and gabbroic gneiss) and ultramafic (meta-harzburgite and -dunite) rocks. The basal tonalite is, therefore, very heterogeneous lithofacies because not only of varied-sized abundant enclaves but also of assimilation and reaction of the tonalitic magma with metamorphic enclaves. Based on these lithofacies and considering effects of the reaction and assimilation, the basal tonalite is further classified into three sub-types: S1-type tonalite with homogeneous tonalite matrix, completely free of metamorphic enclaves, S2-type tonalite with very heterogeneous lithofacies, occurring as a marginal facies around visible metamorphic enclaves, and S3-type tonalite with heterogeneously distributed small melanocratic clots consisting of orthopyroxene, biotite, garnet, plagioclase and quartz.

Among them S1-type tonalite represents a primary rock crystallized from the original tonalitic magma, although this type of tonalite occurs only. All the mineral grains of S1-type tonalite have normal compositional zoning, indicating a simple cooling process. Based on the textural and compositional evidence, the crystallization sequence of the S1-type tonalite is Grt-Pl-Opx-Bt-Qtz-Crd-Kfs. The

range of crystallizing temperature is from 900°C to 700°C, and the magma contained 3-4 wt % H<sub>2</sub>O, according to experimental study (Shimura *et al.*, 1992).

On the other hand, S2-type tonalite occurs widely, intimately associated with metamorphic enclaves. The lithology of S2-type tonalite differs, depending on the lithology of metamorphic enclaves which the tonalite surrounds. The S2-type tonalite, occurring around pelitic enclaves, is very wide up to several meters. This zone consists of normal zoned large garnet grains (0.5-3cm), hypersthene and biotite clots, and large K-feldspar pools that include corroded plagioclase grains. The latter represents anatectic melts issued from the pelitic enclaves. The other S2-type is orthopyroxene bearing leucocratic tonalite that surrounds mafic enclaves. Plagioclase An% in this tonalite is relatively high compared with those of S1-type tonalite. This tonalite was formed by the reaction,

$$\text{Hbl} + \text{primary magma (SiO}_2\text{)} =$$

$$\text{Opx} + \text{secondary magma (rich in Ca, Al and H}_2\text{O)}.$$

The reactions of the tonalite magma with ultramafic enclaves produce peculiar rocks consisting of bronzite, phlogopite and Mg-cordierite, with a few cm to 20cm thick around the enclaves. The ultramafic enclaves are originally serpentinite with relic olivine and chromite spinel, and were trapped as one of ophiolite blocks in the accretionary complex that is the precursor of the Hidaka metamorphic rocks.

The S3-type tonalite is also heterogeneous because of random distribution of dark clots. The bulk chemical composition of the tonalite plots within an intermediate part between those of Grt-Opx granulite (restite) and of S1-type tonalite. The S3-type tonalite is poorer in LIL than S1-type tonalite. The dark clots are restite phases and the S3-type tonalite is a mixture of restites and tonalitic melts.

The primary tonalitic magma generated by crustal anatexis in the deep crust crystallized and differentiated with changing *P-T* conditions during ascent to produce essentially the sequence of granitic rocks from basal to upper types, but locally the assimilation and reaction with metamorphic enclaves produced a variety of granitic rocks.

Komatsu, J., Osani, Y., Toyoshima, T. And Miyashita, S., 1989. Composition and structure of the Hidaka metamorphic belt, northern Japan. In Daly, J.S., Cliff, R.A., and Yardley, B.W.D. (eds), *Evolution of Metamorphic Belts*. Geol. Soc. London Spec. Pub. 43, 487-493.

Shimura, T., Komatsu, M. and Iiyama, J.T., 1992. Genesis of the lower crustal Grt-Opx tonalite (S-type) in the Hidaka Metamorphic Belt,

northern Japan. *Trans. Royal Soc. Edinburgh: Earth Sci.*, **83**, 259-268.

## Magmatic Epidote-Bearing Granitoids from NW Argentina and NE Brazil

<sup>1</sup>Sial, A.N., <sup>2</sup>Toselli, A.J., <sup>3</sup>Saavedra J.,

<sup>1</sup>Ferreira, V.P. and <sup>2</sup>Rossi de Toselli, J.N.

<sup>1</sup>UFPE, Dept. of Geology, Recife, PE, 50732-970, Brazil

<sup>2</sup>Inst. Sup. Correl. Geologica, UNT, Miguel, Lillo 205-4000 Tucuman, Argentina

<sup>3</sup>IRAN, CSIC, Apartado 257, 37080 Salamanca, Spain

The occurrence of magmatic epidote-bearing (mEp) granitoids in South America has been recorded in five Neoproterozoic (Brasiliano Cycle) fold belts in NE Brazil (Serido - *SFB*, Cachoeirinha-Salgueiro - *CSF*, Riacho do Pontal - *RPF*, Pajeu-Paraiba - *PPF* and the Macurure Domain of the Sergipano Fold belt - *MSF*) and in the Early Paleozoic (Famatinian Cycle) Pampean Ranges (Famatina-Los Llanos plutonic belt - *FLL*, and along the Tafi Megafracture - *TMF*, separated by a belt of cordierite granites) in NW Argentina.

In Argentina, mEp-bearing granitoids vary from tonalites to granites (with minor qz monzonites, qz diorites, gabbros and trondhjemitites). In Brazil, they are mostly tonalites and granodiorites, commonly with microgranular qz diorite enclaves, and amphibole-rich clots. Plutons from the *CSF*, *RPF*, *MSF* have similar mineralogy and chemistry. In both countries, epidote is found in four textural relationships: included in plagioclase; with euhedral, allanite core; rimmed by biotite; or along boundaries of hbl in contact with plagioclase, or included in primary muscovite in some of Argentinean two-mica plutons. Brazilian mEp show 27 - 29% Ps (*CSF*) ( $f_{O_2}$  at, or slightly below, NB buffer) and 20 - 24% Ps (*SFB*) compositions ( $f_{O_2}$  between HM and NB buffers). Optical measurements for Famatinian epidotes anticipate compositional range equivalent to the Brazilian ones. In Argentina, epidote is, in some cases, in paragenesis with garnet, while in Brazil with Ca-cpx.

Granitoids in Brazil are essentially metaluminous (with subordinate peraluminous), whereas in Argentina they are distinctly peraluminous (*TMF*), or metaluminous (with subordinate peraluminous) (*FLL*) granitoids. In both countries they are essentially calc-alkalic or trondhjemitic, but tholeiitic members are present in Argentina (e.g. Cerro

Toro and San Agustin granitoids) and shoshonitic ones in Brazil (e.g. Teixeira pluton).

Most mEp-bearing plutons in Brazil intruded intermediate-grade metamorphic rocks, except those in the *CSF* and *RPF*, which pierced low-grade metaturbidites, locally developing unusual ky-bearing thermal aureoles, as they intruded mostly cold, middle crust, at about 6 kbar (Al-in-hbl barometry). In Argentina, same barometry allowed pressures of 6.6 kbar in tonalites which intruded syn-tectonically gneisses (e.g. Cerro Toro pluton), although other granitoids were clearly emplaced at shallower depth. Likely epidote, in the Famatinian granites, crystallized directly from a magma at  $P > 3$  kbar (primary muscovite), though  $< 6$  kbar (4.7 kbar in Cerro Blanco and 5.7 kbar in Paganzo; hbl barometry).

Rb-Sr isochron data from *CSF* microgranular mafic enclaves and host granodiorites (620 Ma) provides a highly linear regression ( $(^{87}\text{Sr}/^{86}\text{Sr})_i = 0.70598$ ), indicating that enclave and host magmas are cogenetic or had been isotopically equilibrated during cooling. Equivalent plutons in the *MSF* (e.g. Coronel João Sá pluton) display higher ( $(^{87}\text{Sr}/^{86}\text{Sr})_i$ ) (0.7080 - 0.7100). In Argentina, peraluminous Cafayate and Loma Pelada plutons exhibit low ( $(^{87}\text{Sr}/^{86}\text{Sr})_i$ ) (0.7043 and 0.7069, respectively), and metaluminous ones of Famatina Ranges show, sometimes, higher values ( $(^{87}\text{Sr}/^{86}\text{Sr})_i = 0.7097$  at Cerro Toro and 0.7046 at Paiman). For the *CSF* plutons in Brazil,  $\epsilon_{\text{Nd}}$  (0.6 Ga) varies from -1.0 to -2.0, with Nd model age from 1.2 to 1.4 Ga ( $t_{\text{DM}}$ ). For the *TMF* granites in Argentina,  $\epsilon_{\text{Nd}}$  (0.4 - 0.5 Ga) varies from -1.0 to -4.0 and Nd model age is in the range observed for the *CSF* granitoids.

Oxygen isotopes for the *CSF* plutons range from +11 to +13‰<sub>SMOW</sub>; their amphibole-rich clots being usually 1.5‰ lower.  $\delta^{34}\text{S}$  values varies from +1 to +9.0‰<sub>CDT</sub>. For the *SFB* plutons,  $\delta^{18}\text{O}$  values are lower (+7 to +10‰). Isotopic data for the *CSF* granitoids support the hypothesis that amphibole-rich clots represent fragments or restites of melting of oceanic floor basalts, hydrothermally altered at low  $T$ . There is no unique petrogenetic model for the granitoids in the *PPF* and *SFB*.

In Argentina, low Sr isotopic ratio in the *TMF* mu-gt-ep-sph-bearing suite vs high Sr initial ratio in the metaluminous *FLL* one, challenge the application of the S-I-M-A classification system. The various calc-alkalic and subalkalic tendencies can be explained by fractional crystallization with variable degree of assimilation and separation of cumulates and intercumulus melts. Peraluminous nature was partially achieved by selective leaching of B, Na and K to the volatile phase. Pegmatites

present in almost every pluton are the witness of such an effective process.

Over 50 plutons have been studied, leading to the conclusion that mEp-bearing granitoids originate from more than one kind of source material and evolve as several magma series. Processes leading to their formation are repeated through geological time, and magmas intrude different crustal levels at different tectonic settings.

### **Contrasting Migmatite Terrains, Tumbledown Mountain Area, West-Central Maine**

Solar, Gary S. and Brown, Michael

*Department of Geology, University of Maryland  
at College Park, MD 20742, USA*

Relationships between development of migmatites and regional tectonic histories in the Northern Appalachians are poorly constrained. It has been argued that some anatectic migmatites were associated with granitic pluton emplacement and with magma ascent; in effect the migmatites record the passage of the granitic pluton from the source. However, the deformation and timing of these migmatites have not been studied in detail. Two types of migmatites occur in the Kearsarge-Central Maine belt in west-central Maine: 1) migmatites found in proximity to granitic plutons; and, 2) migmatites that occur away from exposed granite bodies. The two types of migmatites appear to have been produced by different mechanisms of migmatization (granitic magma injection versus anatexis). Some mappable boundaries between the different migmatites coincide with discontinuities in strain and in the stratigraphy of the host rocks. A coordinated study of the structural, petrological, geochemical, and geochronological characteristics of different migmatite regions should enable evaluation of whether these regions may represent discrete tectonometamorphic terranes, juxtaposed after separate histories.

The Tumbledown Mountain area (7 km north of Rumford, Maine) is an example within the Kearsarge-Central Maine belt where a boundary between terrains characterized by two different types of migmatite occurs. Previous geologic mapping (Moench and Hildreth, 1976) has suggested that: 1) the border of the Tumbledown dome is coincident with a zone of cataclasis (significance

remained open); 2) a regional stratigraphy is traceable into the dome from the north despite the lack of primary structures within the dome; and, 3) the border of the Tumbledown dome is sub-parallel to regional isograd surfaces. Interpretations of tectonic history based on this mapping have been narrowly focused on pre-pluton isoclinal folding (based on regional stratigraphy) and extensive contact metamorphism (*e.g.* Moench and Zartman, 1976; Moench and Pankiwskyj, 1988; Smith and Barreiro, 1990).

These interpretations do not consider regional or orogen-scale ductile structures, styles of migmatization or timing relationships, or the influence of shear zone kinematics on migmatite development. Modern techniques of field geology have not been applied to the Tumbledown Mountain area. As a result, geochemical and geochronologic studies have been restricted to poorly constrained isotopic age data, despite well constrained geothermobarometry and exceptional petrologic observations (*e.g.* Smith and Barreiro, 1990). More modern study of the significance of regional migmatites (*e.g.* Allen, 1994) is necessary to make correlations among tectonic history, metamorphism and granite emplacement; in effect to investigate whether shear zones acted as conduits for granitic magma transport through the crust.

Ongoing field work has led to the production of structural maps that allow an interpretation of the spatial relations of migmatites. These data suggest that the two regions of migmatite in the Tumbledown Mountain area contrast in stratigraphy, amount and style of deformation, nature of migmatite-forming processes (magma injection versus anatexis), and abundance and nature of exposed granitic plutons. These field relations suggest that the different migmatite types and contrasts in strain and stratigraphy may indicate that a major tectonic boundary is coincident with the border of the "Tumbledown dome". Comparisons of migmatite characteristics across the "Tumbledown dome" border and boundary between migmatite types indicate juxtaposition of discrete tectonometamorphic terranes, rather than *in situ* modification of protoliths by plutonic intrusion and doming.

Field data will be integrated with laboratory studies to explore the significance and the timing of these migmatite regions and the boundary between them. The integration of structural (mapping, meso- and microstructural kinematic analysis, fabric trajectories, transpositional relations, etc.), petrological (*P-T-t* paths, metamorphic and deformational conditions, etc.), and geochemical (REE provenance studies, isotopic signatures to trace origin(s) of

granitic material, etc.) characteristics, and high precision geochronology (titanite and monazite [U-Pb system], biotite and muscovite [Rb-Sr system], and multi-mineral separates from selected samples [Sm-Nd system]) will allow quantitative and qualitative comparison. If successful, this integrated approach should be applied to other areas of the Appalachians, and other mountain belts which feature polygenetic migmatites.

- Allen, T., 1994. New Hampshire migmatites: oxygen isotope fractionation during partial melting, and suggestions of structurally enhanced magma migration. *EOS Trans. Am. Geophys. Union*, **75**, 360.
- Moench, R.H. and Hildreth, C.T., 1976. Geologic map of the Rumford quadrangle, Oxford and Franklin Counties, Maine: U.S.G.S. Geol. Quad. Map GQ-1272.
- Moench, R.H. and Pankiwskyj, K.A., 1988. Definition, problems, and reinterpretation of early premetamorphic faults in western Maine and northeastern New Hampshire. In Tucker, R.D. and Marvinney, R.G. (eds), *Studies in Maine Geology*, Maine Geol. Surv., **1**, 35-50.
- Moench, R.H. and Zartman, R.E., 1976. Chronology and styles of multiple deformation, plutonism, and polymetamorphism in the Merrimack Synclinorium of western Maine. *Geol. Soc. Am., Mem.*, **146**, 203-238.
- Smith, H.A. and Barreiro, B., 1990. Monazite U-Pb dating of staurolite grade metamorphism of pelitic schists. *Contrib. Mineral. Petrol.*, **105**, 602-615.

## **Petrology and Geochemistry of Mafic Enclaves in Granitoids of the Robertson River Igneous Suite, Blue Ridge Province, Central Virginia**

Tegeler, J. L.

*Department of Geology, University of Maryland  
at College Park, MD 20742, USA*

The late Neoproterozoic Robertson River Igneous Suite (RRIS) is an elongate batholith that intrudes Grenville age (1.1-1.0 Ga) basement within the Blue Ridge anticlinorium in central Virginia. The RRIS includes eight lithologic units, which were emplaced episodically over a 30 Ma period (730-700 Ma) during an early episode of crustal extension that preceded rifting of Laurentia by approximately 130 Ma. The RRIS is part of a regional supersuite of anorogenic plutons emplaced throughout the Laurentian terrane in Virginia and North Carolina.

Variably sized (0.1-2 meters), dark colored enclaves occur locally in leucocratic granite at several sites in the main batholith of the RRIS. Petrographic and geochemical

evidence indicates that the host rock at two sites is part of the Laurel Mills Granite (LMG), which is one of the oldest and least chemically evolved plutons of the suite. The contact between the enclaves and the granite is very sharp and marked with a concentration of epidote and biotite. The enclaves are fine-grained and display a similar mineralogy to the granite, although the proportions of the minerals are different and the enclaves classify as quartz diorite.

Detailed geochemical analyses of major and trace elements indicate local variation in granite composition immediately adjacent to the enclaves. The granite near the enclaves has a lower SiO<sub>2</sub> content than the LMG, although normative plots indicate that the granite is otherwise very similar to the LMG. Rb, U, Ga, and Nb are lower and Y and Th are higher in the granite adjacent to the enclaves relative to the LMG. Geochemical data for the enclaves indicate broadly andesitic compositions. The data further indicate that the enclaves are alkaline, whereas the majority of mafic rocks in the central Blue Ridge are tholeiitic. The enclaves are enriched in Rb, Sr, Ga, Nb, Zr, and Zn in comparison to both the adjacent granite and the LMG. Trace element compositions of the LMG and the enclaves yield similar plots on discrimination diagrams using Nb-Y and Rb-Y-Nb, falling in the "within-plate granite" field. A comparison of samples taken across a contact between the enclave and the granite shows that from the granite to the enclave, Rb, Sr, Y, Zr, and Zn are enriched. This pattern suggests chemical exchange between the granite and the enclaves. The variation of data between the LMG and the granite adjacent to the enclaves could result from interaction between the LMG and the enclaves, but also may indicate that the host rocks are separate from the LMG.

The RRIS has been shown to have been emplaced in an extensional environment related to the failed rifting of Laurentia. A curious aspect of the early period of regional crustal extension is the paucity of associated mafic rocks. Furthermore all of the mafic rocks documented to date are tholeiitic in composition. However the enclaves in this study represent the first discovery of mafic rocks of alkaline affinity in this region. These are also the first alkaline mafic rocks known to be at least 730 Ma. The alkaline nature of the enclaves is consistent with the tectonic environment of emplacement and with the association of anorogenic granites and may represent the first evidence of a previously unrecognized period of mafic magmatism associated with early crustal extension.

## The Partitioning of Fe and Co Between Plagioclase and Biotite and the $\text{Eu}^{2+}/\text{Eu}^{3+}$ Ratio for Plagioclase in Granitic Rocks from the Inner Zone of Southwest Japan

<sup>1</sup>Terakado, Yasutaka and <sup>2</sup>Fujitani, Tatsuya

<sup>1</sup>*Division of Earth and Environmental Sciences, Faculty of Human Development, Kobe University, Tsurukabuto 3-11, Kobe 657, Japan*

<sup>2</sup>*Marine Technical College, Nishikura-cyo, Ashiya 659, Japan*

Abundances of rare earth elements (REE) and other trace elements were determined for granitic rocks and their mineral separates from the Sanin, Sanyo and Ryoke belts in the Inner Zone of southwest Japan. Among those data, the Fe and Co partition coefficients between plagioclase and biotite show interesting features which may be related to magnetite- or ilmenite-series designation. Moreover, we calculated  $\text{Eu}^{2+}/\text{Eu}^{3+}$  ratios in plagioclase, and will discuss these ratios with relevance to redox states of granite formation processes.

The Inner Zone of southwest Japan is characterized by widespread exposure of Cretaceous to Paleogene granitic rocks which intrude late Paleozoic to Jurassic sedimentary and metamorphic rocks. The Ryoke metamorphic belt, which lies in the Pacific Ocean side of the Inner Zone, is distinguished from the Sanyo belt by the dominant occurrence of gneissose granitic rocks associated with mylonite and metamorphic rocks. The Sanin belt, which lies along the margin of the Japan Sea, is characterized by dominant occurrence of magnetite-series granitoids and of Paleogene rocks. The granitic rocks from the Ryoke belt are mainly ilmenite-series, and the Sanyo belt has intermediate feature with respect to magnetite/ilmenite-series classification.

The plagioclase/biotite partition coefficients for Fe are negatively correlated with those for Co, and the values for the Sanin belt granites are clearly separated from those for the Ryoke belt granites. The Sanin granites have relatively high Fe and low Co partition coefficients, whereas the Ryoke belt granites show relatively low Fe and high Co values. Moreover, the Sanin granites are magnetite-series and the Ryoke belt granites are ilmenite-series. Since the mineral assemblages imply a higher oxygen fugacity in the magnetite-series granites than in the ilmenite-series granites during solidification of the granite magma, the above variations in Fe and Co partitioning may be attributed to the difference in redox states during solidification.

Several other factors, such as effect of inclusion or disequilibrium, were considered, but the redox state seems to have a primary importance. The Sanyo belt samples, which include both types of granites, fall within the range of the Ryoke ilmenite-series granites. The Sanyo belt data suggest that the ilmenite-series granites were converted from a magma with magnetite-series affinity during later solidification stages.

The  $\text{Eu}^{2+}/\text{Eu}^{3+}$  ratios in minerals were calculated by the Philpotts' method in which the equivalence of  $\text{Eu}^{2+}$  and  $\text{Sr}^{2+}$  partitioning is assumed. Although no correlation between  $\text{Eu}^{2+}/\text{Eu}^{3+}$  and  $\text{Fe}^{2+}/\text{Fe}^{3+}$  ratios has been pointed out, the  $\text{Eu}^{2+}/\text{Eu}^{3+}$  ratio in plagioclase from the Sanyo and Ryoke belt granites seems to be correlated with the whole-rock  $\text{Fe}^{2+}/\text{Fe}^{3+}$ . On the other hand, the Sanin belt granites tend to show high plagioclase  $\text{Eu}^{2+}/\text{Eu}^{3+}$  ratios, which deviation is probably due to a disequilibrium caused by rapid solidification. This suggests the possibility that the kinetic effect may more or less affect the magnetite-series granite formation. Furthermore, effect of redox states on the size of the Eu anomaly in plagioclase/melt partition coefficient was examined from the plagioclase  $\text{Eu}^{2+}/\text{Eu}^{3+}$  data of the granites.

## Fluid Inclusion Evidence of the Evolution of Magmatic Fluids in the Harney Peak Leucogranite, Black Hills, South Dakota

Ternes, Kim and Nabelek, Peter I.

*Department of Geological Sciences, University of Missouri, Columbia, MO 65211, USA*

Experimental and theoretical studies have shown that magmatic fluids have strong influence on the phase equilibria of granitic systems. The speciation of magmatic fluids can be determined by microthermometric fluid inclusion analyses; however, to date most studies have focused on altered granites where the bulk of the magmatic fluid stage has been overprinted by externally derived fluids. This study has been undertaken to obtain direct fluid inclusion evidence for the composition and evolution of fluids in a crustally-derived magmatic system. The Proterozoic Harney Peak peraluminous leucogranite (HPG) of the Black Hills, South Dakota, was emplaced at 3-4 kbar as multiple sills, dikes and small intrusions. It is also thought to be genetically related to a large pegmatite field

which surrounds it. The influence of magmatic fluids on crystallization of the granite is demonstrated by prominent local granite-pegmatite layering and chemical heterogeneities. Previous stable isotope study of the granite has shown that the granite has not interacted with non-magmatic fluids since its crystallization (Nabelek *et al.*, 1992). Therefore, any inclusions found in the HPG are of magmatic origin and offer a direct sampling of magmatic fluids associated with a naturally occurring granitic system.

Fluid inclusions were analyzed in tourmaline and quartz. Primary and secondary inclusions were identified. The primary inclusions were identified by their isolated positions within crystals and negative shapes of the enclosing crystals. They consist of variable H<sub>2</sub>O-CO<sub>2</sub>-Salt-(CH<sub>4</sub>) mixtures. The CO<sub>2</sub>-rich inclusions are less salty and yield higher isochore temperatures (calculated using the model of Brown and Lamb, 1989). The range of primary fluid inclusion compositions is ascribed to Rayleigh exsolution of the magmatic fluid which should lead to early CO<sub>2</sub>-rich fluids due to the low solubility of CO<sub>2</sub> in high-silica magmas. The calculated isochore temperatures of the most water-rich primary inclusions are below the granite solidus. However, they may be in error because it was assumed that the only solute is NaCl. Ice melting temperatures, birefringent daughter crystals, phase-equilibria considerations, and alpha-track mapping of B and Li distribution in thin sections, all indicate that K, Li, B and other solutes must be additional constituents in the inclusions.

Using published solubility models for H<sub>2</sub>O and CO<sub>2</sub> in granitic melts (Burnham and Davis, 1974; Stolper *et al.*, 1987) and the average composition of the primary inclusions ( $X_{H_2O} = 0.70$ ), the initial volatile content of the HPG of ~ 5.3 wt % H<sub>2</sub>O ( $X_{H_2O}^m = 0.45$ ) and 650 ppm CO<sub>2</sub>, was calculated using the computer program DEGAS (Holloway and Blank, 1994). At the estimated pressures of melting (5-7 kbar, (Nabelek *et al.*, 1994)), the liquidus temperatures of the HPG melt having 5.3 wt % H<sub>2</sub>O are consistent with the dehydration-melting reactions that lead to the melts and 750-800°C oxygen isotope equilibration temperatures among minerals (Nabelek *et al.*, 1992). It is suggested that saturation of the HPG melt at 3.5 kbar with a CO<sub>2</sub>-rich fluid, that is represented by inclusions with the lowest  $X_{H_2O}$  of 0.20, increased the liquidus temperatures and partially quenched the melt, producing the aplitic segregations of the sills which comprise much of the granite. With further degassing, Rayleigh fractionation produced more H<sub>2</sub>O-rich fluids which resulted in lowering of the solidus and crystallization of pegmatitic

segregations. At subsolidus temperatures the magmatic fluid unmixed into H<sub>2</sub>O-Salt and CO<sub>2</sub>-CH<sub>4</sub> fluids which were trapped as secondary inclusions. This study demonstrates the strong influence of mixed fluid-species on phase equilibria of granitic magmas and provides the first direct evidence for the solubility of volatile species in a natural granite system.

- Brown, P.E. and Lamb, W.M., 1989. P-V-T properties of fluids in the system H<sub>2</sub>O±CO<sub>2</sub>±NaCl: New graphical presentations and implications for fluid inclusion studies. *Geochim. Cosmochim. Acta*, **53**, 1209-1221.
- Burnham, C.W. and Davis, N.F., 1974. The role of H<sub>2</sub>O in silicate melts. II. Thermodynamics and phase relations in the system NaAlSi<sub>3</sub>O<sub>8</sub>-H<sub>2</sub>O, to 10 kbars, 700°C to 1100°C. *Am. J. Sci.*, **274**, 902-940.
- Holloway, J.R. and Blank, J.G., 1994. Application of experimental results to C-O-H species in natural melts. In Carroll, M.R. and Holloway, J.R. (eds), *Volatiles in Magmas: Rev. Mineral.*, **30**, 187-230.
- Nabelek, P.I., Terry, M.P. and Friberg, L.M., 1994. The petrogenesis of the Harney Peak granite, Black Hills, South Dakota, as a consequence of differential uplift of a partially molten crust. *EOS Trans. Am. Geophys. Union*, **75**, 363.
- Nabelek, P.I., Russ-Nabelek, C. and Haeussler, G.T., 1992. Stable isotope evidence for the petrogenesis and fluid evolution in the Proterozoic Harney Peak leucogranite, Black Hills, South Dakota. *Geochim. Cosmochim. Acta*, **56**, 403-417.
- Stolper, E.M., Fine, G.J., Johnson, T. and Newman, S., 1987. The solubility of carbon dioxide in albitic melt. *Am. Mineral.*, **72**, 1071-1085.

### Assessment of Water Content in Granitic Melts Using Melt Inclusion Homogenization Data: Method - Results - Problems

Thomas, R.

GeoForschungsZentrum Potsdam,  
14473 Potsdam, Germany

This contribution presents results of melt inclusion studies of Variscan granites of the Erzgebirge and Fichtelgebirge in Germany, including the highly evolved tin-granites of the Erzgebirge. The primary minerals of rhyolites, granites and pegmatites formed from silicate melts and may trap minute quantities of these melts as inclusions. Much attention has been paid in the past to glass inclusions in volcanic rocks and it is less well known that melt inclusions are also abundant in plutonic rocks. In contrast to melt inclusions in volcanic rocks, which consist of glass and a shrinkage bubble and have diameters

often greater than 20 to 50  $\mu\text{m}$ , the melt inclusions in plutonic rocks are generally very small, average diameters less than 10  $\mu\text{m}$ , and they are typically crystallized; thus they are often overlooked or misidentified as solid inclusions. Silicate melt inclusions in intrusive rocks frequently contain a separate fluid phase with a vapour bubble. This fluid phase results from crystallization of the mostly anhydrous minerals of the melt in the inclusions.

Using a new time and diffusion-controlled quenching technique (Thomas, 1994) water contents and characteristic temperatures (solidus, liquidus, homogenization) of silicate melts can be estimated. With this method we obtain information about  $P$ - $T$  conditions and fluid composition of melts which is otherwise very hard to obtain, particularly for plutonic rocks. In brief, inclusions are heated in evacuated quartz tubes at successive temperatures, quenched and examined microscopically. Because of the slow rates of melting and dissolution, the homogenization temperature ( $T_H$ ) depends on inclusion size. After quenching, smaller melt inclusions may be completely homogenized, larger ones not, and some of intermediate size are just on the verge of homogenization. The latter have the "critical" diameter ( $d_K$ ), which is measured with a micrometer ocular. Using an algorithm based on the Stokes-Einstein equation relating diffusion and viscosity of some liquids, we derive viscosity values from inclusion diameter ( $d_K$ ), run time ( $t$ ) and temperature ( $T$ ) and plot these in the coordinates  $\ln h$  vs.  $10^4/T$ . In the next step, viscosity values at various  $\text{H}_2\text{O}$  contents ( $C_w$ ) are calculated for the host rock composition using Shaw's viscosity model, and these values are plotted as  $\text{H}_2\text{O}$  isopleths on the same diagram. The water contents of melt inclusions are then assessed by interpolation between the  $C_w$ -isopleths. This method eliminates the problematic quantities of the Stokes-Einstein equation.

The water contents estimated by this method are "eq.-wt % water" and the effect of other fluid phases is not explicitly determined. However, we can obtain information about the fluorine content from the solidus shift to low temperatures compared with haplogranite. According to microprobe investigations on melt inclusions the melt of the tin-granites of the Erzgebirge can contain greater than 5 wt % fluorine. By comparison, the highest value determined from bulk rock analyses is about 1 wt %.

It is interesting to note that nearly all high-level granites of the Erzgebirge and Fichtelgebirge, emplaced at shallow levels (1-5 km) in the crust, show evidence of melt evolution to highly fractionated compositions. Regardless of bulk composition, we find  $\text{H}_2\text{O}$ - and F-rich and some-

times P-rich melt inclusions at the end of each intrusive phase. The presence of such inclusions demonstrates an extended period of crystallization, in some cases over 150°C. Understanding the formation of such highly evolved melts is of great importance for the concentration process of ore-forming elements such as Sn, W, Nb, Ta, Be, Mo, U, REE. For example, the so-called "stockscheider"-pegmatites of the Erzgebirge granites are produced by extensive fractionation of the granitic source and efficient separation of the silicate liquid by squeezing out ("filter pressing") of interstitial melt. The pegmatitic magma was a suspension of a F- and P-rich silicate melt with minor immiscible phases of extremely P-rich melt, and crystals of quartz, feldspar, apatite, triplite, berlinite, topaz and other solids. Moreover, during crystallization, a KCl- and NaCl-rich aqueous fluid was exsolved. This complex history of magmatic evolution is recorded in the minute melt- and fluid inclusions.

Thomas, R., 1994. Estimation of the viscosity and the water content of silicate melts from melt inclusion data. *Eur. J. Mineral.*, 6, 511-535.

## ORAL PRESENTATION

### Fertility of Crustal Rocks During Anatexis

Thompson, Alan Bruce

*Department für Erdwissenschaften, ETH Zurich,  
CH-8092, Switzerland*

After many years of systematic experimental investigations, it is now possible to quantify the degree of melting of most common crustal rock types to about 3 GPa, as functions of temperature and  $a_{\text{H}_2\text{O}}$ . Quartzo-feldspathic melting produces steady increases in melt proportion with increasing temperature. The migration of the eutectic/minima radially from quartz in Ab-Or-Qz projections with increasing pressure at various  $a_{\text{H}_2\text{O}}$ , is reflected in quite different rock fertilities to melt production in lower and thickened continental crust. The cotectics including  $\text{CaAl}_2\text{Si}_2\text{O}_8$  in plagioclase show displacements away from Or in Ab-An-Or projections that are large at high  $P_{\text{H}_2\text{O}}$ , but strikingly less at lower pressure and lower  $a_{\text{H}_2\text{O}}$ . These displacements are particularly important when muscovite or biotite proxy for  $\text{KAlSi}_3\text{O}_8$ . The dehydration-melting of micas releases  $\text{H}_2\text{O}$  over narrow temperature intervals resulting in rapid increases in melt quantity, directly

proportional to the amount of hydrate. Mica melting also results in the consumption of  $\text{SiO}_2$  from residual quartz or melt, during the formation of refractory  $\text{Al}_2\text{SiO}_5$ , orthopyroxene, garnet or cordierite.

Pelitic migmatites may be formed during decompression melting in continental collision belts relaxing even from perturbed "normal" geotherms. While anatexis of gneisses could reflect collision of "hot" continents, it is not easy to distinguish enhanced internal heat generation from increased mantle heat supply. Mafic migmatites are diagnostic of an enhanced mantle heat signature. The systematics that have emerged from examination of experimental data should permit deduction of the depth-temperature- $a_{\text{H}_2\text{O}}$  conditions of anatexis of all crustal rock types, simply on the basis of modal mineralogy in migmatites. Deduction of  $P$ - $T$ - $a_{\text{H}_2\text{O}}$  conditions of residual assemblages should permit constraints on the degree of melt extraction from field observations.

### Tectonic Setting and Geochemistry of Granitoids: the Potential and Problems of Discrimination Diagrams

Tischendorf, G., Förster, H.-J.  
and Trumbull, R.B.

*GeoForschungsZentrum Potsdam,  
14473 Potsdam, Germany*

Few would argue that there is some degree of correlation between chemical composition and tectonic setting of granitic rocks, but what are the limits of applicability of tectonic discrimination diagrams? Many workers have used discrimination diagrams suggested by Pearce *et al.* (1984); others have questioned the validity of the method as such. We present here a performance test of Pearce discrimination diagrams based on a compilation of 5000 published analyses of granitic rocks (*s.l.*, volcanic and plutonic) from well-constrained tectonic settings.

Being products of melting, granites must reflect the composition of their source. However, the processes of melting, mobilization, ascent through crustal rocks and final crystallization are manifold, and granitic magma is generally not an isolated system but may interact with wall rocks, mix or mingle with accompanying mafic magmas, and actively adapt to changing  $P$ - $T$  conditions by crystallization or further melting. Two consequences of this for

discrimination are that one must expect transitional types in any discrimination scheme, and granites may be poorly represented by "average" or "representative" chemical analyses; one should consider the compositional spectrum in a given pluton.

As pointed out also by Pearce *et al.* (1984), granite composition depends on source rock composition primarily; tectonic setting is important to the degree that it controls the type of source rocks available and/or the  $P$ - $T$  conditions and extent of melting. Of course, crustal tectonic regimes are far from simple and many orogens are polycyclic. Operation of the Wilson cycle ensures that extension can be superimposed on compressional orogeny and vice versa, leading to overlap of process and mixing of source regions.

With these complexities and caveats in the background, results of our study can be summarized as follows:

*ORG - ocean ridge granitoids* (10 localities). Two groups are distinguishable; those generated by differentiation of basaltic magma ("true M-types") plot within the ORG field but those which formed by partial melting of basaltic sources overlap into the VAG field.

*WPG - within-plate granitoids* (36 localities). These granites are discriminated best and only 4 localities plot with some overlap into the VAG or SyncolG fields; there is no overlap with ORG.

*VAG - volcanic arc granitoids* (70 localities). These granites show virtually no overlap with either the SyncolG or ORG fields, but there are many cases of overlap into the WPG field. This is exemplified in particular by the late Mesozoic and Tertiary rocks of the N. American Cordillera, where extension directly followed arc magmatism (an extreme example is the Trans Pecos, Texas locality). The same situation is found in an oceanic setting in the arcs of Papua New Guinea, New Zealand and Marie Byrd, Antarctica, all of which contain elements of back-arc spreading with which the "WPG-type" samples are associated.

*SyncolG - collisional granitoids* (71 localities). Himalayan granites and granites from some parts of the European Variscides plot within the SyncolG field but many other examples from collisional orogens tend to cluster around the triple point of SyncolG, VAG and WPG fields. Good examples of the spread in compositions encountered are the Tasman fold belt, SE-Asia and the Rheno-Hercynian granites of Germany.

We conclude that only granitoids from within-plate settings, whether oceanic (ORG) or continental (WPG), can be distinguished geochemically with some confidence.

Granitoids from active margins (arc settings) may give data arrays which span the VAG and WPG fields, probably because of the close time and space association with extension. Collisional settings are inherently the most complex in terms of source rocks and process, and do not produce characteristic granitoids in terms of the trace elements used here. We have tested a number of alternative elements or element ratios for discrimination but the compositional overlaps remain because the fundamental problem is rooted in the nature of granite formation, and orogenic processes.

Pearce J.A., Harris, N.B.W. and Tindle, A.G., 1984. Trace element discrimination diagrams for the tectonic interpretation of granitic rocks. *J. Petrol.*, 25, 956-983.

### Polygenetic Microgranitoid Enclave Swarms in Granitic Rocks, Central Sierra Nevada, California

<sup>1</sup>Tobisch, O.T., <sup>2</sup>Vernon, R.H.  
and <sup>1</sup>McNulty, B.A.

<sup>1</sup>*Earth Science Department, University of California,  
Santa Cruz, CA 95064, USA*

<sup>2</sup>*School of Earth Sciences, Macquarie University,  
Sydney, NSW 2109, Australia*

Microgranitoid enclaves in granitic rocks of the central Sierra Nevada batholith have been studied extensively (*e.g.*, Pabst, 1928; Reid *et al.*, 1983; Frost and Mahood, 1987; Dorais *et al.*, 1990; Barbarin, 1991a). Less studied are enclave swarms which have previously been classified compositionally as monogenic or polygenic (Barbarin, 1991b). Composition distributions of enclaves in swarms, however, can vary from nearly homogeneous (*i.e.*, where modal % of mafics, feldspar phenocrysts, etc., varies slightly) to swarms in which the modes of all enclaves vary markedly. The textures/compositions of the swarm matrix varies from matching the host to consisting mostly of coarse-grained aggregates rich in mafic minerals (inferred by us to be cumulates) and accompanied by schlieren layering.

Field observations on swarms in the Dinkey Creek (DCP), Jackass Lakes (JLP) and Mt Givens (MGP) plutons in the central Sierra Nevada indicate they are not necessarily related to pluton boundaries as suggested for some plutons (*e.g.*, Barbarin, 1991a,b; Knopf and Thelan,

1905). Swarms are reasonably common and distributed over much of the DCP, although they tend to concentrate near proposed linear fracture feeding zones within the pluton. Swarms are also abundant in the JLP and are distributed throughout the pluton in zones lying parallel to proposed fracture-controlled pluton boundaries and emplacement sheets. Swarms in the MGP (work in progress) occur at scattered localities, and are much less common than in the other two plutons.

Dimensional range of individual swarms typically is 1-100 m. Swarms in the DCP and MGP are usually <1 m to 4 m wide and several meters in longest dimension, with the maximum length observed ~ 30 m. The largest and most laterally continuous swarms occur in the JLP, where they may be tens of meters wide and extend ~ 100 m along strike. Multiple swarms also occur within complex mingle/mix zones approaching 1-2 km in width and ~5 km in length. Some swarm boundaries can be very sharp and straight and can contain enclaves abruptly truncated by the host magma, as if controlled by a discrete laminar flow surface; other swarm boundaries have gradational boundaries or appear partly dispersed.

The two-dimensional shape of swarms can appear as straight "dikes", meandering layers or "trains", a folded lensoid layer with enclaves aligned ~parallel to the fold axial plane and magmatic foliation, near-circular (pipe-like?) shapes, or irregular masses confined by straight or angular boundaries, among numerous variations. Their three-dimensional geometry is often difficult to document; however in several places we have observed them as lensoid sheets, commonly but not always steeply dipping (plunging?). Two-dimensional axial ratio of enclaves in swarms is generally low to moderate (*i.e.*, <3).

Five possible models, with some overlap (*cf.* also refs. Barbarin, 1991b; Barbarin and Didier, 1992), for producing polygenetic swarms, are: 1) the "log jam" model, in which rafts form by accumulation of enclaves from disparate sources due to blockages in the magma flow (*e.g.*, viscosity "walls", channels too narrow to allow rapid passage, etc.); 2) gravitational sorting, whereby enclaves from disparate sources undergo density and/or size stratification; 3) flow sorting of enclaves and related cumulates from disparate sources (*e.g.*, collection in eddies or zones parallel to flow gradients in host, etc.); and, 4) conduit mix/mingle model, whereby a) during ascent, "mafic" magma incorporates droplets or small batches of felsic magma from the host to produce domains of hybrid magma (repeating this process produces a variety of related compositions), which eventually mingle with the

host and accumulate into swarms by processes 1-3, or b) multiple pulses of evolved hybrid magmas injected near or at the final emplacement site mingle with the host and accumulate via processes 1-3.

- Barbarin, B., 1991a. Enclaves of the Mesozoic calc-alkaline granitoids of the Sierra Nevada batholith, California. In Didier, J. and Barbarin, B. (eds), *Enclaves and Granite Petrology*. Elsevier, Amsterdam, 135-153.
- Barbarin, B., 1991b. Contrasted origins for the "polygenic" and "monogenic" enclave swarms in some granitoids of the Sierra Nevada batholith, California. *TERRA Abstracts*, 3, 32.
- Barbarin, B. and Didier, J., 1992. Genesis and evolution of mafic microgranular enclaves through various types of interaction between coexisting felsic and mafic magmas. *Trans. Royal Soc. Edinburgh: Earth Sci.*, 83, 145-153.
- Didier, J. and Barbarin, B. (eds.), 1991. *Granites and their enclaves. The bearing of enclaves on the origin of granites*. Dev. Petrol., 3. Elsevier, Amsterdam.
- Dorais, M.J., Whitney, J.A. and Roden, M.F., 1990. Origin of the mafic enclaves in the Dinkey Creek pluton, central Sierra Nevada batholith, California. *J. Petrol.*, 31, 853-881.
- Frost, T. and Mahood, G., 1987. Field, chemical and physical constraints on mafic-felsic magma interaction in the Lamarck Granodiorite, Sierra Nevada, California. *Geol. Soc. Am. Bull.*, 99, 272-291.
- Knopf, A. and Thelan, P., 1905. Sketch of the geology of Mineral King, California. *Univ. Calif. Pub. Bull.*, 4, 227-262.
- Pabst, A., 1928. Observations on inclusions in the granitic rocks of the Sierra Nevada. *Univ. Calif. Pub., Dept. Geol. Sci. Bull.*, 17, 325-386.
- Reid, J.B., Jr., Evans, O.C. and Fates, D.G., 1983. Magma mixing in granitic rocks of the central Sierra Nevada, California. *Earth. Planet. Sci. Lett.*, 66, 243-261.

**Petrology and Geochemistry of Late Neoproterozoic Anorogenic Granitoids, Laurentian Appalachians, Virginia and North Carolina: Implications for Extension-Related Encratonic Magmatism**

Tollo, R.P., Hutson, F.E. and Aleinikoff, J.N.

<sup>1</sup>Department of Geology, George Washington University, Washington, DC 20052, USA

<sup>2</sup>Department of Geological Sciences,

University of Texas, Austin, TX 78712, USA

<sup>3</sup>U.S. Geological Survey, Denver, CO 80225, USA

Magmatic activity associated with Late Neoproterozoic regional extension produced more than twenty granitoid

plutons within the Laurentian Appalachians of Virginia and North Carolina. The plutons and associated volcanic rocks form a supersuite that spans an age range of at least 760-700 Ma and defines a period of magmatism that preceded development of an oceanic basin by about 130 Ma. Plutons constituting the supersuite, which includes granitoids of the Crossnore Complex (Virginia and North Carolina) and Robertson River Igneous Suite (central Virginia), among others, intruded Grenville-age (1.2-1.0 Ga) basement of the Blue Ridge province and were metamorphosed at greenschist facies conditions during the Paleozoic.

The plutons are variable in size, typically elongate, and range from monzogranite to alkali feldspar syenite. Most plutons record a sequence of multiple intrusions that, in the large Robertson River batholith (390 km<sup>2</sup>), spanned at least 35 Ma. The plutonic and associated volcanic rocks of the supersuite display many petrologic characteristics of A-type granitoids, including: 1) metaluminous to (relatively rare) mildly peralkaline bulk compositions; 2) high (relative to well-documented I-, S-, and M-types) Zr, Nb, Ga, Y, REE (not Eu), Fe/Mg, and Ga/Al; and, 3) common occurrence of hypersolvus feldspar assemblages, Fe-rich ferromagnesian silicates, fluorite, and REE-bearing accessory phases including allanite. High Ga/Al (9.0 - 2.7) is particularly diagnostic and serves as an effective discriminant between originally metaluminous (< 6) and peralkaline (> 6) bulk compositions. Intrapluton compositional variation is locally significant and reflects both source- and fractionation- (dominantly feldspar and/or accessory minerals) related mechanisms, locally modified by fluid-driven, late- and post-magmatic processes. Trace element data from the most thoroughly studied plutons indicate that the peralkaline rocks are unlikely petrologic derivatives of the more abundant metaluminous types. Moreover, comparison with other well documented suites suggests that the peralkaline rocks exhibit source-related characteristics similar to ocean-island basalts whereas metaluminous units display characteristics similar to bulk continental crust. Results of experimental investigations by other workers in which A-type metaluminous granite melts were produced through melting of charnockitic rocks representative of the Blue Ridge basement support derivation of the metaluminous magmas from local sources. Sm-Nd isotopic data for the Robertson River Igneous Suite have  $\epsilon_{Nd}$  values (calculated for crystallization ages of 730 Ma as indicated by U-Pb isotopic analyses of zircon) ranging from -0.1 to +2.1 and model ages from 1.1 to 1.3 Ga.  $\epsilon_{Nd}$  values increase with decreasing age within the

suite. Older metaluminous units have  $\epsilon_{\text{Nd}}$  values indicative of interaction with evolved crust (-0.1 to +1.4) but the younger peralkaline units show more positive  $\epsilon_{\text{Nd}}$  values (+1.8 to +2.1) that suggest either a change in source characteristics or degree of crustal contamination with time. Collectively, these data indicate that abundant metaluminous magmas associated with the earliest stages of Laurentian extension were produced dominantly through melting of local continental crust and that such melts diversified in composition largely through crystal fractionation. Peralkaline magmas produced during the waning stages of regional magmatic activity were generated through melting of more geochemically primitive sources but the magmas evolved compositionally through similar fractionation mechanisms.

The mode of occurrence, type and range of compositions, and inferred petrogenesis of the supersuite are similar to those of anorogenic, encratonic granitoids documented worldwide. The Laurentian Appalachian supersuite represents a significant, long-lived, temporally episodic period of magmatism that ended with encratonic rifting but not development of oceanic crust. As such, the rocks are indicative of processes operative during the earliest, pre-drift stages of Laurentian extension. A second period of anorogenic magmatism occurred at about 600 Ma and involved abundant mafic and subordinate felsic volcanism. Relatively rare anorogenic granitoids emplaced in Grenville-age basement of the New York promontory during this period are chemically indistinguishable from the supersuite, suggesting that compositional characteristics cannot be used to discriminate between granitoids intruded during the two periods of extension. The more voluminous felsic rocks of the earlier period preserve an otherwise rare record of petrogenetically related plutonic-volcanic sequences and coeval clastic rift deposits associated with encratonic extension and thus provide a unique three-dimensional perspective of crustal processes preceding development of Iapetus.

## Geochemistry and Geochronology of Evolved Granitic Rocks in Southwestern Maine: Tectonic Implications

Tomascak, Paul B., Walker, Richard J.  
and Krogstad, Eirik J.

*Isotope Geochemistry Laboratory,  
Department of Geology, University of Maryland  
at College Park, MD 20742, USA*

The emphasis of this work is the critical assessment of granite generation adjacent to a major shear zone system using comparative elemental and isotope geochemistry and high precision geochronology. The study area is in southwestern Maine and deals with a suite of granitic rocks: the Sebago batholith, small granitic bodies at Brunswick and granitic pegmatites around Topsham.

The Sebago batholith is the largest exposed granite in New England, with an area of *c.* 2600 km<sup>2</sup>. It comprises two-mica granite with varying proportions of the micas, locally contains garnet, and in places displays textures common to pegmatitic leucogranites. It crystallized at  $293 \pm 1$  Ma (concordant U-Pb monazite). Samples have rare earth element (REE) patterns with similar shapes: LREE enriched, gently flattened in the HREE with moderate to strong negative Eu anomalies. Nevertheless, samples fall into three spatially-distinct groups based on REE patterns. Patterns of samples from within the southwestern and central portions of the batholith (Group 1) overlap strongly with a  $(\text{Ce}/\text{Yb})_{\text{CN}} = 10 - 20$ . The bulk of samples peripheral to this region (Group 2) have a greater range in  $(\text{Ce}/\text{Yb})_{\text{CN}}$  (5 - 60) with negative kinks in Nd, yielding higher Sm/Nd. Pegmatitic and aplitic samples from Group 2 show strongly kinked REE patterns with low overall abundances. Samples from the northern extremity of the batholith (Group 3) have steep REE patterns ( $(\text{Ce}/\text{Yb})_{\text{CN}} \sim 60$ ) and in some cases negligible Eu anomalies. The REE patterns of samples with granitic textures are typical of evolved granites derived from anatexis of pelites leaving garnet in the residue. Initial  $\epsilon_{\text{Nd}}$  are as follows: Group 1 = -3.4 to -2.2, Group 2 = -5.6 to -2.8, and Group 3 = -5.2 to -3.9. Depleted mantle Nd model ages are as follows: Group 1 = 0.9-1.2 Ga, Group 2 = 1.2-2.7 Ga, and Group 3 = 1.0-1.2 Ga. The REE and Nd data from Group 1 samples permit their derivation from the same source, potentially by slightly different degrees of melting of long-term LREE-enriched crust. The data permit the origin of Group 2 and 3 samples through

either variability of source materials or contamination of original, somewhat less-evolved magma with material with longer crustal history. In contrast to the Nd isotopic heterogeneity, the batholith displays a homogeneous Pb isotope signature. Severely leached K-feldspars taken from the same suite of whole rock samples have  $^{206}\text{Pb}/^{204}\text{Pb} = 18.41 - 18.75$ ,  $^{207}\text{Pb}/^{204}\text{Pb} = 15.60 - 15.65$  and  $^{208}\text{Pb}/^{204}\text{Pb} = 38.21 - 38.37$ . These Pb isotopic compositions lack the spatial variation seen in the Nd data and overlap the Pb isotopic compositions of felsic igneous rocks from coastal Maine (Ayuso and Bevier, 1991). The data suggest that the Sebago batholith was produced by melting of Proterozoic sediments of variable provenance. The high  $^{206}\text{Pb}/^{204}\text{Pb}$  and  $^{207}\text{Pb}/^{204}\text{Pb}$  of the Sebago batholith common Pb, however, rule out the involvement of North American basement sources (Grenville).

Granitic bodies at Brunswick occur as homogeneous masses of 10-100 m diameter, approximately 7 km from the eastern margin of the Sebago batholith. The granite at Brunswick contains two primary micas and garnet is common. The granite crystallized at  $278 \pm 1$  Ma (U-Pb monazite). Spatially-related evolved granitic pegmatites around Topsham (7-13 km NE) have monazites that record younger crystallization ages of 274-269 Ma. The monazite ages are corroborated by isochron ages of pegmatite apatites (c. 270 Ma) and one uraninite age ( $258 \pm 14$  Ma). The correspondence in ages of granite in Brunswick and pegmatites in Topsham permit the rocks to be related to the same magmatic system. In spite of a documented widespread Permian thermal event, these rocks are the first record of Permian granitic magmatism north of New Hampshire in the Appalachians. The granite at Brunswick has similar bulk chemical composition to the Sebago batholith. REE patterns are kinked in a similar fashion to the Group 2 Sebago batholith granites and samples exhibit a similar range of  $\epsilon_{\text{Nd}}$  (-6.6 to -3.9) and  $t_{\text{DM}}$  (1.4-2.3 Ga). The Sebago batholith is not related to the granite magmatism in the Brunswick area. The granite at Brunswick and Topsham pegmatites postdate high-temperature ductile deformation in the Brunswick area, constraining deformation to  $\geq 280$  Ma. These Permian granitic rocks in southwestern Maine were evidently generated during a spatially isolated thermal event. The limit on the age of ductile deformation in southwestern Maine suggests that final assembly of Avalonian crustal blocks into their current positions may have been diachronous from north to south over c. 250 km in the northern Appalachians

Ayuso, R.A. and Bevier, M.L., 1991. Regional differences in Pb isotopic compositions of feldspars in plutonic rocks of the northern Appalachian mountains, U.S.A., and Canada: A geochemical method of terrane correlation. *Tectonics*, 10, 191-212.

### Li Isotope Geochemistry of the Tin Mountain Pegmatite, Black Hills, South Dakota

Tomascak, Paul B., Lynton, Stephen J., Walker, Richard J. and Krogstad, Eirik J.  
*Isotope Geochemistry Laboratory,  
 Department of Geology, University of Maryland  
 at College Park, MD 20742, USA*

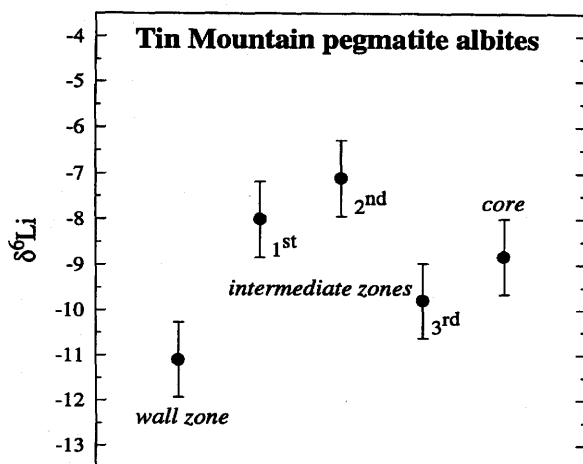
Using newly-established techniques for the separation and analysis of Li isotopes in natural materials, we have analyzed mineral separates from the highly evolved Tin Mountain pegmatite of the Black Hills granite-pegmatite system. Our goals are: 1) to assess the nature of Li isotope variability within the pegmatite; 2) to examine Li isotope fractionation among coprecipitating minerals within interior zones of the pegmatite; and, 3) to compare the Li isotopic compositions of minerals with their oxygen isotopic signature, to determine if criteria might be defined for Li isotope geothermometry.

Based on field relations, geochronology and geochemistry, the Tin Mountain pegmatite is considered to be related to the  $1715 \pm 3$  Ma Harney Peak granite (Walker *et al.*, 1989; Redden *et al.*, 1991; Krogstad and Walker, 1994). The pegmatite constitutes five mineralogically and texturally distinct zones: *wall zone* (albite + quartz + muscovite); *first intermediate zone* (perthite + quartz + albite + muscovite); *second intermediate zone* (perthite + quartz + albite; minor muscovite, spodumene); *third intermediate zone* (albite + quartz + spodumene + muscovite; minor beryl, amblygonite); *core* (quartz + spodumene + muscovite; minor albite, beryl, amblygonite). On the basis of field evidence, geochemistry and intermineral fractionation of oxygen isotopes, Walker *et al.* (1986) determined that the wall zone was first to crystallize among the zones, followed by the first intermediate zone. The remaining intermediate zones and the core then crystallized simultaneously.

Lithium was separated from albite samples via cation exchange chromatography, using a mixture of HCl and ethanol as an eluant. Li isotope ratios were measured via

thermal ionization mass spectrometry, volatilizing  $\text{Li}_2\text{B}_4\text{O}_7$  from a Ta side filament and measuring  $\text{Li}^+$ . The reproducibility of measurements on the NBS L-SVEC ( $\text{Li}_2\text{CO}_3$ ) standard at present permits uncertainties on  $\delta^6\text{Li}$  determinations of  $\pm 0.8\text{‰}$ .

The Li isotope data gathered to date are summarized on the diagram below. The data show the overall isotopic variability of albites is restricted, underscoring the need for high precision isotope ratio measurements in order to distinguish small-scale differences in isotopic composition. The wall zone albite ( $\delta^6\text{Li} = -11.1\text{‰}$ ) is depleted in light Li compared to the first intermediate zone ( $-8.0\text{‰}$ ). The first intermediate zone albite has overlapping  $\delta^6\text{Li}$  with that of second intermediate zone ( $-7.1\text{‰}$ ), within analytical uncertainty. The third intermediate zone albite is light Li depleted ( $-9.8\text{‰}$ ), within uncertainty of the wall zone albite. The isotopic composition of albite from the core is between those of the second and third intermediate zones ( $-8.8\text{‰}$ ). The datum for the wall zone albite is identical to the whole rock value determined by Vocke *et al.* (1990), suggesting Li isotope equilibrium during crystallization of the exterior part of the pegmatite or subsequent reequilibration. The isotopic variations among albites may reflect differences in Li fractionation between different crystallizing assemblages. Changing temperature during pegmatite consolidation could also play a role in the variations demonstrated here. More thorough treatment of these data, however, can only be accomplished with further isotopic measurements on other coexisting minerals (*e.g.* muscovite, quartz, spodumene).



- Krogstad, E.J. and Walker, R.J., 1994. High closure temperatures of the U-Pb system in large apatites from the Tin Mountain pegmatite, Black Hills, South Dakota. *Geochim. Cosmochim. Acta*, **58**, 3845-3853.
- Redden, J.A., Peterman, Z.E., Zartman, R.E. and DeWitt, E., 1991. U-Th-Pb geochronology and preliminary interpretation of Precambrian tectonic events in the Black Hills, South Dakota. In Lewry, J.F. and Stauffer, M.R. (eds), *Geol. Assoc. Can. Spec. Paper* **37**, 229-251.
- Vocke, R.D., Beary, E.S. and Walker, R.J., 1990. High precision Li isotope ratio measurements of samples from a variety of natural sources. *V.M. Goldschmidt Conf. Prog. Abst.*, p.89.
- Walker, R.J., Hanson, G.N., Papike, J.J., O'Neil, J.R. and Laul, J.C., 1986. Internal evolution of the Tin Mountain Pegmatite, Black Hills, South Dakota. *Am. Mineral.*, **71**, 440-459.
- Walker, R.J., Hanson, G.N., and Papike, J.J., 1989. Trace element constraints on pegmatite genesis: Tin Mountain Pegmatite, Black Hills, South Dakota. *Contrib. Mineral. Petrol.*, **101**, 290-300.

## The Carboniferous - Ordovician Connection in the Sardinia-Corsica Batholith: Constraints from the Carboniferous Calc-Alkaline Granitoids and Ordovician Metavolcanics

<sup>1</sup>Tommasini, S., <sup>2</sup>Poli, G.,

<sup>3</sup>Halliday, A.N. and <sup>4</sup>Manetti, P.

<sup>1</sup>Faculteit der Aardwetenschappen,  
Amsterdam, The Netherlands

<sup>2</sup>Department of Earth Sciences, Perugia, Italy

<sup>3</sup>Department of Geological Sciences,

University of Michigan, Ann Arbor, MI 48109, USA

<sup>4</sup>Department of Earth Sciences, Firenze, Italy

Isotopic and trace element signatures of granitoids can yield valuable information to assess the geochemical characteristics of source reservoirs and the importance of new mantle additions to the continental crust during orogenic processes. Also, inferences on the geodynamic setting can be achieved from isotopic signatures of source reservoirs. In spite of this powerful tool, care must be paid when dealing with granitoids because their composition can be affected by open system differentiation processes that could have significantly altered their potential bearings on source characteristics. In the case of the Sardinia-Corsica Batholith, several interaction processes between crust- and mantle-derived magmas formed a wide variety of hybrid magmas ranging from homogeneous tonalitic intrusions to heterogeneous, mafic enclave-bearing granitoids. As such, isotopic and geochemical characteris-

tics of these hybrid magmas cannot be used to assess the nature of source reservoirs during the Hercynian orogeny in Sardinia and Corsica. It is necessary to take into account just those magmas directly originated from source regions to accomplish this task.

Isotopic and trace element data are presented for selected gabbros and I-type granitoids representative of the parental mantle- and crust-derived magmas, respectively. The gabbros belong to normal calcalkaline suites and have marked relative enrichments in Rb, Ba, K and Pb in a primitive mantle-normalized diagram. The granitoids belong to high-K calcalkaline suites and have fairly uniform trace element compositions resembling Volcanic Arc Granitoids (VAG). A significant overlap in Sr and Nd isotope compositions is observed between gabbros and granitoids.

Geochemical and isotopic data provide evidence for the origin of the gabbros from mantle sources enriched in incompatible trace elements through recycling of sediments via subduction zones, whereas the granitoids were derived from crustal sources composed mainly by igneous protoliths with relatively homogeneous composition. Sr and Nd isotope compositions of gabbros and granitoids are consistent with both the mantle enrichment process and the formation of the igneous crustal sources occurring at ~ 450 Ma, during the earlier calc-alkaline igneous activity.

Major and trace element analyses of the Ordovician basic-intermediate metavolcanic rocks provide further evidence for the formation of the igneous crustal sources during this calc-alkaline igneous activity. A partial melting model using mass balance calculations for major elements, direct and inverse estimates for trace elements, and experimental petrology data is consistent with the metavolcanic rocks (or their underplated equivalent) being potential source rocks of the Hercynian I-type granites.

The connection between Hercynian and Ordovician igneous activity has important and new implications for the Paleozoic evolution of the Sardinia and Corsica lithosphere, and permits the Hercynian orogeny to be placed in a wider geodynamic setting, consisting of three main phases. The Ordovician precollisional phase was characterized by a NNE dipping subduction of an oceanic plate under a continental plate with emplacement of acid and subordinate basic-intermediate volcanic and intrusive rocks. The subcontinental mantle underneath Sardinia and Corsica experienced an enrichment event in incompatible trace elements through recycling of sediments via subduction zones. Major crustal accretion also occurred with underplating of basaltic magmas. The Devonian collisional

phase was characterized by the collision of two continental plates after the total consumption of the oceanic plate. Crustal thickening processes took place together with regional metamorphic events that recorded a clockwise *P-T-t* path. The Carboniferous postcollisional phase was characterized by isostatic and thermal readjustments following crustal thickening that caused extensive partial melting processes. Large quantities of I-type granitoids and subordinate gabbroic complexes were emplaced in the middle-upper crust and formed the main frame of the Sardinia-Corsica Batholith.

This geodynamic model is consistent with the Paleozoic evolution of other sectors of Western Europe suggested on the basis of geological, geochronological, and paleomagnetic data. The paleomagnetic restoration of the Late Paleozoic position of Sardinia and Corsica close to Southern France suggests that Sardinia and Corsica could have been portions of the southern edge of the Armorican plate that, during the Siluro-Devonian, collided with the Ibero-Aquitania plate after the total consumption of the Late Cambro-Ordovician South Armorican and/or Massif Central Ocean.

### **Mesozoic Plutonism in Western New Zealand - a 50 Ma Transition from Subduction to Continental Rifting on the Gondwana Margin**

<sup>1</sup>Tulloch, A.J. and <sup>2</sup>Kimbrough, D.L.

<sup>1</sup>*Institute of Geological and Nuclear Sciences,  
Private Bag 1930, Dunedin, New Zealand*

<sup>2</sup>*Department of Geological Sciences, San Diego State  
University, San Diego, CA 92182, USA*

Mesozoic subduction along the New Zealand margin of Gondwana is clearly recorded in the 248-131 Ma calc-alkaline mafic to felsic plutonic and volcanic rocks of the Median Tectonic Zone (MTZ). Silica contents range from 48 - 74 wt % although intermediate compositions dominate. Nd-Sr isotope compositions indicate derivation from mildly depleted mantle.

No more than 5-10 Ma then elapsed before the initiation of magmatism of the alkali-calcic I-type Separation Point Suite (SPS), and its deeper level equivalent, the granulite facies Western Fiordland Orthogneiss (WFO), which stitched the MTZ to the continental margin (126-105

Ma). The SPS/WFO granitoids (56 - 74 wt % SiO<sub>2</sub>) have high Al, Na, Sr and HREE depletions with insignificant Eu anomalies, indicative of derivation from an eclogitic or garnet amphibole source.

Towards the end of SPS/WFO magmatism, at about 105-100 Ma, several metamorphic core complexes formed within the Gondwana margin to the west of the boundary with the recently amalgamated MTZ. Development of these extensional features preceded final rifting of New Zealand from Australia and Antarctica by some 20 Ma. The core complexes appear to form the loci for a further suite of plutons (the transitional I/S-type Rahu Suite; 65 - 75 wt % SiO<sub>2</sub>) which exhibit chemical and isotopic features indicative of significant continental source components. Zircon and monazite U-Pb ages for the Rahu Suite are concentrated in the range 115-107 Ma. In their chemistry, variable isotopic composition, associated appinitic rocks and probable post closure tectonic setting the Rahu Suite has much in common with the Caledonian granites of Scotland. Most of these plutons were emplaced at 10-20 km depth, but were rapidly uplifted on detachment faults which trended subparallel to the continental margin to the east and to the eventual spreading centre of the Tasman Sea to the west.

Although the Early Cretaceous plutonic rocks in the footwalls of the core complexes are dominated by the Rahu Suite, some rocks with SPS/WFO and intermediate characteristics are also present in all complexes. Resetting of Cenozoic displacement on the Alpine Fault strongly suggests that large volumes of WFO underlie the Rahu Suite. Nd-Sr isotopic data suggest that the Rahu Suite was derived from a combination of the SPS/WFO source together with a continental crustal component. Assimilation of old crust is also indicated by Proterozoic zircon inheritance, particularly in the Rahu Suite, but it is also clearly present in some SPS plutons. Traces of Proterozoic inheritance also appear in the younger parts of the MTZ arc rocks, suggesting that in its final stages the locus of MTZ magmatism overlapped the craton margin. Despite a wide range in initial Nd and Sr for the SPS/WFO and Rahu Suites, feldspars in both suites exhibit extremely limited variation in Pb isotopic composition, consistent with crustal scale Pb isotopic homogenisation during, or immediately prior to, melting to produce these granitoid suites.

A likely protolith for the SPS/WFO magmas is the slightly older MTZ arc, which may have achieved the appropriate metamorphic grade within a thick underplate. In detail, models which derive the SPS/WFO from an

MTZ arc protolith (magmatic or tectonic underplating) must account for the ~20 Ma time span of SPS/WFO magmatism and its geographic span from the Permian accreted terrane east (oceanward) of the MTZ, westward across the MTZ and Gondwana margin at least to the present west coast of New Zealand (~140 km across the margin in present configuration), and the observed pattern of Proterozoic zircon inheritance.

Plutonic rocks similar to SPS/WFO in several other parts of the Pacific rim occur inboard of slightly older arc-related batholiths (*e.g.* Eastern Peninsular Ranges Batholith), where they also appear to precede continental extension further inboard and intrude along major sutures between craton and accreted terranes.

Potential derivation of the SPS/WFO suites from an MTZ protolith means that arc characteristics may have been inherited from this source, and thus such features of the SPS/WFO do not necessarily indicate subduction contemporaneous with the SPS. Thus the youngest time at which Mesozoic subduction beneath the New Zealand margin of Gondwana can be shown unambiguously to have occurred using geochemical/magmatic criteria is 140-130 Ma.

Further inboard from the convergent margin a series of increasingly alkaline rocks ranging from gabbro (100 Ma) to A-type granite (83 Ma) and camptonitic lamprophyres (~84 Ma) clearly herald the culmination of extension and the opening of the Tasman Sea between NZ and Australia at, or slightly before, 84 Ma.

## ORAL PRESENTATION

### **Granites from Source to Emplacement: The View from Geophysics**

Vignerresse, Jean Louis

*CREGU, and ENS Géologie, Nancy, France*

Two examples are used to show how the transfer of ideas between disciplines is realized. In the first example, the depth of a pluton floor is estimated from gravity data inversion and correlated to structural measurements registered by the magma when being emplaced. The second example refers to two granitic complexes, very close in time, but very contrasted in their shape at depth, as well as in their petrological pattern.

The pluton of Cabeza de Araya, Estramadura, Spain, intruded late Precambrian micaschists, *c.* 300 Ma, in an extensional zone due to regional shear. The pluton presents a normal petrographic zoning. On its periphery, facies A is porphyritic, gradually passing to facies B, a coarse-grained two-mica granite which is cross-cut by facies C, a leucocratic two-mica variant. 760 gravity stations have been realized, which result in a Bouguer anomaly map. After data inversion and tests on the sensitivity of the results to the density values, the depth of the pluton floor is mapped with an estimated error of 15 %. The pluton is thin with 75% of its volume within 4.5 km of the present erosion level. Its walls dip inward by 30° to 70°.

Structural measurements, using the orientation of K-feldspars, and the anisotropy of magnetic susceptibility provide the orientation and dip of the foliation planes and the lineation. The lineations show a bimodal distribution. Subvertical lineations (> 60°) are located in the southern part of the pluton, in facies C. They also cluster in the north of the pluton. The subset with low plunges (< 30°), located principally in facies A and B, trend with the same azimuth as the pluton. The regions of deep floor and vertical lineations are interpreted as the magma feeding zones.

Two small and unconnected tension cracks, between 6 km and 13 km in depth, served as feeding zones for the magma. Simultaneous infilling by magma during opening was followed by an interruption at the A/B transition before a new stage of progressive opening/infilling led to facies B (gradational contacts). A longer period of quiescence separated the intrusion of facies C (sharp contacts). The magma flow was continuously guided by incremental opening of the walls.

The Hercynian Fichtelgebirge granite, Bayern, Germany, is subdivided into two heterochronous complexes, hereafter designed as the Older Intrusive Complex (OIC) and the Younger Intrusive Complex (YIC), and simplified to equigranular and porphyritic facies. All granitic types have a pronounced peraluminous character.

The porphyritic (OICp) facies is biotite-rich, whereas the equigranular (OICe) facies is mainly medium to fine grained and muscovite rich. The latter is much more peraluminous than the OICp facies, with a compositional gap and distinct chemical variation. The OICe is also more Mg-rich than would be expected from simple biotite fractionation from the OICp. The YICp facies shows a fine grained groundmass containing several different phenocrysts compared to the YICe facies. Both share a typical fractionation trend, reflected by the increase of the

peraluminous character and no discernible gap in the fractionation process.

After gravity data inversion, the OIC is modeled as a thin body, *c.* 1.9 km thick on average. An eastward deepening of the massif to 6 km that coincides with the more evolved facies is interpreted to reflect the root zone. The YIC averages 6 to 7 km in thickness with a nearly flat floor and steeply dipping walls which trend N160°. The western wall, dipping at 70° to the east, is related to the Franconian Line, a major dextral shear zone. The two smaller massifs of the YIC, north of OIC, are connected to the southern unit of the YIC, beneath the OIC unit.

The OIC forms one unique massif on the field and all granitic facies belong to a more or less homogeneously evolving magma. The most fractionated magmas are close to the root zone, whereas the less evolved magma travelled away from its root zone. So, the bulk trend is a higher degree of fractionation with decreasing distance to the root zone. The YIC outcrops in three massifs, each one shows an imbricated disposition of facies. All samples located near the root zone are the least fractionated, with low values of differentiation index and low Th content. Fractionation develops in samples located far from the root zone. These contrasted patterns between OIC and YIC are interpreted as reflecting differences in the magmatic evolution during the emplacement of the two massifs.

In the OIC, two separate magma pulses are defined according to the porphyritic/non-porphyritic character of the rocks, the gap within the fractionation trend, and finally the sharp borders at facies changes. The bulk shape of the floor, with only one root, suggests that this unique root delivers all the magma undergoing an evolving fractionation. Because of the gap in the fractionation pattern, two major pulses of magma have been delivered. The first one invades the region from the east and gives rise to the OICp along an east-west elongated trend. A second pulse of magma immediately follows. It is more evolved and fractionated than the first, and therefore probably more viscous and resistant to flow. It pushes aside the formerly emplaced OICp magma and solidifies as it reaches the uppermost levels to form the present OICe.

In the YIC, the very steep walls and parallel is in to the Franconian line, suggest a tectonic control on emplacement. The geochemical variations within the two main facies are almost identical and show a nearly identical fractionation trend. One single magma generated two facies during successive major steps of continuously opening space filled with granite. During each step of intrusion, the marginal part of the magma crystallized first,

so the remaining magma appears more evolved and forms part of the YICe. Another sequence follows, with lower differentiation index, but with a slope of evolution similar to the first. It also shows a porphyritic and an equigranular facies.

### **Mid-Cretaceous Plutonism Associated with Crustal Extension: The Hohonu Batholith, New Zealand**

Waight, Tod

*Department of Geological Sciences,  
University of Canterbury, Christchurch, New Zealand*

The middle Cretaceous tectonic history of the New Zealand portion of the Gondwana margin was complex, involving subduction, terrane accretion, crustal extension and eventual continental breakup. This history includes emplacement of several distinct pulses of granitoid magmatism. Combined field and petrological investigations have enabled identification of four suites in the Hohonu Batholith, a ~600 km<sup>2</sup> region of granitoids outcropping adjacent to the Alpine Fault on the West Coast of the South Island of New Zealand. A single Devonian pluton represents the oldest magmatism in the batholith, whereas a Late Cretaceous A-type pluton, closely associated with an alkaline mafic dike swarm and the opening of the Tasman Sea at 82 Ma, represents the youngest activity.

The bulk of the batholith comprises the Hohonu supersuite (114-109 Ma) which is characterized by relatively restricted radiogenic isotopic compositions ( $(^{87}\text{Sr}/^{86}\text{Sr})_{(110)} = 0.7062$  to  $0.7085$  and  $\epsilon_{\text{Nd}}(110) = -4.4$  to  $-6.1$ ). The Hohonu supersuite is considered to represent melting of a complicated source combining depleted mantle-derived material and a complex, heterogeneous and largely unconstrained lower continental crustal component. Two constituent suites are recognized within the Hohonu supersuite, the Te Kinga suite and the Deutgam suite. Geochemical contrasts between these two suites are attributed to melting at differing crustal depths, at varying water activities, and in equilibrium with different residual assemblages. The relatively mafic, metaluminous, I-type compositions of the Deutgam suite are ascribed to volatile phase-absent melting in equilibrium with an amphibolitic (plagioclase + amphibole) residue. Residual plagioclase retained Sr, Al<sub>2</sub>O<sub>3</sub>, Na<sub>2</sub>O and Eu and resulted in the low

concentrations of these elements which characterize this suite. In contrast, the peraluminous high silica compositions of the Te Kinga suite are attributed to water-saturated to undersaturated melting in equilibrium with an eclogitic (garnet + amphibole residue) at greater depths in the crust. Residual garnet produced the HREE-depleted nature of the suite, and a lack of residual plagioclase contributed to the characteristically higher Sr, Al<sub>2</sub>O<sub>3</sub>, Na<sub>2</sub>O and Eu contents of the Te Kinga suite.

The Hohonu supersuite was emplaced during a period of rapid tectonic transition along the Gondwana margin. It post-dated crustal thickening and compression associated with subduction, collision and the generation of the "adakitic" Separation Point suite and was also emplaced contemporaneous with the cessation of subduction and the initiation of crustal extension in the Western Province of New Zealand.

#### ORAL PRESENTATION

### **Heterogeneous Sources for Granitic Rocks, Black Hills, South Dakota: Do Granites Really Serve as Interpretable Crustal Probes?**

Walker, Richard J. and Krogstad, Eirik J.

*Isotope Geochemistry Laboratory,  
Department of Geology, University of Maryland  
at College Park, MD 20742, USA*

The Early Proterozoic (1715 Ma) Harney Peak Granite (Black Hills, SD) consists of a complex of hundreds of dikes and sills. In addition, the granite complex is interwoven with, and surrounded by a compositionally diverse pegmatite field. Earlier studies of neodymium (Walker *et al.*, 1986), oxygen (Nabelek *et al.*, 1992) and lead (Krogstad *et al.*, 1993) isotope variations indicated that the Harney Peak Granite complex was not derived from a single source, or even different sources of a single age. New Nd and Pb isotopic results are consistent with a complex source for the Harney Peak Granite. For example, the Harney Peak Granite has  $\epsilon_{\text{Nd}}$  values (1715 Ma) that range from -2.0, indicating an Early Proterozoic (2.2 to 2.3 Ga) crustal source, to -13.4, indicating a Middle Archean (3.1 to 3.2 Ga) crustal source. The Nd isotopic compositions of spatially associated metasedimentary rocks

are consistent with the interpretation that the Early Proterozoic source included local metasedimentary rocks. The Late Archean sources might have included rocks like those exposed on the periphery of the Black Hills.

The Nd and Pb isotopic data for granitic pegmatites display a range similar to that of the Harney Peak Granite suite. For example,  $\epsilon_{Nd}$  values for apatites from the Tin Mountain, Hugo and Peerless pegmatites range from +0.7 to -10.0. There is no obvious correlation between pegmatite type and Nd isotopic composition. However, the interpretation of Nd isotopic data on small, presumably water-rich igneous systems is problematic. The pegmatites evidently exchanged significant Nd with country rocks during their crystallization, and the pegmatites have moderately inhomogeneous Nd isotopic compositions. This observation illustrates potential problems in the study of trace element/isotopic systematics of any fluid-rich granite system.

The range of model ages calculated for the granite-pegmatite system brings into question the viability of using Nd model ages of an evolved granite system to quickly fingerprint the "average" age of the crust in a given region. Because such heterogeneity is present in the magmatic compositions of the Harney Peak Granite, it can be inferred that at least as much heterogeneity was present in the sources. Melts were evidently derived from isolated, heterogeneous zones, and did not have the opportunity to coalesce into large, isotopically homogeneous magma bodies. In this instance, the evidence for source complexity was not lost. Such complexities, however, are likely lost in some systems. This study highlights the danger of drawing inferences from the isotopic data for a few samples of plutonic rocks in studies of regional crustal evolution.

Krogstad, E.J., Walker, R.J., Nabelek, P.I. and Russ-Nabelek, C., 1993.

Lead isotopic evidence for mixed sources of Proterozoic granites and pegmatites, Black Hills, South Dakota, USA. *Geochim. Cosmochim. Acta*, **57**, 4677-4685.

Nabelek, P.I., Russ-Nabelek, C. and Haeussler, G.T., 1992. Stable

isotope evidence for the petrogenesis and fluid evolution in the Proterozoic Harney Peak leucogranite, Black Hills, South Dakota. *Geochim. Cosmochim. Acta*, **56**, 403-417.

Walker, R.J., Hanson, G.N., Papike, J.J. and O'Neil, J.R., 1986. Nd, O, and Sr isotopic constraints on the origin of Precambrian rocks, southern Black Hills, South Dakota. *Geochim. Cosmochim. Acta*, **50**, 2833-2846.

## Crustal Evolution and the Generation of Magmas Akin to Adakites in Western Palmer Land, Antarctic Peninsula

<sup>1</sup>Wareham, Christopher D. and <sup>2</sup>Millar, Ian L.

<sup>1</sup>British Antarctic Survey, High Cross, Madingley Road, Cambridge CB3 0ET, UK

<sup>2</sup>British Antarctic Survey, c/o NERC Isotope Geosciences Laboratory, Keyworth, Nottingham, NG5 5GG, UK

Antarctic Peninsula Mesozoic-Cainozoic magmatism forms part of a belt of subduction-related magmatism that extended along the Pacific margin of Gondwana prior to continental break-up. The east-directed subduction of proto-Pacific and Pacific oceanic plate produced granite magmatism in western Palmer Land between c. 230 Ma and 60 Ma. Subduction in the region ceased between c. 50 and 20 Ma with the formation of a passive margin as a result of ridge-trench collision.

Plutonic magmatism in western Palmer Land ranges in composition from gabbro to granite (s.s.), and is locally overlain by volcanic rocks and intruded by mafic dykes. These plutons intrude basement paragneiss of unknown age. Elsewhere in the peninsula, basement gneiss has yielded whole-rock Rb-Sr and zircon U-Pb ages of up to c. 400 Ma. Intrusions with Proterozoic Nd model ages ( $t_{DM}$ ) and intrusions containing zircons with inherited cores are present throughout the peninsula and suggest that Proterozoic basement may be present.

Many of the granites are LREE-enriched ( $La_N/Yb_N$  up to c. 30), sodic ( $Na/K > 1$ ), have  $Al_2O_3 > 15$  wt %, have high Sr/Y ratios (up to c. 100), and are low in Sc, HFSE and HREE. They have many major element characteristics that are typical of experimental partial melts of metabasalt, leaving a pyroxene - amphibole - garnet restite. These chemical features are also characteristic of Archean tonalite - trondhjemite - dacite suites and Phanerozoic adakites, which are believed to be the products of slab melting. However, the major element composition of many Palmer Land granitoids, such as their  $Na_2O$  and  $MgO$  contents, lies outside the range produced experimentally for melts of metabasalt. Simple trace element modeling suggests that the high Sr content, low Y content, and consequently the high Sr/Y ratios that are characteristic of some of these magmas can not be derived by fluid absent melting of a N-MORB protolith.

$\epsilon_{Nd}(t) = -7 - +5$ , common Pb ( $^{206}Pb/^{204}Pb = 18.638 - 18.796$ ;  $^{207}Pb/^{204}Pb = 15.612 - 15.677$ ;  $^{208}Pb/^{204}Pb =$

38.469 - 38.649) and Sr ( $(^{87}\text{Sr}/^{86}\text{Sr})_i$ ) c. 0.704 - 0.714) isotope studies indicate that magma components were derived from the mantle wedge, mantle lithosphere and sub-arc crust. There is an overall increase in  $\epsilon_{\text{Nd}}$  and decrease in 2-stage Nd model age ( $t_{\text{DM}} = 400 - 1300$  Ma) with decreasing stratigraphic age. Isotope and trace element data are comparable to those obtained on contemporaneous arc basalts in western Palmer Land. These data suggest that the granites were in part generated by the melting of mafic underplate. Major element data and the presence of mafic inclusions in many of the granites indicate that a component of primary mafic magma is also present. The role of mafic magma in the genesis of the Palmer Land granites is two-fold: it is a component of the magmas, whether as a primary melt component or as melted underplate, and it provided the heat necessary for fusion of mafic lower crust.

Juvenile continental crust was produced in western Palmer Land, and elsewhere in the peninsula, during the Mesozoic and Cenozoic. This occurred by underplating, by intraplating and by lateral accretion of magmas in shear zones. Granite magmas in western Palmer Land were largely derived by the melting of underplated mafic magma. Their origin is essentially intra-crustal and consequently their production will have contributed little to the growth of new continental crust. The generation of these magmas will have simply redistributed previously accreted lower crust. The net flux of material into the crust, whether above subduction zones or in intra-continental rift settings, is basaltic in composition. Despite this, the continental crust has a broadly andesitic composition. The melting of underplated basaltic material at the base of the crust can produce a spectrum of granitoid magma compositions and a dense garnet-eclogite residuum. This residuum may detach and sink into the mantle convective system, for example, during continental collision. Therefore, although the generation of granitoids by melting of basaltic underplate may contribute little towards the growth of new continental crust, their production will define the composition of the crust. Thus, subduction zones are not only areas in which new continental crust is formed, but also areas in which the average composition of this crust is refined.

## ORAL PRESENTATION

**Zircon Dissolution and Overgrowth  
in Granitic Melts:  
Effects of Thermal History  
and Local Melt Volume,  
with Implications for Chemical  
Zoning and Relative Core Size  
in Natural Zircons Showing  
an Inherited Isotopic Component**

Watson, E.B. and Hanchar, J.M.

*Department of Earth and Environmental Sciences,  
Rensselaer Polytechnic Institute,  
Troy, NY 12180, USA*

When imaged with cathodoluminescence or back-scattered electrons, individual zircon crystals in granitic rocks commonly exhibit a rounded (sometimes embayed) core overgrown by at least one euhedral, chemically-zoned rim. This multistage record of dissolution and growth suggests a complex history, including survival of zircon during crustal melting—a phenomenon that is not only well documented by U/Pb-isotope studies but also consistent with known systematics of zircon solubility and Zr diffusion in granitic melts. The complexity of the dissolution/growth process is further underscored by the fact that core/rim volume ratios vary widely among individual zircons separated from a single rock.

In an effort to understand the process of zircon dissolution in melts followed by chemically-zoned overgrowth, and to place constraints on the time scales of these processes, we have undertaken a series of finite-difference numerical simulations using existing experimental data on zircon solubility and Zr diffusion in granitic melts containing 3 wt. % dissolved  $\text{H}_2\text{O}$  (Watson and Harrison, 1983; Harrison and Watson, 1983). The simplest models involve linear cooling from an assumed initial temperature at which the melt is saturated in zircon. Cooling from  $750^\circ \rightarrow 650^\circ\text{C}$  over  $10^5$  years produces an overgrowth rim  $5.6 \mu\text{m}$  thick on a preexisting  $100\text{-}\mu\text{m}$  crystal (assuming a physically static system in which no new zircons nucleate). The radial growth rate averages  $1.8 \times 10^{-16} \text{ cm s}^{-1}$ , but is highly non-linear in time, peaking at  $\sim 30\text{K}$  years. The non-linear growth rate could lead to marked chemical zoning in slow-diffusing minor constituents of zircon such as Y, HREE and Hf. A  $100^\circ$  cooling interval extended over 1 Ma results in  $31 \mu\text{m}$  of new zircon growth on an

original 100- $\mu\text{m}$  core. Lower cooling rates yield still thicker overgrowth rims, as do higher initial temperatures.

Our model can incorporate almost any degree of assumed geological complexity, and we are now exploring the consequences to zircon behavior of a heating-cooling cycle appropriate to crustal anatexis. Under such circumstances, protolith zircons can dissolve partially over the heating interval and precipitate new rims upon cooling in what amounts to highly local processing of isotope systems controlled by zircon. For a given melting episode ( $t$ - $T$  path) and a melt reservoir infinitely large relative to the diffusion field around the dissolving (or growing) zircon, the volume ratio of old core to new overgrowth depends only upon the initial size of the zircon. If, however, the melt reservoir is of finite volume in relation to the diffusion field (*e.g.*, a melt pocket on the order of 1 mm in size), the core/rim volume ratio is critically dependent upon melt reservoir volume. A time-dependent reservoir volume (due to melting or crystallization of major mineral phases) leads to additional complexities in both core/rim volume ratios and minor-element zoning in zircons.

Several general conclusions can be drawn from the numerical simulations: 1) zircon growth (and dissolution) rates in granitic melts are very low ( $\sim 10^{-16}$  cm s<sup>-1</sup>) at plausible crustal melting conditions due to the combination of slow Zr diffusion and low zircon solubility in the melt with the high demand for Zr to form zircon; 2) zircon growth and dissolution rates are likely to be highly non-linear in time even for very simple  $t$ - $T$  melting histories; and, 3) during anatexis, "finite reservoir" effects are likely to play a major role in determining the relative core sizes of zircons containing an inherited isotopic component. In the light of these conclusions, the observed complexity and intrapopulation variability of internal structures in natural zircons is not surprising.

Harrison, T.M. and Watson, E.B., 1983. Kinetics of zircon dissolution and diffusion of zirconium in granitic melts of variable water content. *Contrib. Mineral. Petrol.*, **84**, 66-72.

Watson, E.B. and Harrison, T.M., 1983. Zircon saturation revisited: temperature and composition effects in a variety of crustal magma types. *Earth Planet. Sci. Lett.*, **64**, 295-304.

## Geochemical Evidence for Deformation Enhanced Melt Segregation: An Example from the Kirtomy Migmatite Suite, Sutherland, Scotland

Watt, Gordon R. and Burns, Ian M.  
*Geology and Cartography Division,  
Oxford Brookes University,  
Headington, Oxford, OX3 0BP, UK*

The role of accessory phases such as zircon and monazite in controlling the trace and rare-earth element chemistry of granites (Hinton and Paterson, 1994; Montel, 1993), leucogranites (Sevigny *et al.*, 1993) and migmatite leucosomes (Sawyer, 1991; Watt and Harley, 1993) is now well documented. Restricted monazite and zircon dissolution during anatexis, coupled with disequilibrium melting of feldspars (Carrington and Watt, 1995), may give rise to melts with characteristic low LREE and HREE contents and positive Eu anomalies. Dissolution may be prevented by armouring of accessories or by removal of melt before equilibration with the source lithology (Brown, 1994; Sawyer, 1994). Compilations of melt segregation rates show that melt percolation velocities are more rapid than diffusion velocities in silicates, and if segregation occurs by channelised migration along veins or high-porosity pathways then melt migration may be more rapid still (Bedard, 1989). Disequilibrium melt compositions may therefore be generated and extracted during water saturated melting, if melt removal is rapid. Evidence for channelised flow and deformation enhanced melt segregation on a hand specimen and outcrop scale (boudin necks, veins, melt migration into micro-shears) is present in semi-pelitic migmatitic gneisses of the Kirtomy Migmatite Suite (KMS) in Sutherland. These amphibolite facies semi-pelitic and pelitic migmatites are interpreted to have formed during evolution of the Caledonian Moine Nappe pile and record metamorphic conditions of 680-700°C, 4-6 kbar. Melt migration distances are on an outcrop to 100m scale. Leucosomes in the KMS have low Zr contents and positive Eu anomalies, similar to those of granitic sheets in the Scourian Complex (Rollinson, 1994) and mafic migmatites described by Sawyer (1991). REE patterns of this type can be produced by removal of leucosome before complete equilibration with source due to the inhibited dissolution of LREE bearing accessory phases in water-undersaturated melts. Melting in the KMS,

however, occurred at or near the wet granite solidus, forming biotite as a restitic phase. Experimental work shows that during water-saturated melting conditions accessory phase dissolution is near instantaneous, and therefore slow accessory phase dissolution because of low melt H<sub>2</sub>O contents cannot be responsible for the geochemical signatures witnessed in the KMS. Furthermore, detailed back-scattered electron imaging shows that accessory phases were not armoured during melting. We suggest that deformation enhanced melt extraction was responsible for the REE and trace element chemistry of the KMS leucosomes - rapid migration of melt from the melting site on a timescale of less than 10000 years prevented leucosomes from equilibrating with zircon and monazite before extraction.

- Barbero, L. and Villaseca, C., 1992. The Layos Granite, Hercynian Complex of Toledo (Spain): an example of a parautochthonous restite-rich granite in a granulitic area. *Trans. Royal Soc. Edinburgh: Earth Sci.*, **83**, 127-138.
- Bedard, J. H., 1989. Disequilibrium mantle melting. *Earth Planet. Sci. Lett.*, **91**, 359-66.
- Brown, M., 1994. Melt segregation mechanism controls on the geochemistry of crustal melts. *Mineral. Mag.* **58A**, 124-125.
- Carrington D. P. and Watt, G. R., 1995. A geochemical and experimental study of the role of K-Feldspar during water-undersaturated melting of metapelites. *Chem. Geol.*, in press.
- Hinton, R. W. and Paterson, B. A., 1994. Crystallisation history of granitic magma: evidence from trace element zoning. *Mineral. Mag.*, **58A**, 416-417.
- Montel, J. M., 1993. A model for monazite/melt equilibrium and application to the generation of magmas. *Chem. Geol.*, **110**, 127-146.
- Rollinson, H., 1994. Origin of felsic sheets in the Scourian granulites: new evidence from rare earth elements. *Scott. J. Geol.*, **30**, 121-129.
- Sawyer, E. W., 1991. Disequilibrium melting and the rate of melt-residuum separation during migmatization of mafic rocks from the Grenville Front, Quebec. *J. Petrol.*, **32**, 701-738.
- Sawyer, E. W., 1994. Melt segregation in the continental crust. *Geology*, **22**, 1019-1022.
- Sevigny, J. H., Parrish, R. R. and Ghent, E. D. 1993. Petrogenesis of peraluminous granites, Monashee Mountains, south-eastern Canadian Cordillera. *J. Petrol.*, **30**, 557-581.
- Watt G. R. and Harley, S. L. 1993. Accessory phase controls on the geochemistry of crustal melts and restites produced by dehydration melting. *Contrib. Mineral. Petrol.*, **114**, 550-566.

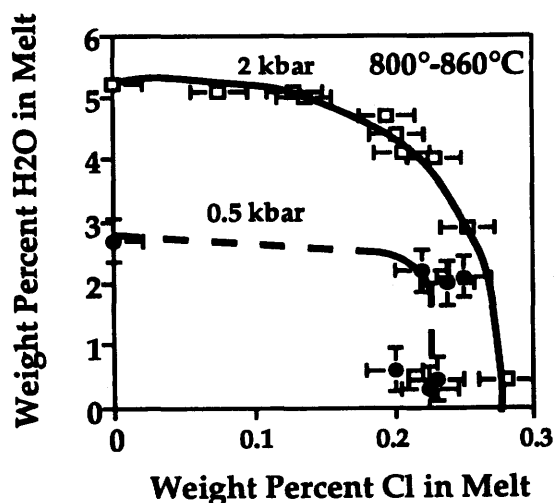
## Early Exsolution of Chlorine-Enriched "Fluids" From Felsic Magmas: A Crucial But Poorly-Understood Process

Webster, James D.

*Department of Earth and Planetary Sciences,  
American Museum of Natural History,  
Central Park West at 79th Street,  
NY, NY 10024-5192, USA*

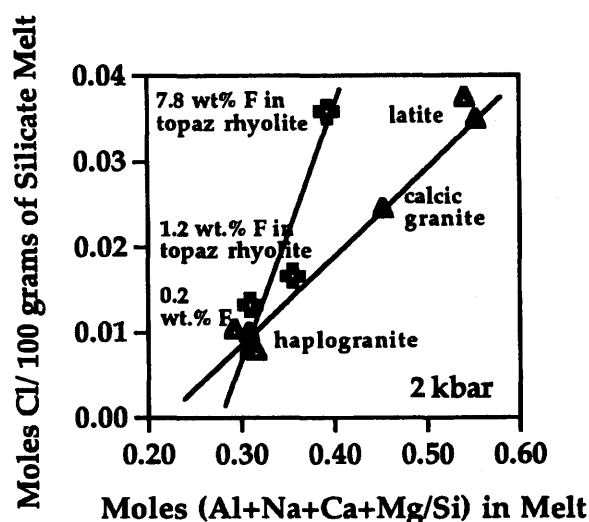
The exsolution and subsequent movement of aqueous fluids within aluminosilicate magmas can profoundly affect heat and mass transfer in and around magma reservoirs, alter magma composition, and may also control late-stage processes such as hydrothermal brecciation-mineral deposition and volcanic eruptions. Experimental studies have shown that fluid exsolution from silicate melt is a function of the solubilities of all volatiles present, and hence aqueous fluids will exsolve from magma that is nominally water undersaturated if comparatively small quantities of other volatiles such as CO<sub>2</sub> or SO<sub>2</sub> are also dissolved in the magma. In this context, new experiments have been conducted at 0.5 and 2 kbar to determine the solubility of chlorine and water in a variety of F-deficient and F-enriched felsic melts. The results can be used to predict the exsolution of supercritical Cl-bearing aqueous fluids, coexisting brine plus vapor, and/or marginally hydrous alkali chloride melts from silicate melt. This combination of volatiles is particularly significant for mineralizing magmatic systems because it pairs the most abundant magmatic volatile (water) with one of the most important complexing anions in hydrothermal fluids (the chloride ion).

The solubility of H<sub>2</sub>O plus Cl in silicate melt is a strong function of pressure. For example, the reciprocal solubilities of these volatiles in fluid saturated haplogranite melt were determined at two pressures by equilibrating alkali chloride melts with silicate melt or by equilibrating Cl-bearing fluids with silicate melt. The following figure shows a reduction in solubility for both volatiles with decreasing pressure; 2 kbar data are shown as squares and 0.5 kbar as circles.



Consequently, highly-evolved (F-poor) felsic magmas at 2 kbar will exsolve a fluid phase (*i.e.*, an alkali chloride melt) with as little as 1 wt % H<sub>2</sub>O in melt if at least 0.28 wt % Cl is also present. These results are consistent with recent studies of glass inclusions from barren and mineralized felsic volcanic systems which indicate that many rhyolite magmas contain from 0.2 to greater than 0.5 wt % Cl prior to eruption.

The reciprocal solubilities of H<sub>2</sub>O and Cl are also a strong function of F, Ca, Na, Mg, and Al in melt. For example, H<sub>2</sub>O-deficient, F-bearing topaz rhyolite melts (crosses) dissolve significantly more Cl than anhydrous haplogranite melt; the solubility of Cl in haplogranite melt is one-fourth that of topaz rhyolite melt containing > 7 wt % F. Chloride solubilities at 2 kbar and 800 - 1075°C are shown in the following figure.



In addition, H<sub>2</sub>O-deficient, Ca- and Mg-rich (F-poor) melts (triangles) also exhibit enhanced Cl solubility relative to haplogranite melt; Cl solubility in latite melt is about 4 times that in haplogranite melt under similar conditions.

Extrapolation of these experimentally-determined Cl and H<sub>2</sub>O solubilities to the higher pressures required for the generation of felsic magmas by partial melting in the lower crust suggests that the solubilities of both volatiles in such melts will be quite high. Hence, it follows that Cl-enriched fluids may not be stable in the presence of felsic silicate melt at these conditions. Conversely, as felsic magmas begin their ascent toward the surface and subsequently undergo magmatic differentiation, supercritical Cl-bearing aqueous fluids, coexisting brine plus vapor, and/or marginally hydrous alkali chloride melts may exsolve even if the melts contain only minimal H<sub>2</sub>O contents. Thus, exsolution Cl-enriched fluids may occur early, after either minimal fractional crystallization of H<sub>2</sub>O- and Cl-poor minerals or after minimal ascent and pressure reduction.

These results are also applicable to processes of magmatic-hydrothermal ore deposition because they are compatible with the presence of salt-rich fluid inclusions (exhibiting magmatic homogenization temperatures) in many molybdenum- and copper- mineralized porphyritic magmas. Such inclusions imply that highly saline fluids do exsolve directly from mineralizing, felsic magmas; saline fluids are not generated solely as a result of fluid boiling.

## ORAL PRESENTATION

### Diapirism of Crustal Magmas

Weinberg, Roberto F.

Research School of Earth Sciences,  
Australian National University,  
Canberra, ACT 0200, Australia

There has been considerable discussion surrounding the mechanisms of transport of felsic magma through the continental crust. This work questions the recent tendency in the literature to attribute magma ascent mostly to dykes, and the emphasis given to their relation to plutons and shear zones. It first discusses the difficulties involved in the propagation of felsic dykes away from the source into

cold crust, and then describes recent results which suggest that diapirism may be an efficient mechanism of magma and heat transport through the lower crust.

Several segregation mechanisms may operate within the magma source region: a) upwards porous flow; b) magma overpressure and cataclasis when external strain rates are faster than the rate with which the melt can flow out of the system (Dell'Angelo and Tullis, 1988); c) flow of magma towards low pressure sites (Robin, 1979; Stevenson, 1989). These mechanisms give rise to melt pockets, veins and magma-filled fractures oriented mainly parallel to the direction of maximum compressional stress. Although melt segregation may occur within the source region, Rubin (1993) suggested that crustal (felsic) melts might be unable to leave the source region as dykes because the high viscosity magma freezes faster than dykes propagate. If this is the case, the source becomes increasingly buoyant and may start to dome. Doming initiates preferentially in the low pressure areas where melt has accumulated, and as it proceeds melt flows preferentially to the top of the dome to form a granitic cap underlain by restites and low-melt migmatites. It is important to stress that diapirism does not require the source to reach the rheological critical melt percentage before it is able to start rising, in fact even a solid buoyant body may rise diapirically. Shear zones are generally weak areas softened by strain. If major crustal shear zones (active or inactive) cut across a partially molten region submitted to regional stresses, they will attract melt from the surroundings because of their low pressure. In this way shear zones may localise the sites of diapir initiation and provide a preferential path for magma ascent, thereby controlling the ascent without necessarily having any influence on the ascent mechanism or on the creation of space for the magma.

It has been considered that diapirs rise too slowly to travel a significant distance through the crust before freezing. However, assuming power-law rheology of crustal rocks, low effective crustal viscosity allows much faster ascent than that predicted for Newtonian crust, thus allowing diapirs to rise to mid-crustal levels prior to solidification (Weinberg and Podladchikov, 1994 and *in press*). Fast diapirs are able to pull the lower crust and the isotherms upwards. A dry lower crust may then melt due to diapir-driven decompression. The buoyancy of the wall rocks due to partial melting will further enhance the diapir's velocity and its ability to penetrate the crust. A combination of power-law crustal rheology and decompression melting of the surrounding might greatly enhance the effectiveness of diapirs in transporting magmas through the

crust. Despite recent developments in the theory of diapirism, field evidence has yet to identify their ascent path. The difficulty in determining the pathways may be due to a combination of relatively rare exposure of lower crustal sections with the often observed complexity of structures in these terranes and the interaction between structures related to the passage of diapirs and syn- and post-emplacement regional structures. The steeply plunging kilometre-scale sheath folds mapped in the granulite terrane of central Australia (Goscombe, 1992) may conceivably represent such structures.

- Dell'Angelo, L. N. and J. Tullis, 1988. Experimental deformation of partially melted granitic aggregates, *J. metamorphic Geol.*, **6**, 495-515.
- Goscombe, B., 1992. High-grade reworking of central Australian granulites. Part 1: Structural evolution. *Tectonophysics*, **204**, 361-399.
- Robin, P.-Y., 1979. Theory of metamorphic segregation and related processes, *Geochim. Cosmochim. Acta*, **43**, 1587-1600.
- Rubin, A. M., 1993. On the thermal viability of dikes leaving magma chambers, *Geophys. Res. Lett.*, **20**, 257-260.
- Stevenson, D. J., 1989. Spontaneous small-scale melt segregation in partial melts undergoing deformation, *Geophys. Res. Lett.*, **16**, 1067-1070.
- Weinberg, R. F., and Podladchikov, Y., 1994. Diapiric ascent of magmas through power-law crust and mantle, *J. Geophys. Res.*, **99**, 9543-9559.
- Weinberg, R. F., and Podladchikov, Y. The rise of solid-state diapirs, *J. Struct. Geol.*, in press.

## Diapirism and Decompression Melting

Weinberg, Roberto F.

*Research School of Earth Sciences,  
Australian National University,  
Canberra, ACT 0200, Australia*

In a dry crust, rapid decompression caused by the upward drag of a rising diapir may lead to partial melting of the surrounding rocks. These rocks become buoyant and accelerate the original diapir, further enhancing decompression melting in a "runaway" process, that ends only when the diapir reaches cold crust and decelerates due to loss of buoyancy caused by freezing and high crustal viscosity. Decompression melting depends on the buoyancy of the diapir, the thermal structure of the crust and the solidus curve of the wall rocks, and considerably enhances diapir penetration through the crust. In contrast with the hot-Stokes models, in which thermal softening of

the wall rocks accelerates the diapir but leads also to rapid freezing of the diapiric magma, decompression melting accelerates the diapir without rapidly consuming its thermal energy. In fact the diapir may regain some of the thermal and mechanical energy lost during ascent when the surrounding rocks become buoyant due to melting. Diapirism and decompression melting are studied here numerically, and assuming an initial warm, molten diapir within solid lower crust (Fig. 1a). The model crust has Newtonian viscosity, which increases upwards by four orders of magnitude due to the geothermal gradient. The temperature at the base of the crust equals the solidus temperature of the model crust and decreases upwards slower than the crustal temperature. This means that, with the exception of the initial diapir, the whole crust is solid. The volume of partially molten crust and the depth at which the diapir freezes are presented in dimensionless parameters based on the buoyancy of the diapir, the rheology of the crust, the geothermal gradient and solidus curve, and absolute temperature at the base of the crust. It is shown that a diapir may treble its volume by partially melting the wall rocks (Fig. 1b) and that the increased buoyancy, rather than the decreased viscosity of the wall rocks, allows diapirs to travel much further through the crust before freezing. Most melting occurs below the diapir, a region that is heated during the passage of the diapir, but more importantly, where hot lower crustal rocks are dragged upwards by the diapir. If the partially molten crust is denser than the diapir, as would be the case for most granitoid diapirs, the partially molten crust remains below the diapir (Fig. 1b), and only if segregation occurs will the newly formed melt rise to join the original diapir. If, on the other hand, the partially molten crust is lighter than the diapir (*e.g.* if there are large amounts of melt in the wall rocks of a relatively dense tonalite/diorite diapir), the partially molten crust will invade the diapir from below and occupy its core. The results suggest that the buoyancy added to the diapir by decompression melting of the surroundings may be much more important in enhancing diapiric ascent of magmas than thermal softening of the wall rocks. Furthermore, the results show how the volume of crustal melt produced may depend not only on the thermal structure of the crust but also on the dynamics of magma emplacement.

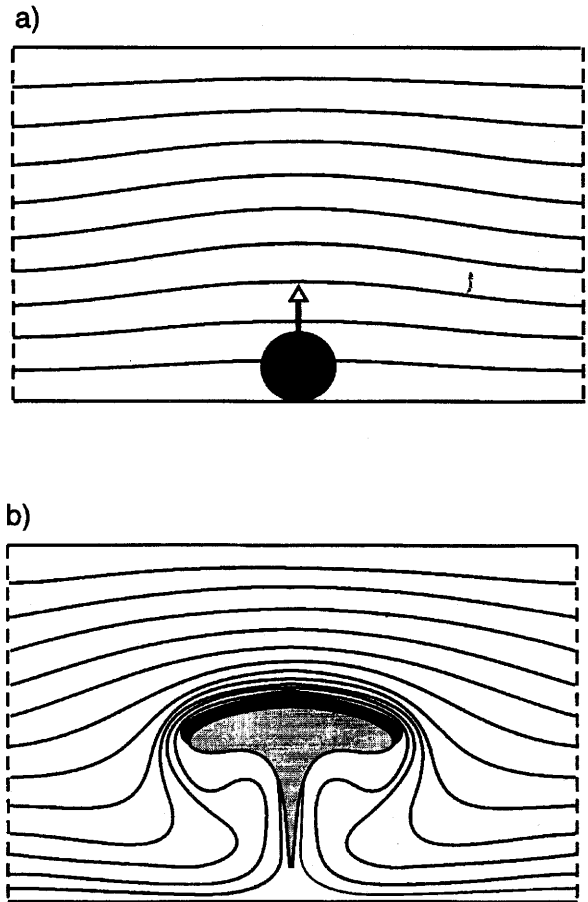


Figure 1. a) The starting geometry of the numerical model. The black circle is the initial diapir, the arrow shows the ascent direction and the lines indicate isotherms controlling the upward increase in viscosity. b) The diapir causes partial melting of the crust along its tail (grey area) partly due to heat transferred to its wall rocks during passage, but mainly due to upward drag of the hot lower crust. The partially molten crust in this model is lighter than the solid rocks but denser than the diapir. The lateral spread of the original diapir is due to the upward increase in viscosity and to the addition of the buoyant partially molten crust to its tail.

## ORAL PRESENTATION

**Mafic-Silicic Layered Intrusions**

Wiebe, R.A.

*Department of Geosciences,  
Franklin and Marshall College,  
Lancaster, PA 17604, USA*

Plutonic complexes that consist of interlayered mafic and silicic rocks, "mafic-silicic layered intrusions" (MASLI), are common and occur in a wide range of tectonic settings. Recent work on the coast of Maine and a review of earlier work indicate that these complexes have generally formed by multiple injections of basaltic magma into floored silicic magma chambers rather than by multiple sill-like injections of silicic magma into pre-existing, partly-solidified mafic rocks. Some MASLI are basin-form - up to 3 km thick and 30 km in diameter. Most appear to have been emplaced at shallow crustal levels. Field relations, petrography and geochemistry indicate that the silicic layers tend to be cumulates and that the basal parts of many mafic layers are quenched basaltic liquids. MASLI appear to be the plutonic expression of composite magma chambers that have long been inferred from the study of silicic volcanic rocks.

MASLI typically contain macrorhythmic units, from less than one to several 10s of meters thick, characterized by a chilled gabbroic base that grades upward to medium-grained gabbro, diorite or highly evolved silicic cumulates. Each chilled base records the introduction of new basaltic magma into the magma chamber. The top of each unit is truncated by the chilled base of the overlying unit. Cumulates beneath the chilled base of a macrorhythmic unit vary widely in composition, suggesting that the level at which the basaltic magmas ponded was controlled by a rapid inward drop in crystallinity and viscosity rather than by neutral buoyancy. Density inversion is demonstrated by load-cast structures which occur at the bases of many units and silicic pipes and veins which extend from the underlying unit into the base of the overlying unit. Where the input of new mafic magma was small, gabbro typically occurs as discontinuous zones of chilled pillows.

Thick macrorhythmic units that grade upward from chilled gabbro to highly silicic cumulates preserve a record of double-diffusive convection with stably stratified, hotter, denser mafic magma beneath silicic magma. The lower gabbroic rocks are commonly hornblende-rich with large corroded biotite crystals; the upper silicic rocks of many

units are relatively anhydrous. Intermediate rocks provide evidence for mechanical mixing of crystals and selective exchange of H<sub>2</sub>O, alkalis and isotopes. Crystallization of biotite and hornblende in mafic magma at the boundary contributed to exchange of H<sub>2</sub>O and alkalis. Although diffusion and turbulent mixing were probably restricted to a thin boundary layer, convection away from that boundary transferred the effects of hybridization into the interior of both magmas. Systematic variation in (<sup>87</sup>Sr/<sup>86</sup>Sr)<sub>i</sub> occurs over tens of meters in some units. The apparent lack of comparable variation in Nd isotopes is consistent with the lower diffusivity of Nd. When mafic infusions established a long-lasting basal layer of mafic magma, mixing and fractional crystallization contributed to producing an intermediate layer of magma highly enriched in incompatible elements.

The compositional and thermal effects of repeated infusions of basaltic magma may greatly affect the character of granite that crystallizes from overlying silicic magma. In Maine, processes that operated in MASLI have had profound and varying effects on the evolution of overlying granites. In the Cadillac Mountain granite, basaltic infusions converted an I-type, subsolvus, biotite hornblende granite into a hypersolvus, A-type granite. The characteristic trace-element enrichments shown by A-type granites were produced by interactions with incompatible element-rich intermediate magmas that evolved near the base of the chamber. In the Gouldsboro granite repeated injections of basaltic magma mainly promoted exchange of alkalis and led to the development of a low-K (trondhjemitic) magma layer beneath normal granitic magma. The contrasting responses of these two silicic systems may be largely related to differences in the rates of influx of mafic magma.

MASLI demonstrate that basaltic infusions into silicic magma chambers can significantly effect the thermal and chemical character of granites even in shallow-level chambers. If comparable interactions occur at deeper crustal levels, it is possible that selective thermal, chemical and isotopic exchange may be even more efficient. Because the mafic magmas crystallize first and relatively rapidly, silicic magmas that rise away from deep composite chambers may eventually show little obvious record of their prior involvement with mafic magma. In addition, heat transfer from mafic to silicic magma may play an important role in permitting crystal-poor silicic magmas to reach high crustal levels.

**Enclave-Rich Zones in the  
Gouldsboro Granite, Maine:  
A Record of Eruption and  
Compositional Stratification in a  
Silicic Magma Chamber**

Wiebe, R. A. and Adams, S. D.

*Department of Geosciences,  
Franklin and Marshall College,  
Lancaster, PA 17604, USA*

The Gouldsboro granite is a shallow-level Silurian intrusive complex, roughly 350 km<sup>2</sup> in area, located on the Maine coast. Except for a heterogeneous mixture of granitic, hybrid, and mafic rocks near the base of the complex, it consists of leucocratic, biotite hornblende granite. In the highest-level exposures of the granite there are zones up to 300 meters in width and at least 1 km in length that contain roughly 30 to 50 percent of chilled intermediate to silicic globular enclaves (ranging in diameter from tens of cms to several meters) in a matrix of granite. In the largest of these zones, there are two different types of enclaves (high-K<sub>2</sub>O and low-K<sub>2</sub>O) with identical SiO<sub>2</sub>. For most major and trace elements plotted against SiO<sub>2</sub>, both enclaves and host granite produce coherent trends with SiO<sub>2</sub>, ranging from 65 and 71% in the globules and from 71 to 78% in the granite. The compositional variation of these enclaves and the host granite strongly suggest they evolved within the same chamber. The low-K enclaves are concentrated in the central axis of the zone, while the high-K enclaves are dominant in the margins. Scarce chilled pillows and angular fragments of basalt occur only in the low-K enclaves. Some of these are unusually rich in K<sub>2</sub>O. Most enclaves contain some amygdules filled with feldspar and quartz, and the basaltic inclusions are weakly vesicular. Some enclaves are composite, consisting of both high-K and low-K types separated by a sharp but highly irregular, crenulate boundary. This zone of enclaves appears to be the locus of an eruption from within the chamber through its partly crystallized granitic roof, and the enclaves probably preserve a record of magma compositions within the chamber at the time of eruption. On the basis of models for magma withdrawal, the distribution of the two types of enclaves suggests that the chamber was compositionally stratified with low-K magma below high-K magma. The restriction of scarce chilled basalt inclusions to the low-K type suggests that basaltic magma entered the

base of the chamber shortly before the eruption and may have triggered it.

The main compositional differences between the two types of silicic magmas are in K, Na, Rb, and Ba concentrations. Each group shows a fairly wide range in alkalis, and the compositional gap between the two groups is nearly bridged by a few samples. The high-K enclaves have alkali contents that are comparable to the dominant host granite. The low-K (trondhjemitic) enclaves have alkali contents that are matched only by a small volume of high-SiO<sub>2</sub>, very low-K trondhjemite that seems only to occur in the vicinity of enclaves. Basaltic inclusions in the low-K enclaves are commonly K-rich. These relations suggest that the low-K magma could have been derived from the high-K magma by selective exchange of alkalis between mafic and silicic magmas.

More mafic, chilled enclaves dominate another zone of similar size in the granite. These have SiO<sub>2</sub> that varies from about 54 to 59%; their major- and trace-element compositions form very tight trends against SiO<sub>2</sub> except for alkalis which vary widely at a constant value of SiO<sub>2</sub> (*e.g.* K<sub>2</sub>O varies from 0.4 to 1.6% at about 56% SiO<sub>2</sub>). In terms of most elements, these mafic enclaves have compositions which suggest they evolved largely by fractionation from a basaltic parent. The host granite near these enclaves has highly variable K<sub>2</sub>O and ranges from normal granite to trondhjemite with very low K<sub>2</sub>O. The compositional variation of alkalis in both enclaves and granitic host can best be explained by selective exchange during commingling.

The layer of low-K (trondhjemitic) silicic magma that developed near the base of chamber was probably generated by alkali-exchange between resident silicic magma with normal K<sub>2</sub>O and multiple injections of mafic magma. On a small scale, comparable exchange of alkalis is commonly observed at the margins of chilled pillows in granite. With many replenishments of basaltic magma into a silicic chamber, it may be possible to generate a hotter, drier (and, hence, denser) layer of low-K silicic magma between stratified mafic and granitic magmas. This process may play an important role in the origin of some trondhjemites.

## Testing Fault-Controlled Magma Emplacement Mechanisms

Yoshinobu, A.S., Okaya, D.A.,  
Paterson, S.R. and Fowler, T.K.

*Department of Earth Sciences,  
University of Southern California,  
Los Angeles, CA 90089-0740, USA*

When shear zones are mapped in or around granitoids, is it reasonable to conclude that these faults produced the space now occupied by the pluton? The preponderance of fault-controlled magma emplacement models in the current literature indicates that this model is accepted as a viable mechanism for magma emplacement in arcs. However, no adequate tests have been carried out to establish the validity of the above hypothesis. In order for a fault or set of faults to create space for magma emplacement, a number of structural conditions must be met which include the following: 1) faults should exist that bound the plutons; 2) these faults should have significant displacements relative to the size of the pluton and continue into the country rocks far beyond the structural aureoles of the intrusions; 3) it should be possible to "balance" the map by removing the pluton and restoring the country rocks along the faults back to their initial pre-emplacement configuration; 4) where exposed, the roofs (and floors) of the magma chambers should be highly extended or detached by sub-horizontal shear zones; 5) the pluton orientation should have a predictable relationship with arc-scale faults; and, 6) the rates of processes must be compatible with slip rates in modern arcs.

We can also test the fault-controlled hypothesis utilizing 1-D and 2-D finite difference thermal modeling which constrains the thermal requirements needed to create and maintain a chamber during the successive emplacement of magma into space created by the simultaneous displacement of country rock along faults. The results of our preliminary modeling indicate that early crystallized sheeted complexes should form along the margins of plutons emplaced by dilation within fault zones, consistent with published modeling.

Do real plutons meet these thermal and structural conditions? We are currently examining the spatial and temporal relations of proposed space-making faults in the Late Cretaceous Sierra Nevada batholith, California and the Permian Colanguil batholith, northwestern Argentina, using both field data and thermomechanical modeling.

Voluminous granitoid intrusive suites along the eastern edge of the Sierra Nevada in the age range of 80-90 Ma. have been hypothesized to be emplaced into a) tensional cracks and dilational jogs within arc-parallel strike slip faults, or b) zones of dilation bridging en echelon p-shear fault arrays within the upper crust. However, based on published mapping and our own reconnaissance field work, we conclude the following: 1) plutons within these intrusive suites are locally to regionally discordant to country rock markers; 2) the plutons are irregularly shaped; 3) the proposed space-making faults generally do not completely bound the plutons, nor do they show evidence of large displacements; 4) locally preserved roof rocks are not extended nor detached; 5) the granitoids do not have significant sheeted border phases; and, 6) country rock markers cannot be reconstructed by removing the plutons and restoring the faults.

Plutons within the Colanguil batholith have been postulated to be emplaced during Permian trench-parallel arc extension. We have examined two of these plutons in detail, and a third in reconnaissance fashion; all were emplaced into an older fold-and-thrust belt at shallow depths. Although these plutons locally contain syn-magmatic dikes parallel to the long dimension of the magma chamber (~ 3 % of the total map area in one pluton), our mapping indicates that: 1) country rock roofs capping the plutons are neither detached nor extended; 2) no significant faults of the appropriate age exist in the field area; 3) no marginal sheeted phase was recognized as predicted by the thermal modeling; and, 4) country rock markers cannot be reconstructed.

The discordant nature of these batholiths indicates that stoping has played an important role at least during the final emplacement of the magmas into the upper crust. Although it is permissible that stoping by younger intrusive pulses could effectively "erase" earlier evidence of marginal sheeting, we note that the inability to reconstruct regional country rock markers and the lack of significant pluton-bounding faults with large displacements suggest to us that faults did not produce the space for these magmas. We contend that the relationships described above are widespread in arcs. The resulting implication is that the majority of country rock material displaced by the plutons moved downwards rather than laterally along intra-arc faults.

## One-Dimensional Thermal Modelling of Crustal Anatexis in an Extensional Regime

Zen, E-an

Department of Geology, University of Maryland  
at College Park, Maryland 20742, U.S.A.

One-dimensional thermal modelling using the 1DT program (Haugerud, 1986) was used to test the idea that mid-crustal anatexis of fertile sedimentary material in an extensional environment could produce large volumes of granitic melt. The actual Neogene-to-Recent crustal, tectonic, and thermal conditions of the Basin and Range Province (B&R) of western United States guided the modelling. Table 1 compares the model parameters with data for B&R (Zen, 1995).

Table 1. Model Parameters and Basin and Range Data

	MODEL	B&R
Thermal Conductivity	2.0 W/m/K	
Heat Capacity	900 J/K/Kg	
Rock Specific Gravity	2780 kg/m <sup>3</sup>	
Depth to mid-crustal discontinuity, km	22, 26, or 32	15-25
Duration of Extension, Ma	30	>20
Extensional Strain Rate	3%/Ma (1x10 <sup>-15</sup> /sec)	~3-10%/Ma
Heat Productivity, A, uW/m <sup>3</sup>	2 or 3	<3, mostly ~2
Productivity/Depth Relations	linearly decreasing to 0 at, or constant to, 20/30 km	
Subcrustal Flux, mW/m <sup>2</sup>		
Initial	30	
Maximum	60 or 75	60-80
Surface Heat Flow at Maximum Flux	80 to 165 mW/m <sup>2</sup>	c. 90 mW/m <sup>2</sup> ; Battle Mt. High, 120-160 mW/m <sup>2</sup>
Time Interval for Adjusting Thermal Profile	2.0 Ma	
Final Monitor Depth	30 km or rises with deletion	

Extension is simulated by 15 iterations of deletion, mostly at 2 Ma intervals, of a 2-km cell from an initial 60-km thickness. The deleted material is accounted for by linear extension mostly at a strain rate of 1x10<sup>-15</sup>s<sup>-1</sup>. The heat productivity, A, specified at the surface, either remains constant to a depth Z' (Z' = 20 or 30 km) or tapers linearly to 0 at that depth (nearly all the runs used tapered A). The subcrustal flux is increased by a constant amount with every deletion to attain its peak value,

corresponding to the effect of mafic underplating and thinning of the subcrustal mantle. The monitor depth (~base of the crust) either is stationary or rises with deletion; after termination of deletion the flux either remains at the peak value or drops back toward the pre-extension value.

Melting is stepwise, with the parametric heat of fusion, h<sub>f</sub> defined as  $\Delta H_f/C_p = 300^\circ\text{C}$ , i.e., 1% melting equals 3 degrees of virtual cooling. The incremental melting scheme is: 700°C (solidus), 15%; 740°C, 20%; 780°C, 15%; 820°C, 10%; 860°C and 900°C, 5% each. The volumes of melts generated for 40 runs are given in Table 2; the magma volumes would be augmented by lateral pooling, residual material, and melt formed below the deletion zone.

Table 2. Percentages of Melt Volume, in km<sup>3</sup>/km<sup>2</sup>, Formed Above Deletion Depth

Volume Range	0-1	1-2	2-3	3-4	4-5	5-6	6-7	7-8	8-9
End of Deletion	32.5	22.5	17.5	17.5	5.0	5.0	0	0	0
18 Ma later	17.5	12.5	25.0	10.0	7.5	10.0	7.5	5.0	5.0

Prolonged extension using thermal, tectonic, and melting properties that are geologically realistic can lead to voluminous anatexis of fertile material at pressures as low as 4 kbar *provided* that fertile source material is available at the proper depths.

I applied the results to the granitic plutons of the Lachlan Belt (LB), southeastern Australia. There, the strongly peraluminous, S-type granite, granodiorite, and rare tonalite must have been derived from fertile sedimentary source rocks. The An contents of the residual cores ("restitic") and magmatic overgrowth of plagioclase are demarked at about An<sub>50</sub> and suggest melting within a temperature range of c. 150°C; rare An<sub>80</sub> cores could mean that the source layer was as much as 3 km thick. A mid-Paleozoic extensional episode lasting a few tens of Ma for LB is controversial but permissive. If the process did happen, then the model-predicted steep average thermal gradient of c. 50°C/km would explain the *in situ* anatexis at Cooma (pressure above the Al-silicate triple point). The model also provides an alternative explanation for the I-S line as the mid-crustal boundary of the limit of extension.

In the model, the upper crust is passive and stationary and the pressure-temperature-time paths are isobaric lines. Results of many model runs predict progressive low-pressure, high-temperature metamorphism for the upper crust as the P-T-t paths traverse through the

andalusite field into the sillimanite field, and may even reach the breakdown of muscovite+quartz in equilibrium with plagioclase (the second sillimanite isograd).

Haugerud, R.A., 1986. 1DT - an interactive, screen-oriented microcomputer program for simulation of 1-dimensional geothermal histories: *U.S. Geological Survey, Open-file Report* 86-511.

Zen, E-an, 1995. Crustal magma generation and low-pressure, high-temperature regional metamorphism in an extensional environment: possible application to the Lachlan Belt, Australia. *Am. J. Sci.*, 295, in press.

## **Anatomy and Genesis of Shuiximiao Asymmetrically Layered Pegmatite-Aplite Dikes**

Zhu, Jinchu, Rao, Bing and Xiong, Xiaolin

*Department of Earth Science,  
Nanjing University,  
Nanjing 210008, China*

The Sn-Ta bearing Shuiximiao granite of Guangxi Autonomous Region, South China, is a concealed granite cupola of Early Jurassic age. It is hosted by a Carboniferous limestone sequence and characterized by a well expressed vertical zonation. From the exocontact downwards to the endocontact within a distance of some 400-500 m, the following zones are successively developed: 1) lepidolite - fluorite stringers; 2) Sn/W bearing (K feldspar-) quartz veins; 3) Sn/Ta bearing pegmatite - sodic aplite dikes and pegmatoid stockscheider; 4) Sn/Ta bearing albite-rich topaz granite; 5) albite granite; and, 6) microcline-albite granite. Because the zones 2, 3 and 4 are mined for Sn, W, Ta and Nb by underground works, the relationship between the dikes and granite cupola is very clear.

Several subparallel NS trending pegmatite-sodic aplite dikes are rooted in the roof part of the albite-rich topaz granite and pegmatoid stockscheider of the cupola. They are gently to steeply dipping, tabular in shape, >200 m long along the strike, >100 m deep and 2-20 m thick. The dikes are mostly asymmetrically layered. The footwall portions are usually the albite-rich granitic aplite consisting of Ab, Qz, Kf, Top and mica; the hangingwall portions are usually the granitic pegmatite consisting of Qz, Kf, Ab, mica and Top; the middle portions are usually the alternating bands of sodic aplite and pegmatite up to

about one hundred layers. Sometimes porphyritic fine-grained aplite with Kf phenocrysts are also developed. The average aplite versus pegmatite volume ratio is about 1:1.

Multiphase juxtaposed composite intrusives, igneous gravitational crystal settling, metasomatism, magmatic flowage and stressed dynamic metamorphism all may be considered as the main controlling mechanism for formation of this kind of dikes. A combination of the following factors is considered to be responsible for their genesis: 1) the parental magma of the dikes is derived from the Ab-rich topaz granite melt at the top of the cupola which is the late differentiate of granite fractionation, rich in Na, H<sub>2</sub>O, F, Li, Ta, Nb, Sn, W, but not necessarily be water-oversaturated; 2) At certain degree of undercooling and a range of water content, the Ab + Q assemblage is usually the first liquidus phases of granite crystallization yielding sodic aplite at the footwall portions for gentle to normal dikes; 3) fluctuation of F content in the melt and episodic crystallization of topaz would result in consequent change of eutectic composition of the moving crystallization front. Disequilibrium crystallization of the residual granitic melt with changing composition is responsible for the alternating layering; and, 4) the above-mentioned hypothesis can be used only to interpret the compositional layering. The frequently existing textural layering is believed to be related to the crystallization kinetics of the residual granite melt which is poorly understood at the present. Further experiments at proper temperatures, pressures, water contents and initial compositions are critically needed.

## AUTHOR INDEX

Abbey, W.J.	7	Clemens, John D.	52,126,127	Guimarães, I.P.	60
Acosta, Antonio	7	Cocherie, Alain	36,128	Haapala, I.	61
Adams, S.D.	165	Cole, David R.	10	Halliday, A.N.	152
Åhäll, K.-I.	39	Coler, D.G.	132	Hammer, J.	46,62
Al-Saleh, Ahmad	8	Collins, W.	37,38,79,86	Hammouda, T.	116
Aleinikoff, J.N.	7,149	Creaser, Robert A.	27,32,38	Hanchar, J.M.	158
Allen, Charlotte M.	25	Crossland, A.	57	Hanson, R. Brooks	63
Anderson, J. Lawford	9,93	Cruz, M.J.M.	49	Harley, S.L.	64
Anovitz, Lawrence M.	10,24	Dall'Agnol, Roberto	135	Harris, Nigel	86
Arth, J.G.	11	Dalla Salda, L.H.	91	Heizler, M.T.	18,95
Atherton, M.P.	73	Darbyshire, D.P.F.	39,138	Herve, F.	111
Ayuso, R.A.	11	Da Silva Filho, A.F.	60	Hess, K.	42
Bagaric, Steve	107	Davies, G.R.	65,117	Heumann, A.	65
Baker, Leslie	12	Davis, A.	40	Himmelberg, Glen R.	29
Baldo, E.	120	Dean, A.A.	41	Hodkinson, D.	66
Barbarin, Bernard	13	Defant, Marc J.	44	Hogan, J.P.	67,68
Barboza, Scott A.	14	Delaloye, M.	50	Holden, Peter	18
Bargossi, G.M.	129	Del Moro, A.	129	Holtz, Francois	70
Barnes, C.G.	15	Dingwell, D.B.	42	Hook, S.J.,	95
Barovich, Karin M.	76	D'Lemos, R.S.	42,113	Horak, Jana M.	71
Barr, Sandra M.	16	Drinkwater, James L.	29	Horita, Juske	10
Barton, Mark D.	17,18	Drummond, Mark S.	44	Hutson, F.E.	72,149
Bea, Fernando	19,20,51	Duchesne, J.C.	45	Hutton, D.H.W.	98
Beard, James S.	21,112	Duthou, Jean-Louis	58	Jackson, M.D.	73
Bergantz, George W.	14,21	Eidam, J.	46,62	Jacques, J.M.	74
Berza, T.	45	Elburg, Marlina A.	47	James, E.	15
Blakey, Suzanne	23	Eleftheriadis, G.	105	Jensen, Charles	106
Blencoe, James G.	10,24	Enrique, P.	48,50	Johannes, Wilhelm	74
Blevin, Phillip L.	25	Falkner, C.M.	95	John, Barbara E.	75
Blundy, Jonathan D.	75	Fallick, A.E.	49	Johnson, Clark M.	76
Bonin, Bernard	26	Fanning, C.M.	56	Jovic, V.	53
Bouchez, Jean-Luc	100,105	Ferreira, V.P.	49,141	Kalakay, Thomas J.	77
Brandon, Alan D.	27	Ferres, M.	50	Karlstrom, K.E.	110
Braun, I.	28	Fershtater, G.B.	51	Kawano, Yoshinobu	78
Brew, David A.	29	Flinders, James	52	Keay, S.	79
Brewer, T.S.	39	Flood, R.H.	53	Kepezhinskas, Pavel K.	44
Brown, Michael	30,66,142	Ford, Arthur B.	29	Ketcham, D.H.	79
Bryant, Colleen J.	25	Forizs, I.	53	Khalili, M.	80
Burns, Ian M.	159	Förster, H.-J.	54,147	Kimbrough, D.L.	153
Caggianelli, A.	129	Foster, D.A.	56	King, T.R.	42
Candela, P.A.	31,115,121	Fowler, T. K., Jr.	57,111,166	Kloetzli, U.S.	82
Carrington, D.	64	Fujitani, Tatsuya	144	Knoche, R.	42
Carroll, William	106	Galan, Gumer	58	Kohút, M.	81
Chacko, Thomas	27,32	Gallego, Marcos	90	Koller, F.	82
Chappell, Bruce W.	25,34	Gasparotto, G.	129	Komatsu, Masayuki	139
Cheadle, M.J.	73	Ghidotti, Gregory	18	Kotov, A.B.	81
Chown, E.H.	35	Gibbons, Wes	71	Kovach, V.P.	80
Christiansen, Eric H.	35	Gilbert, M.C.	68	Krogstad, E.J.	40,66,150,151,156
Christofides, G.	105	Glascoock, Michael D.	103	Kubo, Kazuya	83
		Goodwin, Laurel	18	Kumar, Santosh	83
		Gray, Karen J.	59	Kutsukake, Toshio	84

Lahtinen, Raimo	85	Piccoli, P.M.	115	Thirlwall, M.F.	23
Landenberger, B.	86	Pichavant, Michel	116,135	Thomas, R.	145
Larson, S.-Å.	39	Pin, Christian	58	Thompson, Alan Bruce	93,146
Law, Richard	100	Pinarelli, L.	129	Tischendorf, G.	147
Lee, Y.F.S.	95	Poli, G.	117,152	Tobisch, Othmar T.	94,148
LeFort, Patrick	86	Price, J.D.	68	Todd, V.R.	139
Leslie, Karen	87	Pupin, Jean-Pierre	118	Tollo, R.P.	7,72,149
Liegeois, J.P.	45	Rämö, O. Tapani	61,109	Tomascak, Paul B.	150,151
Litvinovsky, B.A.	88	Rao, B.	168	Tommasini, S.	117,152
London, David	89,90,99	Rapela, C.W.	119,120	Tong, Weixing	94
Long, L.E.	79	Ratajeski, K.	121	Toselli, A.J.	141
López de Luchi, M.G.	91	Reavy, R.J.	74	Tribe, I.R.	42
Lowenstern, Jacob B.	92	Reed, Marshall	122	Trumbull, R.B.	147
Luedke, R.G.	99	Reed, Robert M.	124	Tulloch, A.J.	153
Lund, S.P.	136	Renno, A.D.	125	Ulmer, Peter	93
Lynton, Stephen J.	151	Rhede, D.	54	Unkefer, J.	95
Manetti, P.	152	Roberts, Malcolm P.	126,127	Vernon, R.H.	148
Matile, Lusius	93	Roddick, James A.	128	Vignerresse, Jean Louis	154
Mattey, David	86	Rossi, Philippe	36,128	Volborth, A.	61
Mayo, David P.	93	Rossi de Toselli, J.N.	141	Vukov, M.	53
McNulty, Brendan A.	94,148	Rottura, A.	129	Waight, T.	156
Menéndez, Luis G.	7	Rushmer, Tracy	130,132	Walker, Richard J.	150,151,156
Menzies, M.A.	23	Rutherford, Malcolm J.	12	Wareham, Christopher D.	157
Michalko, J.	81	Saavedra, J.	120,141	Watson, E.B.	158
Millar, Ian L.	157	Saint Blanquat de, Michel	100	Watt, Gordon R.	159
Miller, C.F.	95	Salnikova, E.B.	81	Weaver, S.D.	102,111
Miller, J.S.	95	Sampson, S.	132	Webb, S.L.	42
Miller, Robert B.	97,111	Sawyer, E.W.	38,133,134	Webster, J.D.	160
Molyneux, S.J.	98	Scaillet, Bruno	70,135	Weinberg, Roberto F.	161,162
Montero, Pilar G.	98	Schmidt, K.L.	136	Wickham, S.M.	88
Morgan, G.B. VI	90,100	Seaman, S.J.	137	Wiebe, R.A.	164,165
Morgan, Sven	100	Sewell, R.J.	138	Williams, M.L.	137
Moukhsil, Abdelali	101	Shannon, W.M.	15	Wolf, Michael B.	90
Muir, R.J.	102	Shaw, S.E.	53,139	Wooden, Joseph L.	93,95
Nabelek, Peter I.	103,144	Shimura, Toshiaki	139	Wright, J.E.	68
Nakajima, Takashi	104	Shirey, Steven B.	76	Xiong, X.	168
Nédélec, A.	105	Sial, A.N.	49,79,141	Yoshinobu, A.	57,166
Neiva, A.M.R.	105	Singh, Jagmohan	74	Zanvilevich, A.N.	88
Nekvasil, Hanna	106	Smith, D.R.	15	Zen, E-an	167
Newton, R.C.	88	Snoke, Arthur W.	77	Zhu, J.	168
Nicholls, Ian	107	Solar, Gary S.	142		
Nironen, M.	109	Soldatos, T.	105		
Nyman, M.W.	110	Sole, J.	50		
O'Neill, Michael	16	Speer, J.A.	132		
Okaya, D.A.	166	Staudigel, H.	65		
Pankhurst, R.J.	111,119,120	Stephens, W.E.	105		
Paterson, S.R.	57,97,111,136,166	Stunitz, Holger	75		
Patiño Douce, Alberto E.	112	Tatu, M.	45		
Patrick, D.W.	95	Tegeler, J.L.	143		
Pembroke, J.W.	42,113	Terakado, Yasutaka	144		
Petford, Nick	114	Ternes, Kim	144		



